HIGHLY STEREOSELECTIVE *INTERMOLECULAR* HALOFUNCTIONALIZATION OF OLEFINS

By

Bardia Soltanzadeh

A DISSERTATION

Submitted to
Michigan State University
in partial fulfillment of the requirements
for the degree of

Chemistry-Doctor of Philosophy

2018

ABSTRACT

HIGHLY STEREOSELECTIVE INTERMOLECULAR HALOFUNCTIONALIZATION OF OLEFINS

By

Bardia Soltanzadeh

Since the inception of organic chemistry more than a 200 years ago, halogenation of olefins has been a mainstay reaction. Yet, this venerable reaction had not succumbed to an enantioselective process. Two major issues that have thwarted the development of asymmetric alkene halogenations are the rapid stereochemical degradation of chiral halonium ions by olefin-to-olefin halonium transfer, and by isomerization of halonium ions to the open β-halocarbenium ions. The latter scenario changed in 2010, when our lab, among others, successfully demonstrated stereoselective reactions for the intramolecular halocyclization of alkenes with tethered nucleophiles. Not surprisingly, most early examples reported on the *intramolecular* capture of halonium ions *via* tethered nucleophiles; the proximity-driven rate enhancement of the cyclization step presumably outcompetes any stereorandomizing event. Enantioselectivities of >95:5 are routinely obtained with a variety of halonium precursors and nucleophiles. In contrast, enantioselective *intermolecular* halofunctionalizations have been more difficult to achieve due to reduced reaction rates, limited choice of compatible nucleophiles, and lack of regiochemical control. This dissertation highlights my efforts towards optimizing a variety of *intermolecular*

halofunctionalization methodologies. First, our results that show excellent control of stereo and enantioselectivity in haloetherification and haloesterification of both activated and non-activated olefins will be discussed. The resulting lessons from the latter were parlayed into developing a highly selective olefin dihalogenation, demonstrating the ability to overcome regiochemical scrambling through catalyst controlled process, as opposed to substrate control selectivity, which limits the chemistry to activated olefins. Most recently, the chemistry has been extended to enantioselective haloamination of olefins, setting the stage for the synthesis of privileged moieties found in natural products, bioactive reagents, and pharmaceuticals. Finally, our preliminary mechanistic investigations suggest that a concerted mechanistic pathway is responsible for product formation. The dependence of the course of the reaction on the nature of the nucleophile leads to a suggested explanation for the observed divergence in product facial selectivity.

To my lovely parents

ACKNOWLEDGMENTS

During the course of my graduate studies numerous people were helping me, and without their support, this process would be impossible. My advisor professor Babak Borhan was one of those people that influence me not only in scientific way but also in personal perspective. His mentorship was led me to grow as a scientist and thought me how to think and fix scientific problems. I am grateful to my committee members, Prof. William Wulff, Prof. James Jackson and Prof. Daniel Jones for their advice and support. I am thankful to Dr. Richard Staples for X-ray crystallography, Dr. Daniel Holmes for helping me to run kinetic studies by means of NMR instruments. Arvind has been fantastic senior for me; he kindly taught me to be a better chemist. I also want to send my thanks to Dr. Chrysoula Vasileiou for her help and encouragement. I am thankful to those graduate students that collaborate with me on different projects- Daniel, Yi and Aritra.

Mostly, I express my gratitude to my parents, brother, sister and Hamideh for their unconditional support and love. Without their encouragement and support, this long journey would have been impossible.

TABLE OF CONTENTS

LIST OF TABLES

LIST OF FIGURES

KEY TO SYMBOLS AND ABBREVIATIONS

Å	Angstrom
[α]	Specific rotation
δ	Chemical shift
Ac	Acetyl
Alk	Alkyl
Ar	Aryl
br	Broad (spectral peak)
Cl_2	Chlorine
CsCl	Cesium chloride
d	Day
DCDMH	1,3-Dichloro-5,5-dimethylhydantoin
DCDPH	1,3-Dichloro-5,5-diphenylhydantoin
DCM	Dichloromethane
DHQ	Dihydroquinine
DHQD	Dihydroquinidine
(DHQ)2PHAL	Dihydroquinine 1,4-phthalazinediyl diether
(DHQD)2PHAL	Dihydroquinidine 1,4-phthalazinediyl diether
DIAD	Diisopropyl diazadicarboxylate
DMAP	4-Dimethylaminopyridine
DMSO	Dimethylsulfoxide

dr	Diastereoselectivity ratio
ee	Enantioselectivity excess
ESI	Electrospray ionization
Et	Ethyl
EtOAc	Ethyl Acetate
$(Et)_2O$	Diethyl ether
EtOH	Ethanol
h	Hour
Me	Methyl
MeCN	Acetonitrile
MHz	Megahertz
Min	Minutes
Mol	Molar
MS	Molecular sieves
NaOH	Sodium hydroxide
*n*Bu	*n*-butyl
NBS	N-bromosuccinimide
NCS	N-chlorosuccinimide
NMR	Nuclear magnetic resonance
Ph	Phenyl
PHAL	phthalazine
R	Substituent

rr	Regioselectivity ratio
rt	Room temperature
Sat	Saturated
TEA	Triethylamine
TEAC	Tetra ethyl ammonium chloride
THF	Tetrahydrofuran
tBu	tert-butyl
TFE	2,2,2-trifluoroethanol
TLC	Thin layer chromatography

Chapter I: Highly Stereoselective Intermolecular Haloetherification and Haloesterification of Allyl Amides

I-1 Introduction

Methodologies for enantioselective alkene halofunctionalization have grown at a fast pace in recent years.[1-43] The chiral carbon-halogen bond is a versatile motif in bioactive and natural compounds, and also of value in the traceless total synthesis of natural products. [44-46]

Figure I-1: Natural products with stereo defined carbon-halogen bonds

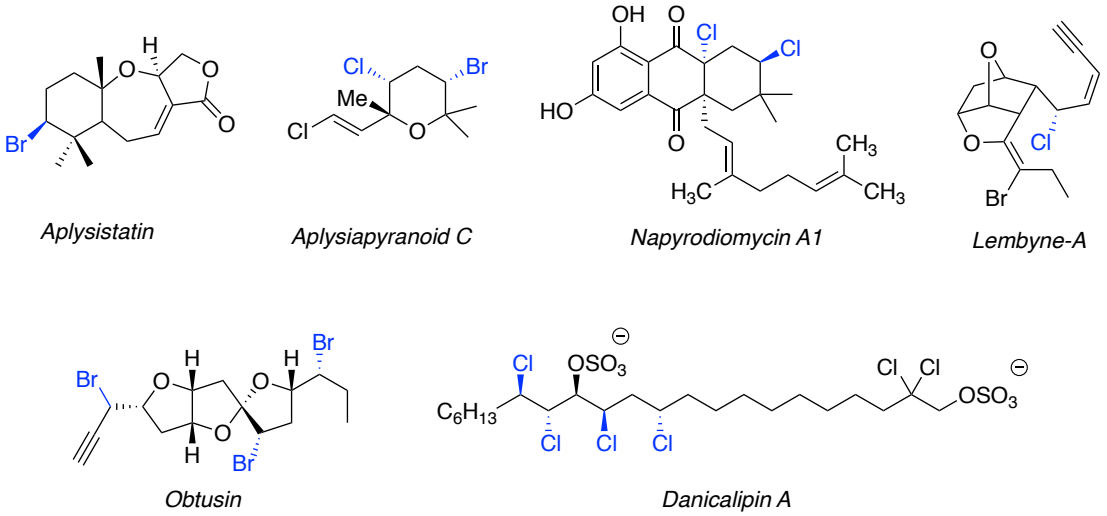

Over 4000 natural compounds exhibit carbon-halogen bond

In the last 37 years, various catalytic enantioselective alkene functionalization reactions, such as epoxidation,[47] dihydroxylation,[48] aziridination[49] and others were successfully developed, exhibiting high stereoselectivity. Encouragingly, during the last seven years tremendous advances have been made in asymmetric halogenation of alkenes. There are

two different established methodologies for forming chiral halofunctionalized molecules, intramolecular and intermolecular halogenation (Figure I-2a). In halocyclization (intramolecular version), after the alkenes are activated with various halogen donors, the tethered nucleophiles capture the putative chiral halonium ions and deliver enantioenriched-halogenated products. In the latter case, the nucleophiles are not attached to the alkenes and intermolecularly trap the halonium ions.

Figure I-2: (a) Intramolecular vs intermolecular halofunctionalization (b) Racemization of chiral halonium ion

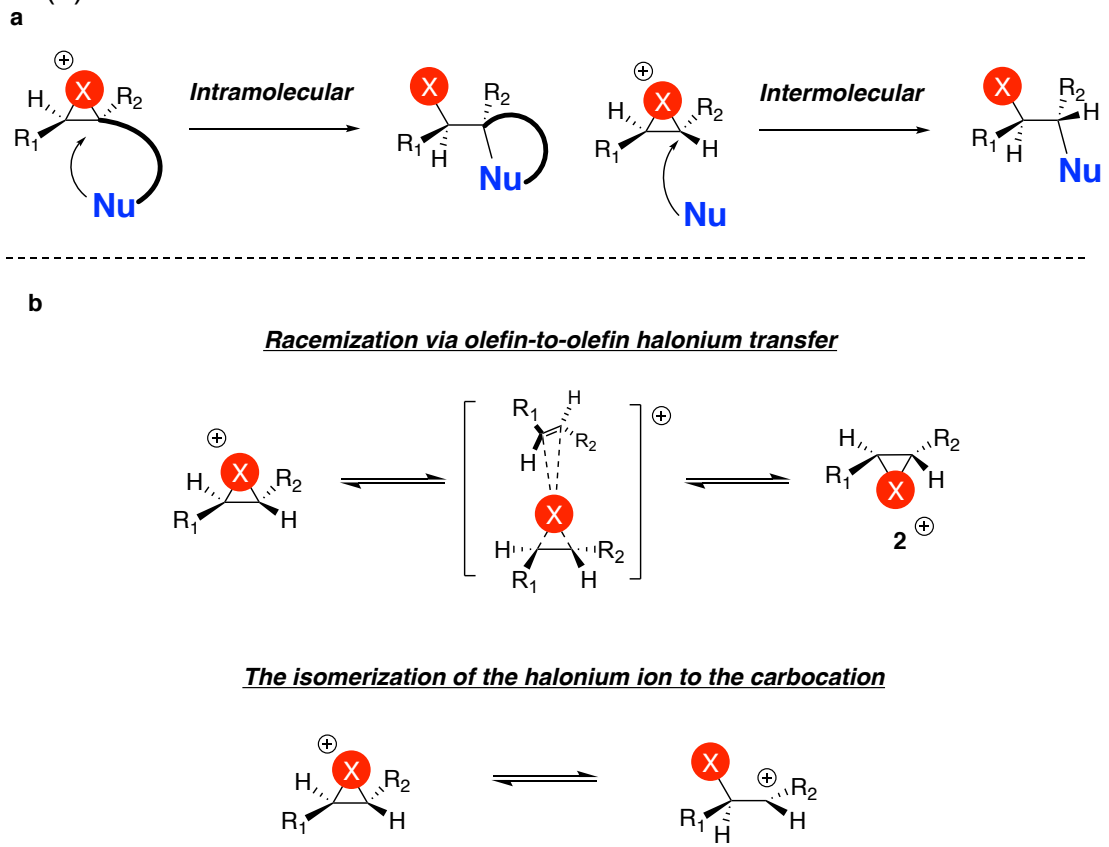

Although some excellent reports have shown a great deal of progress in the halocyclization area,[5, 10, 13, 50-51] enantioselective intermolecular halogenation

still remains challenging due to poor levels of enantioselectivity and limited substrate scope.[7] Two of the major issues in the development of intermolecular halofunctionalization are the rapid racemization of the chiral halonium ion by olefin-to-olefin transfer,[52-53] and the isomerization of cyclic halonium ions to acyclic β-halocarbenium ions (Figure I-2b).[32, 54] These two stereorandomizing events will be discussed in the next sections. Not surprisingly, the most early examples were reported on the intermolecular capture of halonium ions with tethered nucleophiles; the proximity rate enhancement of the cyclization step presumably competes with stereorandomizing (olefin to olefin transfer and isomerization) events. Enantioselectivities of more than 95:5 *er* are routinely obtained with a variety of halonium precursors and tethered nucleophiles in halocyclization reactions.

I-1-1 Racemization of chiral halonium ion by olefin to olefin halenium transfer

In 2010, Professor Denmark and his coworkers cleverly showed that the chiral bromonium ions undergo rapid stereochemical degradation by olefin-to-olefin halenium ion transfer.[52] Hexafluoroisopropyl alcohol (HFIP) was selected as a solvent to provide a strong ionizing medium, thus treatment of compound **I-1** with sodium acetate as a nucleophile forms product **I-2** in high yield. The *anti* diastereoselectivity of product **I-2** is evident for *in-situ* formation of bromonium ion (Figure I-3). It was shown that acetolysis of chiral compound **I-1** with two equivalents n-Bu_4NOAc in the presence of one equivalent of *trans*-4-octene **I-3**

and HFIP as solvent forms acetate product with 80% enantiospecificity (Figure I-3). Interestingly, increasing the amount of n-Bu_4NOAc to 5 equivalents led to enhancement in enantiospecificity to 94% *es* (Figure I-3). These results are consistent with the proximity rate increase of trapping bromonium ion in the presence of higher equivalents of nucleophiles, which can decrease the erosion of stereoselectivity caused by olefin-to-olefin halonium ion transfer. A similar experiment with chloronium ion shows

Figure I-3: Partial stereorandomization of bromonium ion by olefin to olefin halenium ion transfer

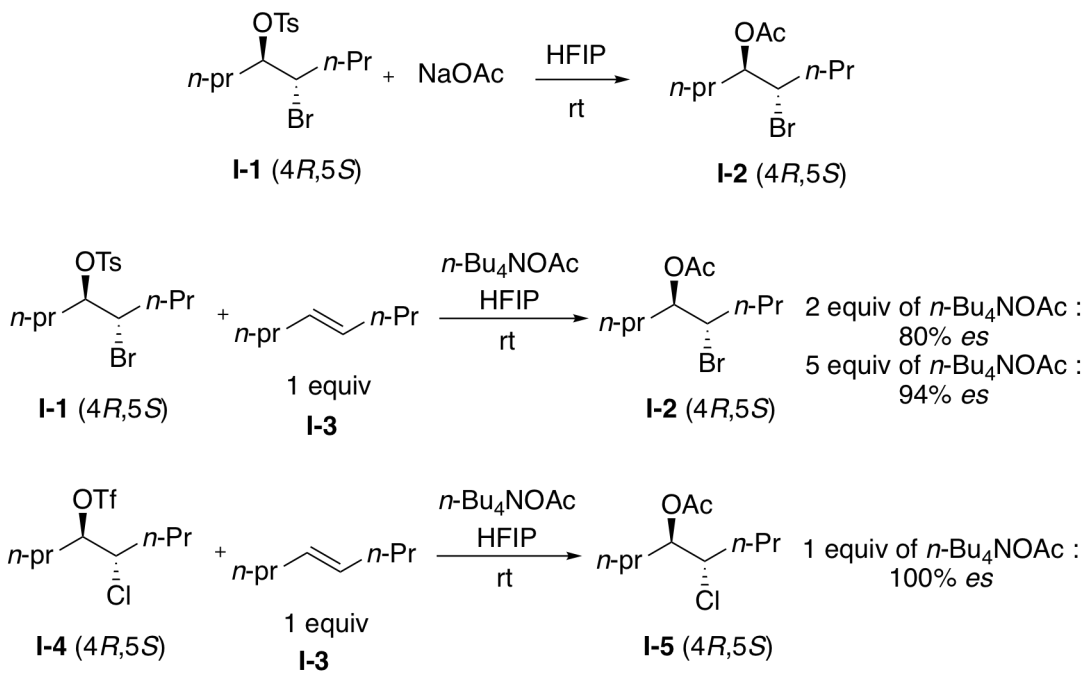

racemization would not happen in the case of *in situ* formation of chloronium ion in the presence of excess amount of alkenes. The acetolysis of compound **I-4** in

the presence of n-Bu_4NOAc and alkene **I-3** produces product **I-5** with 100% *es* (Figure I-3).

Based on Denmark's report, development of enantioselective cholorofunctionalization of alkenes is feasible. Unfortunately, the isomerization of active chloronium ion to β-chlorocarbenium ion can lead to erosion of stereoselectivity. Studies that have evidence for isomerization will be discussed in the next section.

Olah and his coworkers reported landmark studies for trapping various halonium ions and characterizing them under super acid conditions.[55] In one instance, the treatment of 1,2 dibromobutane **I-6 or I-7** with antimony-pentafluoride-sulfur dioxide at -78 °C forms bridged 1,2-dimethylethylenebromonium ion (**I-8** and **I-9** in a ratio of 3:7). Warming up the reaction in the NMR test tube to -40 °C produces different bromonium ions. It was suggested that the bridged bromonium ion opens up to produce a carbenium ion, subsequently followed by 1,2-hydrogen shift and a 1,2-methyl shift to form compound **I-11** (Figure I-4).

Figure I-4: Rapid equilibrium between cyclic and acyclic bromonium ion

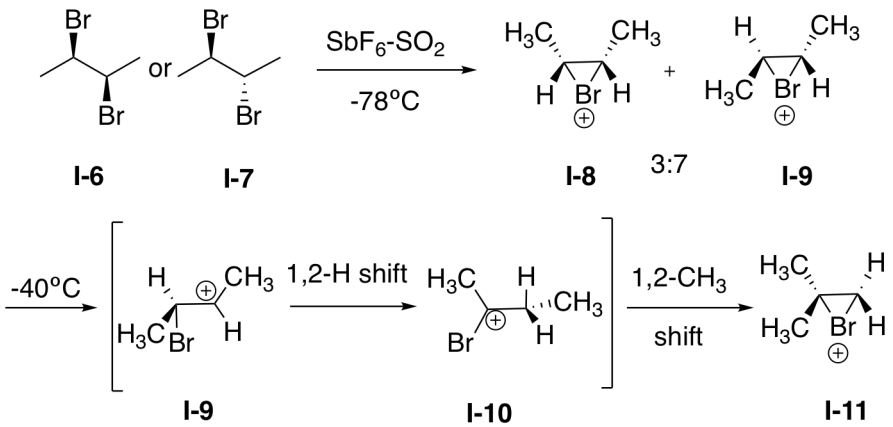

This transformation suggests that the bridged halonium ion and the acyclic β-bromenium ion are in rapid equilibrium. Interestingly, the *trans* and *cis* 1,2 dimethylethylenebromonium ions (**I-8** and **I-9)** were obtained in 7:3 ratio, respectively, regardless of super acid treatment with *syn* or *anti* dibromobutane (**I-6 or I-7)**. This latter observation is in line with the expectation that the bromonium ion should exchanges via a rapid equilibrium and isomerizes to β-bromenium ion (Figure I-4).

In recent reports, Ohta and coworkers investigated the structure of chloronium and bromonium ions by isotopic perturbation of equilibrium.[56] The ^{13}C NMR shift was consistent with a rapid equilibrium rather than a singular structure such as cyclic halonium ion (Figure I-5).

Figure I-5: The isotopic perturbation of degenerate equilibrium

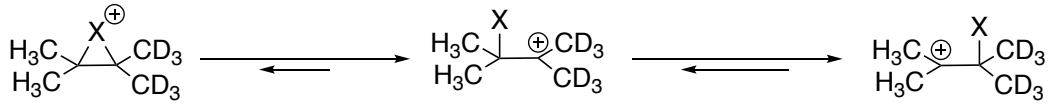

I-12-A (X = Cl)
I-12-B (X = Br)

I-13-A (X = Cl)
I-13-B (X = Br)

I-14-A (X = Cl)
I-14-B (X = Br)

Despite these mechanistic limits for developing intermolecular halofunctionalization reactions, a number of good reports have shown progress in this area. Intermolecular aminohalogenation,[4, 36-37] haloesterification,[34, 38] halohydrin formation,[39-41] and dihalogenation[42-43] have all been reported. Nonetheless, alcohols have not been shown to be viable nucleophiles in the reported transformation, despite the improvement seen in halocycloetherification

1-1-2 Literature precedence for enantioselective intermolecular halo-functionalization of alkenes

Tang and coworkers published the first enantioselective bromoesterification of unfunctionalized alkenes with moderate yield and enantioselectivity (up to 77% yield and 85:15 *er*).[38] The chiral binol backbone based Brønsted acid **I-18** and *n*-bromo succinamide **I-19** were employed as a chiral catalyst and halonium source, respectively. An ion pair of chiral catalyst and halogen source (NBS) has been suggested to explain the stereoselectivity of this reaction. Although, this chemistry is the first asymmetric intermolecular bromoesterification, it is limited to cycloalkenes like **I-16** as the substrate. Additionally, the reported enantioselectivities in most cases are lower than 75:25 *er*.

Figure I-6: First asymmetric intermolecular bromoesterification catalyzed by chiral Brønsted acid

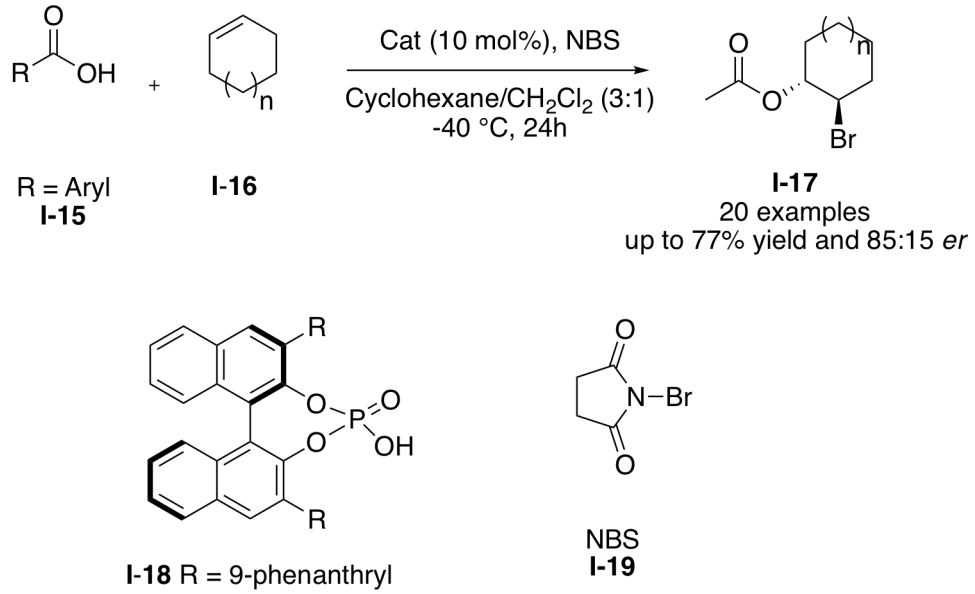

Toste and coworkers disclosed chiral oxyfluorination of enamides using chiral phosphoric acid **I-23** as a chiral catalyst.[39] Selectofluor **I-21** was employed as the fluorine donor, contains sufficient moisture to enable as hydroxyl nucleophile for *in situ* formation of hemiaminal (Figure I-7). Interestingly, both *cis* and *trans* enamide deliver oxy-fluorinated product in *syn* diastereoselectivity as a primary product with high enantioselectivity. As shown in this report that the yield and stereoselectivity for the *syn* products are promising, but it suffers in delivering *anti* oxyfluorinated products in high yield and enantioselectivity.

Figure I-7: Phosphoric acid catalyst for oxyfluorination of enamide

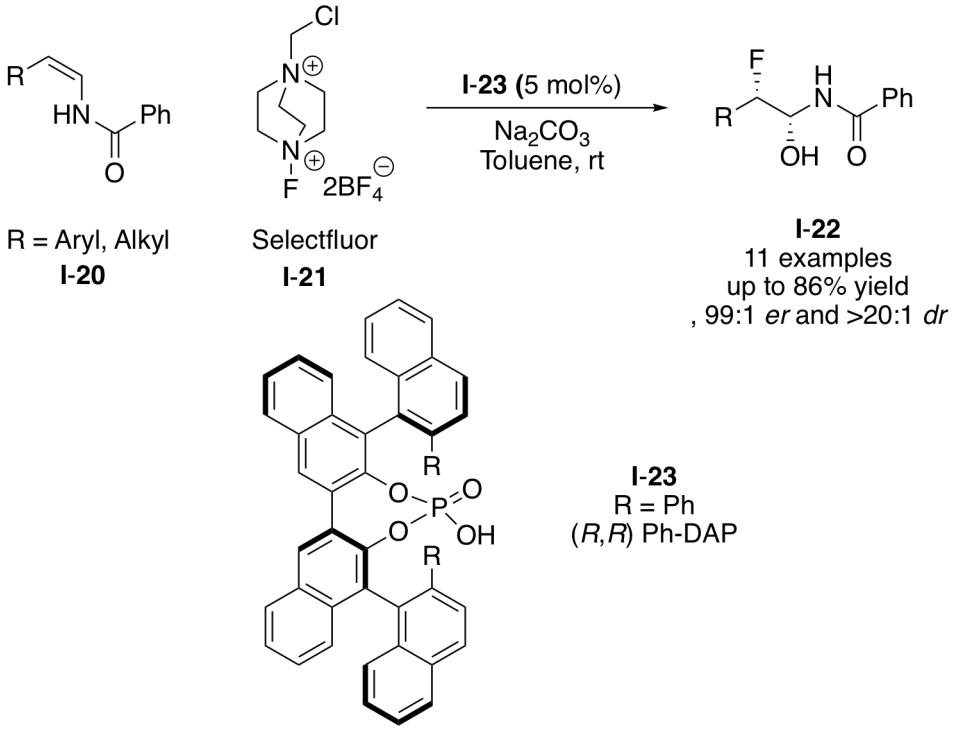

Ma and coworkers reported the catalytic asymmetric intermolecular bromohydroxylation of 2-aryl-substituted allylic alcohols **I-24** with quinine-derived alkaloid **I-29** as a chiral catalyst in 2013 (Figure I-7).[40] Allylic alcohol **I-24** reacts with boronic acid and forms boronate ester. The amino group of the chiral catalyst forms a complex with boron and increases the nucleophilicity of the remaining hydroxyl group on the boronate ester. In the mean time, NBS can get activated by the chiral catalyst and deliver the bromonium ion. This tight complexion of a substrate, chiral catalyst, and bromonium donor (Complex **I-26)** would produce cyclic boronate ester **I-27;** in the second step treating the crude mixture with H_2O_2 oxidized **I-27** and formed chiral bromohydrin **I-25** with high enantioselectivity (Figure I-8). The substrate scope shows these transformations

are successful for 1,1- disubstituted allylic alkenes. However, the authors have not reported any other kind of allylic alcohols as substrates in this study.

Figure I-8: Asymmetric bromohydroxylation of allyl alcohols by quinine-derived catalysts

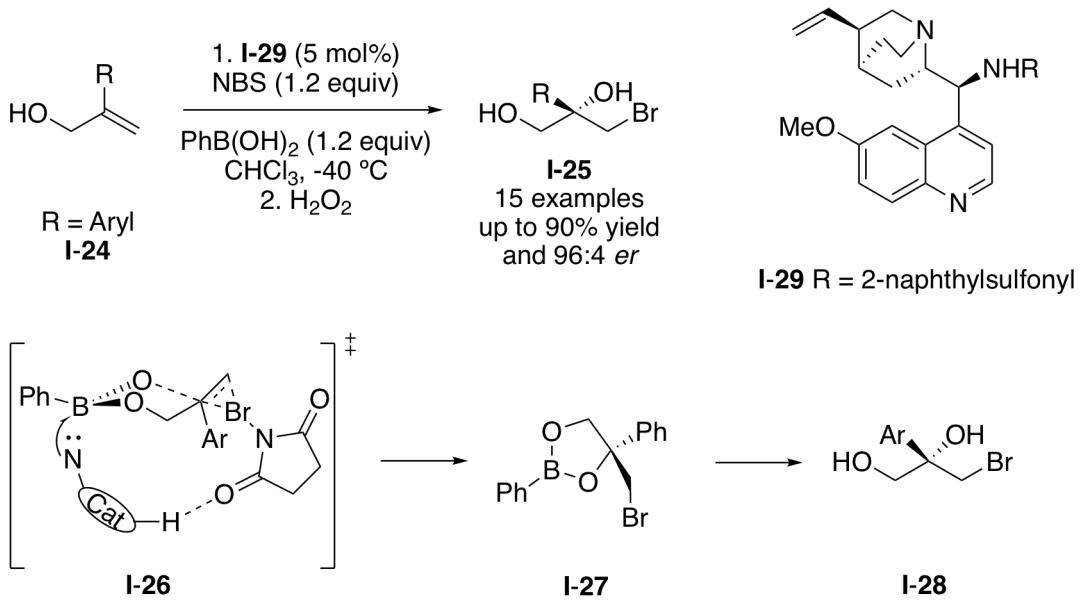

In 2013, Tang's lab developed the enantioselective bromoesterification of allylic sulfonamides in the presence of $(DHQD)_2PHAL$ as the chiral catalyst.[34] Using triflate as the protecting group for amines plays an important role to tune the acidity of nitrogen–hydrogen bond, putatively forming the tighter hydrogen bond with phthalazine of $(DHQD)_2PHAL$. On the other hand, employing CSA clearly improves the enantioselectivity. Based on these results the authors suggest that the nitrogen of the phthalazine ring in the $(DHQD)_2PHAL$ forms a hydrogen bond with the hydrogen atom of the allylic sulfonamide in the substrate. At the same time, one unit of the quinuclidine in the dimeric chinchona alkoxide catalyst activates the NBS, thus explaining the high enantioselectivity for this

transformation (see **I-31,** Figure I-9**)**. The *trans* aryl allylic sulfonamides **I-29** deliver final products **I-30** with moderate to high enantioselectivity (Figure I-9). Unfortunately, employing *cis* isomer of the aliphatic allyl sulfonamide results in bromo-esterified products with low yield and enantioselectivity. Also, nucleophiles other than benzoic acid were not evaluated in this report.

Figure I-9: Enantioselective intermolecular bromoesterification of allylic sulfonamides

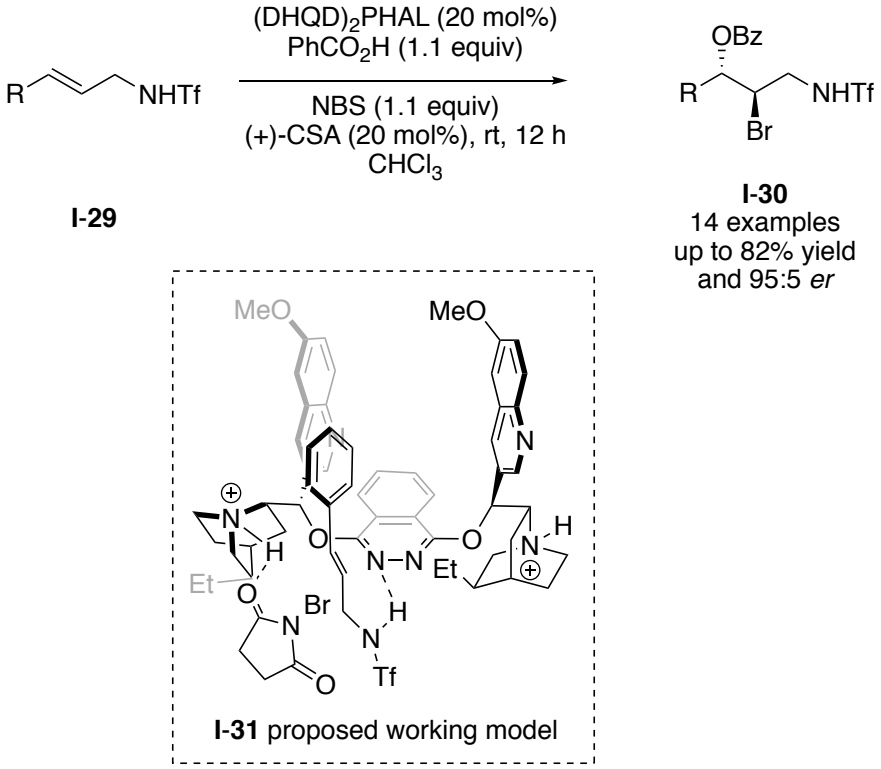

Snyder and coworkers employed chiral sulfur-derived halonium reagents to accomplish the enantioselective iodohydroxylation on unfunctionalized alkenes. Treatment of chiral dimethyl thiolane **I-32** with iodine monochloride in the presence of antimony pentachloride forms the chiral iodo sulfonium ion **I-33** in 76% yield (Figure I-10a).[41] Optimization studies showed that treating 1.2-

dihydronaphthalene **I-34** with chiral dimethyl iodo sulfonium ion **I-33,** and subsequently quenching the reaction with water forms iodohydrin product **I-35** in 67% yield and 81:19 *er* (Figure I-10b). Developing chiral sulfur-derived halonium reagents as both chiral promoter and halogen donor is fascinating. However, the low enantioselectivity and narrow substrate scope is a shortcoming of this study.

Figure I-10: Potential of chiral sulfonium reagents to effect asymmetric halonium additions to isolated alkenes

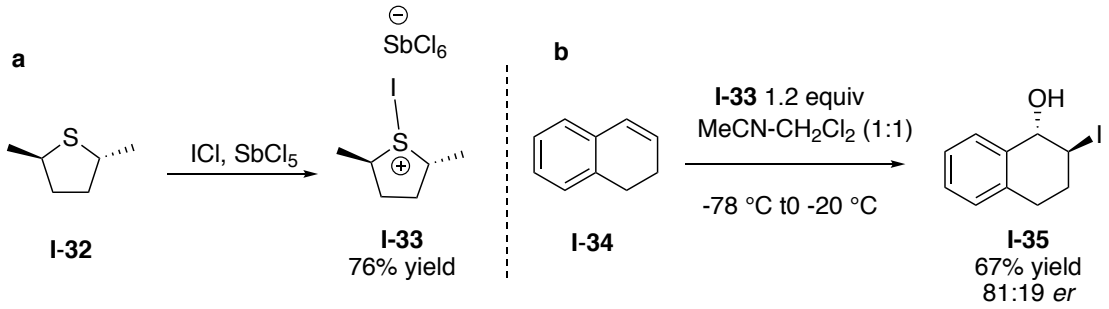

Despite this progress, challenges remain. First, alcohols are yet to be demonstrated as viable nucleophiles in intermolecular haloetherification despite the success seen in halo-*cycloetherification* reactions. Second, substrates with alkyl substituents on the alkene are known to afford poor to moderate levels of enantioselectivity at best. For example, the best enantioselectivity for aliphatic substrate in vicinal haloesterification was reported by Tang and his coworkers in 60:40 *er* (Figure I-11a).[34] Additionaly, Ma reported the enantioselective halohydrin synthesis with 84:16 *er* (Figure I-11b).[40] Third, substrate scope studies were limited to 'electronically biased' alkenes and hence possible regioselectivity issues have remained unaddressed. Finally, none of the catalytic

systems were demonstrated to be promiscuous enough to allow for the use of different halenium sources and nucleophiles with the same substrates.

Figure I-11: (a) Enantioselective bromoesterification of aliphatic alkenes (b) Chiral halohydrin synthesis of aliphatic olefins

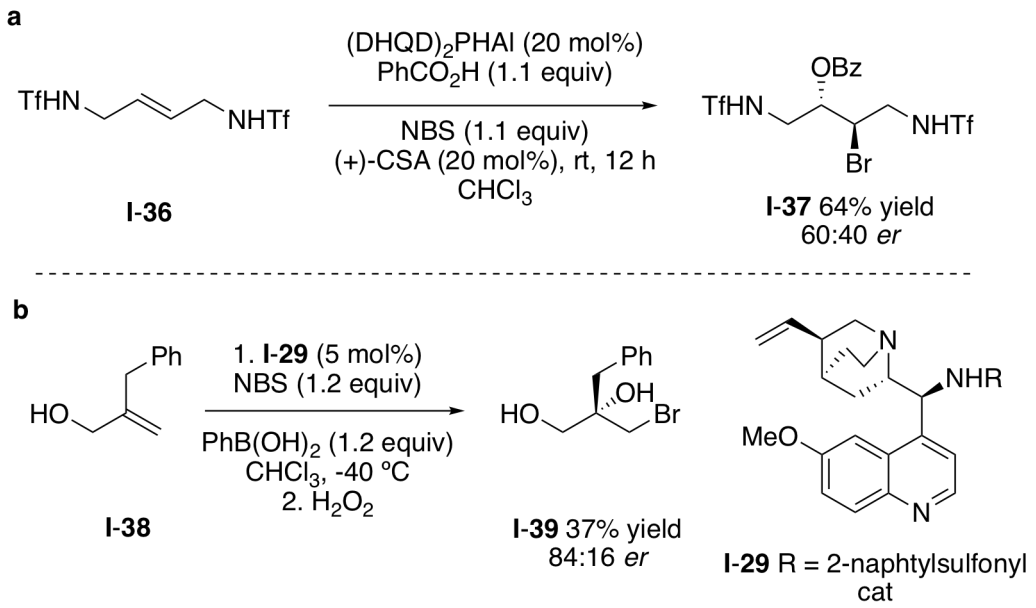

We sought to develop an enantioselective intermolecular haloetherification reaction with the intention of both demonstrating the feasibility of this unprecedented transformation and addressing some of the limitations detailed above. The rest of this Chapter will deal with efforts to discover and optimiz the first enantio-, diastereo- and regioselective intermolecular chloroetherification of a variety of alkenes including those with no dominant bias for regioselectivity (i.e. alkenes with alkyl substituents).

I-2 Results and discussion

I-2-1 Preliminary results

I-2-1-1 TFE-incorporated products was a hint for development of a methodology for intermolecular halofunctionalization

In 2010, our lab disclosed the first enantioselective chlorocyclization of alkenoic acid. Commercially available $(DHQD)_2PHAL$ as chiral organocatalyst and DCDPH (5,5-diphenyl-1,3-dichlorohydantoin) **I-42** as chloronium donor were employed in this transformation. DCDPH is not commercially available. Nonetheless, our lab has developed the one-step synthesis of DCDPH from the corresponding commercially available hydantoin. In this chemistry, various lactone molecules were synthesized, with up to 89% yield and 95:5 *er* (Figure I-12a).[28]

Later on, we demonstrated that the same catalytic system along with DCDMH **I-45** with little modification could yield products from the enantioselective chlorocyclization of unsaturated amide **I-43** as well. The facile, formation of dihydrooxazoles and dihydrooxazines can overcome many problems, most notably avoiding usage of the stoichiometric amount of chiral amino alcohols. In this work, we had indicated that the non-nucleophilic CF_3CH_2OH as the reaction medium was crucial for obtaining high yields and enantioselectivities for intramolecular cyclization of aryl substituted allyl amides. As reported, various dihydrooxazine rings **I-44** with different substituents were synthesized, with up to 90% yield and >99:1 *er* (Figure I-12b).[16]

Figure I-12: An organocatalytic asymmetric chlorolactonization reaction of alkenoic acid

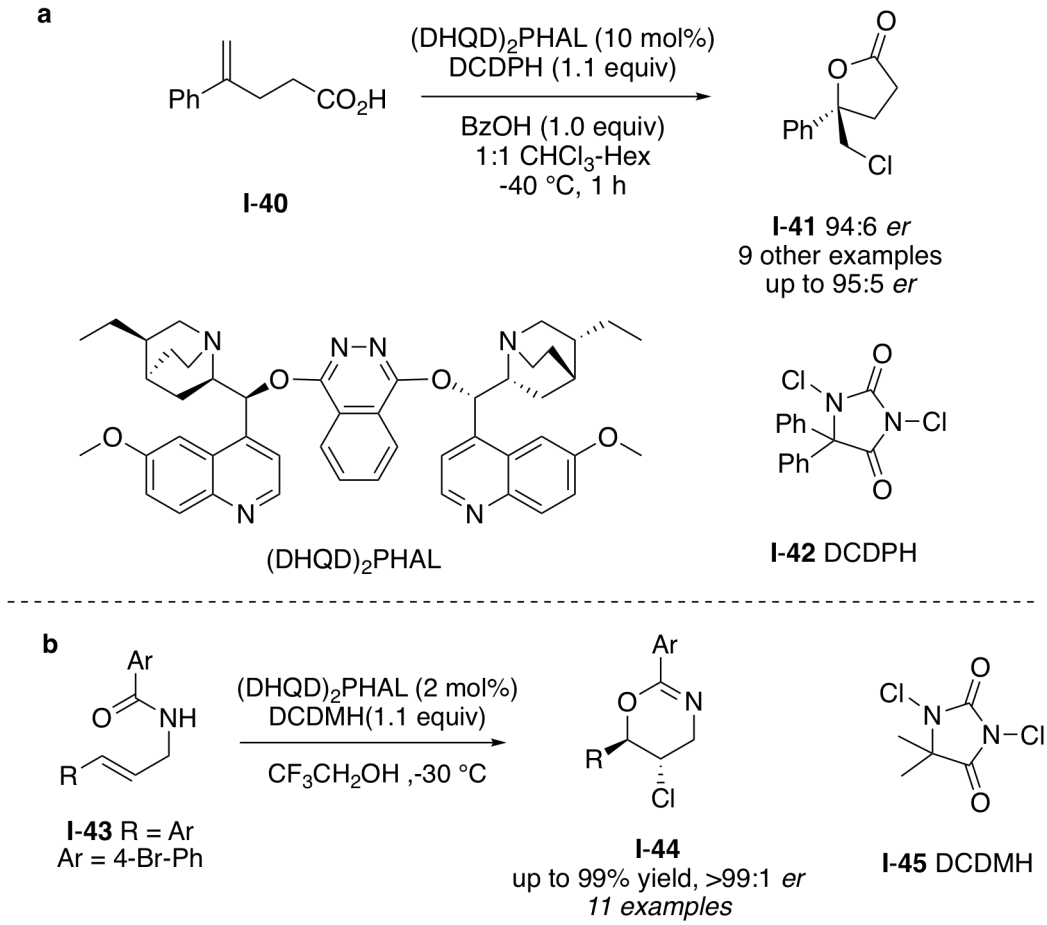

In our prior work, we had demonstrated a highly diastereo- and enantioselective chlorocyclization of unsaturated amides to furnish dihydrooxazine and oxazoline heterocycles.[16] The use of CF_3CH_2OH as the reaction medium was crucial for obtaining high enantioselectivities. In the attempted chlorocyclization of *E*-**46a**-Br under optimized reaction conditions, *a*-**47a**-*TFE*-Br was isolated in 82:18 *er* and 35% yield (>10:1 *dr* and >10:1 *rr*) along with the desired product *t*-**48a**-Br (40%, 99.5:0.5 *er*; see Figure I-13a). The reader is referred to the next paragraph for a detailed explanation of our naming

system for the starting materials and products in this chapter. The rate of intramolecular nucleophilic capture of the putative chloriranium ion by the pendant amide nucleophile for this substrate is presumably slow enough to allow for a competing intermolecular nucleophilic capture even by the weakly nucleophilic CF_3CH_2OH. In the event, a simple solvent-switch from CF_3CH_2OH to *n*-$PrNO_2$ as the reaction medium alleviated the problem of chemodivergence, affording exclusively *t*-**48a**-Br in good yield and excellent enantioselectivity (77%, >99.5:0.5 *er*, Figure I-13b).[16] While the enantioselectivity and the yield of *a*-**47a**-*TFE*-Br were not synthetically useful, we were intrigued by the excellent diastereo- and regioselectivity of this by-product arising from the intermolecular nucleophilic capture of a sterically and electronically unbiased chloronium/chlorocarbenium ion intermediate. As such, this result represented a good starting point for developing a practical and general intermolecular chlorofunctionalization reaction of alkenes.

We have opted to use a systematic naming system that enables the reader to identify the relevant components of the starting materials and products easily. Since all starting materials are substituted allyl amides, they are defined as *E* or *Z* (where appropriate), followed by a number (**46a**, **46b**, ...) that is unique to the substitution on the olefin. The naming is completed by defining the phenyl substituent of the amide moiety (NO_2, Br, ...), which is always on the *para* position. The naming of the intermolecular products precedes by '*a*' or '*s*' (*anti* or *syn*), followed by a number (**47a**, **47b**, ...) that corresponds to the substituent on

the parent olefin. The third component (in *italics*) is the identity of the nucleophile (*OMe*, *OH*, ...), followed by the substituent on the phenyl group of the amide. The 6-member ring intramolecular products are identified as either *cis* or *trans* ('*c*' or '*t*'), followed by the number that corresponds to the substituent on the parent olefin (**48a**, **48b**, ...), and then the identifier of the phenyl substituent for the amide. The 5-member ring products are named as above, with the exception of having '*a*' or '*s*' (*anti* or *syn*) that precedes the numbering (**49a**, **49b**, ...).

Figure I-13: (a) Discovery of an asymmetric intermolecular chloroetherification of allyl amides (b) Using Non-nucleophilic 1-nitropropane yielded cyclized products exclusively

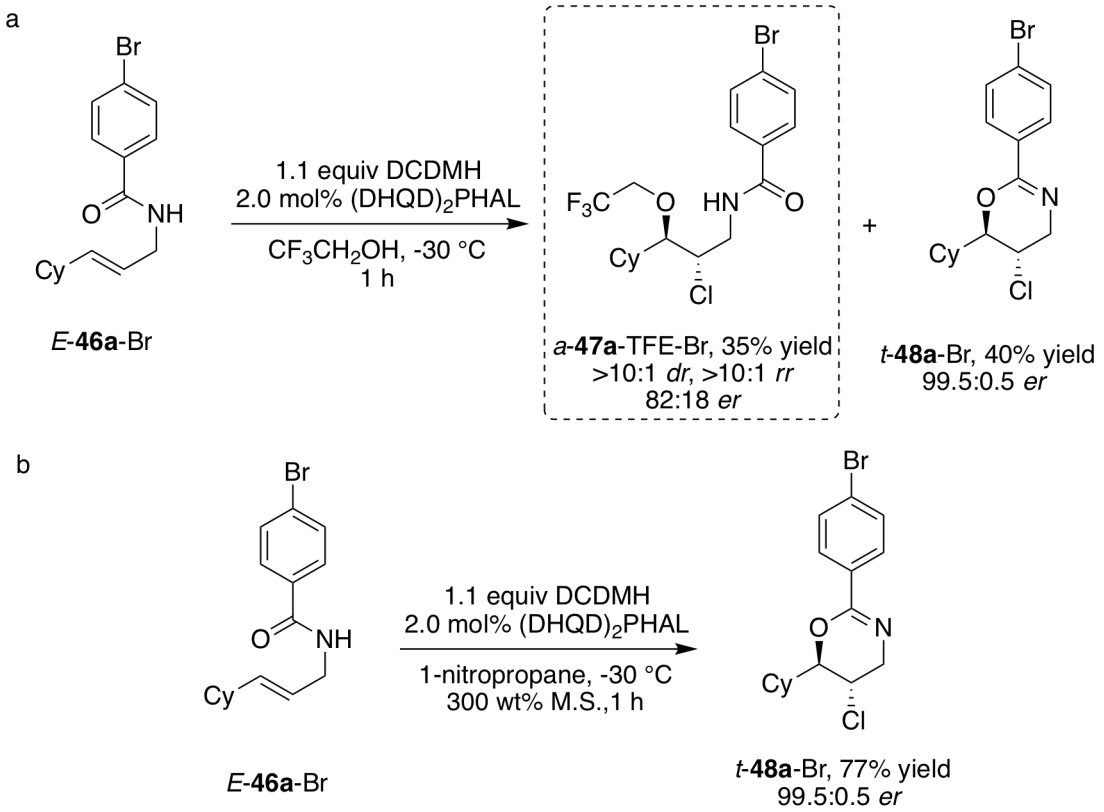

I-2-1-2 Additive studies to improve enantioselectivity of chlorocyclization of amides lead to the development of intermolecular halofunctionalization

In line with the above observation, additive studies were performed on the enantioselective allyl amide chlorocyclization reaction to understand the role of TFE as a crucial solvent for this transformation.[16] Under optimized conditions, employing TFE as solvent produces cyclic product *t*-**48b**-Br in >99:1 *er* (Table I-1, entry 1). Switching the solvent to acetonitrile erodes the enantioselectivity of the product to 90:10 *er* (Table I-1, entry 2).

Table I-1: Additive studies in chlorocyclization of allyl amides reaction

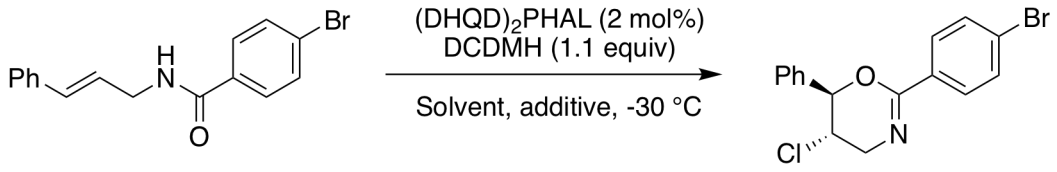

E-**46b**-Br

t-**48b**-Br

Entry	Solvent	Additive	*er*%[a]	Yield%[b]
1	TFE	None	>99:1	89
2	CH_3CN	None	90:10	84
3	CH_3CN	1 equiv TFE	96:4	87
4	CH_3CN	5 equiv TFE	98:2	89

[a] Determined by NMR; [b] Determined by chiral HPLC

Nonetheless, illuminating results were obtained when TFE was used as an additive for the reaction. As shown in Table I-1, the enantioselectivity of the chlorocyclized product *t*-**48b**-Br was enhanced drastically by employing 1 or 5 equivalents of TFE as an additive (Table I-1, entry 3, 4).

These results intrigued us to test ethanol as a solvent to see the effect of different alcohols in these reactions. However, employing ethanol as solvent forms the intermolecular chloroetherified product *a*-**47b**-*OEt*-Br in 58%yield and 79:21 *er* along with cyclized *t*-**48b**-Br product (42% yield and 91:9 *er*, see Figure I-14). As such, this result is in line with TFE-incorporated product that was discussed in the section above, and represented a good starting point for developing a practical and general intermolecular chlorofunctionalization reaction of alkenes.

Figure I-14: Intermolecular chloroetherification of allyl amides

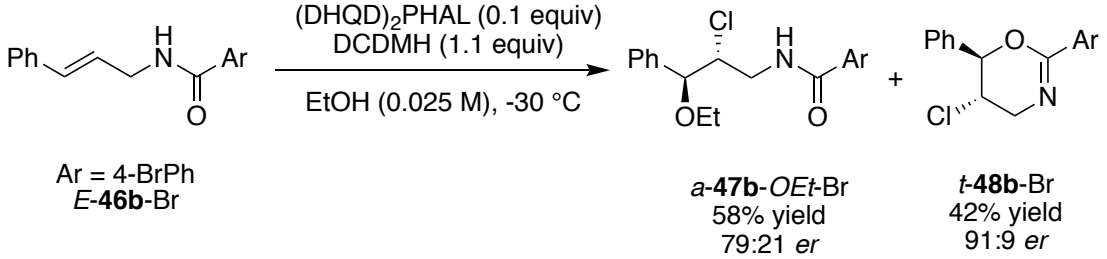

I-2-2 Optimization of reaction variables

I-2-2-1 Influence of the identity and stoichiometry of the chlorenium source on the stereoselectivity of the reaction.

We chose the intermolecular reaction of *E*-**46b**-Br with a chlorenium source and EtOH as the test bed to optimize the process. $(DHQD)_2$PHAL was employed as the chiral catalyst along with various chloronium sources. With the exception of *N*-chlorophthalimide (NCP, entry 3, Table I-2), all other chlorenium sources gave complete conversion to products. The identity of the chlorenium source does not influence the ratio of **47b:48b** in a significant manner (ratio was ~6:4). Using 1.1 equivalent of DCDMH and DCDPH showed similar *er* (80:20) for product *a*-**47b**-*OEt*-Br (Table I-2, entries 1 and 2). Increasing the DCDMH loading to 2 equiv improved the enantiomeric ratio (entry 5). Further increase in the DCDMH loading to 5 or 10 equivalents did not lead to any improvement in the enantioselectivity (Table 2, entries 5 and 6) for *a*-**47b**-*OEt*-Br**.**

Table I-2: Chlorenium source optimization

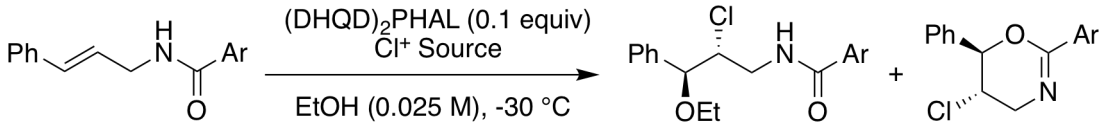

Ar = 4-BrPh
E-**46b**-Br

a-**47b**-*OEt*-Br

t-**48b**-Br

Entry	Source	equiv of Cl^+	Conv. %	Ratio[a] **47b**:**48b**	*er* (**47b**)[b,c]
1	DCDMH	1.1	100	6:4	80:20
2	DCDPH	1.1	100	6:4	80:20
3	NCP	1.1	0	nd	0
4	NCSach	1.1	100	6:4	78:22
5	**DCDMH**	**2**	**100**	**6:4**	**81:19**
6	DCDMH	5	100	6:4	78:22
7	DCDMH	10	100	6:4	78:22

[*a*] Determined by NMR; [*b*] Determined by chiral HPLC: [c] for compound *a*-2**b**-*OEt*-Br

I-2-2-2 Influence of reaction solvent on enantioselectivity of chloro etherified products

Using ethanol as a solvent gave products *a*-**47b**-*OEt*-Br and *t*-**48b**-Br in the ratio of 6:4 and enantiomeric ratio of 81:19 for *a*-**47b**-*OEt*-Br (entry 1, Table I-3). Adding 10 equivalents of TFE decreased the enantioselectivity (entry 2). A 1:1 MeCN-EtOH cosolvent mixture gave slightly improved enantioselectivity (entry 3). Changing the ratio of MeCN to EtOH to 7:3 produced both products in equimolar amounts, but with higher *er* (entry 4, Table I-3). Finally, decreasing the

temperature to -30 °C gave higher enantioselectivity of 84:16 *er* (entry 5, Table I-3).

Table I-3: Influence of co-solvent additives on the chemo- and stereoselectivity of the reaction

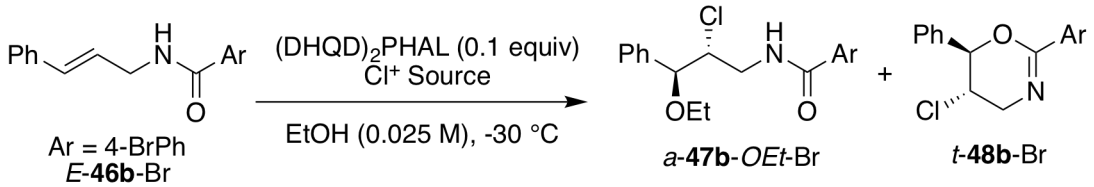

Entry	Temp	Solvent	Ratio of **47b:48b**[a]	*er* (**47b**) [b,c]
1	-30	EtOH	6:4	81:19
2	-30	EtOH with 10 equiv TFE	6:4	77:23
3	-30	MeCN:EtOH(1:1)	6:4	81:19
4	rt	MeCN:EtOH (7:3)	1:1	82:18
5	-30	MeCN:EtOH (7:3)	1:1	84:16

[*a*] Determined by NMR; [*b*] Determined by chiral HPLC: [c] for compound *a*-**47b**-*OEt*-Br

I-2-2-3 Effect of substituents on the amide moiety in the chloro etherification reaction selectivity

Other optimization studies were focused on varying the expandable amide moiety. In this study we used MeOH as nucleophile, and the diastreomeric ratio for acyclic haloetherified product was easily obtained with H-NMR.

At ambient temperature both the desired chloroether product *a*-**47b**-*OMe*-Br and the cyclized product *t*-**48b**-Br were observed (93% combined yield) in a 1.8:1 ratio. In line with our prior studies, the cyclized product *t*-**48b**-Br had excellent enantioselectivity (96:4 *er*), whereas *a*-**47b**-*OMe*-Br exhibited lower

67:33 *er*. Lower temperatures and lower concentrations led to slightly improved enantioselectivity for *a*-**47b**-*OMe*-Br while not significantly improving the *dr* or the **47b:48b** ratio (see entries 2 and 3 in Table I-4). Further experimentation revealed that employing MeOH as a co-solvent in MeCN led to a significant improvement in the enantioselectivity of *a*-**47b**-*OMe*-Br (Table I-4, entry 4).

Other studies focused on varying the expendable amide moiety. Changing the 4-bromobenzamide motifs to 4-methoxybenzamide gave practically identical results (entry 5 in Table I-4). Nonetheless, employing the electron deficient 4-NO_2-benzamide gave a significant improvement in the enantioselectivity of *a*-**47b**-*OMe*-NO_2 (92:8 *er*, entry 6, Table I-4). As evident from these preliminary results, although useful levels of enantioinduction were seen for the intermolecular chloroetherification of *E*-**46b**-NO_2, the *dr* (3.4:1) as well the ratio of **47b**:**48b** (~1:1) were not ideal.

Table I-4: Orienting studies for enantioselective intermolecular chloroetherification of ***E*-46b-(Br/OMe/NO$_2$)**

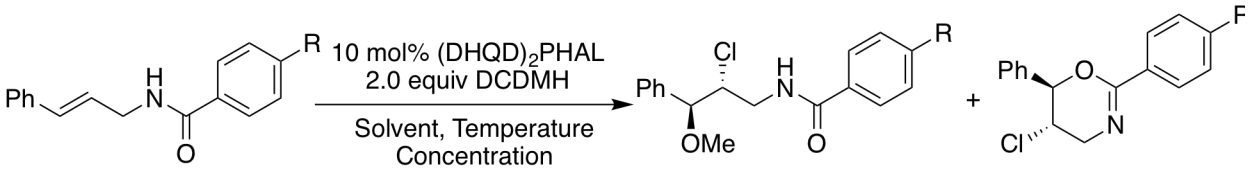

E-**46b**-Br: R = Br
E-**46b**-OMe: R = OMe
E-**46b**-NO$_2$: R = NO$_2$

a-**47b**-*OMe*-Br: R = Br
a-**47b**-*OMe*-OMe: R = OMe
a-**47b**-*OMe*-NO$_2$: R = NO$_2$

t-**48b**-Br: R = Br
t-**48b**-OMe: R = OMe
t-**48b**-NO$_2$: R = NO$_2$

Entry	Substrate	Solvent	%Yield[a]	**47b**:**48b**[b]	*dr* (*a*-**47b**:*s*-**47b**)[b]	*er*(**47b**)[g]	*er*(**48b**)[g]
1[c,e]	*E*-**46b**-Br	MeOH	93	1.8:1	6.8:1	67:33	96:4
2[d,e]	*E*-**46b**-Br	MeOH	94	1.8:1	6.8:1	73:27	98:2
3[f]	*E*-**46b**-Br	MeOH	76	1.8:1	5.7:1	71:29	98:2
4[h,f]	*E*-**46b**-Br	MeOH:MeCN	76	1.3:1	5.8:1	85:15	99:1
5[h,f]	*E*-**46b**-OMe	MeOH:MeCN	86	1.3:1	5.0:1	83:17	97:3
6[h,f]	*E*-**46b**-NO$_2$	MeOH:MeCN	85	1.1:1	3.4:1	92:8	96:4

[a] Combined yield of *a*-**47b**, *s*-**47b** and **48b** as determined by NMR analysis with MTBE as added external standard; [b] Determined by NMR; [c] The reaction occurs at room temperature [d] the reaction occurs at -30 °C [e] The concentration of reaction was 0.03 M [f] the concentration of reaction was 0.01 M [g] Determined by chiral HPLC; [h] MeOH:MeCN ratio was 3:7.

I-2-2-4 Reaction optimization for aliphatic substrates

Gratifyingly, replacing the Ph substituent on the alkene in substrate *E*-**46b**-Br with the aliphatic *n*-C_3H_7 group gave exclusively the desired intermolecular product a-**47c**-OMe-Br with near complete diastereo- and regioselectivity (>99:1 *dr* and *rr,* see entry 1 in Table I-5) on employing the best conditions from the pilot studies. More importantly, *a*-**47c**-*OMe*-Br was isolated in 92% yield and 81:19 *er*,

and the formation of the cyclized product was suppressed to a mere 5%. Under the premise that decreasing the nucleophilicity of the amide might completely suppress the formation of the cyclized product, the 4-bromobenzamide was substituted with the 4-NO_2-benzamide. Indeed, this change afforded exclusively *a*-**47c**-*OMe*-NO_2 (entry 2, Table I-5) in 86% yield, 87:13 *er*, >20:1 *rr*, and >99:1 *dr*. *cis*-Allylic amides were even better substrates for this chemistry as compared to the *trans*-allylic amide counterparts. Substrate *Z*-**46c**-NO_2 gave the corresponding product *s*-**47c**-*OMe*-NO_2 in 87% yield and 99:1 *er* (entry 3, Table I-5). Reactions that were run at ambient temperatures or with lower catalyst loadings showed no loss in the diastereo- and regioselectivity and only a small decrease in the enantioselectivity (97:3 *er*; see entries 4 and 5 in Table I-5). Nonetheless, the yields were lower (75–79%) owing to the formation of side products arising from the competing addition of MeCN across the alkene. While the lack of a cation-stabilizing group can explain the exquisite diastereoselectivity with aliphatic substrates, the origin of the *regioselectivity* with such an unbiased system is not easily explained.

Table I-5: Reaction optimization for aliphatic substrates.

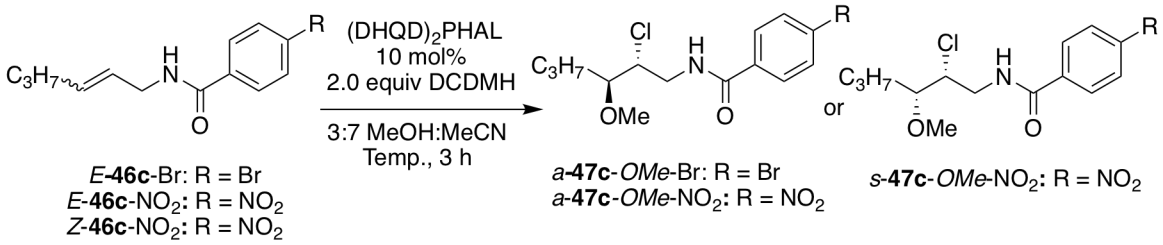

Entry[a]	Substrate	Temp °C	Product	Yield%[b]	*er*[d]
1	*E*-**46c**-Br	-30	*a*-**47c**-OMe-Br	92[c]	81:19
2	*E*-**46c**-NO_2	-30	*a*-**47c**-OMe-NO_2	86	87:13
3	*Z*-**46c**-NO_2	-30	*s*-**47c**-OMe-NO_2	87	99.5:0.5
4	*Z*-**46c**-NO_2	24	*s*-**47c**-OMe-NO_2	75	97:3
5[e]	*Z*-**46c**-NO_2	-30	*s*-**47c**-OMe-NO_2	79	97:3

[a] The *rr* was >20:1 and *dr* was >99:1 in all instances; [b] Determined by NMR using MTBE as added external standard; [c] 5% of cyclized product was also seen by NMR; [d] Determined by chiral HPLC. [e] 2 mol% catalyst was used.

I-2-3 Substrate scope for the intermolecular chloroetherification reaction

I-2-3-1 Substrate with MeOH as the nucleophile

In an effort to map out the generality of this transformation, a number of *trans*-disubstituted allyl amides were initially exposed to the optimized reaction conditions. Compounds *E*-**46b**-NO_2 and *E*-**46d**-NO_2 (Figure I-15) with aryl substituents on the alkene gave moderate isolated yields (due to competing chlorocyclization) and fair diastereoselectivity for the corresponding products *a*-**47b**-*OMe*-NO_2 and *a*-**47d**-*OMe*-NO_2 (56% and 64% yields, respectively; ~3.4:1 *dr*, mass balance in both cases was the cyclized product *t*-**48b**-NO_2 and *t*-**48d**-NO_2, respectively, Figure I-15). Nonetheless, the chloroether products were

formed with good enantioselectivity. *Trans*-substrates with alkyl substituents on the olefin (*a*-**47c**/**47a**/**47e**-*OMe*-NO_2) predictably gave products with exquisite levels of diastereo- and regioselectivity. Additionally, high yield and *er* was observed for *a*-**47c**-*OMe*-NO_2 (R_1=*n*-C_3H_7). The *er* dropped significantly on introduction of the bulky cyclohexyl group (see *a*-**47a**-*OMe*-NO_2, 75:25 *er*). The benzyloxy substituted compound gave only moderate yields and *rr* (62%, 7:1 *rr*), although the enantioselectivity was good (Figure I-15, see *a*-**47e**-*OMe*-NO_2, 89:11 *er*).

Figure I-15: Substrate Scope for intermolecular chloroetherification for *trans* allyl amides substrate

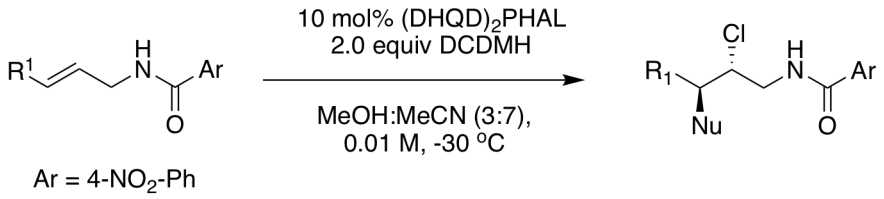

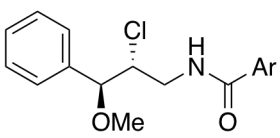

a-**47b**-*OMe*-NO_2[d]
56%, (49%) yield[a,c]
3.4:1 *dr*, >20:1 *rr*
92:8 *er*[b]

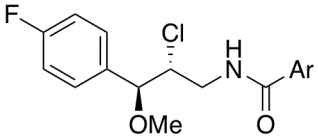

a-**47d**-*OMe*-NO_2[d]
64%[a], (58%) yield[a,c]
3.4:1 *dr*, >20:1 *rr*
90:10 *er*[b]

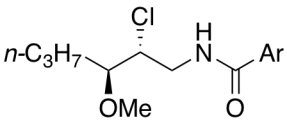

a-**47c**-*OMe*-NO_2
86%, (79%) yield[a]
>99:1 *dr*, >20:1 *rr*
87:13 *er*[b]

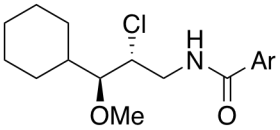

a-**47a**-*OMe*-NO_2
79% yield[a]
>99:1 *dr*, >20:1 *rr*
75:25 *er*[b]

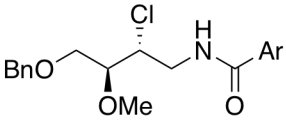

a-**47e**-*OMe*-NO_2
62%, (57%) yield[a]
>99:1 *dr*, 7:1 *rr*
89:11 *er*[b]

[a]Yield determined by NMR with MTBE as standard. Numbers in parantheses reflect yields of isolated product on 0.1 mmol scale; [b]Enantioselectivity determined by chiral -phase HPLC; [c]Combined yield of diastereomers, 15 equivalents of Li_2CO_3 was used as additive; [d]Mass balance was the cyclized product

Aryl substituted *Z*-alkenes were exceptional substrates, leading to the intermolecular product exclusively, in good yields (73% to 80%, Figure I-16), excellent regioselectivity (>99:1 *rr)* and high enantioselectivity (≥98:2 *er,* see Figure I-16, *s*-**47b**/**47f**/**47g**-*OMe*-NO_2). Intriguingly, the diastereoselectivity progressively decreases going from a Ph substituent (3.3:1 *dr* for *s*-**47b**-*OMe*-NO_2) to the anisyl substituent (1:1 *dr* for *s*-**47g**-*OMe*-NO_2, Figure I-16) with the *p*-

toluyl substituted compound *Z*-**46f**-NO_2 giving an intermediate 1.3:1 *dr*. These results likely suggest an increased carbocation character at the benzylic position in the transition state with increasing electron density of the aryl substituent. Noteworthy, the minor diastereomer for each reaction still retains high levels of enantioselectivity (see values in parentheses, Figure 16, for products *s*-**47b**/**47f**/**47g**-*OMe*-NO_2). *Z*-alkyl substituted olefins afforded the desired products in near complete regio-, diastereo-, and enantioselectivity (see Figure 16, products *s*-**47h**/**47c**/**47i**/**47e**/**47j**-*OMe*-NO_2). Trisubstituted alkene **46k**-NO_2 also gives the desired product in moderate yield and excellent enantioselectivity (59%, 99:1 *er*).

Figure I-16: Substrate scope of intermolecular chloroetherification for *cis* allyl amide substrates

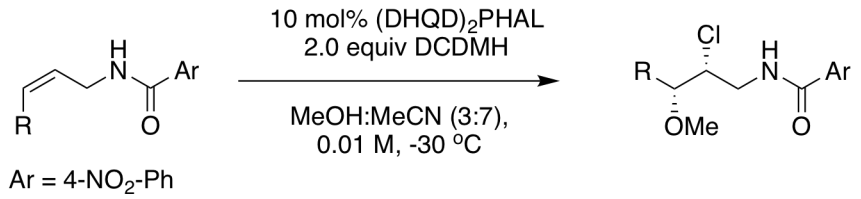

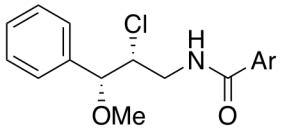

s-**47b**-*OMe*-NO_2
93%, (82%) yield[a,c]
3.3:1 *dr*, 99:1 *rr*
99.5:0.5 *er*[b]
(90:10% *er*)[b,d]

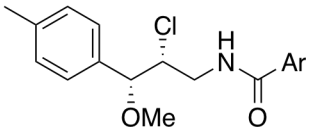

s-**47f**-*OMe*-NO_2
87% yield[a,c]
1.3:1 *dr*, 99:1 *rr*
98:2 *er*[b]
(97:3 *er*)[b,d]

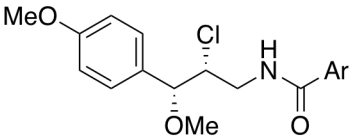

s-**47g**-*OMe*-NO_2
80% yield[a,c]
1:1 *dr*, 99:1 *rr*
99.:1 *er*[b]
(92.:8 *er*)[b,d]

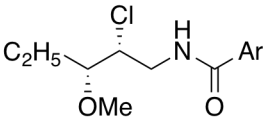

s-**47h**-*OMe*-NO_2
83%, (77%) yield[a]
>99:1 *dr*, >20:1 *rr*
98:2 *er*[b]

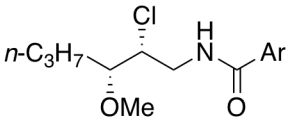

s-**47c**-*OMe*-NO_2
87%, (79%)[e] yield[a]
>99:1 *dr*, >20:1 *rr*
99.5:0.5 *er*[b]
(99.5:0.5 *er*)[e]

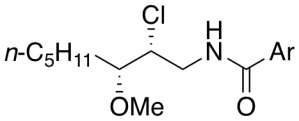

s-**47i**-*OMe*-NO_2
83%, (74%) yield[a]
>99:1 *dr*, >20:1 *rr*
99.5:0.5 *er*[b]

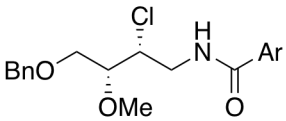

s-**47e**-*OMe*-NO_2
60%, (53%) yield[a]
>99:1 *dr*, 7:1 *rr*
99.5:0.5 *er*[b]

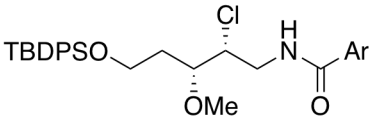

s-**47j**-*OMe*-NO_2
79% yield[a]
>99:1 *dr*, >20:1 *rr*
99.5:0.5 *er*[b]

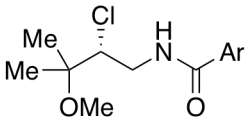

47k-*OMe*-NO_2
59%. (53%) yield[a],
>20:1 *rr*, 99:1 *er*[b]

---

[a]Yield determined by NMR with MTBE as standard. Numbers in parantheses reflect yields of isolated product on 0.1 mmol scale; [b]Enantioselectivity determined by chiral -phase HPLC; [c]Combined yield of diastereomers, 15 equivalents of Li_2CO_3 was used as additive; [d]The er values are for the minor diastereomer; [e]The result in paranthesis is from a 1 g reaction scale

I-1-3-2 Nucleophile scope for the intermolecular chloroetherification reaction

Finally, we sought to explore the scope of this reaction with regards to the nucleophilic and electrophilic components (see Figure I-17). We were delighted to discover that a variety of alcohols and even carboxylic acids may be employed as viable nucleophiles in this chemistry with little or no modification of the optimized reaction conditions. Replacing MeOH with other alcohols such as ethanol, allyl alcohol, and propargyl alcohol as the co-solvents cleanly affords the desired products in >20:1 *dr* and ≥98:2 *er* (see *s*-**47c**-*OEt*-NO_2, *s*-**47c**-*OAllyl*-NO_2 and *s*-**47c**-*OPropargyl*-NO_2 in Figure I-17). These results demonstrate the feasibility of introducing diverse functional handles into the products using this chemistry, in addition to the highly stereoselective C-Cl and C-O bond installations during the course of the reaction.

Acetic acid can be employed also as the nucleophilic co-solvent to furnish the corresponding chloroesters with excellent enantioselectivity with *Z-, E-,* as well as tri-substituted alkene substrates (≥93:7 *er,* see *s*-**47c**-*OAc*-NO_2**,** *a*-**47c**-*OAc*-NO_2 and **47k**-*OAc*-NO_2 in Figure I-17). Employing water as the nucleophile leads directly to the corresponding chlorohydrins in excellent yields and *er*s (see *s*-**47c**-*OH*-NO_2 and *s*-**47h**-*OH*-NO_2 in Figure I-17).

Figure I-17: Nucleophile scope for the intermolecular chloroetherification reaction[a]

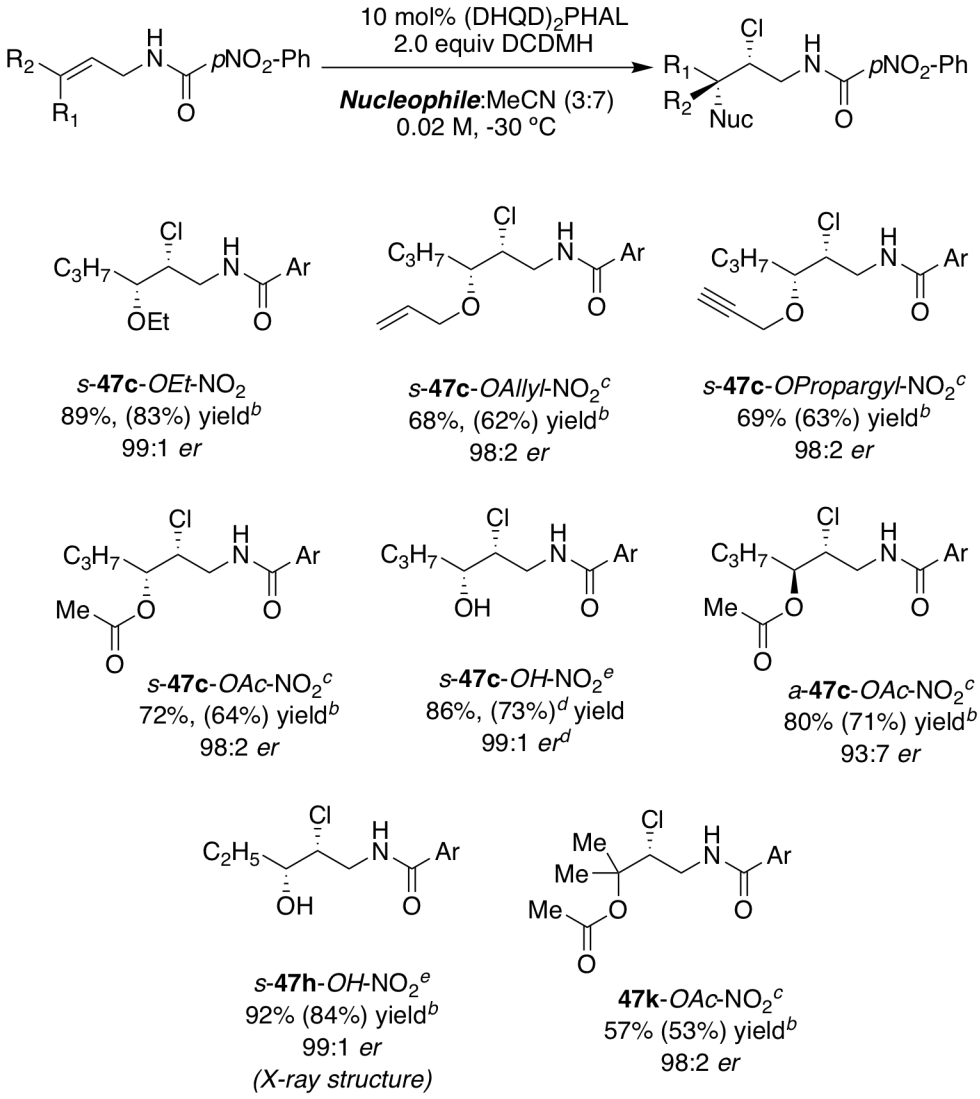

[a] The *rr* was >20:1 and *dr* was >99:1 in all instances; [b]Yield determined by NMR. Numbers in parantheses reflect yields of isolated products on a 0.1 mmol scale. Enantioselectivity determined by chiral HPLC; [c]Reaction was run under nitrogen in the presence of molecular sieves; [d]The results reflect a 1 g scale reaction; [e]The ratio of MeCN:H_2O was 9:1, reaction temperature was -10 °C

I-2-3-3 Substrate scope for asymmetric bromination of allyl amide substrates

Finally, employing NBS in lieu of DCDMH leads to the corresponding bromoether and bromohydrin products in good yields and *ers.* The substrate in optimized condition along with NBS forms *s*-**47c'**-*OMe*-NO_2 in 92% yield and 99:1 *er* (Figure I-18). Combination of water as nucleophile and NBS as bromonium source is compatible with this chemistry and forms *s*-**47c'**-*OH*-NO_2, *a*-**47c'**-*OH*-NO_2 in 99.5:0.5 *er* and 85:15 *er*, respectively. Tri-substituted alkene **46k**-NO_2 forms corresponding brominated product in 62% yield and 99.5:0.5 *er* (see **46k**-*OMe*-NO_2, Figure I-18, The mass balance for this reaction was cyclized product).

Figure I-18: Substrate scope for asymmetric bromination of allyl amide substrates[a]

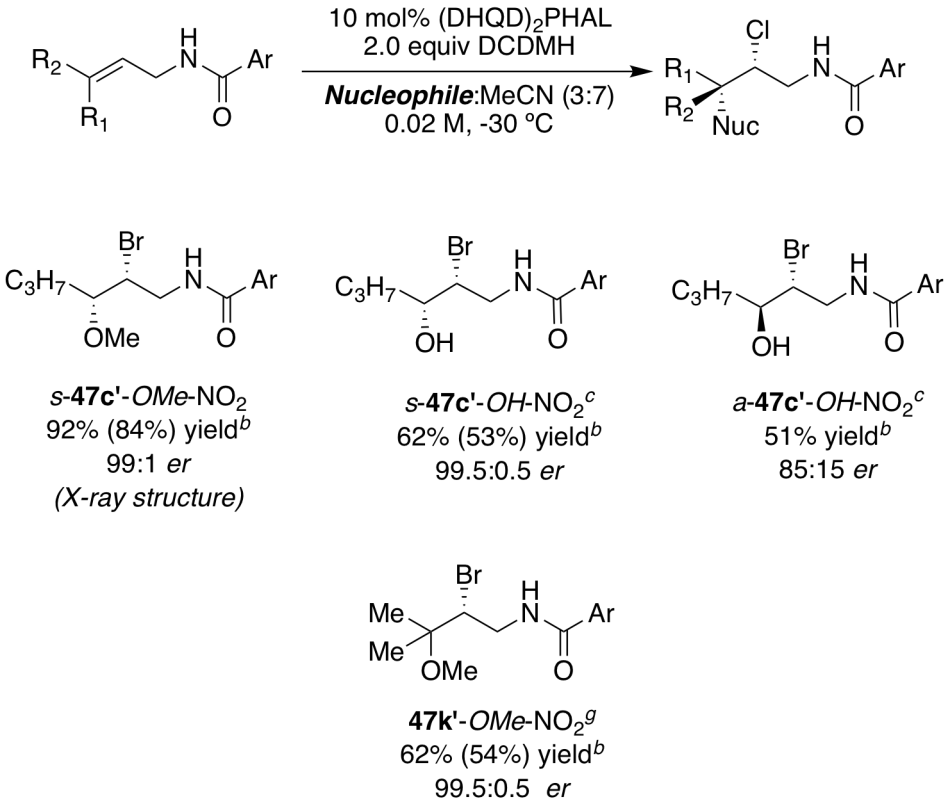

[a]The *rr* was >20:1 and *dr* was >99:1 in all instances; [b]Yield determined by NMR. Numbers in parantheses reflect yields of isolated peoducts on a 0.1 mmol scale. Enantioselectivity determined by chiral HPLC; [c]The ratio of MeCN:H_2O was 9:1, reaction temperature was -10 °C.

I-2-3-4 Substrate scope for the intermolecular chloroesterification reaction by employing quasi-enantiomeric catalyst

The *quasi*-enantiomeric $(DHQ)_2PHAL$, was also evaluated with different substrates, yielding enantiomeric products in comparable yields and selectivities (Figure I-19). The exception was the result with the least successful category of substrates (*trans*-substituted aryls) which forms *ent*-a-**47b**-*OMe*-NO_2 in 75:25 *er*,

and does not mirror the $(DHQD)_2PHAL$ catalyzed reaction well, yielding product with lower than expected enantioselectivity. However, the *cis* allyl amide substrates (*Z*-**46f**-NO_2 and *Z*-**46c**-NO_2) gave practically identical results favoring the opposite enantiomeric antipode of the products (Figure I-19, *ent*-s-**47f**-*OMe*-NO_2 and *ent*-s-**47c**-*OMe*-NO_2). Tri substituted alkene **46k**-NO_2 produced product end exactly mirrored the result with $(DHQD)_2PHAL$ catalyzed reaction well (Figure I-19).

Figure I-19: Substrate scope for the intermolecular chloroesterification reaction by employing quasi-enantiomeric catalyst

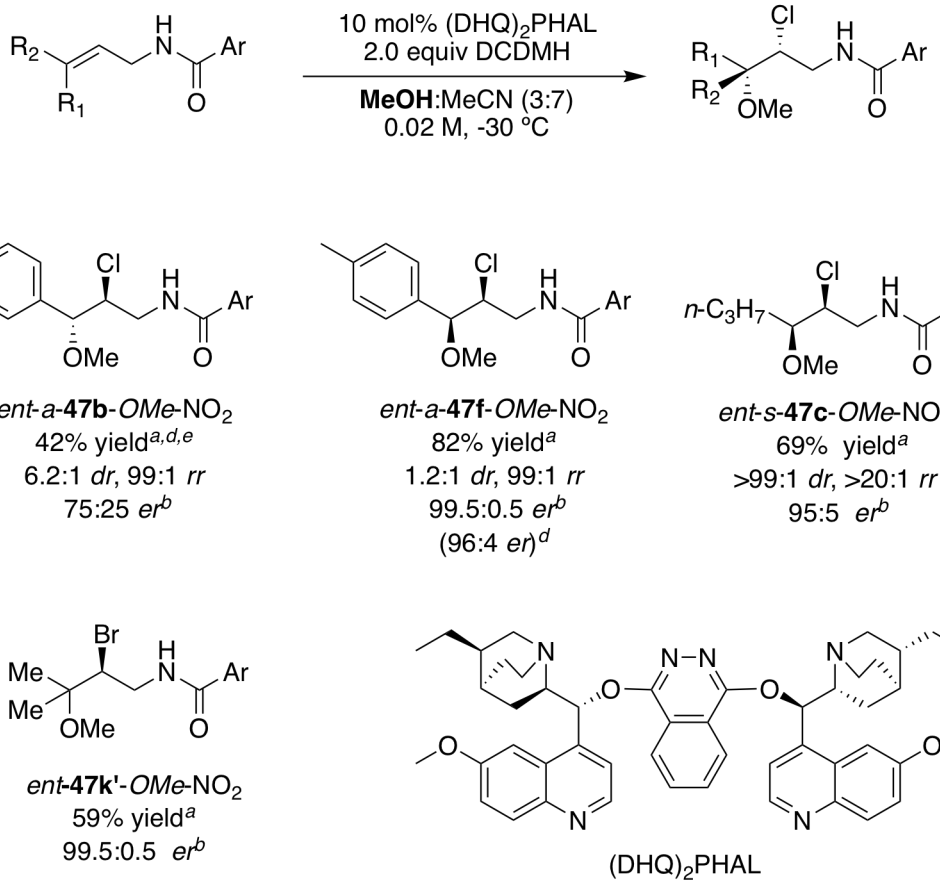

---

[a]Yield determined by NMR with MTBE as standard; [b]Enantioselectivity determined by chiral-phase HPLC; [c]Combined yield of diastereomers, 15 equivalents of Li_2CO_3 was used as additive; [d]The *er* values are for the minor diastereomer; [e] Mass balance was the cyclized products

It warrants emphasis that a large excess of the nucleophile (>100 equiv) is currently required to prevent the formation of cyclized products. Our lab is currently in the process of addressing this limitation to enable the use of highly functionalized nucleophiles in this chemistry.

I-2-4 Product distribution arising due to substrate-control and catalyst-control for the intermolecular chloroetherification reaction.

The different ratios observed for the regioselectivity of the chiral chloroetherified products require an attempted rationalization. As shown in Figure I-20, the aryl substituted allyl amide forms a chiral product in 99:1 *rr*, but switching from aryl substituent to alkyl allyl amide, yields products with lower regioselectivity ratios (Figure I-20). MeOH as the nucleophile can open up the putative chloronium ion from both sites and forms two regioisomers. However, in the case of aryl substituents, one regioisomer is obtained due to benzylic stabilization of the carbocation. Interestingly unbiased alkene *Z*-**46c**-NO_2 forms corresponding product with high regioselectivity (24:1 *rr*, *s*-**47c**-OMe-NO_2, Figure I-20). The benzyloxy group (OBn) results in a drop in regioselectivity (7:1 *rr*, Figure I-20, *s*-**47e**-OMe-NO2,). However, adding one carbon restores the *rr* and yields product with 23:1 *rr* (Figure I-20, *s*-**47j**-OMe-NO_2). These results show that the electron-donating group as a substituent can stabilize the carbocation and forms the product with higher regioselectivity.

Figure I-20: The regioselectivity for different products in enantioselective chloroetherification reaction

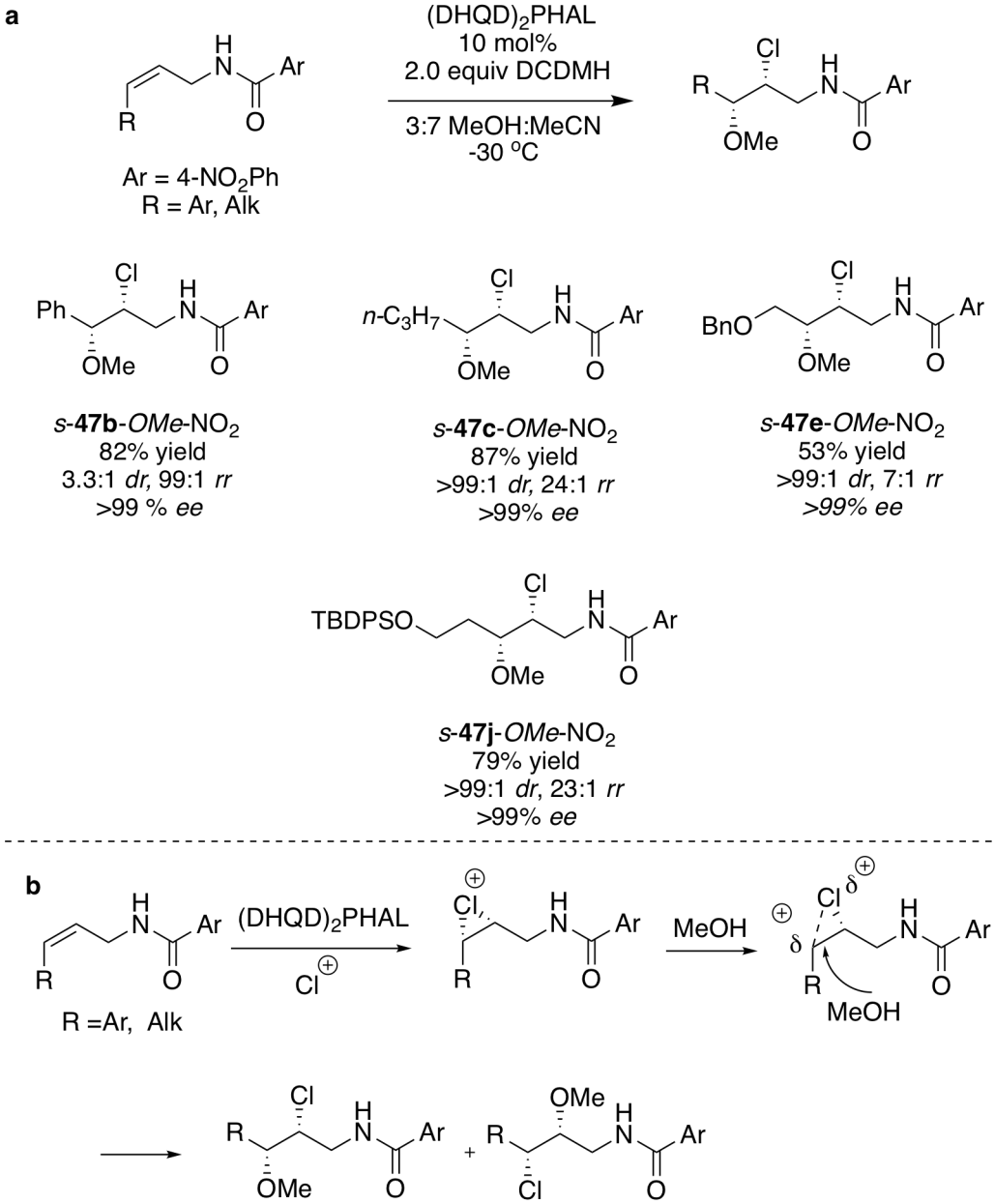

With these observations, we questioned whether the observed regioselectivity is only as a result of substrate control or the chiral catalyst

(DHQD)$_2$PHAL has some role in determining the ratio of the two regio isomers.

Figure I-21: Products distribution For *Z*-allyl amides

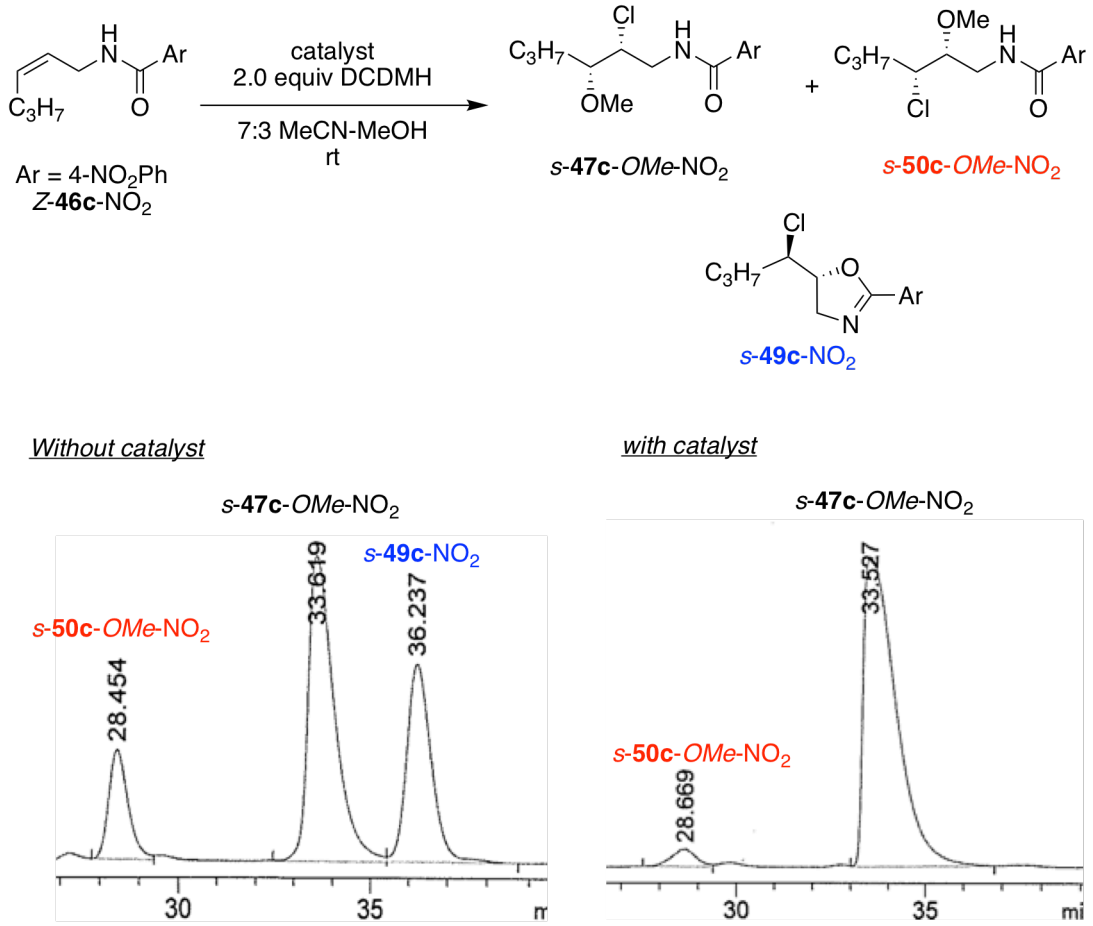

Reactions run in the absence of any catalyst gave a mixture of numerous products for the intermolecular chloroetherification reaction of both *E*- and *Z*- allyl amides. In contrast, reactions run in the presence of (DHQD)$_2$PHAL gave predominantly the desired chloroether product. The numerous products seen in the latter reactions were meticulously isolated and characterized. The *Z*-**46c**-NO$_2$ gave 3 major products. As seen from the HPLC trace of the crude reaction mixture, along with the desired product s-**47c**-*OMe*-NO$_2$, the constitutional

isomer *s*-**50c**-*OMe*-NO_2 as well as the cyclized oxazoline product *s*-**49c**-NO_2 was seen (Figure I-21). Under optimized reaction conditions that employed $(DHQD)_2$PHAL, the major product was the chloroether *s*-**47c**-*OMe*-NO_2. Small amount of the constitutional isomer *s*-**50c**-*OMe*-NO_2 was seen; no cyclized products were observed. A similar analysis was also performed with the *E*-**46c**-NO_2. As seen from the scheme below, the non-catalyzed reaction gave 2 constitutional isomers for both the chloroether product as well as the cyclized product. Although all these compounds were seen in the $(DHQD)_2$PHAL catalyzed reaction as well, the selectivity for the desired chloroether product was significantly higher (Figure I-22).

Figure I-22: Product distribution for *E*-allyl amides

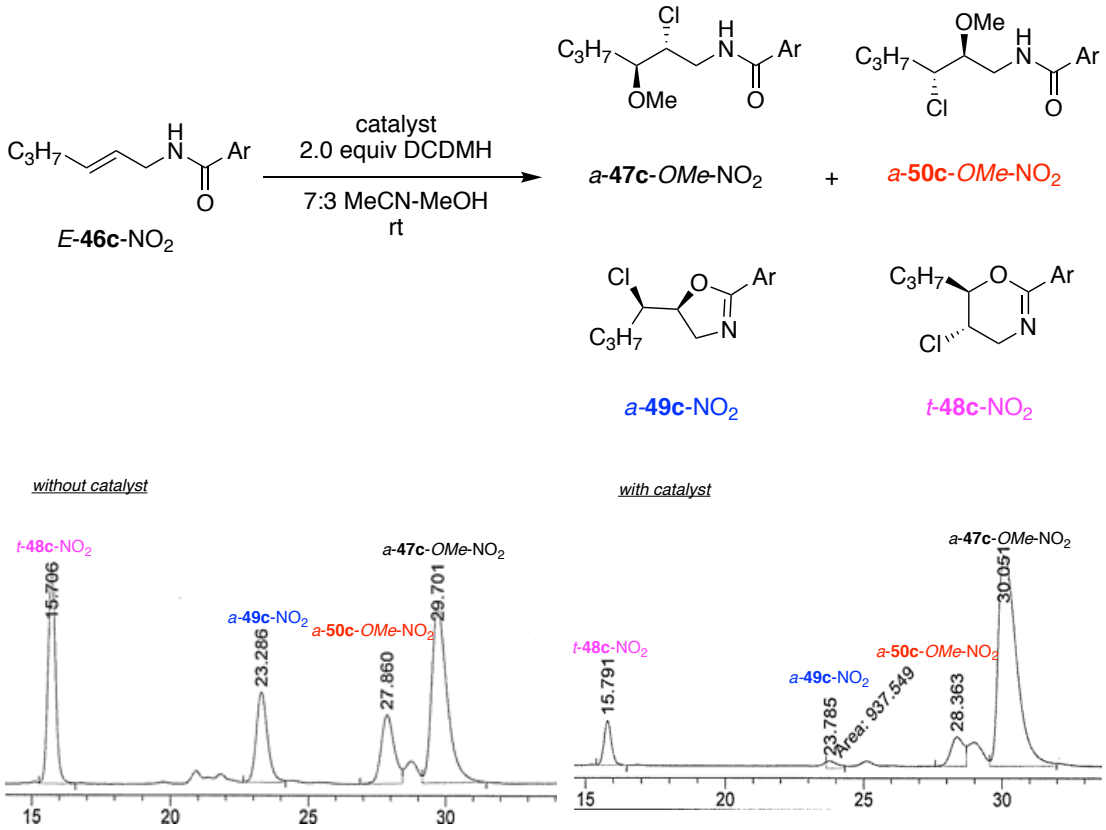

I-2-5 Absolute stereochemistry of the chloroetherification reactions

I-2-5-1 Absolute stereochemistry of the chloroetherification products derived from *E*- alkene

Attention must be drawn to the fact that the Cl bearing stereocenter has the same chirality for products derived from either the *cis* or *trans*-alkene substrates. The absolute stereochemistry of *s*-**47h**-*OH*-NO_2 and *s*-**47c**-*OMe*-NO_2, and the relative stereochemistry of *a*-**47c**-*OH*-NO_2 were established by single crystal X-ray diffraction. Since the absolute stereochemistry of *a*-**47c**-*OH*-NO_2 could not be determined from X-ray analysis, we resorted to the chemical transformations detailed in Figure I-23 for proof of structure. This was verified by

the TPAP-NMO mediated oxidation of the diastereomeric chlorohydrins *s*-**47c**-*OH*-NO_2 and *a*-**47c**-*OH*-NO_2, derived from substrates *Z*-**46c**-NO_2 and *E*-**46c**-NO_2, respectively (see Figure I-23). Both substrates gave the chloroketone product with the same absolute stereochemistry (verified by both, HPLC and optical rotation). This is only possible if the face selectivity of the chlorenium delivery was the same for these two classes of substrates.

Figure I-23: Determination of absolute stereochemistry of Cl-bearing stereocenter

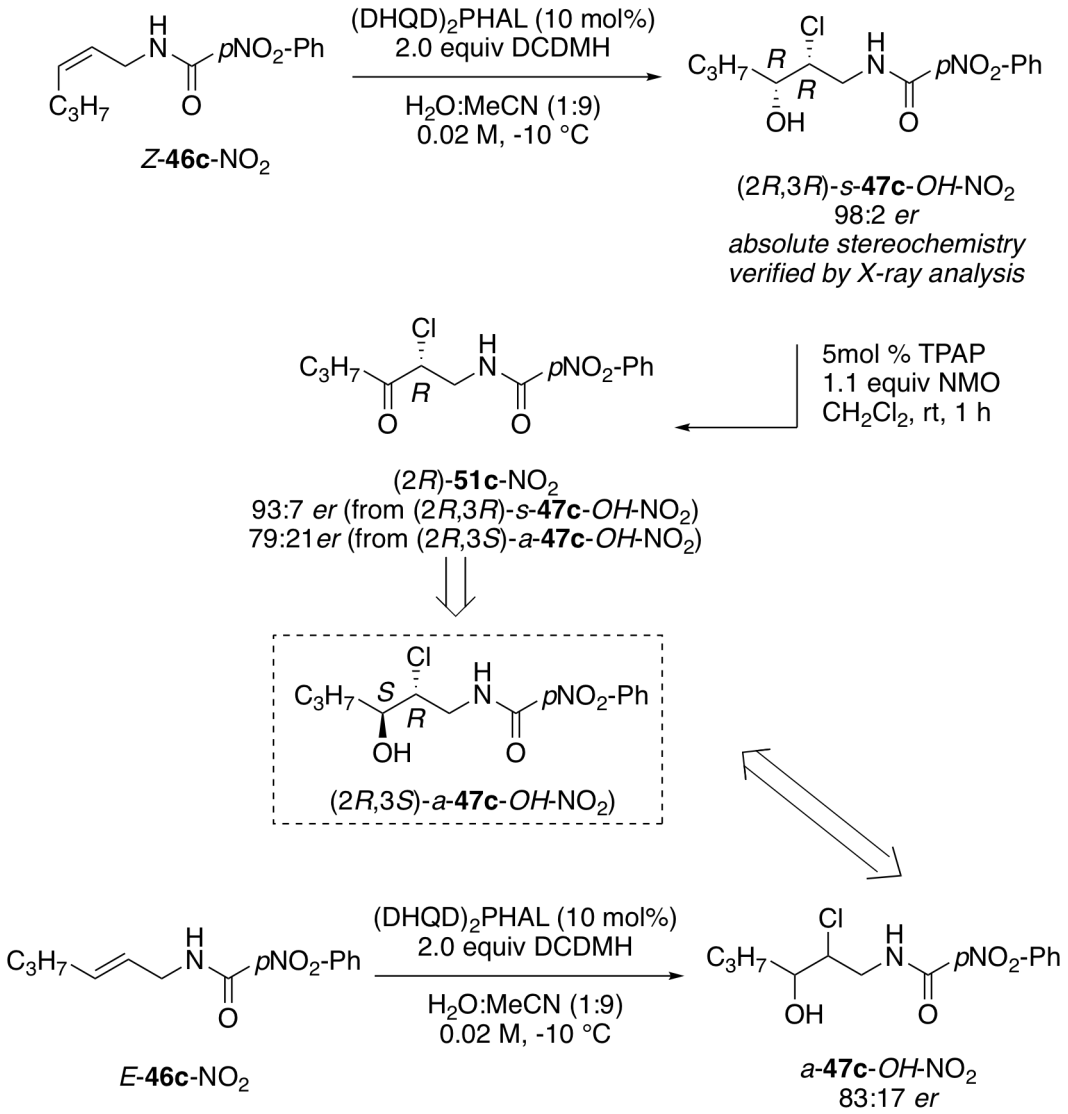

I-2-5-2 Stereodivergence in the formation of halohydrin and oxazoline products

The intermolecular chloroetherification reaction of many substrates gave variable amounts of the chlorocyclized products in addition to the desired products. Intriguingly, the Cl-bearing stereocenter of both these products formed

in the same reaction had the opposite stereochemistry based on chemical transformations and corroborating crystallographic evidence detailed below. While the chloroether product had an *R*-configuration for the Cl-bearing stereocenter, the chlorocyclized product had an *S*-configuration. With crystallographic evidence supporting the latter observation, we sought to unequivocally establish this divergence in stereoselectivity by chemical derivatization. An attempted synthesis of halohydrin *a*-**47b**-*OH*-Br from substrate *E*-**46b**-Br gave the chlorocyclized product *t*-**3b**-Br (36%, 97:3 *er*) in addition to the desired product *a*-**47b**-*OH*-Br (43%, 82:18 *er*). The stereochemistry of the Cl bearing stereocenter of *t*-**48b**-Br was assigned as *S* based on our prior studies. The absolute stereochemistry of the Cl-bearing stereocenter in *a*-**47b**-*OH*-Br**,** on the other hand was inferred to be *R* (based on the crystal structures of *s*-**47c**-*OMe*-NO_2 and *s*-**47h**-*OH*-NO_2 and chemical transformations illustrated in Figure I-24a). In order to unequivocally establish this stereodivergence, *t*-**48b**-Br was transformed to *a*-**47b**-*OH*-Br by means of a two-step transformation shown in Figure I-23a. Optical rotation as well as HPLC co-injection confirmed that it was indeed the enantiomer of *a*-**47b**-*OH*-Br that had resulted from this transformation (Figure I-24b). These results lead us to conclude that two distinct mechanisms are in play that leads to either the cyclized dihydrooxazine products or the desired intermolecular addition of the nucleophile and halenium ion across the alkene in the *same* reaction.

Figure I-24: (a) Stereodivergence in the formation of halohydrin and oxazoline products. (b) HPLC trace for halohydrins

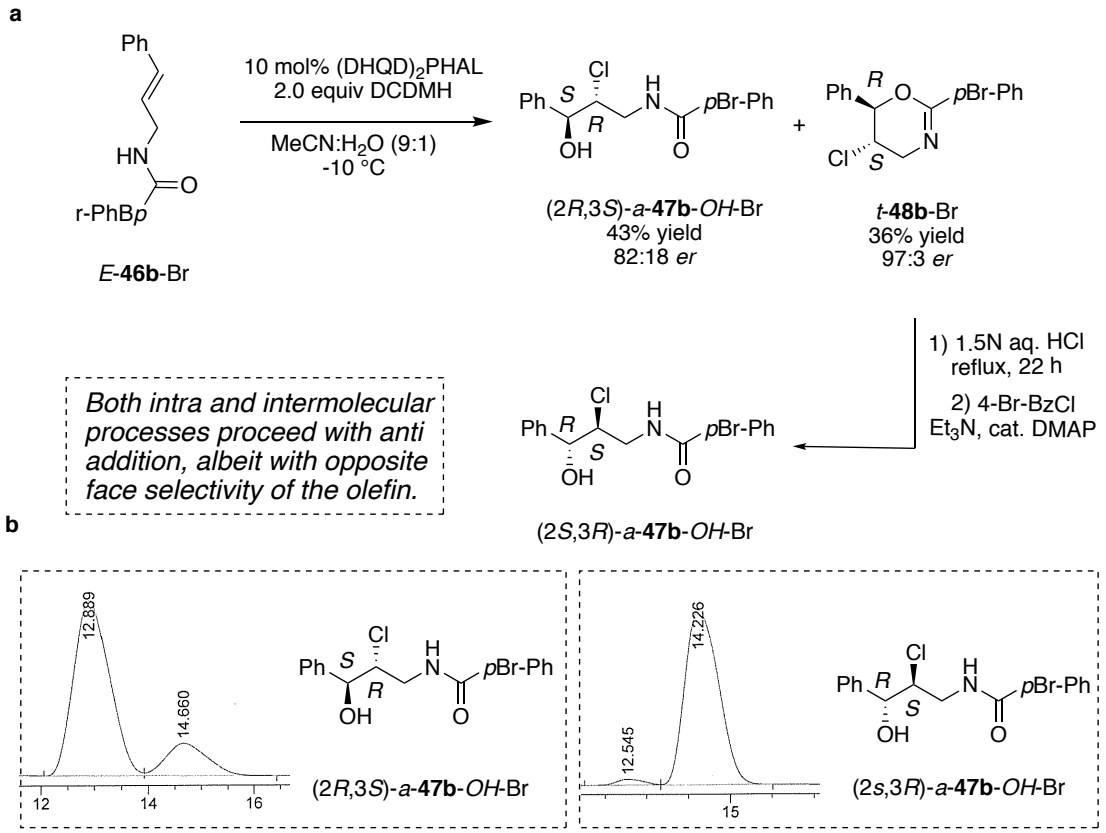

I-2-6 Experimental section

I-2-6-1 General information

Commercially available reagents were purchased from Sigma-Aldrich or Alfa-Aesar and used as received. CH_2Cl_2 and acetonitrile were freshly distilled over CaH_2 prior to use. THF was distilled over sodium-benzophenone ketyl. All other solvents were used as purchased. ^1H and ^{13}C NMR were recorded on 500 MHz Varian NMR machines using $CDCl_3$ or CD_3CN as solvent and were referenced to residual solvent peaks. Flash silica gel (32-63 mm, Silicycle 60 Å)

was used for column chromatography. Enantiomeric excess for all products was determined by HPLC analysis using DAICEL CHIRALCEL® OJ-H and OD-H or CHIRALPAK® IA and AD-H columns. Optical rotations of all products were measured in chloroform.

I-2-6-2 General procedure for optimization of catalytic asymmetric intermolecular haloetherification/haloesterification of unsaturated amides

The substrate (0.04 mmol, 1.0 equiv) was suspended in acetonitrile (MeCN, 2.8 mL) in a screw-capped vial equipped with a stir bar. The resulting suspension was cooled to -30 ° C in an immersion cooler. $(DHQD)_2PHAL$ (3 mg, 10 mol%) and 1.2 mL of methanol or acetic acid was then introduced. After stirring for 2 min DCDMH (15.8 mg, 0.08 mmol, 2.0 equiv) or NBS (14.3 mg, 2.0 equiv) was added. The stirring was continued at -30 °C till the reaction was complete (TLC). The reaction was quenched by the addition of saturated aq. Na_2SO_3 (1 mL) and diluted with DCM (3 mL). The organics were separated and the aqueous layer was extracted with DCM (3 × 3 mL). The combined organics were dried over anhydrous Na_2SO_4, concentrated and dissolved in 1 mL of $CDCl_3$. An equivalent amount (0.04 mmol) of MTBE was added and the solution was analyzed by NMR to obtain the NMR yield of the desired product. This solution was then concentrated in the presence of small quantity of silica gel. Column chromatography (SiO_2/EtOAc – Hexanes gradient elution) gave the desired product.

Following modifications were used for halohydrin synthesis: MeCN:H_2O ratio was 9:1; Reaction temperature: -10 °C.

I-2-6-3 General procedure for substrate scope analysis for catalytic asymmetric intermolecular haloetherification/haloesterification of unsaturated amides

The substrate (0.1 mmol, 1.0 equiv) was suspended in acetonitrile (MeCN, 7.0 mL) in a screw-capped vial equipped with a stir bar. The resulting suspension was cooled to -30 ° C in an immersion cooler. $(DHQD)_2PHAL$ (7.8 mg, 10 mol%) and 3.0 mL of methanol or acetic acid was then introduced After stirring for 2 min DCDMH (39.4 mg, 0.2 mmol, 2.0 equiv) or NBS (35.6 mg, 2.0 equiv) was added. The stirring was continued at -30 °C till the reaction was complete (TLC). The reaction was quenched by the addition of saturated aq. Na_2SO_3 (4 mL) and diluted with DCM (3 mL). The organics were separated and the aqueous layer was extracted with DCM (3 × 3 mL). The combined organics were dried over anhyd. Na_2SO_4 and concentrated in the presence of small quantity of silica gel. Column chromatography (SiO_2/EtOAc – Hexanes gradient elution) gave the desired product.

Following modifications were used for halohydrin synthesis: MeCN:H_2O ratio was 9:1; Reaction temperature: -10 °C.

I-2-6-4 Procedure for gram scale catalytic asymmetric intermolecular haloetherification/haloesterification of unsaturated amides

Z-**1c**-NO_2 (1.0 g, 4.0 mmol, 1.0 equiv) was suspended in acetonitrile (MeCN, 14.0 mL) in a screw-capped vial equipped with a stir bar. The resulting

suspension was cooled to -30 ° C in an immersion cooler. $(DHQD)_2PHAL$ (311.6 mg, 10 mol%), 7.0 mL of methanol was then introduced. After stirring for 2 min DCDMH (1500 mg, 8.0 mmol, 2.0 equiv) was added. The stirring was continued at -30 °C till the reaction was complete (TLC). The reaction was quenched by the addition of saturated aq. Na_2SO_3 (20 mL) and diluted with DCM (15 mL). The organics were separated and the aqueous layer was extracted with DCM (3 × 15 mL). The combined organics were dried over anhyd. Na_2SO_4 and concentrated in the presence of silica gel. Column chromatography (SiO_2/EtOAc – Hexanes gradient elution) gave the desired product.

Following modifications were used for gram scale synthesis of halohydrin *s-2c-OH*-NO_2: MeCN:H_2O ratio was 9:1 (20 mL); catalyst loading: 2 mol% $(DHQD)_2PHAL$, Reaction temperature: -10 °C.

Allyl alcohols **I-52** was synthesized from the corresponding aldehydes or ketone by a Horner-Wadsworth-Emmons (HWE) olefination reaction follow by DIBAL reduction of resulting ester.[16]

I-2-6-5 Synthesis of unsaturated amide substrates for chlorofunctionalization[57-58]

Figure I-25: General procedure for synthesis of substrates

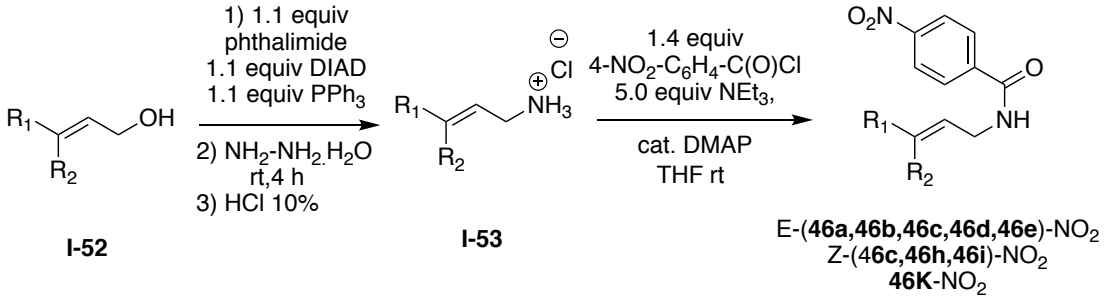

Allyl alcohols **I-52** (1.0 equiv), phthalimide (1.1 equiv) and PPh_3 (1.1 equiv) was added to the reaction vessel and dissolved in THF (5 mL/mmol). The flask was immersed in an ice bath and DIAD (1.1 equiv) was added drop wise. After TLC analysis revealed the complete consumption of starting material (~30 min), 3 equivalents of hydrazine hydrate was added to the reaction vessel and the resulting suspension was stirred overnight at room temprature. The reaction was diluted with water, concentrated HCl (3 mL) was added, and the resulting suspension was stirred for further 30 min at ambient temperature. The precipitated solids were filtered and the filter cake was washed with 10% aq. HCl (2 × 2 mL). The combined filtrates were washed with ether (3 × 5 mL) and the aqueous phase was concentrated under reduced pressure giving the amine salts **I-53**, which were used in the next reaction without any purification.

A solution of crude ammonium chloride salt **I-53** from the previous step (1 equiv), triethyl amine (5 equiv) and catalytic amount of DMAP in THF (20 mL) were cooled in an ice bath. To this suspension was added *p*-nitro benzoyl chloride (1.5 equiv). After the addition was completed, the reaction was warmed

to room temperature. After 3 h, the reaction was quenched with methanol (1.0 mL) and then diluted with an equal amount of water, concentrated under reduced pressure, and extracted with DCM (3 × 25 mL). The combined organic layer was washed with brine (1 × 20 mL), dried over anhyd. Na_2SO_4 and concentrated under reduced pressure in the presence of silica gel. Column chromatography (EtOAC-Hexanes gradient elution) gave the desired products (*E*-(**46a,46b,46c,46d,46e**)-NO_2, *Z*-(**46c,46h,46i**)-NO_2, **46k**-NO_2).

I-2-6-6 General procedure for synthesis of aromatic *Z*-allyl amides

Figure I-26: General procedure for synthesis of aromatic *Z*-allyl amides

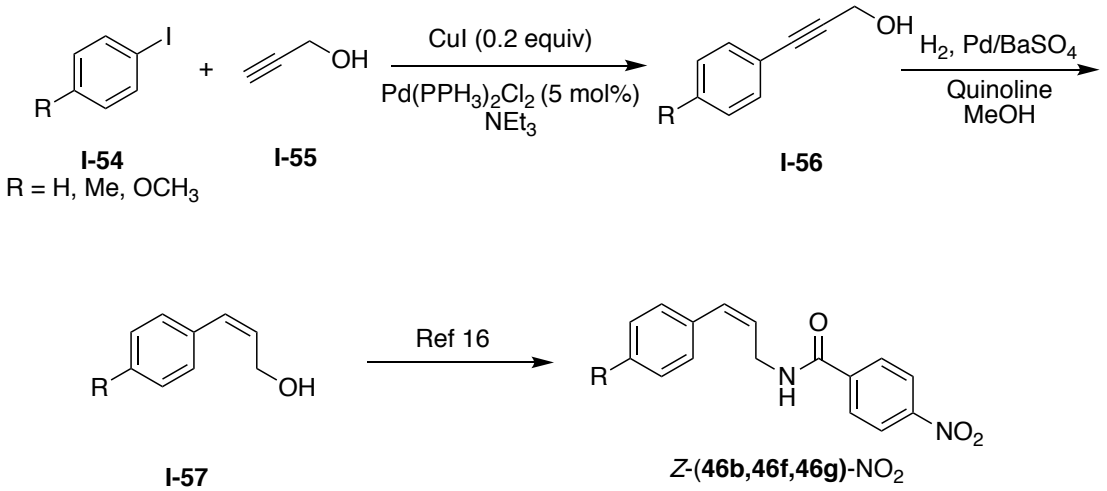

Iodo benzene **I-54** (1.0 equiv) and propargyl alcohol was dissolved in triethylamine (10 mL/mmol) at room temperature after which CuI (0.2 equiv) and $Pd(PPh_3)Cl_2$ (5 mol%) were added to reaction vessel. After TLC analysis revealed consumption of starting material, the reaction was diluted with water, concentrated under reduced pressure, and extracted with DCM (3 × 25 mL). The

combined organic layer was washed with brine (1 × 20 mL), dried over anhyd. Na_2SO_4 and concentrated under reduced pressure in the presence of silica gel. Column chromatography (20% EtOAC-Hexanes gradient elution) gave the desired products **I-56**. (70-85 % yield for different substrates)

3-Phenylprop-2-yn-1-ol **I-56** (1.0 equiv), palladium on barium sulfate (10 wt%) and quinoline were dissolved in methanol (10 mL/mmol). The reaction vessel was purged with hydrogen gas and then stirred under balloon pressure of H_2. When GC analysis revealed complete consumption of starting material, the catalyst was filtered and the filtrate was concentrated. Column chromatography (EtOAC-Hexanes gradient elution) gave the desired products (**I-57**).

Allyl amides *Z*-(**46b,46f,46g**)-NO_2 were synthesized as reported previously.[16]

I-2-6-7 General procedure synthesis of substrates *Z*-46e-NO_2 – *Z*-46j-NO_2

Figure I-27: General procedure for the synthesis of substrates *Z*-**46e**-NO_2 – *Z*-**46j**-NO_2

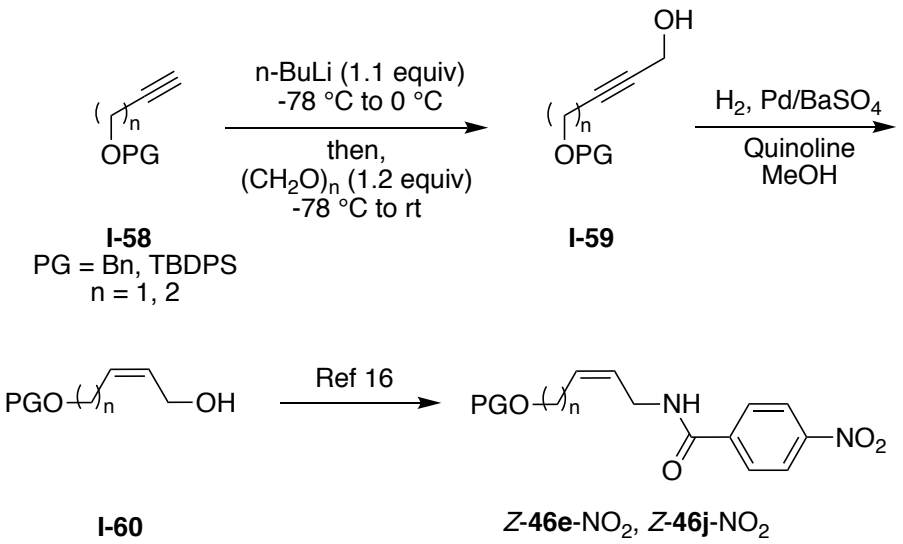

Alkyne **I-58** (1.0 equiv) was dissolved in THF in a flamed dried round bottom flask. *n*-BuLi (1.1 equiv) was added to cooled solution at -78 °C. The reaction was then warmed to 0 °C. After 30 min paraformaldehyde (1.2 equiv) was added in a single portion at -78 °C and the reaction was warmed to room temperature. After 2 h, the reaction was quenched with sat. aq. NH_4Cl solution (15.0 mL). The mixture was diluted with water and concentrated under reduced pressure and then extracted with DCM (3 × 10 mL). The combined organic layer was washed with brine (1 × 10 mL), dried over anhyd. Na_2SO_4, and concentrated under reduced pressure in the presence of silica gel. Column chromatography (EtOAC-Hexanes gradient elution) gave the desired products **I-59**.

The *Z* allylic alcohol **I-60** was synthesized from alkynol **I-59** by a Lindlar reduction that was reported in page 49.

Allyl amides *Z*-**46e**-NO_2, *Z*-**46j**-NO_2 were synthesized as reported previously.[16]

I-2-6-8 Analytical data for products

a-**47b**-*OMe*-NO_2**:** *N*-((2*R*,3*S*)-2-chloro-3-methoxy-3-phenylpropyl)-4-nitrobenzamide

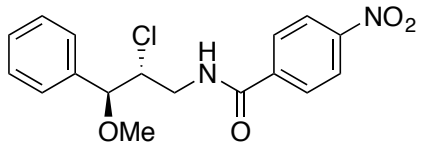

R_f : 0.20 (30%EtOAc in hexanes, UV)

^{1}H NMR (500 MHz, $CDCl_3$) δ 8.29 (d, *J* = 9.0 Hz, 2H), 7.88 (d, *J* = 9.0 Hz, 2H), 7.40-7.33 (m, 5H), 6.82 (br s, 1H), 4.45 (d, *J* = 4.5 Hz, 1H), 4.25-4.22 (m, 1H), 4.11-4.06 (m, 1H), 3.66-3.61 (m, 1H), 3.34 (s, 3H)

^{13}C NMR (125 MHz, $CDCl_3$) δ 165.26, 149.64, 139.66, 136.87, 137.22, 128.76, 128.12, 127.18, 123.87, 86.33, 62.60, 57.98, 42.54

HRMS analysis (ESI): Calculated for $[M+H]^+$: $C_{17}H_{18}ClN_2O_4$: 349.0955; Found: 349.0950

Resolution of enantiomers: DAICEL Chiralcel® Oj-H column, 20% IPA-Hexanes, 1.0 mL/min, 265 nm, RT1 (minor) = 27.0 min, RT2 (major) = 30.1 min

$[\alpha]_D^{20}$ = +46.7 (c 0.5, $CHCl_3$, *er* = 92:8)

a-**47d**-*OMe*-NO_2**:** *N*-((2*R*,3*S*)-2-chloro-3-(4-fluorophenyl)-3-methoxypropyl)-4-nitrobenzamide

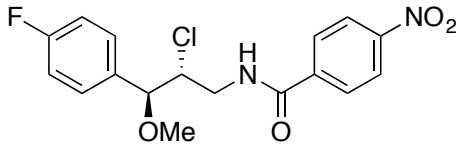

R_f : 0.19 (30% EtOAc in hexanes, UV)

^{1}H NMR (500 MHz, $CDCl_3$) δ 8.29 (d, *J* = 9.0 Hz, 2H), 7.91 (d, *J* = 9.0 Hz, 2H), 7.33-7.30 (m, 2H), 7.09-7.06 (m, 2H), 6.77 (br s, 1H), 4.38 (d, *J* = 4.5 Hz, 1H) 4.19-4.18 (m, 1H), 4.13-4.09 (m, 1H), 3.65-3.63 (m, 1H), 3.31 (s, 3H)

^{13}C NMR (125 MHz, $CDCl_3$) δ 165.32, 149.65, 139.81, 133.74, 129.08 (d, J_{CF} = 30 Hz) 128.12, 123.91, 115.81, 115.63, 85.55, 62.79, 57.79, 42.77

HRMS analysis (ESI): Calculated for $[M+H]^+$: $C_{17}H_{17}ClFN_2O_4$: 367.0861; Found: 367.0844

Resolution of enantiomers: CHIRALCEL OJ-H 12% IPA-Hexane, 0.7 ml/min, RT1 (minor) = 64.6, RT2 (major) = 69.6; $[\alpha]_D^{20}$ = -5.0 (c 0.1, $CHCl_3$, *er* = 89:11)

a-**47c**-*OMe*-NO_2**:** *N*-((2*R*,3*S*)-2-chloro-3-methoxyhexyl)-4-nitrobenzamide

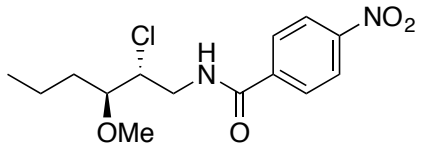

R_f : 0.38 (30% EtOAc in hexanes, UV)

^{1}H NMR (500 MHz, $CDCl_3$) δ 8.29 (d, *J* = 9.0 Hz, 2H), 7.93 (d, *J* = 9.0 Hz, 2H), 7.24 (br s, 1H), 4.16-4.10 (m, 2H), 3.60-3.56 (m, 1H), 3.49-3.47 (m, 4H), 1.68-1.62 (m, 2H), 1.54-1.35 (m, 2H), 0.95 (m, 3H)

^{13}C NMR (125 MHz, $CDCl_3$) δ 165.40, 149.70, 139.86, 128.14, 123.90, 83,90, 61.78, 59.37, 42.92, 33.69, 18.46, 14.09

HRMS analysis (ESI): Calculated for $[M-H]^-$: $C_{14}H_{18}ClN_2O_4$: 313.0955; Found: 313.0953

Resolution of enantiomers: DAICEL Chiralcel® AD-H column, 7% IPA-Hexanes, 0.5 mL/min, 254 nm, RT1 (major) = 32.6 min, RT2 (major) = 34.7 min.

$[\alpha]_D^{20}$ = -30 (c 0.25, $CHCl_3$, *er* = 87:13)

a-**47a**-*OMe*-NO_2**:** *N*-((2*R*,3*S*)-2-chloro-3-cyclohexyl-3-methoxypropyl)-4-nitrobenzamide

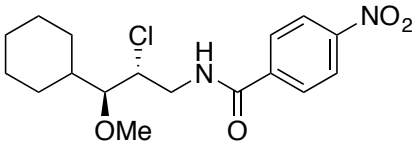

R_f : 0.36 (30% EtOAc in hexanes, UV)

^1H NMR (500 MHz, $CDCl_3$) δ 8.29 (d, *J* = 9.0 Hz, 2H), 7.92 (d, *J* = 9.0 Hz, 2H), 7.00 (br s, 1H), 4.33-4.30 (m, 1H), 4.15-4.10 (m, 1H), 3.63-3.58 (m, 4H), 3.22-3.20 (dd, J =7.0, 4.0 Hz 1H), 1.94-1.91(m, 1H), 1.77-1.74 (m, 2H), 1.68-1.63 (m, 2H), 1.27-1.05 (m, 6H)

^{13}C NMR (125 MHz, $CDCl_3$) δ 165.40, 149.69, 139.91, 128.12, 123.88, 89.50, 62.64, 60.87, 42.71, 41.32, 29.67, 28.70, 26.20, 25.99, 25.86

HRMS analysis (ESI): Calculated for $[M-H]^-$: $C_{17}H_{22}ClN_2O_4$: 353.1268; Found: 353.1261

Resolution of enantiomers: DAICEL Chiralcel® OJ-H column, 10% IPA-Hexanes, 1.0 mL/min, 254 nm, RT1 (major) = 11.8 min, RT2 (minor) = 16.1 min.

$[\alpha]_D^{20}$ = -4.0 (c 0.6, $CHCl_3$, *er* = 75:25)

a-**47e**-*OMe*-NO_2**:** *N*-((2*R*,3*S*)-4-(benzyloxy)-2-chloro-3-methoxybutyl)-4-nitrobenzamide

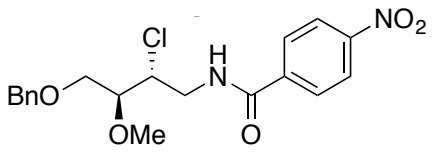

R_f: 0.16 (30% EtOAc in hexanes, UV)

^{1}H NMR (500 MHz, $CDCl_3$) δ 8.25 (d, *J* = 9.0 Hz, 2H), 7.85 (d, *J* = 9.0 Hz, 2H), 7.35-7.29, (m, 5H), 6.87 (br s, 1H), 4.56 (d, *J* = 1 Hz, 2H), 4.36-4.33 (m, 1H), 3.99-3.95 (m, 1H), 3.83-3.79 (m, 1H), 3.75-3.72 (dd, *J*=10.0, 5.0 Hz, 1H), 3.69-3.66 (dd, *J*=10.0, 5.0 Hz, 1H), 3.49 (s, 3H)

^{13}C NMR (125 MHz, $CDCl_3$) δ 165.24, 149.60, 139.78, 137.45, 128.55, 128.11, 128.02, 127.83, 123.83, 82.33, 73.76, 68.17, 59.11, 59.08, 24.90

HRMS analysis (ESI): Calculated for $[M-H]^-$: $C_{19}H_{20}ClN_2O_5$: 391.1061; Found: 391.1057

Resolution of enantiomers: DAICEL Chiralcel® IA column, 20% IPA-Hexanes, 1.0 mL/min, 254 nm, RT1 (major) = 11.0 min, RT2 (minor) = 11.8 min.

$[\alpha]_D^{20}$ = +5.2 (c 0.5, $CHCl_3$, *er* = 88:12)

s-**47b**-*OMe*-NO_2**:** *N*-((2*R*,3*R*)-2-chloro-3-methoxy-3-phenylpropyl)-4-nitrobenzamide

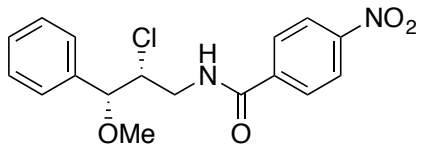

R_f : 0.22 (30% EtOAc in hexanes, UV)

^{1}H NMR (500 MHz, $CDCl_3$) δ 8.27 (d, *J* = 9.0 Hz, 2H), 7.86 (d, *J* = 9.0 Hz, 2H), 7.41-7.24 (m, 5H), 6.57 (br s, 1H), 4.41 (d, *J* = 4.5 Hz, 1H), 4.29-4.28 (m, 1H), 4.00-3.95 (m, 1H), 3.56-3.52 (m, 2H), 3.27(s, 3H)

^{13}C NMR (125 MHz, $CDCl_3$) δ 165.32, 149.75, 139.66, 136.83, 123.84, 128.68, 128.13, 127.49, 123.87, 85.03, 63.63, 57.44, 43.80

HRMS analysis (ESI): Calculated for $[M+H]^+$: $C_{17}H_{18}ClN_2O_4$: 349.0955; Found: 349.0955

Resolution of enantiomers: DAICEL Chiralcel® AD-H column, 10% IPA-Hexanes, 1.0 mL/min, 254 nm, RT1 (major) = 22.8 min, RT2 (minor) = 29.9 min.

$[\alpha]_D^{20}$ = -8.0 (c 0.1, $CHCl_3$, *er* = 99.5:0.5)

a-**47f**-*OMe*-NO_2**:** *N*-((2*R*,3*R*)-2-chloro-3-methoxy-3-(*p*-tolyl)propyl)-4-nitrobenzamide

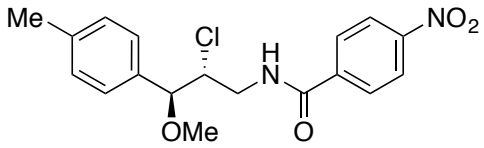

R_f : 0.27 (30% EtOAc in hexanes, UV)

^{1}H NMR (500 MHz, $CDCl_3$) δ 8.29 (d, *J* = 9.0 Hz, 2H), 7.89 (d, *J* = 9.0 Hz, 2H), 7.22-7.18 (m, 4H), 6.86 (br s, 1H), 4.24 (d, *J* = 5.5 Hz, 1H), 4.23-4.20 (m, 1H), 4.10-4.05 (m, 1H), 3.65-3.60 (m, 1H), 3.33 (s, 3H), 2.34 (s, 3H)

^{13}C NMR (125 MHz, $CDCl_3$) δ 165.27, 149.67, 139.64, 138.74, 133.73, 129.41, 128.13, 127.38, 123.86, 84.94, 63.72, 57.29, 43.75, 21.21

HRMS analysis (ESI): Calculated for $[M-H]^-$: $C_{18}H_{18}ClN_2O_4$: 361.0955; Found: 361.0955

Resolution of enantiomers: DAICEL Chiralcel® AD-H column, 15% IPA-Hexanes, 1.0 mL/min, 265 nm, RT1 (major) = 13.6 min, RT2 (minor) = 16.6 min.

$[\alpha]_D^{20}$ = +14.9 (c 0.7, $CHCl_3$, *er* = 97:3)

s-**47f**-*OMe*-NO_2**:** *N*-((2*R*,3*R*)-2-chloro-3-methoxy-3-(*p*-tolyl)propyl)-4-nitrobenzamide

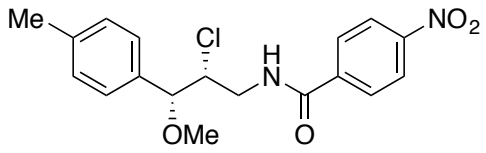

R_f : 0.27 (30% EtOAc in hexanes, UV)

^{1}H NMR (500 MHz, $CDCl_3$) δ 8.29 (d, *J* = 9.0 Hz, 2H), 7.85 (d, *J* = 9.0 Hz, 2H), 7.22-7.10 (m, 4H), 6.55 (br s, 1H), 4.39 (d, *J* = 5.0 Hz, 1H), 4.38-4.24 (m, 1H), 3.95-3.94 (m, 1H), 3.55-3.50 (m, 1H), 3.30 (s, 3H), 2.35 (s, 3H)

^{13}C NMR (125 MHz, $CDCl_3$) δ 165.22, 149.63, 139.91, 138.63, 134.15, 129.46, 128.12, 127.10, 123.85, 86.22, 62.65, 57.86, 42.56, 21.19

HRMS analysis (ESI): Calculated for $[M-H]^-$: $C_{18}H_{18}ClN_2O_4$: 361.0955; Found: 361.0955

Resolution of enantiomers: DAICEL Chiralcel® OD-H column, 15% IPA-Hexanes, 1.0 mL/min, 254 nm, RT1 (major) = 17.8 min, RT2 (minor) = 25.0 min.

$[\alpha]_D^{20}$ = -7.1 (c 0.6, $CHCl_3$, *er* = 99:1)

47g-*OMe*-NO_2**:** *N*-2-chloro-3-methoxy-3-(4-methoxyphenyl)propyl)-4-nitrobenzamide (note: the relative stereochemistry of the two diastereomeric products below was not identified.)

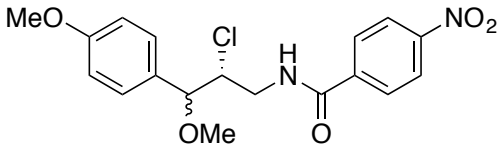

R_f : 0.16 (30% EtOAc in hexanes, UV)

^{1}H NMR (500 MHz, $CDCl_3$) δ 8.28 (d, *J* = 9.0 Hz, 2H), 7.87 (d, *J* = 9.0 Hz, 2H), 7.28 (d, *J* = 8 Hz, 2H), 6.92 (d, *J* = 8 Hz, 2H), 6.57 (br s, 1H), 4.37 (d, *J* = 5.5 Hz, 1H), 4.27-4.23 (m, 1H), 3.96-3.92 (m, 1H), 3.80 (s, 3H), 3.53-3.48 (m, 1H), 3.29 (s, 3H)

^{13}C NMR (125 MHz, $CDCl_3$) δ 165.24, 159.87, 149.64, 139.89, 129.09, 128.44, 128.13, 123.87, 114.10, 85.91, 62.79, 57.70, 55.28, 42.67

HRMS analysis (ESI): Calculated for $[M-H]^-$: $C_{18}H_{18}ClN_2O_5$ 377.0904; Found: 377.0899

Resolution of enantiomers: DAICEL Chiralcel® OD-H column, 2% IPA-Hexanes, 01.0 mL/min, 254 nm, RT1 (minor) = 21.6 min, RT2 (major) = 25.7 min.

$[\alpha]_D^{20}$ = +17 (c 0.25, $CHCl_3$, *er* = 99:1)

epi-**47g**-*OMe*-NO_2**:**, *N*-((2*R*,3*R*)-2-chloro-3-methoxy-3-(4-methoxyphenyl)propyl)-4-nitrobenzamide

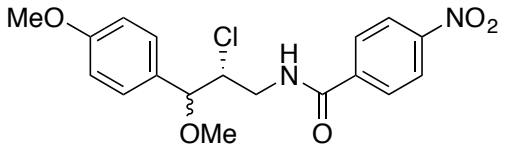

R_f : 0.16 (30% EtOAc in hexanes, UV)

^{1}H NMR (500 MHz, $CDCl_3$) δ 8.29 (d, *J* = 9.0 Hz, 2H), 7.90 (d, *J* = 9.0 Hz, 2H), 7.26 (d, *J* = 8.0 Hz, 2H), 6.91 (d, *J* = 8.0 Hz, 2H), 6.85 (br s, 1H), 4.39 (d, *J* = 6.0 Hz, 1H) 4.22-4.18 (m, 1H), 4.11-4.06 (m, 1H), 3.80 (s, 3H), 3.65-3.60 (m, 1H), 3.31 (s, 3H)

^{13}C NMR (125 MHz, $CDCl_3$) δ 165.27, 159.97, 149.68, 139.63, 128.69, 128.12, 123.86, 114.08, 84.66, 63.83, 57.18, 55.27, 43.71

HRMS analysis (ESI): Calculated for $[M-H]^-$: $C_{18}H_{18}ClN_2O_5$ 377.0904; Found: 377.0901

Resolution of enantiomers: DAICEL Chiralcel® IA column, 20% IPA-Hexanes, 1.0 mL/min, 254 nm, RT1 (major) = 11.9 min, RT2 (minor) = 13.8 min.

$[\alpha]_D^{20}$ = -13.0 (c 0.25, $CHCl_3$, *er* = 92:8)

s-**47h**-*OMe*-NO_2**:** *N*-((2*R*,3*R*)-2-chloro-3-methoxypentyl)-4-nitrobenzamide

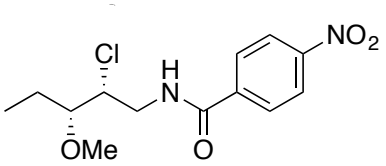

R_f : 0.20 (30% EtOAc in hexanes, UV)

^{1}H NMR (500 MHz, $CDCl_3$) δ 8.30 (d, *J* = 9.0 Hz, 2H), 7.94 (d, *J* = 9.0 Hz, 2H), 6.83 (br s, 1H), 4.28-4.25 (m, 1H), 4.14-4.09 (m, 1H), 3.60-3.51 (m, 1H), 3.46 (s, 3H), 3.61-3.34 (m, 1H), 1.75-1.69 (m, 2H), 0.98 (t, *J* = 7.5 Hz, 3H)

^{13}C NMR (125 MHz, $CDCl_3$) δ 165.49, 149.69, 139.69, 128.16, 123.90, 84.10, 60.96, 58.21, 43.92, 22.90, 9.92

HRMS analysis (ESI): Calculated for $[M+H]^+$: $C_{13}H_{16}ClN_2O_4$ 299.0799; Found: 299.0796

Resolution of enantiomers: DAICEL Chiralcel® AD-H column, 7% IPA-Hexanes, 1.0 mL/min, 254 nm, RT1 (minor) = 22.2 min, RT2 (major) = 24.7 min.

$[\alpha]_D^{20}$ = +30.0 (c 0.39, $CHCl_3$, *er* = 98:2)

s-**47c**-*OMe*-NO_2**:** *N*-((2*R*,3*R*)-2-chloro-3-methoxyhexyl)-4-nitrobenzamide

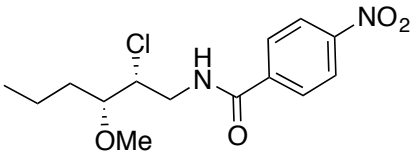

R_f : 0.25 (30% EtOAc in hexanes, UV)

^{1}H NMR (500 MHz, $CDCl_3$) δ 8.29 (d, *J* = 9.0 Hz, 2H), 7.93 (d, *J* = 9.0 Hz, 2H), 6.79 (br s, 1H), 4.25-4.23 (m, 1H), 4.13-4.08 (m, 1H), 3.61-3.55 (m, 1H), 3.45 - 3.41(m, 4H), 1.68-1.62 (m, 2H), 1.54-1.35 (m, 2H), 0.95 (t, *J* = 7.5 Hz, 3H)

^{13}C NMR (125 MHz, $CDCl_3$) δ 165.44, 149.74, 139.73, 128.14, 123.90, 82,70, 61.04, 58.27, 43.78, 32.08, 18.90, 14.04

HRMS analysis (ESI): Calculated for $[M+H]^+$: $C_{14}H_{20}ClN_2O_4$: 315.1112; Found: 315.1116

Resolution of enantiomers: DAICEL Chiralcel® AD-H column, 10% IPA-Hexanes, 1.0 mL/min, 254 nm, RT1 (major) = 12.1 min, RT2 (minor) = 14.0 min.

$[\alpha]_D^{20}$ = +19.0 (c 0.1, $CHCl_3$, *er* = 99.5:0.5)

Absolute stereochemistry was determined by single crystal X-ray diffraction (XRD). Crystals for XRD were obtained by crystallization from CH_2Cl_2 layered with hexanes in a silicone-coated vial.

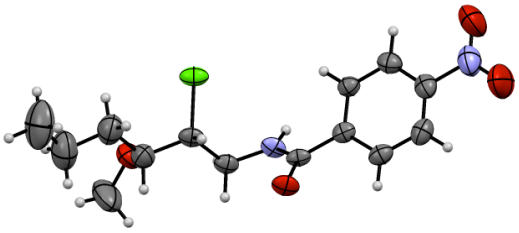

*ent-s-***47c**-*OMe*-NO_2**:** *N*-((2*S*,3*S*)-2-chloro-3-methoxyhexyl)-4-nitrobenzamide

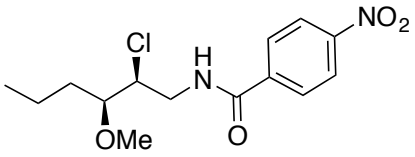

R_f : 0.25 (30% EtOAc in hexanes, UV) 64% yield with $(DHQ)_2PHAl$

^1H NMR (500 MHz, $CDCl_3$) δ 8.29 (d, *J* = 9.0 Hz, 2H), 7.93 (d, *J* = 9.0 Hz, 2H), 6.79 (br s, 1H), 4.25-4.23 (m, 1H), 4.13-4.08 (m, 1H), 3.61-3.55 (m, 1H), 3.45 - 3.41(m, 4H), 1.68-1.62 (m, 2H), 1.54-1.35 (m, 2H), 0.95 (t, *J* = 7.5 Hz, 3H)

^{13}C NMR (125 MHz, $CDCl_3$) δ 165.44, 149.74, 139.73, 128.14, 123.90, 82,70, 61.04, 58.27, 43.78, 32.08, 18.90, 14.04

HRMS analysis (ESI): Calculated for $[M+H]^+$: $C_{14}H_{20}ClN_2O_4$: 315.1112; Found: 315.1116

Resolution of enantiomers: DAICEL Chiralcel® AD-H column, 10% IPA-Hexanes, 1.0 mL/min, 254 nm, RT1 (minor) = 11.4 min, RT2 (major) = 14.4 min.

$[\alpha]_D^{20}$ = -19.8 (c = 0.5, $CHCl_3$, *er* = 95.0:5.0)

s-**47i**-*OMe*-NO_2**:** *N*-((2*R*,3*R*)-2-chloro-3-methoxynonyl)-4-nitrobenzamide

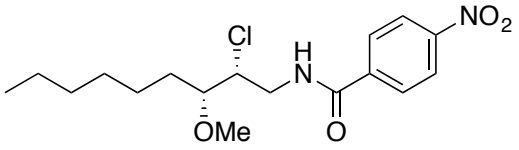

R_f : 0.30 (30% EtOAc in hexanes, UV)

^1H NMR (500 MHz, $CDCl_3$) δ 8.33 (d, *J* = 9.0 Hz, 2H), 7.97 (d, *J* = 9.0 Hz, 2H), 6.85 (br s, 1H), 4.30-4.27 (m, 1H), 4.16-4.15 (m, 1H), 3.64-3.58 (m, 1H), 3.45 (s, 3H), 3.44-3.41 (m, 1H), 1.72-1.68 (m, 2H), 1.39-1.25 (m, 8H), 0.90 (t, *J* = 7.0 Hz, 3H)

^{13}C NMR (125 MHz, $CDCl_3$) δ 165.46, 149.70, 139.70, 128.15, 123.91, 82.90, 61.09, 58.25, 43.82, 31.68, 29.92, 29.25, 25,57, 22.55, 14.06

HRMS analysis (ESI): Calculated for $[M-H]^-$: $C_{16}H_{22}ClN_2O_4$: 341.1268; Found: 341.1272

Resolution of enantiomers: DAICEL Chiralcel® AD-H column, 10% IPA-Hexanes, 1.0 mL/min, 254 nm, RT1 (major) = 10.5 min, RT2 (minor) = 12.7 min.

$[\alpha]_D^{20}$ = +16.5 (c 0.6, $CHCl_3$, *er* = 95:5)

s-**47e**-*OMe*-NO_2**:** *N*-((2*R*,3*R*)-4-(benzyloxy)-2-chloro-3-methoxybutyl)-4-nitrobenzamide

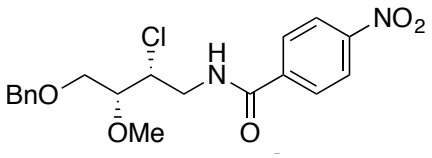

R_f : 0.23 (30% EtOAc in hexanes, UV)

^{1}H NMR (500 MHz, $CDCl_3$) δ 8.25 (d, *J* = 9.0 Hz, 2H), 7.85 (d, *J* = 9.0 Hz, 2H), 7.34-7.32 (m, 5H), 6.79 (br s, 1H), 4.55 (s, 2H), 4.38-4.35 (m, 1H), 4.17-4.03 (m, 1H), 3.80-3.77 (dd, *J* = 9.5, 4.5 Hz, 1H), 3.78-3.67 (m, 3H), 3.48 (s, 3H)

^{13}C NMR (125 MHz, $CDCl_3$) δ 165.40, 149.60, 139.76, 137.46, 128.53, 128.01, 127.82, 123.83, 81.28, 73.82, 68.40, 59.72, 58.85, 43.76

HRMS analysis (ESI): Calculated for $[M-H]^-$: $C_{19}H_{20}ClN_2O_5$: 391.1061; Found: 391.1060

Resolution of enantiomers: DAICEL Chiralcel® IA column, 10% IPA-Hexanes, 1.0 mL/min, 254 nm, RT1 (minor) = 24.6 min, RT2 (major) = 26.8 min.

$[\alpha]_D^{20}$ = +4.1 (c 0.45, $CHCl_3$, *er* = 99:1)

***s*-47j-*OMe*-NO_2:** *N*-((2*R*,3*R*)-5-((*tert*-butyldiphenylsilyl)oxy)-2-chloro-3-methoxypentyl)-4-nitrobenzamide

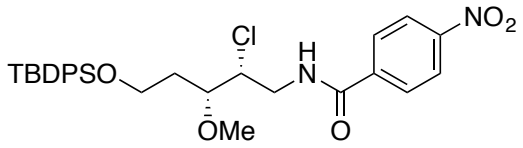

R_f : 0.38 (30% EtOAc in hexanes, UV)

^{1}H NMR (500 MHz, $CDCl_3$) δ 8.28 (d, *J* = 9.0 Hz, 2H), 7.92 (d, *J* = 9.0 Hz, 2H), 7.65-7.63 (m, 5H), 7.41-7.37 (m, 5H), 6.77 (br s, 1H), 4.27 (m, 1H) 4.10-4.07 (m, 1H), 3.81-3.76 (m, 3H), 3.61-3.58 (m, 1H), 3.42 (s, 3H), 1.99-1.94 (m, 1H), 1.81-1.78 (m, 1H), 1.25-1.21 (m,2H), 1.04 (s, 9H)

^{13}C NMR (125 MHz, $CDCl_3$) δ 165.37, 149.73, 139.76, 135.54, 133.49, 133.44, 129.77, 128.13, 127.74, 123.90, 79.76, 61.18, 59.98, 58.42, 43.73, 32.90, 26.86, 19.18

HRMS analysis (ESI): Calculated for $[M+H]^+$: $C_{29}H_{36}ClN_2O_5Si$: 555.2082; Found: 555.2089

Resolution of enantiomers: DAICEL Chiralcel® AD-H column, 3% IPA-Hexanes, 0.7 mL/min, 254 nm, RT1 (minor) = 34.3 min, RT2 (major) = 37.0 min.

$[\alpha]_D^{20}$ = +17.0 (c 0.1, $CHCl_3$, *er* = 99.5:0.5)

47k-*OMe*-NO_2: (*R*)-*N*-(2-chloro-3-methoxy-3-methylbutyl)-4-nitrobenzamide

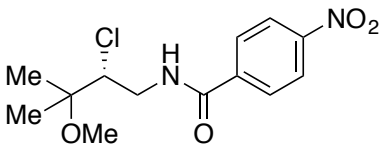

R_f : 0.20 (30% EtOAc in hexanes, UV)

^{1}H NMR (500 MHz, $CDCl_3$) δ 8.29 (d, *J* = 9.0 Hz, 2H), 7.93 (d, *J* = 9.0 Hz, 2H), 6.93(br s, 1H), 4.23-4.19 (m, 1H) 4.07-4.054 (m, 1H), 3.25-3.48 (m, 1H), 3.56-3.52 (m, 1H), 3.30 (s, 3H), 1.35 (s, 3H), 1.32 (s, 3H)

^{13}C NMR (125 MHz, $CDCl_3$) δ 165.32, 149.68, 139.89, 128.10, 123.86, 77.38, 66.77, 49.95, 42.89, 22.97, 21.09

HRMS analysis (ESI): Calculated for $[M+H]^+$: $C_{13}H_{18}ClN_2O_4$: 301.0955; Found: 301.0959

Resolution of enantiomers: DAICEL Chiralcel® OJ-H column, 5% IPA-Hexanes, 0.7 mL/min, 254 nm, RT1 (minor) = 28.3 min, RT2 (major) = 31.0 min.

$[\alpha]_D^{20}$ = +14.0 (c 0.1, $CHCl_3$, *er* = 99.5:0.5)

s-**47c**-*OEt*-NO_2**:** *N*-((2*R*,3*R*)-2-chloro-3-ethoxyhexyl)-4-nitrobenzamide

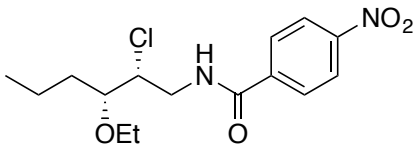

R_f : 0.25 (30% EtOAc in hexanes, UV)

^{1}H NMR (500 MHz, $CDCl_3$) δ 8.29 (d, *J* = 8.5 Hz, 2H), 7.94 (d, *J* = 8.5 Hz, 2H), 6.92 (br s, 1H), 4.25-4.24 (m, 1H), 4.12-4.07 (m, 1H), 3.64-3.57 (m, 3H), 3.55-3.52 (m, 1H), 1.72-1.66 (m, 1H), 1.61-1.55 (m, 1H), 1.55-1.43 (m, 1H), 1.43-1.35 (m, 1H), 1.20 (t, *J* = 6.5 Hz 3H), 0.95 (t, *J* = 7.5 Hz, 3H)

^{13}C NMR (125 MHz, $CDCl_3$) δ 165.35, 149.68, 139.75, 128.15, 123.90, 81.33, 66.15, 60.75, 43.70, 32.30, 19.03, 15.61, 14.05

HRMS analysis (ESI): Calculated for $[M-H]^-$: $C_{15}H_{22}ClN_2O_4$: 329.1268; Found: 329.1273

Resolution of enantiomers: DAICEL Chiralcel® IA column, 5% IPA-Hexanes, 1.0 mL/min, 254 nm, RT1 (major) = 20.3 min, RT2 (minor) = 22.0 min.

$[\alpha]_D^{20}$ = +21.3 (c 0.7, $CHCl_3$, *er* = 99.5:0.5)

s-**47c**-*OAllyl*-NO_2**:** *N*-((2*R*,3*R*)-3-(allyloxy)-2-chlorohexyl)-4-nitrobenzamide

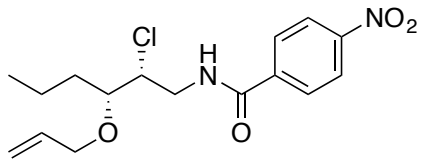

R_f : 0.40 (30% EtOAc in hexanes, UV)

^{1}H NMR (500 MHz, $CDCl_3$) δ 8.28 (d, *J* = 9.0 Hz, 2H), 7.93 (d, *J* = 8.5 Hz, 2H), 6.87 (br s, 1H), 5.94-5.87 (m, 1H), 5.30 (dd, *J* = 15.0, 1.5 Hz, 1H), 5.21 (dd, *J* = 15.0, 1.5 Hz, 1H), 4.26-4.23 (m, 1H), 4.12-4.06 (m, 3H), 3.64-3.59 (m, 2H), 1.72-1.70 (m, 1H), 1.64-1.57 (m, 1H), 1.54-1.37 (m, 2H), 0.93 (t, *J* = 9 Hz, 3H)

^{13}C NMR (125 MHz, $CDCl_3$) δ 165.36, 149.69, 139.65, 134.22, 128.20, 123.86, 118.10, 80.57, 71.44, 60.62, 43.70, 32.20, 18.97, 14.04

HRMS analysis (ESI): Calculated for $[M-H]^-$: $C_{16}H_{20}ClN_2O_4$: 339.1112; Found: 339.1107

Resolution of enantiomers: DAICEL Chiralcel® IA column, 7% IPA-Hexanes, 1.0 mL/min, 254 nm, RT1 (minor) = 16.9 min, RT2 (major) = 17.8 min.

$[\alpha]_D^{20}$ = +13.7 (c 0.5, $CHCl_3$, *er* = 99.5:0.5)

s-**47c**-*OPropargyl*-NO_2**:** *N*-((2*R*,3*R*)-2-chloro-3-(prop-2-yn-1-yloxy)hexyl)-4-nitrobenzamide

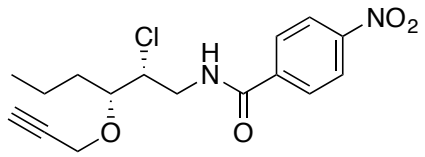

R_f : 0.40 (30% EtOAc in hexanes, UV)

^{1}H NMR (500 MHz, $CDCl_3$) δ 8.28 (d, *J* = 9.0 Hz, 2H), 7.93 (d, *J* = 8.5 Hz, 2H), 6.87 (br s, 1H), 4.36-4.33 (dd, *J* = 16.5, 2.5 Hz, 1H), 4.32-4.29 (m,1H), 4.25-4.21 (dd, *J* = 16.5, 2.5 Hz, 1H), 4.10-4.05 (m, 1H), 3.83-3.80 (m, 1H), 3.69-3.64 (m, 1H), 1.72-1.70 (m, 1H), 1.64-1.57 (m, 1H), 1.54-1.37 (m, 2H), 0.96 (t, *J* = 9 Hz, 3H)

^{13}C NMR (125 MHz, $CDCl_3$) δ 165.49, 149.72, 139.70, 128.21, 123.88, 79.61, 79.02, 75.15, 60.60, 56.67, 43.70, 31.90, 18.72, 14.05

HRMS analysis (ESI): Calculated for $[M-H]^-$: $C_{16}H_{18}ClN_2O_4$: 337.0955; Found: 337.0951

Resolution of enantiomers: DAICEL Chiralcel® IA column, 10% IPA-Hexanes, 1.0 mL/min, 265 nm, RT1 (minor) = 18.8 min, RT2 (major) = 20.3 min.

$[\alpha]_D^{20}$ = +14.0 (c 0.1, $CHCl_3$, *er* = 98:2)

s-**47c**-*OAc*-NO_2**:** (2*R*, 3R)-2-chloro-1-(4-nitrobenzamido)hexan-3-yl acetate

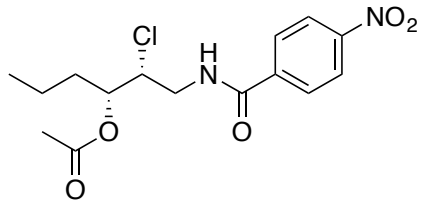

R_f : 0.30 (30% EtOAc in hexanes, UV)

^{1}H NMR (500 MHz, $CDCl_3$) δ 8.30 (d, *J* = 8.5 Hz, 2H), 7.97 (d, *J* = 8.5 Hz, 2H), 7.10 (br s, 1H), 5.17-5.14 (m, 1H), 4.16-4.13 (m, 1H), 4.00-3.95 (m, 1H), 3.36-3.24 (m, 1H), 2.17 (s, 3H), 1.84-1.81 (m, 1H), 1.63-1.61 (m, 1H), 1.35-1.31 (m, 2H), 0.91 (t, *J* = 7.5, 3H)

^{13}C NMR (125 MHz, $CDCl_3$) δ 172.10, 165.13, 149.83, 139.21, 128.20, 123.92, 72.11, 60.32, 42.70, 33.68, 20.92, 18.65, 13.64

HRMS analysis (ESI): Calculated for $[M+H]^+$: $C_{15}H_{20}ClN_2O_5$: 343.1061; Found: 343.1062

Resolution of enantiomers: DAICEL Chiralcel® AD-H column, 7% IPA-Hexanes, 01.0 mL/min, 254 nm, RT1 (major) = 17.6 min, RT2 (minor) = 18.9 min.

$[\alpha]_D^{20}$ = -8.0 (c 0.1, $CHCl_3$, *er* = 98:2)

s-**47c**-*OH*-NO_2**:** *N*-((2*R*,3*R*)-2-chloro-3-hydroxyhexyl)-4-nitrobenzamide

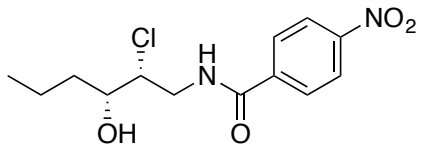

R_f : 0.12 (30% EtOAc in hexanes, UV)

^{1}H NMR (500 MHz, CD_3CN) δ 8.28 (d, *J* = 9.0 Hz, 2H), 7.98 (d, *J* = 8.5 Hz, 2H), 6.93 (br s, 1H), 4.14-4.11 (dt, *J* = 7.0, 2.0 Hz, 2H), 3.90-3.84 (m, 1H), 3.79-3.76 (m, 1H), 3.60-3.55 (m,1H) 3.41 (d, *J* = 6.5 Hz, 1H), 1.60-1.56 (m, 1H), 1.53-1.42 (m, 2H), 1.36-1.31 (m, 1H), 0.91 (t, *J* = 7.5 Hz, 3H)

^{13}C NMR (125 MHz, $CDCl_3$) δ 166.39, 150.08, 140.11, 128.83, 124.02, 70.37, 65.07, 43.79, 36.47, 19.04, 13.61

HRMS analysis (ESI): Calculated for $[M-H]^-$: $C_{13}H_{16}ClN_2O_4$: 299.0799; Found: 299.0796

Resolution of enantiomers: DAICEL Chiralcel® IA column, 15% IPA-Hexanes, 1.0 mL/min, 265 nm, RT1 (major) = 12.3 min, RT2 (minor) = 13.8 min.

$[\alpha]_D^{20}$ = +14.6 (c 0.9, $CHCl_3$, *er* = 99:1)

a-**47c**-*OAc*-NO_2**:** (2*R*,3*S*)-2-chloro-1-(4-nitrobenzamido)hexan-3-yl acetate

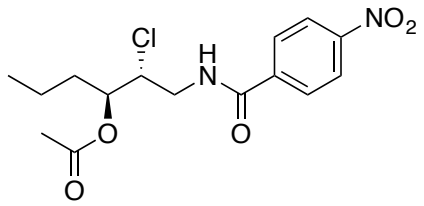

R_f : 0.28 (30% EtOAc in hexanes, UV)

^{1}H NMR (500 MHz, $CDCl_3$) δ 8.30 (d, *J* = 9.0 Hz, 2H), 7.94 (d, *J* = 9.0 Hz, 2H), 6.65 (br s, 1H), 5.13 (m, 1H), 4.19 (m, 2H), 3.49 (m, 1H), 2.19 (s, 3H), 1.79-1.70 (m, 2H), 1.42-1-33 (m, 2H), 0.95 (t, *J* = 7.5 Hz, 3H)

^{13}C NMR (125 MHz, $CDCl_3$) δ 170.81, 165.26, 149.73, 139.60, 128.20, 123.93, 73.53, 61.47, 42.00, 33.34, 20.95, 18.34, 13.77

HRMS analysis (ESI): Calculated for $[M-H]^-$: $C_{15}H_{18}ClN_2O_5$: 341.0904; Found: 341.0903

Resolution of enantiomers: DAICEL Chiralcel® AD-H column, 10% IPA-Hexanes, 1.0 mL/min, 254 nm, RT1 (major) = 12.95 min, RT2 (minor) = 13.9 min.

$[\alpha]_D^{20}$ = +14.0 (c 0.15, $CHCl_3$, *er* = 93:7)

s-**47h**-*OH*-NO_2**:** *N*-((2*R*,3*R*)-2-chloro-3-hydroxypentyl)-4-nitrobenzamide

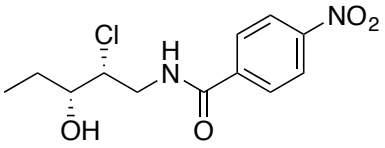

R_f : 0.20 (30% EtOAc in hexanes, UV)

^{1}H NMR (500 MHz, CD_3CN) δ 8.29 (d, *J* = 9.0 Hz, 2H), 7.99 (d, *J* = 9.0 Hz, 2H), 7.60 (br s, 1H), 4.17-4.14 (dt, *J* = 6.5, 1.5 Hz, 1H), 3.90-3.85 (m, 1H), 3.70-3.65 (m, 1H), 3.61-3.55 (m, 1H), 3.42 (d, *J* = 6.5 Hz, 1H), 1.66-1.54 (m, 2H), 0.93 (t, *J* = 8.0 Hz, 3H)

^{13}C NMR (125 MHz, CD_3CN) δ 166.38, 150.10, 140.12, 128.84, 124.03, 72.10, 64.63, 43.77, 27.37, 9.87

HRMS analysis (ESI): Calculated for $[M-H]^-$: $C_{12}H_{14}ClN_2O_4$: 285.0642; Found: 285.0645

Resolution of enantiomers: DAICEL Chiralcel® IA column, 15% IPA-Hexanes, 1.0 mL/min, 254 nm, RT1 (minor) = 13.7 min, RT2 (major) = 15.2 min.

$[\alpha]_D^{20}$ = +6.0 (c 0.45, $CHCl_3$, *er* = 99:1)

Absolute stereochemistry was determined by single crystal X-ray diffraction

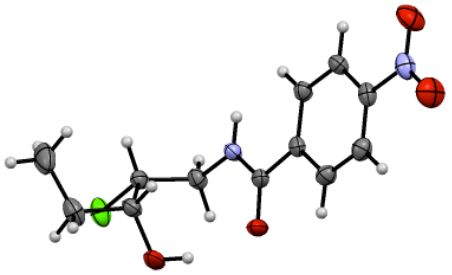

(XRD). Crystals for XRD were obtained by crystallization from CH_2Cl_2 layered with hexanes in a silicone-coated vial.

47k-*OAc*-NO_2**:** ((*R*)-3-chloro-2-methyl-4-(4-nitrobenzamido)butan-2-yl acetate

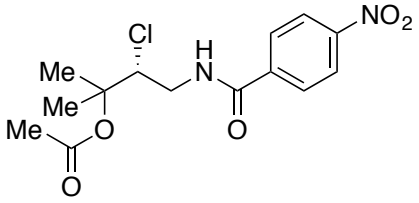

R_f : 0.20 (30% EtOAc in hexanes, UV)

^{1}H NMR (500 MHz, $CDCl_3$) δ 8.30 (d, *J* = 9.0 Hz, 2H), 7.93 (d, *J* = 8.5 Hz, 2H), 6.54 (br s, 1H), 4.60-4.58 (dd, *J* =10.0, 2.5 Hz, 1H) 4.31-4.26 (m, 1H), 3.39-3.33 (m, 1H), 2.03 (s, 3H), 1.62 (s, 3H),1.60 (s, 3H)

^{13}C NMR (125 MHz, $CDCl_3$) δ 170.04, 165.45, 149.80, 139.57, 128.19, 123.93, 82.13, 66.63, 42.44, 23.62, 22.78, 22.17

HRMS analysis (ESI): Calculated for $[M+H]^+$: $C_{14}H_{17}ClN_2O_5$: 329.0904; Found: 304.0906

Resolution of enantiomers: DAICEL Chiralcel® AD-H column, 10% IPA-Hexanes, 1.0 mL/min, 254 nm, RT1 (major) = 22.1 min, RT2 (minor) = 24.4 min.

$[\alpha]_D^{20}$ = +39.2 (c 0.7, $CHCl_3$, *er* = 98:2)

s-**47c'**-*OMe*-NO_2**:** *N*-((2*R*,3*R*)-2-bromo-3-methoxyhexyl)-4-nitrobenzamide

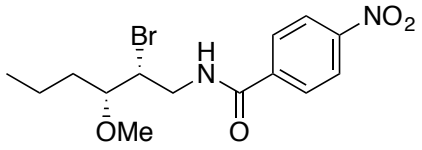

R_f : 0.20 (30% EtOAc in hexanes, UV)

^{1}H NMR (500 MHz, $CDCl_3$) δ 8.30 (d, *J* = 9.0 Hz, 2H), 7.94 (d, *J* = 8.5 Hz, 2H), 6.84 (br s, 1H), 4.38-4.35 (m, 1H), 4.19-4.12 (m, 1H), 3.73-3.68 (m, 1H), 3.39-3.36 (m, 1H), 1.79-1.73 (m, 2H), 1.45-1.39 (m, 2H), 0.98 (t, *J* = 8.0 Hz, 3H)

^{13}C NMR (125 MHz, $CDCl_3$) δ 165.33, 149.70, 139.70, 128.14, 123.92, 82.75, 58.12, 54.75, 44.23, 32.99,18.90,14.02

HRMS analysis (ESI): Calculated for $[M+H]^+$: $C_{14}H_{29}BrN_2O_4$: 359.0606; Found: 359.0604

Resolution of enantiomers: DAICEL Chiralcel® IA column, 10% IPA-Hexanes, 1.0 mL/min, 254 nm, RT1 (major) = 11.9 min, RT2 (minor) = 12.6 min.

$[\alpha]_D^{20}$ = +24.4 (c 0.9, $CHCl_3$, *er* = 99:1)

Absolute stereochemistry was determined by single crystal X-ray diffraction (XRD). Crystals for XRD were obtained by crystallization from CH_2Cl_2 layered with hexanes in a silicone-coated vial.

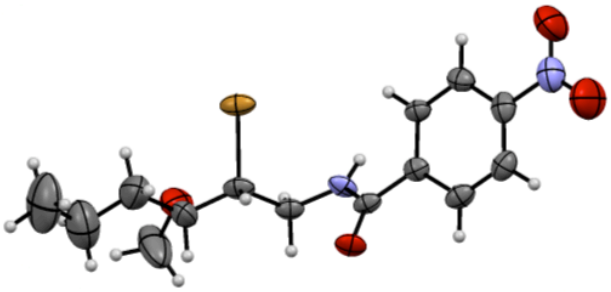

s-**47c'**-*OH*-NO_2**:** *N*-((2*R*,3*R*)-2-bromo-3-hydroxyhexyl)-4-nitrobenzamide

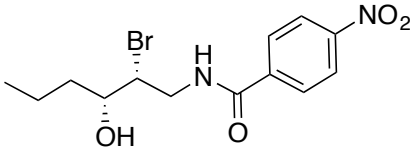

R_f : 0.15 (30% EtOAc in hexanes, UV) 62 % yield

^{1}H NMR (500 MHz, $CDCl_3$) δ 8.29 (d, *J* = 9.0 Hz, 2H), 7.94 (d, *J* = 9.0 Hz, 2H), 6.89 (br s, 1H), 4.30-4.27 (m, 1H), 4.22-4.16 (m, 1H), 3.75-3.70 (m, 1H), 3.65 - 3.62 (m, 4H), 2.17 (d, *J* = 8 Hz), 1.70-1.63 (m, 1H), 1.58-1.35 (m, 3H), 0.95 (t, *J* = 7.0 Hz, 3H)

^{13}C NMR (125 MHz, $CDCl_3$) δ 165.82, 149.78, 139.39, 128.21, 123.94, 71.79, 60.17, 45.04, 38.31, 18.73, 13.88

HRMS analysis (ESI): Calculated for $[M+H]^+$: $C_{13}H_{18}BrN_2O_4$: 345.0450; Found: 345.0434

Resolution of enantiomers: DAICEL Chiralcel® Ia column, 10% IPA-Hexanes, 1.0 mL/min, 254 nm, RT1 (major) = 22.9 min, RT2 (minor) = 24.7 min.

$[\alpha]_D^{20}$ = +11.6 (c = 0.5, $CHCl_3$, *er* = 99.5:0.5)

a-**47c'**-*OH*-NO_2: *N*-((2*R*,3*S*)-2-bromo-3-hydroxyhexyl)-4-nitrobenzamide

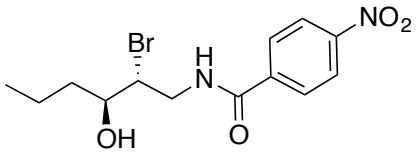

R_f : 0.20 (30% EtOAc in hexanes, UV) 51% yield

^{1}H NMR (500 MHz, $CDCl_3$) δ 8.32 (d, *J* = 9.0 Hz, 2H), 7.97 (d, *J* = 9.0 Hz, 2H), 6.89 (br s, 1H), 4.39-4.32 (ddd, *J* = 15.5, 7.5, 4.0 Hz, 1H), 4.14 (d, *J* = 4.0 Hz 1H), 407-4.04 (m, 1H), 3.73 -3.68 (ddd, J = 15.0, 5.5, 3.5 Hz, 1H), 3.66-3.63 (m, 1H), 1.82-1.77 (m, 1H), 1.61-1.49 (m, 2H), 1.41-1.35 (m, 1H), 0.93 (t, *J* = 7.0 Hz, 3H)

^{13}C NMR (125 MHz, $CDCl_3$) δ 166.88, 149.94, 138.89, 128.34, 124.01, 72.00, 58.49, 42.87, 35.90, 18.94, 13.94

HRMS analysis (ESI): Calculated for $[M+H]^+$: $C_{13}H_{18}BrN_2O_4$: 345.0450; Found: 345.0439

Resolution of enantiomers: DAICEL Chiralcel® OD-H column, 10% IPA-Hexanes, 1.0 mL/min, 254 nm, RT1 (minor) = 24.5 min, RT2 (major) = 29.7 min.

$[\alpha]_D^{20}$ = -15.6 (c = 0.6, $CHCl_3$, *er* = 85.0:15.0)

47k'-*OMe*-NO_2**:** (*S*)-*N*-(2-bromo-3-methoxy-3-methylbutyl)-4-nitrobenzamide

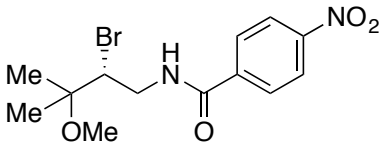

R_f : 0.25 (30% EtOAc in hexanes, UV) 62% yield

^{1}H NMR (500 MHz, $CDCl_3$) δ 8.33 (d, *J* = 9.0 Hz, 2H), 7.97 (d, *J* = 9.0 Hz, 2H), 6.99 (br s, 1H), 4.31-4.23 (m, 2H), 3.65-3.60 (m, 1H), 3.33 (s, 3H), 1.42 (d, *J* = 8.5 Hz, 6H)

^{13}C NMR (125 MHz, $CDCl_3$) δ 165.22, 149.66, 139.86, 128.12, 123.91, 77.06, 61.19, 50.05, 43.45, 23.41,22.42

HRMS analysis (ESI): Calculated for $[M+H]^+$: $C_{13}H_{18}ClN_2O_4$: 345.0450; Found: 345.0441

Resolution of enantiomers: DAICEL Chiralcel® OJ-H column, 10% IPA-Hexanes, 1.0 mL/min, 254 nm, RT1 (minor) = 28.8 min, RT2 (major) = 33.9 min.

$[\alpha]_D^{20}$ = +23.8 (c = 0.7, $CHCl_3$, *er* = 99.5:0.5)

ent-**47k'**-*OMe*-NO_2**:** (*S*)-*N*-(2-bromo-3-methoxy-3-methylbutyl)-4-nitrobenzamide

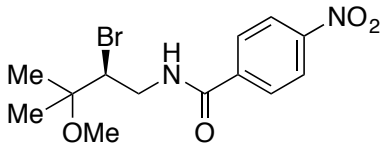

R_f : 0.25 (30% EtOAc in hexanes, UV) 59% yield with $(DHQ)_2$PHAll

^{1}H NMR (500 MHz, $CDCl_3$) δ 8.33 (d, *J* = 9.0 Hz, 2H), 7.97 (d, *J* = 9.0 Hz, 2H), 6.99 (br s, 1H), 4.31-4.23 (m, 2H), 3.65-3.60 (m, 1H), 3.33 (s, 3H), 1.42 (d, *J* = 8.5 Hz, 6H)

^{13}C NMR (125 MHz, $CDCl_3$) δ 165.22, 149.66, 139.86, 128.12, 123.91, 77.06, 61.19, 50.05, 43.45, 23.41,22.42

HRMS analysis (ESI): Calculated for $[M+H]^+$: $C_{13}H_{18}ClN_2O_4$: 345.0450; Found: 345.0439

Resolution of enantiomers: DAICEL Chiralcel® OJ-H column, 10% IPA-Hexanes, 1.0 mL/min, 254 nm, RT1 (major) = 27.8 min, RT2 (minor) = 32.4 min.

$[\alpha]_D^{20}$ = -33.8 (c = 1.0, $CHCl_3$, *er* = 99.5:0.5)

I-2-6-9 Analytical data for byproduct

47c-*NHAc*-NO_2: *N*-(3-acetamido-2-chlorohexyl)-4-nitrobenzamide

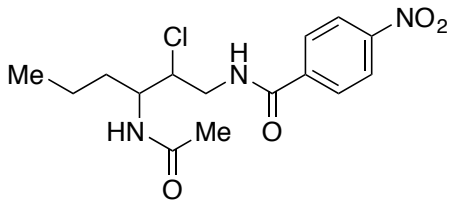

Note: Relative and absolute stereochemistry was not established.

R_f : 0.10 (20% EtOAc in hexanes, UV)

^{1}H NMR (500 MHz, $CDCl_3$) δ 8.30 (d, *J* = 9.0 Hz, 2H), 8.25 (br s, 1H), 8.07 (d, *J* = 9.0 Hz, 2H), 5.58 (d, *J* = 9.5 Hz, 1H), 4.34-4.26 (m, 2H), 4.13-4.09 (m, 1H), 2.93-2.87 (m, 1H), 2.85 (s, 3H), 1.67-1.53 (m, 2H), 1.37-1.32 (m, 2H), 0.88 (t, *J* = 7.5 Hz, 3H)

^{13}C NMR (125 MHz, $CDCl_3$) δ 172.09, 164.76, 149.71, 139.19, 128.35, 123.85, 61.12, 49.31, 42.35, 34.75, 23.29, 19.24, 13.65

HRMS analysis (ESI): Calculated for $[M+H]^+$: $C_{15}H_{21}ClN_3O_4$: 342.1221; Found: 342.1229

I-2-6-10 Analytical data for substrates

E-**1b-**NO_2**:** *N*-cinnamyl-4-nitrobenzamide

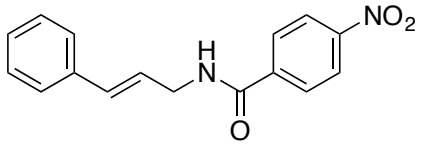

R_f : 0.31 (30% EtOAc in hexanes, UV)

^{1}H NMR (500 MHz, $CDCl_3$) δ 8.28 (d, *J* = 8.5 Hz, 2H), 7.95 (d, *J* = 8.5 Hz, 2H), 7.34-7.25 (m, 5H), 7.23(d, *J* =16.0 Hz, 1H), 6.62 (br s, 1H), 6.59-6.23 (m, 1H), 4.25 (t, *J* = 6.5 Hz, 2H)

^{13}C NMR (125 MHz, $CDCl_3$) δ 165.25, 149.57, 139.90, 136.11, 133.26, 128.65, 128.14, 128.02, 126.39, 124.42, 123.83, 42.44

HRMS analysis (ESI): Calculated for $[M+H]^+$: $C_{16}H_{15}N_2O_3$: 283.1083; Found: 283.1085

E-**1d-**NO_2: (*E*)-*N*-(3-(4-fluorophenyl)allyl)-4-nitrobenzamide

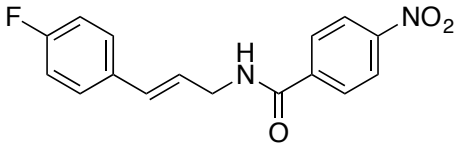

R_f : 0.30 (30% EtOAc in hexanes, UV)

^{1}H NMR (500 MHz, $CDCl_3$) δ 8.32 (d, *J* = 8.5 Hz, 2H), 7.98 (d, *J* = 8.5 Hz, 2H), 7.34-7.31 (m, 2H), 7.01-6.97 (m, 1H), 7.58 (d, *J* =15.5 Hz, 1H), 6.28 (br s, 1H), 6.21-6.15 (m, 1H), 4.25 (t, *J* = 6.0 Hz, 2H)

^{13}C NMR (125 MHz, $CDCl_3$) δ 165.23, 149.69, 139.91, 132.18, 128.14, 128.02 (d, J_{CF} = 30 Hz) , 124.26 (d, J_{CF} = 7.5 Hz) 123.89, 115.70, 115.53, 42.39

HRMS analysis (ESI): Calculated for $[M+H]^+$: $C_{16}H_{14}FN_2O_3$: 301.0988; Found: 301.0991

E-**1c-**NO_2: (*E*)-*N*-(hex-2-en-1-yl)-4-nitrobenzamide

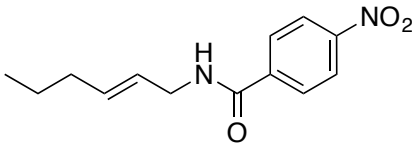

R_f : 0.30 (30% EtOAc in hexanes, UV)

^{1}H NMR (500 MHz, $CDCl_3$) δ 8.27 (d, *J* = 9.0 Hz, 2H), 7.92 (d, *J* = 9.0 Hz, 2H), 6.14 (br s, 1H), 5.72-5.68 (m, 1H) 5.55-5.51 (m, 1H), 4.02 (t, *J* = 6.0 Hz, 2H), 2.03-1.995 (m, 2H), 1.41-1.37 (m, 2H), 0.89 (t, *J* = 7.0 Hz, 3H)

^{13}C NMR (125 MHz, $CDCl_3$) δ 165.09, 149.58, 140.21, 134.96, 128.08, 124.90, 123.81, 42.35, 34.30, 22.19, 13.65

HRMS analysis (ESI): Calculated for $[M+H]^+$: $C_{13}H_{17}N_2O_3$: 249.1239; Found: 249.1243

E-**1a-**NO_2: (*E*)-*N*-(3-cyclohexylallyl)-4-nitrobenzamide

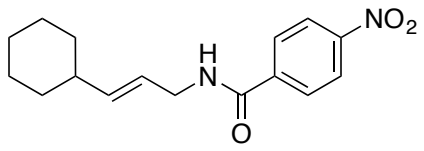

R_f : 0.44 (30% EtOAc in hexanes, UV)

^{1}H NMR (500 MHz, $CDCl_3$) δ 8.27 (d, *J* = 9.0 Hz, 2H), 7.92 (d, *J* = 9.0 Hz, 2H), 6.12 (br s, 1H), 5.67-5.50 (m, 1H), 5.48-5.44 (m, 1H), 4.02 (t, *J* = 6.0 Hz, 2H), 1.94 (m, 1H), 1.71-1.54 (m, 5H), 1.28-1.041 (m, 5H)

^{13}C NMR (125 MHz, $CDCl_3$) δ 165.07, 140.86, 140.22, 128.09, 123.80, 122.26, 116.59, 42.47, 40.36, 32.71, 26.06, 25.93

HRMS analysis (ESI): Calculated for $[M+H]^+$: $C_{16}H_{21}N_2O_3$: 289.1552; Found: 289.1541

E-**1e-**NO_2: (*E*)-*N*-(4-(benzyloxy)but-2-en-1-yl)-4-nitrobenzamide

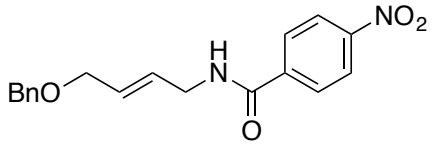

R_f : 0.20 (30% EtOAc in hexanes, UV)

^{1}H NMR (500 MHz, $CDCl_3$) δ 8.26 (d, *J* = 8.0 Hz, 2H), 7.91 (d, *J* = 8.0 Hz, 2H), 7.32-7.26 (m, 4H), 6.27 (br s, 1H), 5.83 (m, 2H), 4.51 (s, 2H), 4.10-4.01(m, 4H)

^{13}C NMR (125 MHz, $CDCl_3$) δ 165.18, 149.62, 139.91, 137.96, 129.87, 128.42, 128.11, 127.99, 127.76, 127.75, 123.82, 72.66, 69.91, 41.67

HRMS analysis (ESI): Calculated for $[M+H]^+$: $C_{18}H_{19}N_2O_4$: 327.1345; Found: 327.1336

Z-**1c-**NO_2: (*Z*)-*N*-(hex-2-en-1-yl)-4-nitrobenzamide

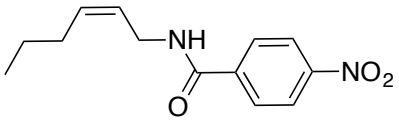

R_f : 0.33 (30% EtOAc in hexanes, UV)

^{1}H NMR (500 MHz, $CDCl_3$) δ 8.25 (d, *J* = 9.0 Hz, 2H), 7.92 (d, *J* = 9.0 Hz, 2H), 6.17 (br s, 1H), 5.63-5.60 (m, 1H), 5.51-5.46 (m, 1H), 4.01 (t, *J* = 6.0 Hz, 2H), 2.12-2.077 (m, 2H), 1.42-1.39 (m, 2H), 0.90 (t, *J* = 7.0 Hz, 3H)

^{13}C NMR (125 MHz, $CDCl_3$) δ 158.14, 142.24, 133.03, 127.60, 120.97, 117.17, 116.67, 30.34, 22.31, 15.46, 6.57

HRMS analysis (ESI): Calculated for $[M+H]^+$: $C_{13}H_{17}N_2O_3$: 249.1239; Found: 249.1244

Z-**1h-**NO_2: (*Z*)-4-nitro-*N*-(pent-2-en-1-yl)benzamide

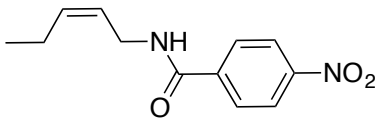

R_f : 0.35 (30% EtOAc in hexanes, UV)

^{1}H NMR (500 MHz, $CDCl_3$) δ 8.28 (d, *J* = 9.0 Hz, 2H), 7.92 (d, *J* = 9.0 Hz, 2H), 6.08 (br s, 1H), 5.66-5.62 (m, 1H), 5.47-5.43 (m, 1H), 4.12 (t, 6.0 Hz, 2H), 2.17-2-19 (m, 2H), 1.02 (t, *J* = 8.0 Hz, 3H)

^{13}C NMR (125 MHz, $CDCl_3$) δ 165.27, 149.50, 140.10, 136.47, 128.09, 123.79, 123.49, 37.35, 20.76, 14.13

HRMS analysis (ESI): Calculated for $[M+H]^+$: $C_{12}H_{25}N_2O_3$: 235.1083; Found: 235.1079

Z-**1i**-NO_2: (*Z*)-4-nitro-*N*-(non-2-en-1-yl)benzamide

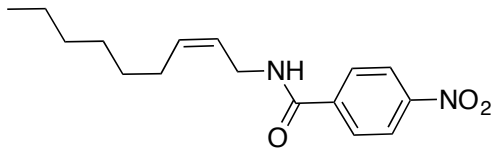

R_f : 0.27 (30% EtOAc in hexanes, UV)

^{1}H NMR (500 MHz, $CDCl_3$) δ 8.27 (d, *J* = 9.0 Hz, 2H), 7,92 (d, *J* = 9.0 Hz, 2H), 6.08 (br s, 1H), 5.65-6.61 (m, 1H), 5.50-5.47 (m, 1H), 4.11 (t, *J* =5.5 Hz, 2H), 2.14 (dd, *J* = 14.0, 7.0 Hz, 2H), 3.46-3.43 (m, 1H), 1.72-1.68 (m, 2H), 1.39-1.25 (m, 8H,) 0.90 (t, *J* = 7.0 Hz, 3H)

^{13}C NMR (125 MHz, $CDCl_3$) δ 165.25, 149.54, 140.11, 135.13, 128.07, 123.99, 123.88, 73.45, 31.67, 29.41, 28.92, 27.46, 22.60, 14.07

HRMS analysis (ESI): Calculated for $[M+H]^+$: $C_{16}H_{23}N_2O_3$: 291.1709; Found: 291.1708

1k-NO_2: *N*-(3-methylbut-2-en-1-yl)-4-nitrobenzamide

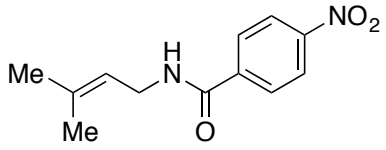

R_f : 0.30 (30% EtOAc in hexanes, UV)

^{1}H NMR (500 MHz, $CDCl_3$) δ 8.26 (d, *J* = 7.5 Hz, 2H), 7.91 (d, *J* = 7.5 Hz, 2H), 6.08 (br s, 1H), 5.28 (t, *J* = 5.5 Hz, 1H), 4.03 (t, *J* = 5.5 Hz, 2H), 1.74 (s, 3H), 1.71 (s, 3H)

^{13}C NMR (125 MHz, $CDCl_3$) δ 165.95, 149.53, 140.24, 137.71, 128.73, 123.33, 119.29, 38.38, 25.67, 17.96

HRMS analysis (ESI): Calculated for $[M+H]^+$: $C_{12}H_{15}ClN_2O_3$: 235.1083; Found: 235.1085

Z-**1b-**NO_2: (*Z*)-4-nitro-*N*-(3-phenylallyl)benzamide

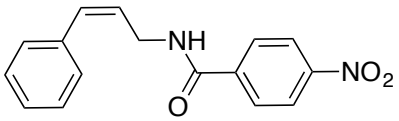

R_f : 0.31 (30% EtOAc in hexanes, UV)

^{1}H NMR (500 MHz, $CDCl_3$) δ 8.25 (d, *J* = 9.0 Hz, 2H), 7.86 (d, *J* = 9.0 Hz, 2H), 7.37-7.26 (m, 5H), 6.41 (d, *J* = 11.5 Hz, 1H), 6.22 (br s, 1H), 5.78-5.73 (m, 1H) 4.39-4.36 (m, 2H)

^{13}C NMR (125 MHz, $CDCl_3$) δ 165.25, 149.62, 139.94, 136.09, 123.62, 128.71, 128.47, 128.08, 127.55, 126.85, 123.81, 38.60

HRMS analysis (ESI): Calculated for $[M+H]^+$: $C_{16}H_{15}N_2O_3$: 283.1083; Found: 283.1091

Z-**1f**-NO_2: (*Z*)-4-nitro-*N*-(3-(*p*-tolyl)allyl)benzamide

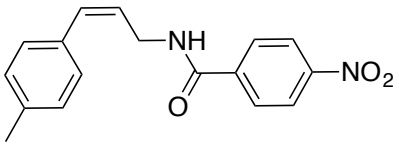

R_f : 0.32 (30% EtOAc in hexanes, UV)

^{1}H NMR (500 MHz, $CDCl_3$) δ 8.26 (d, *J* = 9 Hz, 2H), 7.87 (d, *J* = 9 Hz, 2H), 7.17-7.13 (m, 4H), 6.64 (d, *J* = 12.0 Hz, 1H), 6.17 (br s, 1H), 5.73-5.68 (m, 1H) 4.39-4.36 (m, 1H), 2.34 (s, 3H)

^{13}C NMR (125 MHz, $CDCl_3$) δ 165.29, 149.47, 139.89, 137.39, 133.13, 132.31, 129.10, 128.62, 128.09, 126.12, 123.17, 38.66, 21.15

HRMS analysis (ESI): Calculated for $[M+H]^+$: $C_{117}H_{17}N_2O_3$: 297.1239; Found: 297.1234

Z-**1g-**NO_2: (*Z*)-*N*-(3-(4-methoxyphenyl)allyl)-4-nitrobenzamide

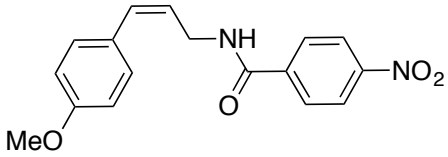

R_f : 0.25 (30% EtOAc in hexanes, UV)

^{1}H NMR (500 MHz, $CDCl_3$) δ 8.27 (d, *J* = 9.0 Hz, 2H), 7.89 (d, *J* = 9.0 Hz, 2H), 7.20 (d, *J* = 8.0 Hz, 2H), 6.90 (d, *J* = 8.0 Hz, 2H), 6.61 (d, *J* = 11.5 Hz), 6.17 (br s, 1H), 5.68-5.63 (m, 1H), 4.39-4.36 (m, 2H), 3.80 (s, 3H)

^{13}C NMR (125 MHz, $CDCl_3$) δ 165.29, 158.96, 149.54, 139.94, 132.08, 130.04, 128.59, 128.13, 125.10, 123.80, 113.85, 55.28, 38.68

HRMS analysis (ESI): Calculated for $[M-H]^-$: $C_{17}H_{15}N_2O_4$: 311.1032; Found: 311.1027

Z-**1e-**NO_2: (*Z*)-*N*-(4-(benzyloxy)but-2-en-1-yl)-4-nitrobenzamide

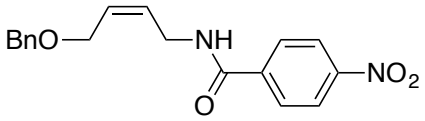

R_f : 0.27 (30% EtOAc in hexanes, UV)

^{1}H NMR (500 MHz, $CDCl_3$) δ 8.15 (d, *J* = 9.0 Hz, 2H), 7.73 (d, *J* = 9.0 Hz, 2H), 7.33-7.28 (m, 5H), 6.47 (br s, 1H), 5.92-5-80 (m, 2H), 4.53 (s, 2H), 4.17 (d, *J* = 16.0 Hz, 2H), 4.11 (t, 2H)

^{13}C NMR (125 MHz, $CDCl_3$) δ 164.96, 149.43, 139.82, 137.63, 130.36, 129.22, 128.60, 128.06, 128.04, 128.00, 123.71, 73.00, 65.85, 37.22

HRMS analysis (ESI): Calculated for $[M+H]^+$: $C_{18}H_{19}N_2O_4$: 327.1345; Found: 327.1350

Z-**1j-**NO_2: (*Z*)-*N*-(5-((*tert*-butyldiphenylsilyl)oxy)pent-2-en-1-yl)-4-nitrobenzamide

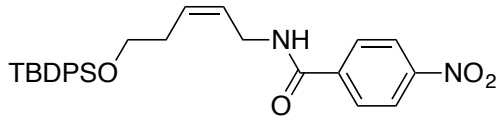

R_f : 0.35 (30% EtOAc in hexanes, UV)

^{1}H NMR (500 MHz, $CDCl_3$) δ 8.18 (d, *J* = 8.0 Hz, 2H), 7.76 (d, *J* = 8.0 Hz, 2H), 7.66-7.63 (m, 5H), 7.37-7.24 (m, 5H), 6.02 (br s, 1H), 5.70-5.67 (m, 1H) 5.62-

5.60 (m, 1H) 4.06 (t, *J* = 6.5 Hz, 2H), 3.74 (t, *J* =6.5 Hz, 2H), 2.40 (dt, *J* = 6.5 Hz, 2H), 1.03 (s, 9H)

^{13}C NMR (125 MHz, $CDCl_3$) δ 165.22, 149.47, 140.02, 135.53, 135.48, 133.75, 131.24, 129.72, 128.02, 127.70, 126.16, 123.80, 123.72, 63.21, 37.41, 30.85, 26.87, 26.77, 19.28

HRMS analysis (ESI): Calculated for $[M+H]^+$: $C_{28}H_{33}N_2O_4Si$: 489.2210; Found: 489.2214

I-2-6-11 Analytical data for different products of chloroetherification reaction without catalyst

s-**5c**-*OMe*-NO_2: 3-chloro-2-methoxyhexyl)-4-nitrobenzamide

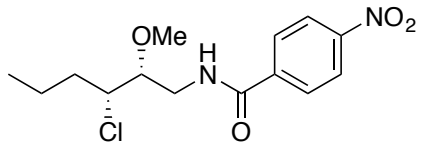

^{1}H NMR (500 MHz, $CDCl_3$) δ 8.29 (d, *J* = 9.0 Hz, 2H), 7.93 (d, *J* = 9.0 Hz, 2H), 6.52 (br s, 1H), 4.05-4.02 (m, 1H), 3.92-3.86 (m, 1H), 3.63-3.54 (m, 2H), 3.51 (s, 3H), 1.87-1.72 (m, 2H), 1.66-1.59 (m, 1H), 1.47-1.38 (m, 1H), 0.95 (t, *J* = 7.5 Hz, 3H)

^{13}C NMR (125 MHz, $CDCl_3$) δ 165.49, 149.73, 139.79, 128.11, 123.92, 81,53, 62.18, 59.22, 40.56, 35.49, 19.93, 13.4

s-**4c**-NO_2: 1-chlorobutyl-2-(4-nitrophenyl)-4,5-dihydrooxazole

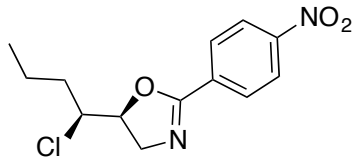

^{1}H NMR (500 MHz, $CDCl_3$) δ 8.27 (d, *J* = 8.5 Hz, 2H), 8.12 (d, *J* = 8.5 Hz, 2H), 4.93-4.89 (m, 1H), 4.22 (dd, *J* = 15.0, 10.0 Hz, 1H), 4.17 (dd, *J* = 15.0, 10.0 Hz, 1H), 3.99-3.97 (m, 1H), 1.85-1.71 (m, 2H), 1.69-1.63 (m, 1H), 1.51-1.45 (m, 1H), 0.97 (t, *J* =7.5 Hz, 3H)

^{13}C NMR (125 MHz, $CDCl_3$) δ 162.22, 149.57, 132.98, 129.27, 123,59, 81.69, 62.92, 57.85, 35.51, 19.66, 13.45

HRMS analysis (ESI): Calculated for $[M+H]^+$: $C_{13}H_{16}N_2O_3Cl$: 283.0849; Found: 283.0861

Relative stereochemistry was determined by single crystal X-ray diffraction (XRD). Crystals for XRD were obtained by crystallization from CH_2Cl_2 layered with hexanes in a silicone-coated vial.

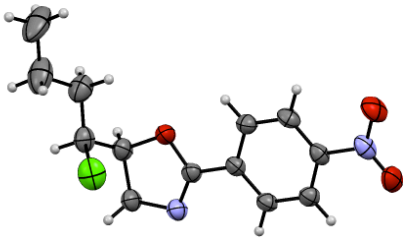

a-**5c**-*OMe*-NO_2: 3-chloro-2-methoxyhexyl)-4-nitrobenzamide

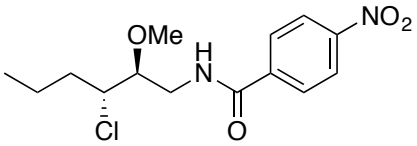

^1H NMR (500 MHz, $CDCl_3$) δ 8.29 (d, *J* = 9.0 Hz, 2H), 7.93 (d, *J* = 9.0 Hz, 2H), 6.55 (br s, 1H), 4.11-4.07 (m, 1H), 3.99-3.95 (m, 1H), 3.56-3.51 (m, 1H), 3.50-3.47 (m, 4H), 1.84 -1.79 (m, 1H), 1.69-1.63 (m, 1H), 1.48-1.41 (m, 2H), 0.97 (t, *J* = 7.5 Hz, 3H)

^{13}C NMR (125 MHz, $CDCl_3$) δ 165.46, 149.63, 139.86, 128.12, 123.89, 81.70, 61.21, 57.93, 39.79, 36.26, 19.96, 13.53

a-**4c**-NO_2: chlorobutyl-2-(4-nitrophenyl)-4,5-dihydrooxazole

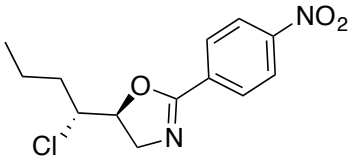

^{1}H NMR (500 MHz, $CDCl_3$) δ 8.26 (d, *J* = 8.5 Hz, 2H), 8.10 (d, *J* = 8.5 Hz, 2H), 4.82-4.77 (m, 1H), 4.21 (dd, *J* = 16.0, 10.0 Hz, 1H), 4.09-4.03 (m, 2H), 1.85-1.83 (m, 1H), 1.69-1.66 (m, 2H), 1.47-1.43 (m, 1H), 0.98 (t, *J* =7.5 Hz, 3H)

^{13}C NMR (125 MHz, $CDCl_3$) δ 161.86, 149.54, 133.11, 129.19, 123.59, 82.03, 63.02, 57.96, 35.85, 19.28, 13.49

t-**3c**-NO_2: 5-chloro-2- (4-nitrophenyl)-6-propyl-5,6-dihydro-4*H*-1,3-oxazine

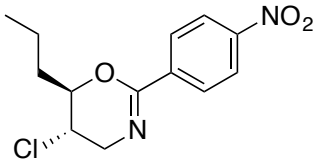

^{1}H NMR (500 MHz, $CDCl_3$) δ 8.21 (d, *J* = 8.5 Hz, 2H), 8.06 (d, *J* = 8.5 Hz, 2H), 4.26 (dt, *J* = 8.5, 3.0 Hz, 1H), 3.02-3.94 (m, 2H), 3.70 (dd, *J* = 16.5, 7.0 Hz, 1H), 1.99-194 (m, 1H), 1.71-1.64 (m, 2H), 1.55-1.51 (m, 1H), 1.03 (t, *J* =7.5 Hz, 3H)

^{13}C NMR (125 MHz, $CDCl_3$) δ 153.32, 149.22, 138.64, 128.19, 123.30, 78.85, 52.44, 50.48, 34.48, 18.02, 13.84

HRMS analysis (ESI): Calculated for $[M+H]^+$: $C_{13}H_{16}N_2O_3Cl$: 283.0849; Found: 283.0863

Relative stereochemistry was determined by single crystal X-ray diffraction (XRD). Crystals for XRD were obtained by crystallization from CH_2Cl_2 layered with hexanes in a silicone-coated vial.

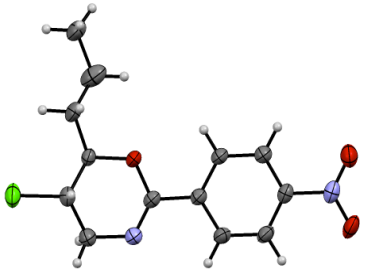

REFERENCES

REFERENCES

1. Arai, T.; Watanabe, O.; Yabe, S.; Yamanaka, M., Catalytic Asymmetric Iodocyclization of N-Tosyl Alkenamides using Aminoiminophenoxy Copper Carboxylate: A Concise Synthesis of Chiral 8-Oxa-6-Azabicyclo[3.2.1]octanes. *Angew. Chem. Int. Ed. Engl.* **2015,** *54* (43), 12767-71.

2. Ashtekar, K. D.; Marzijarani, N. S.; Jaganathan, A.; Holmes, D.; Jackson, J. E.; Borhan, B., A new tool to guide halofunctionalization reactions: the halenium affinity (HalA) scale. *J. Am. Chem. Soc.* **2014,** *136* (38), 13355-62.

3. Cai, Y.; Zhou, P.; Liu, X.; Zhao, J.; Lin, L.; Feng, X., Diastereoselectively switchable asymmetric haloaminocyclization for the synthesis of cyclic sulfamates. *Chem. Eur. J.* **2015,** *21* (17), 6386-9.

4. Cai, Y. F.; Liu, X. H.; Hui, Y. H.; Jiang, J.; Wang, W. T.; Chen, W. L.; Lin, L. L.; Feng, X. M., Catalytic Asymmetric Bromoamination of Chalcones: Highly Efficient Synthesis of Chiral alpha-Bromo-beta-Amino Ketone Derivatives. *Angew. Chem. Int. Ed.* **2010,** *49* (35), 6160-6164.

5. Castellanos, A.; Fletcher, S. P., Current methods for asymmetric halogenation of olefins. *Chem. Eur. J.* **2011,** *17* (21), 5766-76.

6. Chen, G.; Ma, S., Enantioselective halocyclization reactions for the synthesis of chiral cyclic compounds. *Angew. Chem. Int. Ed. Engl.* **2010,** *49* (45), 8306-8.

7. Chen, J.; Zhou, L., Recent Progress in the Asymmetric Intermolecular Halogenation of Alkenes. *Synthesis-Stuttgart* **2014,** *46* (5), 586-595.

8. Cheng, Y. A.; Yu, W. Z.; Yeung, Y. Y., Recent advances in asymmetric intra- and intermolecular halofunctionalizations of alkenes. *Org. Biomol. Chem.* **2014,** *12* (15), 2333-43.

9. Cheng, Y. A.; Yu, W. Z.; Yeung, Y. Y., Carbamate-catalyzed enantioselective bromolactamization. *Angew. Chem. Int. Ed. Engl.* **2015,** *54* (41), 12102-6.

10. Denmark, S. E.; Kuester, W. E.; Burk, M. T., Catalytic, asymmetric halofunctionalization of alkenes--a critical perspective. *Angew. Chem. Int. Ed. Engl.* **2012,** *51* (44), 10938-53.

11. Dobish, M. C.; Johnston, J. N., Achiral Counterion Control of Enantioselectivity in a Brønsted Acid-Catalyzed Iodolactonization. *J. Am. Chem. Soc.* **2012,** *134* (14), 6068-6071.

12. Fang, C.; Paull, D. H.; Hethcox, J. C.; Shugrue, C. R.; Martin, S. F., Enantioselective Iodolactonization of Disubstituted Olefinic Acids Using a Bifunctional Catalyst. *Org. Lett.* **2012,** *14* (24), 6290-6293.

13. Hennecke, U., New catalytic approaches towards the enantioselective halogenation of alkenes. *Chem. Asian J.* **2012,** *7* (3), 456-465.

14. Hennecke, U.; Wilking, M., Desymmetrization as a Strategy in Asymmetric Halocyclization Reactions. *Synlett* **2014,** *25* (12), 1633-1637.

15. Jaganathan, A.; Borhan, B., Chlorosulfonamide salts are superior electrophilic chlorine precursors for the organocatalytic asymmetric chlorocyclization of unsaturated amides. *Org. Lett.* **2014,** *16* (14), 3616-9.

16. Jaganathan, A.; Garzan, A.; Whitehead, D. C.; Staples, R. J.; Borhan, B., A catalytic asymmetric chlorocyclization of unsaturated amides. *Angew. Chem. Int. Ed. Engl.* **2011,** *50* (11), 2593-6.

17. Jaganathan, A.; Staples, R. J.; Borhan, B., Kinetic resolution of unsaturated amides in a chlorocyclization reaction: concomitant enantiomer differentiation and face selective alkene chlorination by a single catalyst. *J. Am. Chem. Soc.* **2013,** *135* (39), 14806-13.

18. Ke, Z.; Tan, C. K.; Chen, F.; Yeung, Y. Y., Catalytic asymmetric bromoetherification and desymmetrization of olefinic 1,3-diols with C2-symmetric sulfides. *J. Am. Chem. Soc.* **2014,** *136* (15), 5627-30.

19. Mizar, P.; Burrelli, A.; Gunther, E.; Softje, M.; Farooq, U.; Wirth, T., Organocatalytic stereoselective iodoamination of alkenes. *Chem. Eur. J.* **2014,** *20* (41), 13113-6.

20. Murai, K.; Fujioka, H., Recent Progress in Organocatalytic Asymmetric Halocyclization. *Heterocycles* **2013,** *87* (4), 763-805.

21. Nakatsuji, H.; Sawamura, Y.; Sakakura, A.; Ishihara, K., Cooperative activation with chiral nucleophilic catalysts and N-haloimides: enantioselective iodolactonization of 4-arylmethyl-4-pentenoic acids. *Angew. Chem. Int. Ed. Engl.* **2014,** *53* (27), 6974-7.

22. Tan, C. K.; Yeung, Y. Y., Recent advances in stereoselective bromofunctionalization of alkenes using N-bromoamide reagents. *Chem. Commun.* **2013,** *49* (73), 7985-96.

23. Tan, C. K.; Zhou, L.; Yeung, Y. Y., Organocatalytic Enantioselective Halolactonizations: Strategies of Halogen Activation. *Synlett* **2011,** (10), 1335-1339.

24. Toda, Y.; Pink, M.; Johnston, J. N., Bronsted acid catalyzed phosphoramidic acid additions to alkenes: diastereo- and enantioselective halogenative cyclizations for the synthesis of C- and P-chiral phosphoramidates. *J. Am. Chem. Soc.* **2014,** *136* (42), 14734-7.

25. Tripathi, C. B.; Mukherjee, S., Catalytic Enantioselective 1,4-Iodofunctionalizations of Conjugated Dienes. *Org. Lett.* **2015,** *17* (18), 4424-7.

26. Veitch, G. E.; Jacobsen, E. N., Tertiary aminourea-catalyzed enantioselective iodolactonization. *Angew. Chem. Int. Ed. Engl.* **2010,** *49* (40), 7332-5.

27. Wang, Y.-M.; Wu, J.; Hoong, C.; Rauniyar, V.; Toste, F. D., Enantioselective Halocyclization Using Reagents Tailored for Chiral Anion Phase-Transfer Catalysis. *J. Am. Chem. Soc.* **2012,** *134* (31), 12928-12931.

28. Whitehead, D. C.; Yousefi, R.; Jaganathan, A.; Borhan, B., An Organocatalytic Asymmetric Chlorolactonization. *J. Am. Chem. Soc.* **2010,** *132* (10), 3298-3300.

29. Wilking, M.; Muck-Lichtenfeld, C.; Daniliuc, C. G.; Hennecke, U., Enantioselective, desymmetrizing bromolactonization of alkynes. *J. Am. Chem. Soc.* **2013,** *135* (22), 8133-6.

30. Xie, W.; Jiang, G.; Liu, H.; Hu, J.; Pan, X.; Zhang, H.; Wan, X.; Lai, Y.; Ma, D., Highly enantioselective bromocyclization of tryptamines and its application in the synthesis of (-)-chimonanthine. *Angew. Chem. Int. Ed. Engl.* **2013,** *52* (49), 12924-7.

31. Yin, Q.; You, S. L., Asymmetric chlorocyclization of indole-3-yl-benzamides for the construction of fused indolines. *Org. Lett.* **2014,** *16* (9), 2426-9.

32. Yousefi, R.; Ashtekar, K. D.; Whitehead, D. C.; Jackson, J. E.; Borhan, B., Dissecting the stereocontrol elements of a catalytic asymmetric

chlorolactonization: syn addition obviates bridging chloronium. *J. Am. Chem. Soc.* **2013,** *135* (39), 14524-7.

33. Zeng, X.; Miao, C.; Wang, S.; Xia, C.; Sun, W., Asymmetric 5-endo chloroetherification of homoallylic alcohols toward the synthesis of chiral beta-chlorotetrahydrofurans. *Chem. Commun.* **2013,** *49* (24), 2418-20.

34. Zhang, W.; Liu, N.; Schienebeck, C. M.; Zhou, X.; Izhar, I. I.; Guzei, I. A.; Tang, W. P., Enantioselective intermolecular bromoesterification of allylic sulfonamides. *Chem. Sci.* **2013,** *4* (6), 2652-2656.

35. Zheng, S. Q.; Schienebeck, C. M.; Zhang, W.; Wang, H. Y.; Tang, W. P., Cinchona Alkaloids as Organocatalysts in Enantioselective Halofunctionalization of Alkenes and Alkynes. *Asian J. Org. Chem.* **2014,** *3* (4), 366-376.

36. Cai, Y. F.; Liu, X. H.; Jiang, J.; Chen, W. L.; Lin, L. L.; Feng, X. M., Catalytic Asymmetric Chloroamination Reaction of alpha,beta-Unsaturated gamma-Keto Esters and Chalcones. *J. Am. Chem. Soc.* **2011,** *133* (15), 5636-5639.

37. Cai, Y. F.; Liu, X. H.; Li, J.; Chen, W. L.; Wang, W. T.; Lin, L. L.; Feng, X. M., Asymmetric Iodoamination of Chalcones and 4-Aryl-4-oxobutenoates Catalyzed by a Complex Based on Scandium(III) and a N,N '-Dioxide Ligand. *Chem. Eur. J.* **2011,** *17* (52), 14916-14921.

38. Li, G.-x.; Fu, Q.-q.; Zhang, X.-m.; Jiang, J.; Tang, Z., First asymmetric intermolecular bromoesterification catalyzed by chiral Brønsted acid. *Tetrahedron: Asymmetry* **2012,** *23* (3–4), 245-251.

39. Honjo, T.; Phipps, R. J.; Rauniyar, V.; Toste, F. D., A doubly axially chiral phosphoric acid catalyst for the asymmetric tandem oxyfluorination of enamides. *Angew. Chem. Int. Ed. Engl.* **2012,** *51* (38), 9684-8.

40. Zhang, Y.; Xing, H.; Xie, W.; Wan, X.; Lai, Y.; Ma, D., Asymmetric, Regioselective Bromohydroxylation of 2-Aryl-2-porpen-1-ols Catalyzed by Quinine-Derived Catalysts. *Adv. Synth. Catal.* **2013,** *355*, 68-72.

41. Brucks, A. P.; Treitler, D. S.; Liu, S.-A.; Snyder, S. A., Explorations into the Potential of Chiral Sulfonium Reagents to Effect Asymmetric Halonium Additions to Isolated Alkenes. *Synthesis-Stuttgart* **2013,** *45* (13), 1886-1898.

42. Nicolaou, K. C.; Simmons, N. L.; Ying, Y. C.; Heretsch, P. M.; Chen, J. S., Enantioselective Dichlorination of Allylic Alcohols. *J. Am. Chem. Soc.* **2011,** *133* (21), 8134-8137.

43. Hu, D. X.; Shibuya, G. M.; Burns, N. Z., Catalytic Enantioselective Dibromination of Allylic Alcohols. *J. Am. Chem. Soc.* **2013,** *135* (35), 12960-12963.

44. Gribble, G. W., Naturally occurring organohalogen compounds--a comprehensive survey. *Fortschr. Chem. Org. Naturst.* **1996,** *68*, 1-423.

45. Gribble, G. W., Introduction. *Fortschr. Chem. Org. Naturst.* **2010,** *91*, 1.

46. Gribble, G. W., Occurrence of halogenated alkaloids. *Alkaloids Chem. Biol.* **2012,** *71*, 1-165.

47. Katsuki, T.; Sharpless, K. B., The first practical method for asymmetric epoxidation. *J. Am. Chem. Soc.* **1980,** *102* (18), 5974-5976.

48. Jacobsen, E. N.; Marko, I.; Mungall, W. S.; Schroeder, G.; Sharpless, K. B., Asymmetric dihydroxylation via ligand-accelerated catalysis. *J. Am. Chem. Soc.* **1988,** *110* (6), 1968-1970.

49. Evans, D. A.; Faul, M. M.; Bilodeau, M. T.; Anderson, B. A.; Barnes, D. M., Bis(oxazoline)-copper complexes as chiral catalysts for the enantioselective aziridination of olefins. *J. Am. Chem. Soc.* **1993,** *115* (12), 5328-5329.

50. Chemler, S. R.; Bovino, M. T., Catalytic Aminohalogenation of Alkenes and Alkynes. *ACS Catal.* **2013,** *3* (6), 1076-1091.

51. Hennecke, U., A new approach towards the asymmetric fluorination of alkenes using anionic phase-transfer catalysts. *Angew. Chem. Int. Ed. Engl.* **2012,** *51* (19), 4532-4534.

52. Denmark, S. E.; Burk, M. T.; Hoover, A. J., On the Absolute Configurational Stability of Bromonium and Chloronium Ions. *J. Am. Chem. Soc.* **2010,** *132* (4), 1232-1233.

53. Neverov, A. A.; Brown, R. S., Br+ and I+ Transfer from the Halonium Ions of Adamantylideneadamantane to Acceptor Olefins. Halocyclization of 1,ω-Alkenols and Alkenoic Acids Proceeds via Reversibly Formed Intermediates. *J. Org. Chem.* **1996,** *61* (3), 962-968.

54. Olah, G. A.; Bollinger, J. M., Stable carbonium ions. 33. Primary alkoxycarbonium ions. *J. Am. Chem. Soc.* **1967,** *89* (12), 2993-6.

55. Olah, G. A.; Westerman, P. W.; Melby, E. G.; Mo, Y. K., Onium ions. X. Structural study of acyclic and cyclic halonium ions by carbon-13 nuclear

magnetic resonance spectroscopy. Question of intra- and intermolecular equilibration of halonium ions with haloalkylcarbenium ions. *J. Am. Chem. Soc.* **1974,** *96* (11), 3565-3573.

56. Ohta, B. K.; Hough, R. E.; Schubert, J. W., Evidence for beta-chlorocarbenium and beta-bromocarbenium ions. *Org. Lett.* **2007,** *9* (12), 2317-20.

57. Lei, A.; Wu, S.; He, M.; Zhang, X., Highly Enantioselective Asymmetric Hydrogenation of α-Phthalimide Ketone: An Efficient Entry to Enantiomerically Pure Amino Alcohols. *J. Am. Chem. Soc.* **2004,** *126* (6), 1626-1627.

58. Panzik, H. L.; Mulvaney, J. E., Polyampholyte synthesis by cyclopolymerization. *J. Polym. Sci., Part A: Polym. Chem.* **1972,** *10* (12), 3469-3487.

Chapter II: Highly Regio-and Enantioselective Vicinal Dihalogenation of Allyl Amides

II-1 Introduction

Halogenated natural products represent a class of structurally diverse molecules with some estimates suggesting that greater than 4000 molecules belong to this ever-growing class of natural products.[1-4] They are challenging synthetic targets, at least in part, due to the paucity of methods available to install C-halogen bonds in an enantioselective fashion. The development of enantioselective vicinal dihalogenation of easily accessed alkenes represents a straightforward means of accessing these motifs and avoids circuitous functional group transformations to convert chiral alcohols or epoxides to alkyl halides. With the advent of numerous methodologies for asymmetric halofunctionalization of alkenes in recent years,[5-43] the challenging asymmetric vicinal dihalogenation reaction of alkenes has come into focus. Most of the well-established asymmetric halofunctionalizations reported till date, have achieved enantioselective C-X (X = Cl, Be, I or F) bond formation along with a concomitant formation of a C-O, C-N or even a C-C bond formation depending on the nucleophile employed in intercepting the putative intermediate. In contrast, halide nucleophiles that could lead to dihalogenated products have not been employed with the same levels of success.

II-1-1 Racemization of chiral halonium ion by olefin to olefin halenium transfer

Olefin dihalogenation proceeds in two steps: first the halonium ion is formed followed by subsequent nucleophilic attack to the putative halonium ion, the absolute configuration of the dihalide products is decided during the first step (formation of halonium ion intermediate). For producing chiral halonium ion, the halenium ion transfers to alkenes from the halogenating agent should be irreversible, and the halonium ion should be stable prior to nucleophilic trapping (Figure II-1).

Figure II-1: Alkene dihalogenation reaction proceeding by a two-step mechanism

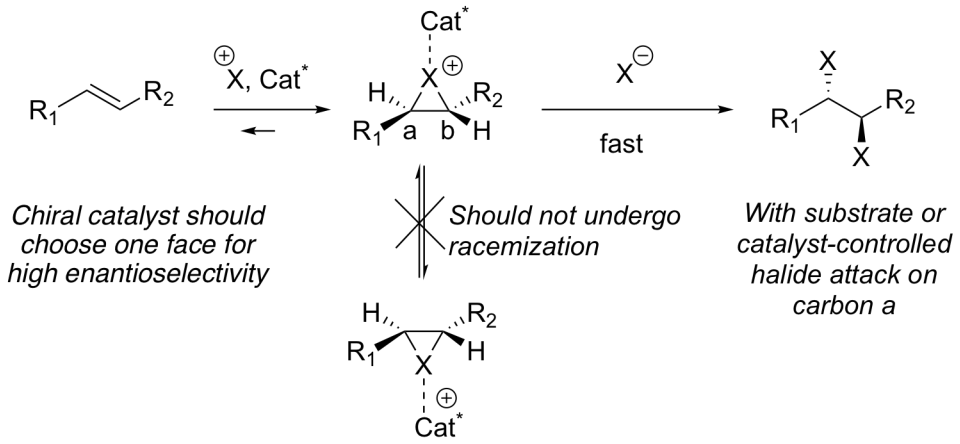

A simple difficulty in formation of enantioselective halonium ion is the distance between olefin and chiral catalyst that is covalently or through hydrogen binding associated with the halogen donor. This range arises because the alkene should approach the σ^* orbital of the Cat*-X bond. The anticipated coordination geometry for this approach is 180°. This stereoelectronic approach leads to a

significant distance between the chiral catalyst and the alkene, thus induction of enantioselectivity from the catalyst to alkenes for the formation of chiral halonium ion is difficult (Figure II-2a). Generally, electrophilic species such as osmium tetraoxide that can approach to alkenes with π^* orbitals enable more diverse geometries.[15] Therefore, the enantiomeric induction and communication between the catalyst and alkenes is simpler than the first case (Figure II-2a). As we mentioned in Section **I-1-2**, even if chiral halonium ions can be formed with high enantioselectivity, these chiral intermediates (especially bromonium ions) are most likely undergo through rapid stereochemical degradation by olefin-to-olefin halonium tion ransfer (Figure II-2b).[44]

Figure II-2: (a) Challenges in stereochemical communication (b) Racemization via olefin-to-olefin halenium transfer

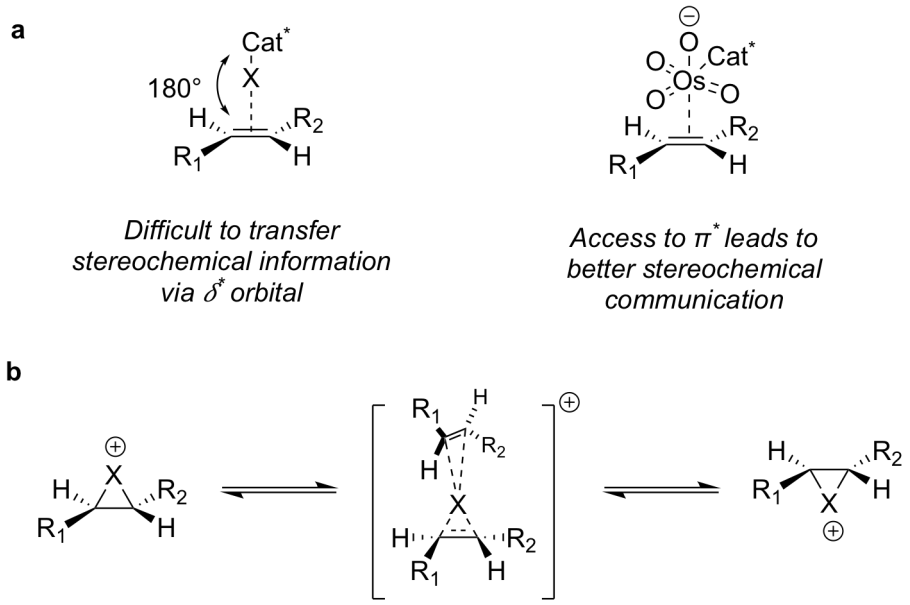

If the chiral halonium ion is formed and the nucleophilic attack event is kinetically more competitive than olefin-to-olefin racemization, still dihalogenation

transformation represents a unique challenge in that a poor *regioselectivity* in the halide opening of the putative chiral halonium ion intermediate can erode the *enantioselectivity* of the transformation; the two 'constitutional isomers' resulting from the regioselectivity of the transformation are in fact the two enantiomers of the product (see Figure II-3). Hence, in addition to exquisite face selectivity in alkene halogenation, excellent control of regioselectivity is also imperative (Figure II-3). It is perhaps not surprising that many of the substrates that have succumbed to highly enantioselective dihalogenations are *electronically biased* – employing styryl systems leads to an inherent bias for the halide opening at the benzylic position.[15, 45] The development of a *catalyst-controlled* regioselectivity as opposed to a substrate controlled process holds promise in significantly improving the scope of the transformation and thereby offers an efficient means to synthesizing natural products.

Figure II-3: Mechanistic challenges for asymmetric dihalogenation

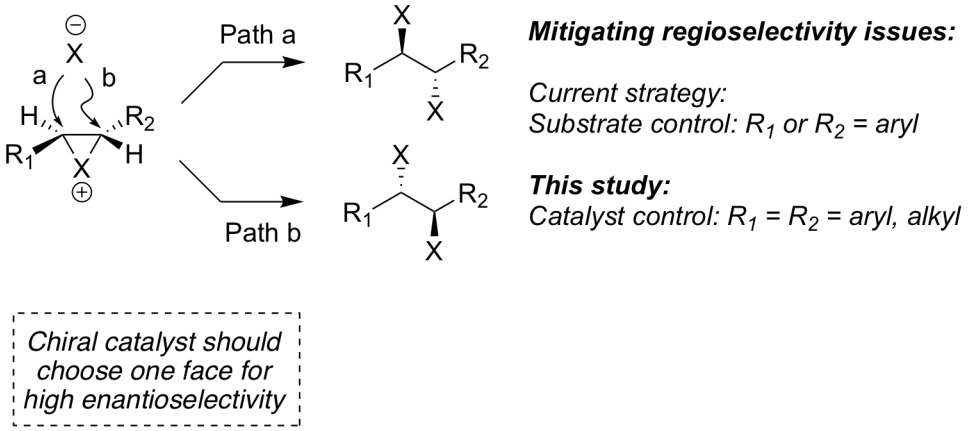

II-1-2 Literature precedence for enantioselective vicinal dihalogenation of alkenes

A few landmark achievements in dihalogenation chemistry merit mention. Snyder's group has reported an enantioselective total synthesis of (-)-Napyradiomycin **II-4** that featured an asymmetric dichlorination of an advanced precursor using chlorine gas and an excess of a chiral 1,1′-biphenanthryl **II-3** promoter.[46] Employing four equivalents of chiral dialkoxyboranes forms a chiral 2:1 complex with alkene **II-1**, subsequent treatment with Cl_2 gas resulted in dichloride product **II-2** in 93.5:6.5 *er*. In the proposed working model, it was suggested that the chiral borane would coordinate to carbonyl groups of the precursor and shield one enantioface of the alkene.

Figure II-4: Stoichiometric, enantioselective dichlorination of alkene en route to (-)-Napyradiomycin

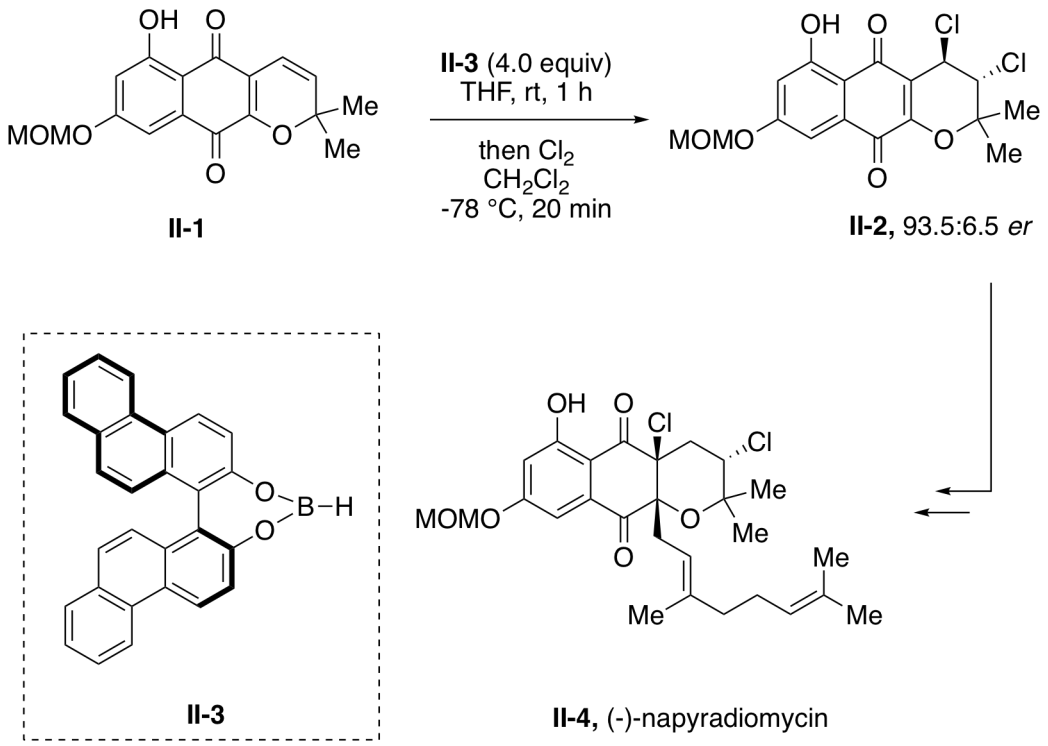

The same group has also reported the asymmetric dichlorination of unfunctionalized olefins with a chiral sulfide compound as a stoichiometric chiral reagent.[46] However, employing the chiral sulfonium salt **II-6** in the presence of dihydronaphthalene **II-5** in CH_2Cl_2 delivers dichlorinated product **II-7** in 57% yield but the enantioselectivity is only 57:43 *er* (Figure II-5).

Figure II-5: Stoichiometric, enantioselective dichlorination of alkenes by employing chiral sulfonium ion salt

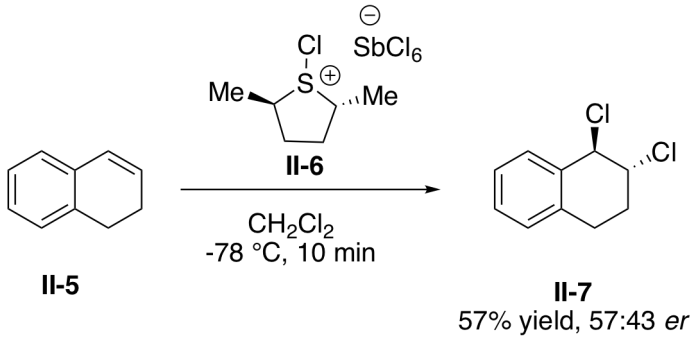

The Nicolaou group reported the first practical, catalytic asymmetric dichlorination of allyl alcohols using the $(DHQ)_2PHAL/ArICl_2$ (**II-10)** reagent system.[45] The *trans* cinnamyl alcohols **II-8** produce the dichlorinated product **II-9** in moderate to good yield (Figure II-6a). However, *cis* cinnamyl alcohols and aliphatic substituted allyl alcohols are generally less selective and form the final product with low enantioselectivity. In the stereoinduction model, the author suggests that the quinuclidine nitrogen of the chiral catalyst activates the iodine (III) of the dichlorinating agent **II-10**. Notably, the potential hydrogen bonding between the hydroxyl group of the substrate and the nitrogen atom of the phthalazine ring of $(DHQ)_2PHAL$ would bring the allyl alcohols in the chiral catalyst's binding pocket and produce vicinal dichlorinated products in high enantioselectivities (Figure II-6b).

Figure II-6: (a) Asymmetric dichlorination of styryl allyl alcohol (b) Proposed working model

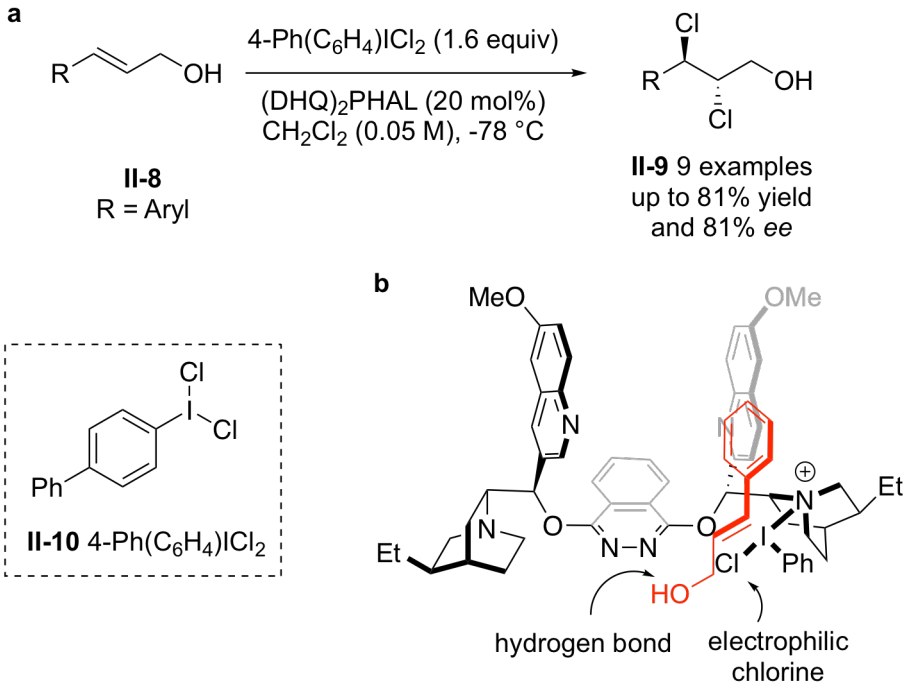

Burns and coworkers demonstrated that cinnamyl alcohols **II-11** in the presence of 20 mol% of a chiral diol (TADDOL) **II-13** and dibromomalonate **II-14** (as the bromonium source), and a bromotitanium triisopropoxide (as a bromide source) would deliver dibrominated products **II-12** up to 72% yield and 92:8 *er*.[47] Slightly higher enantioselectivities (5 to 10% *ee*) can be obtained when one equivalent of TADDOL **II-13** was used (Figure II-7).

Figure II-7: Catalytic enantioselective dibromination of allyl alcohols

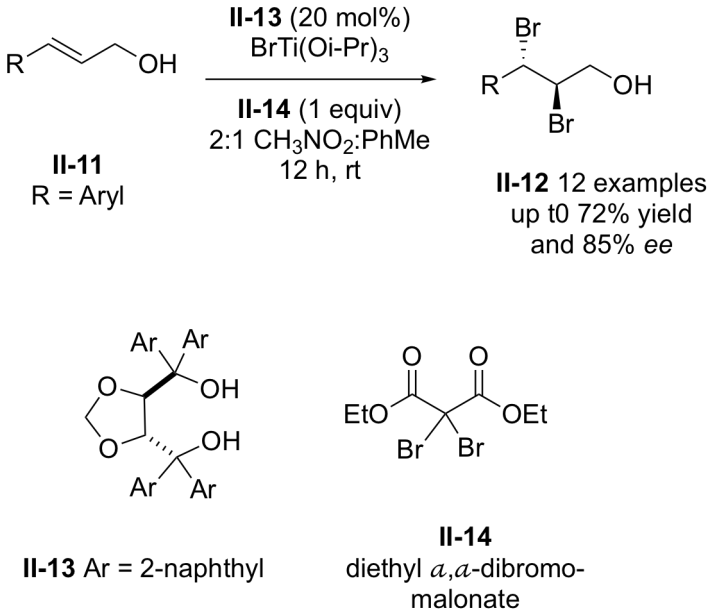

The catalytic cycle for this transformation showed that the ligand exchange on titanium might form the coordinatively saturated complex **II-15**, that contains the substrate, bromide ion, diethyl dibromomalonate **II-14** and chiral diol **II-13**. The species in this complex are arranged in a manner to allow for both intramolecular bromonium delivery and intramolecular bromide capture. Charge separation in complex **II-16** may increase the nucleophilicity of the bromide, which then can add to bromonium ion through transition state **II-17** (Figure II-8). Ligand exchange at Ti with *i*-PrOH is reversible and releases the dibrominated product. In this mechanistic scenario, the authors claimed the bromonium ion formation is reversible, and the bromide delivery is the enantiodetermining step. If that is true, this scenario may manifest itself through dynamic kinetic resolution. However, the authors did mention that the enantiodetermining irreversible

bromonium ion formation, or even concerted dibromination step, could not be ruled out with the results in hand.

Figure II-8: Proposed catalytic cycle

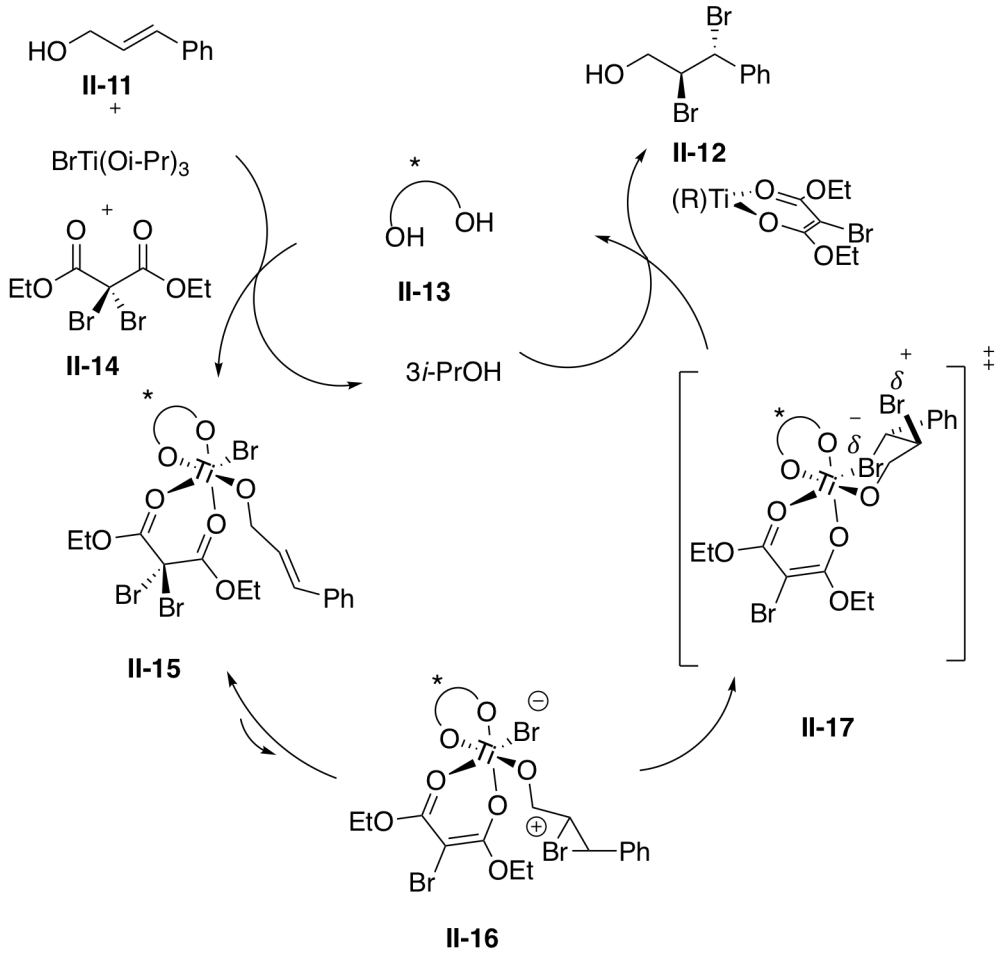

In a further development, the highly regio- and enantioselective vicinal asymmetric chlorobromination of aliphatic allyl alcohols using N-bromosuccinimide/ClTi(O*i*-Pr)$_3$ reagent system was also reported by the same group.[48] Using 50 mol% of the chiral diol **II-13**, the chlorobrominated products were produced with 1:2 site selectivity. Interestingly, Schiff base as the chiral catalyst **II-18** forms the chlorobrominated product **II-20** exclusively (>20:1, see

Table II-1, entry 2). Based on these results, **II-18** can overturn the intrinsic (substrate control) site selectivity of the chloride ion addition to bromonium ion intermediate.

Table II-1: Catalyst-controlled regioselective chlorobromination of allyl alcohols

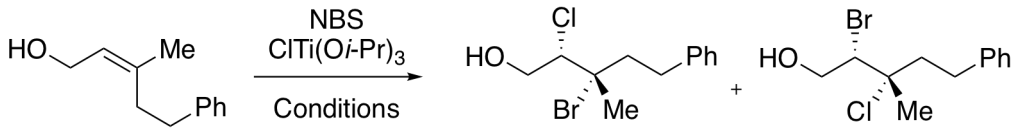

II-19 **II-20** **II-21**

entry	Conditions	**20**:**21**	*ee*% (**20**), *ee*% (**21**)
1	50 mol% **II-13**, CH_2Cl_2, rt	1:2	6:8
2	10 mol% **II-18**, hexane, -20 °C	>20:1	94,nd

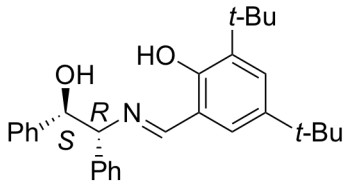

II-18

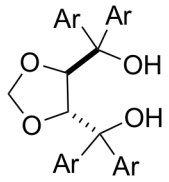

II-13 Ar = 2-naphthyl

The substrate scope for this regioselective chlorobromination indicates that using (10–30 mol%) tridentate Schiff base **II-18** as catalyst in the presence of chlorotitanium triisopropoxide forms intermediate **II-23**. Subsequently, formation of the bromonium ion and nucleophilic attack with chloride would form the chlorobrominatad product **II-24** in 89% yield, 96:4 *er* and >20:1 *rr* (Figure II-9).

Figure II-9: Catalytic chemo- regio- and enantioselective bromochlorination of allylic alcohols

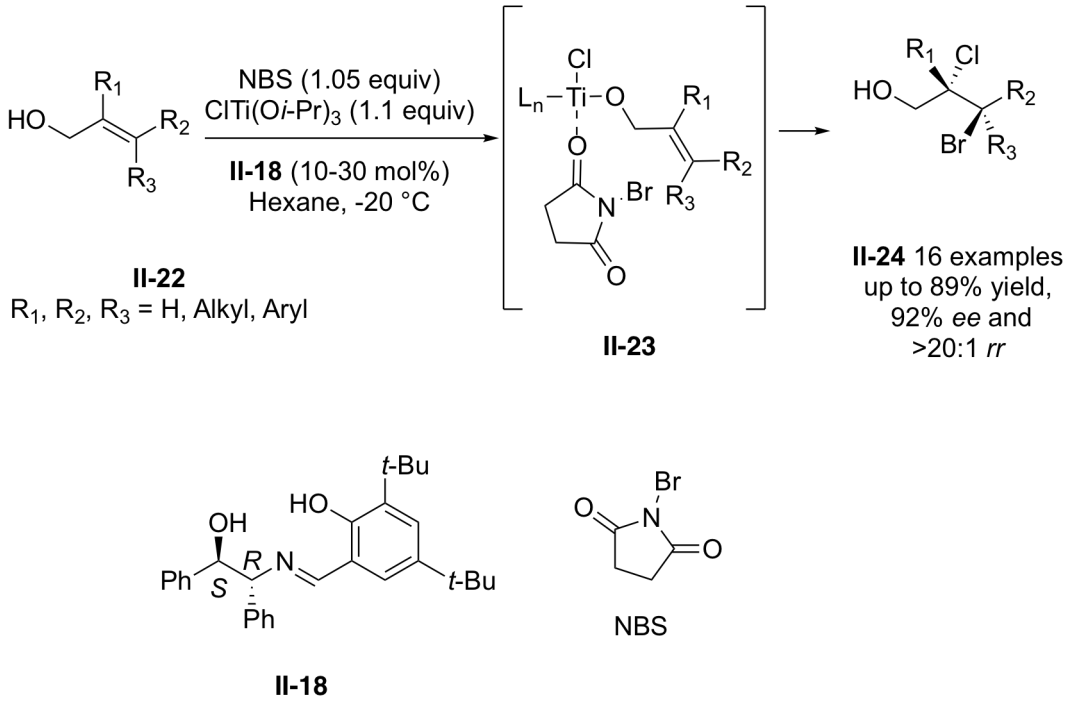

For the application of this new method, Burns and coworkers employed this enantioselective chlorobromination for the gram-scale total synthesis of (+)-bromochloromyrcene **II-28** (Figure II-10).[49] It was the first time the asymmetric dihalogenation reaction was used in a total synthesis, and the catalyst-controlled regio site selectivity in the halogenation step is impressive.

Figure II-10: Enantioselective synthesis of (+)-bromochloromyrcene

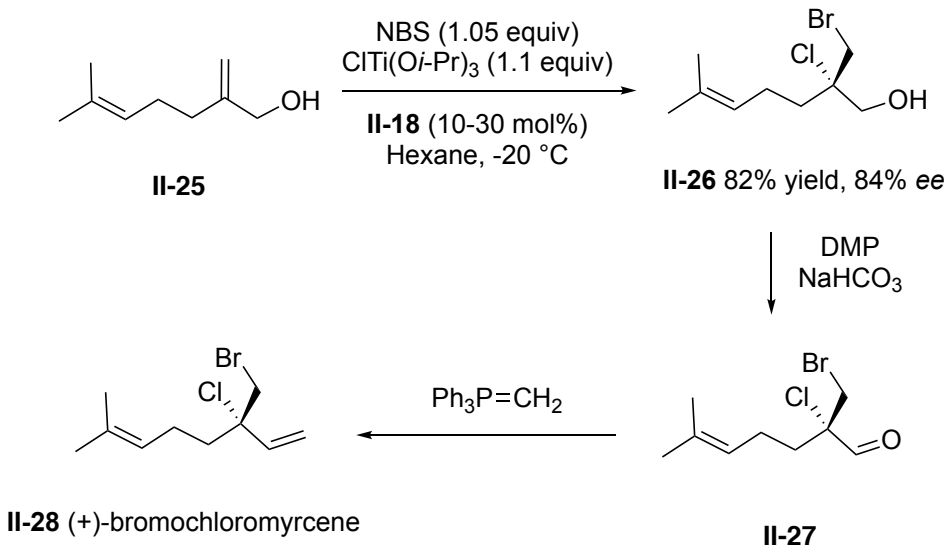

After this development in enantioselective dihalogenation reactions, Burns and coworker reported preliminary results for the catalytic and enantioselective dichlorination of allylic alcohols that have aliphatic substituents.[50] The formation of vicinal dichlorinated products is a powerful means of entry to chlorosulfolipids natural products synthesis. In this area dichlorinated aliphatic allyl alcohol is known as an essential motif for the synthesis of deschloromytilipin A **II-29**, mytilipin A **II-30**, danicalipin A **II-31** and malhamensilipin A **II-32** (Figure II-11). Due to lack the of enantioselective dichlorination methodology, these natural products are either synthesized in a racemic fashion[51] or in the case of danicalipin A, the kinetic resolution of epoxide opening was used as a precursor for the formation of chiral vicinal dichloride products.[52]

Figure II-11: Structure of chlorosulfolipid natural products

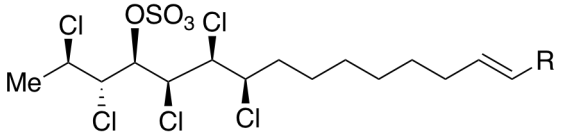

II-29 (+)-deschloromytilipin A (R = H)
II-30 (+)-mytilipin A (R = Cl)

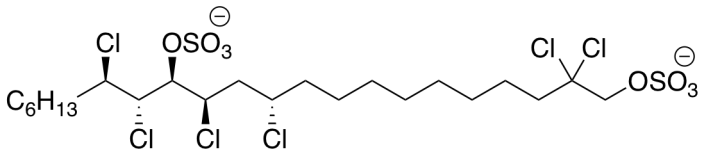

II-31 (+)-danicalipin A

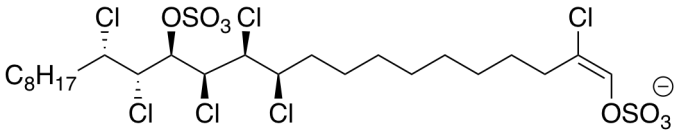

II-32 (+)-malhamensilipin A

In the developed enantioselective dichlorination of aliphatic allyl alcohols, the *tert*-butyl hypochlorite (*t*-BUOCl) was used as the Cl^+ source.[50] However, the chiral catalyst and halide sources were the same as in other reports. As shown in Figure II-12, allyl alcohol **II-33** produces the corresponding dichlorinated product **II-34** in 95:5 *er* by employing 30 mol% Schiff base **II-18.** In this transformation, *t*-BuOCl and $ClTi(O\textit{i}\text{-}Pr)_3$ were used as chloronium and chloride sources, respectively.

Figure II-12: Example of asymmetric alkene dichlorination

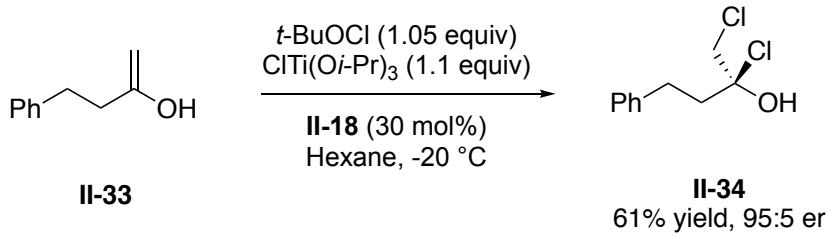

Notably, these results indicate the first regio-enantioselective dihalogenation of unbiased (non-aryl-substituted) alkenes, but still, two shortcomings are apparant with these methodologies; 1: the enantioselectivities for dichlorination of the aliphatic alcohols are moderate (around 81% *ee*); 2: the hydroxyl group was used as the chiral catalyst-directing group. Thus, this transformation could only be used for the alkenes that are tethered to the hydroxyl group. With these shortcomings in mind, I sought to develop highly a regio-, diastereo- and enantioselective dihalogenation methodologies for alkenes.

II-2 Results and discussions

II-2-1 Catalyst-controlled regioselectivity in enantioselective haloetherification reaction

As discussed in Chapter I, our group has recently reported a highly enantioselective intermolecular haloetherification and haloesterification reaction of unsaturated amides (Figure II-13).[29] One of the key features of the transformation was the excellent catalyst-controlled regioselectivity that renders a wide variety of alkyl-substituted alkenes as compatible substrates for the chemistry.

Figure II-13: Catalytic asymmetric intermolecular halohydrin formation, haloetherification and haloesterification

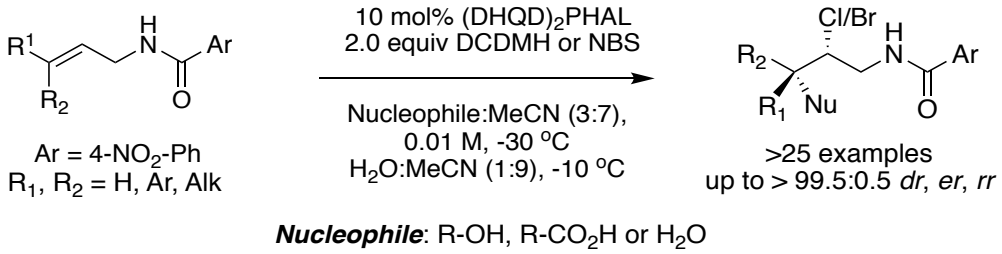

To figure out if the enantioselective chloroetherification methodology can extend to catalytic enantioselective dihalogenation reactions, we designed the control experiment to indicate whether the catalyst dictates the regioselectivity for the haloetherification reactions. The chloroetherification reaction of *Z*-allyl amide **II-35** was conducted in optimized conditions without $(DHQD)_2PHAL$ as the chiral catalyst. In line with desired product **II-36,** the regioisomer product **II-37** and cyclized product **II-38** were formed in the ratio of 57:16:27, respectively (Table II-2, entry 1). However employing $(DHQD)_2PHAL$ produced chloroetherified product **II-36** with high selectivity (Table II-2, entry 2).

Table II-2: Catalyst-controlled regioselectivity in chloroetherification reactions of *Z*-allyl amide **II-35**

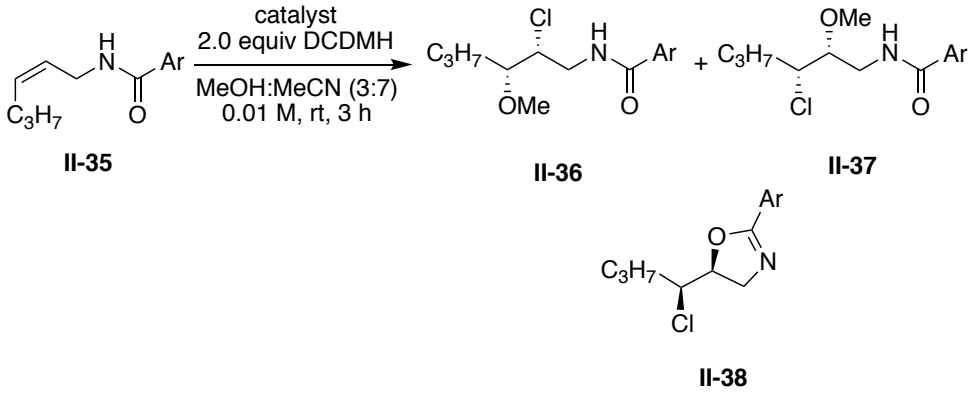

Entry	Catalyst	**II-36**:**II-37**:**II-38**[a]	*rr* (**II-36**:**II-37**) [a]
1	None	57:16:27	4:1
2	10% $(DHQD)_2PHAL$	96:4:0	24:1

[a]Regioselectivity and ratio of uncyclized to cyclized products were determined by HPLC

Notably, the same control experiment was conducted with *E*-allyl amide **II-39** and in this case a mixture of regioisomers (**II-40**, **II-41**) and cyclic products (**II-42**, **II-43**) were formed in the ratio of 43:15:26:16, respectively (Table II-3, entry 1). Interestingly, when the chiral catalyst is employed, the desired chloroetherified product **II-40** forms in high selectivity (87%, Table II-3, entry 2). Noteworthy is the fact that the chiral catalyst is responsible not only for the high enantioselectivities but also for the exquisite regioselectivity for the reactions employing aliphatic substrates (for example, noncatalyzed reactions gave *rr* values of ~4:1 for substrate **II-35** and 3:2 for substrate **II-39**). These results hint at extensive pre-organization of the substrate–nucleophile–catalyst complex in

addition to the halogen source catalyst H-bonded complex that we have previously established.

Table II-3: Catalyst-controlled regioselectivity in chloroetherification reactions of *E*-allyl amide **II-39**

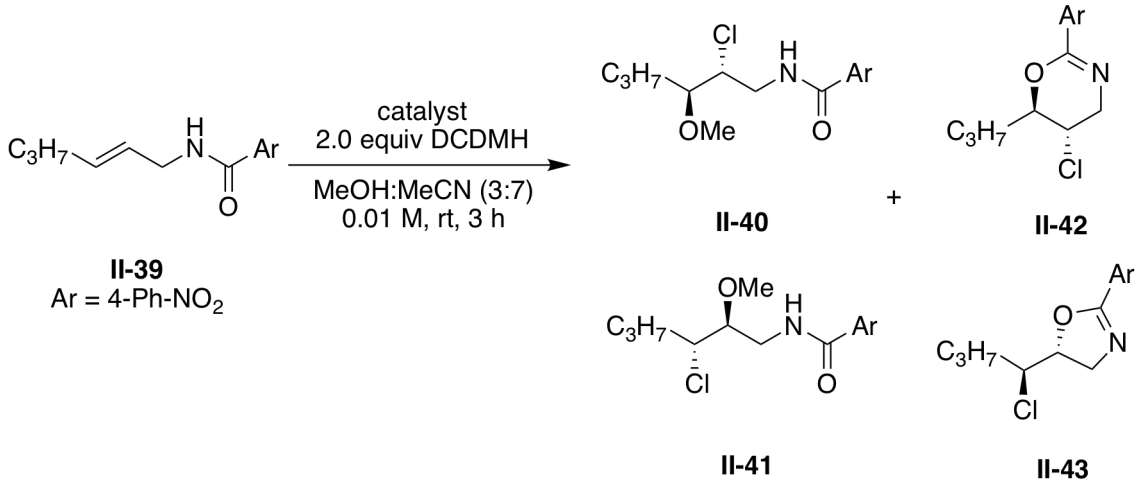

Entry	Catalyst	**II-40**:**II-41**:**II-42**:**II-43**[a]	*rr* (**II-40**:**II-41**) [a]
1	None	43:15:26:16	3:2
2	10% $(DHQD)_2$PHAL	87:4:7:2	10:1

[a]Regioselectivity and ratio of uncyclized to cyclized products were determined by HPLC

II-2-2 Extension of haloetherification to the enantioselective dihalogenation of alkenes

Based on these results, we realized the potential to extend the asymmetric chloroetherification chemistry to the enantioselective dihalogenation of alkenes by discovering an appropriate halide salt to intercept the same halonium putative intermediate (Figure II-14).

Figure II-14: Potential to extend asymmetric chloroetherification chemistry to the enantioselective dihalogenation reaction

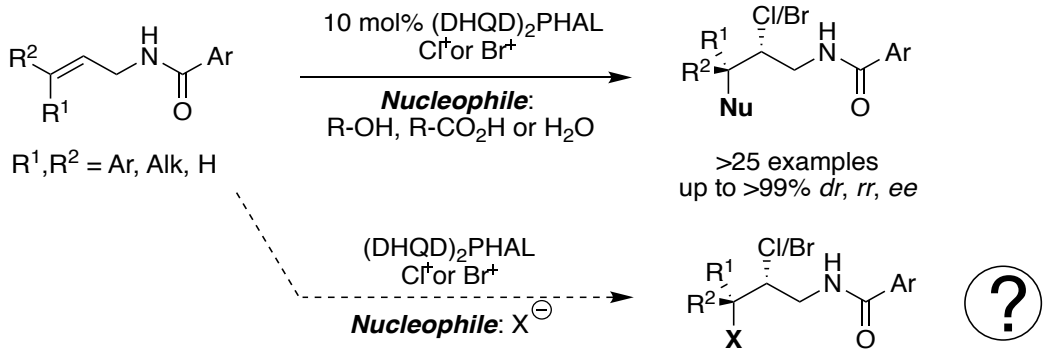

Our studies commenced with identifying conditions that could transform II-35 to II-44. Pilot studies indicated that the best enantioselectivities were seen when MeCN or CF_3CH_2OH (TFE) was used as the solvent. It should be noted that competing intermolecular processes such as interception of the intermediate by the solvent leads to side products II-45 (from TFE incorporation) or II-47 (the Ritter product when CH_3CN is employed). Also, the intramolecular halocyclization path yields the oxazoline II-46 as a side product. Our initial screening of reaction conditions had to not only deliver the desired dihalogenated products in acceptable yields and enantioselectivity, but also avoid the production of side products II-45-II-47 (see Table II-4).

Numerous chloride sources were evaluated for this test reaction in the presence of 2.0 equivalents of DCDMH, 10 mol% of $(DHQD)_2PHAL$ and acetonitrile (ACN) as a solvent. Initially, soluble quaternary ammonium chloride salts were evaluated. Disappointingly, a mixture of products with a marginal preference for the desired product II-44 as a racemate were produced (II-44:II-46

=55:45, 50:50 *er*, Table II-4, entry 1). Use of NaCl predominantly produces the Ritter product II-47 (Table II-4, entry 2). Encouragingly, LiCl fared much better despite its sparing solubility in organic solvents. Reactions run at ambient temperature with 15 equivalents of LiCl gave significant amounts of the chlorocyclized by-product II-46 (II-44:II-46 = 79:21, Table II-4, entry 3). Lowering the temperature to -30 °C gave the dichlorinated product exclusively (II-44:II-46 = 95:5 and 92:8 *er*, entry 4); although encouraging, this result gave significantly lower enantioselectivity for other substrates (see Table II-5, in Section II-2-5).

Further experimentation revealed that employing trifluoroethanol (CF_3CH_2OH, TFE) as the reaction solvent gave reproducibly exquisite enantioselectivity for the desired product, albeit at the expense of the product yield (ca. 40%) due to the formation of II-45 (Table II-4, entry 5). Formation of by-product II-45 could be greatly mitigated by simply increasing the stoichiometry of LiCl from 15 to 100 equiv (>20:1 II-44:II-45, Table II-4, entry 7). These results were particularly surprising given the low solubility of LiCl in TFE (ca. 20 mg/mL).

Table II-4: Summary of optimization studies for dichlorination

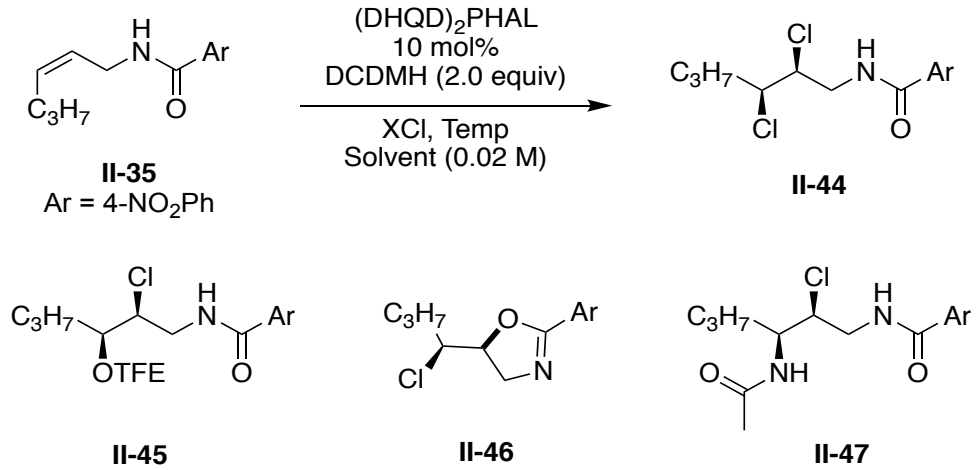

Entry	Solvent	Conc	Temp (°C)	XCl	XCl (equiv)	**44**:**45**:**46**:**47**[a]
1	MeCN	0.02	23	TEAC	15	55:0:45:0
2	MeCN	0.02	23	NaCl	15	0:0:13:87
3	MeCN	0.02	23	LiCl	15	79:0:21:0
4	MeCN	0.02	-30	LiCl	15	95:0:5:0
5	TFE	0.02	-30	LiCl	15	45:56:0:0
6	TFE	0.02	-30	LiCl	50	86:14:0:0
7	TFE	0.02	-30	LiCl	100	95:5:0:0
9	TFE	0.40	-30	LiCl	100	95:5:0:0

[a]Determined by NMR; TFE = 2,2,2-trifluoroethanol; TEAC = Tetraethylammonium chloride

II-2-3 Dichlorination of allyl amides in acetonitrile

Using acetonitrile as the solvent for dichlorination of **II-54A** produced the corresponding product **II-54B** in moderate yield and stereoselectivity (entry 1, Table II-5). Under the same conditions **II-39B** was formed in high yield and diastereoselectivity (99:1 *dr*) albeit in low enantioselectivity (61.5:38.5 *er,* entry 2,

Table II-5). However, performing the dichlorination reaction in trifluroethanol (TFE) gave a significant improvement in stereoselectivity of **II-54B** and **II-39B** (>99:1 *er* and 93:7 *er*, respectively, see Figure II-15 and II-16 in Section **II-2-5-1** and **II-2-5-2**).

Table II-5: Dichlorination of allyl amides in acetonitrile

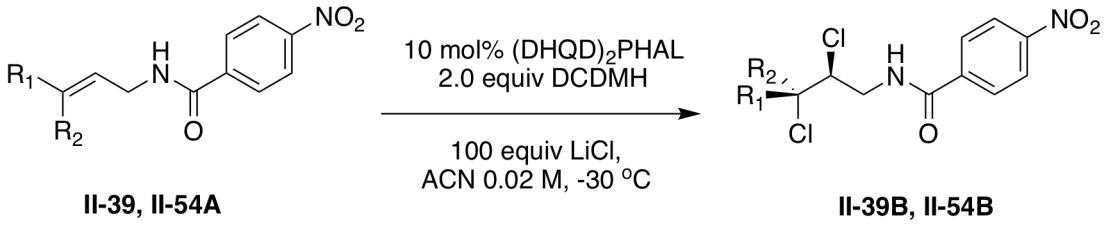

Entry	R_1	R_2	Prod	%Yield[a]/*dr*	*er*[b]
1	H	Ph	**II-54B**	59/>6.3:1	91:9
2	C_3H_7	H	**II-39B**	89/>99:1	61.5:38.5

[a]Combined yield, Determined by NMR; [b]Determined by chiral HPLC

II-2-4 Role of the counterion of chloride in selectivity of dichlorination reactions

Intrigued by the effect of solid LiCl, we investigated the role of the counterion under the optimized conditions with various chloride salts that have a wide range of solubilities in TFE. The fully soluble tetraethylammonium chloride (TEAC) produced a mixture of products with a marginal preference for the desired product II-44 in high enantioselectivity (93:7 *er*, Table II-6, entry 2). Treating compound II-35 with sparingly soluble NaCl in TFE (0.03 M solubility) returned predominantly the TFE incorporated product II-45 (Table II-6, entry 3).

These results are in complete contrast with LiCl (entry 1), which delivers the desired product in high chemo- and enantioselectivity. CsCl, exhibiting similar solubility as LiCl in TFE (0.53 M for CsCl vs. 0.40 M for LiCl) also fails to deliver the product in high selectivity, yielding a nearly 1:1 ratio of II-44:II-45. From these results, it is evident that while solubility of the chloride source might be an important factor that dictates product distribution, the counterion is equally important. Additionally, the presence of undissolved LiCl is also essential for good selectivity. Finally, we ruled out the possibility that *in-situ* generated Cl_2 gas might be the active chlorenium and chloride source; in this instance very low selectivity was observed for the desired product (Table II-6, entry 5). Numerous control experiments suggest that these reactions likely occur at the solid-liquid interface. These experiments are discussed later in the chapter.

Table II-6: Role of chloride counter ion in selectivity of the dichlorination reaction

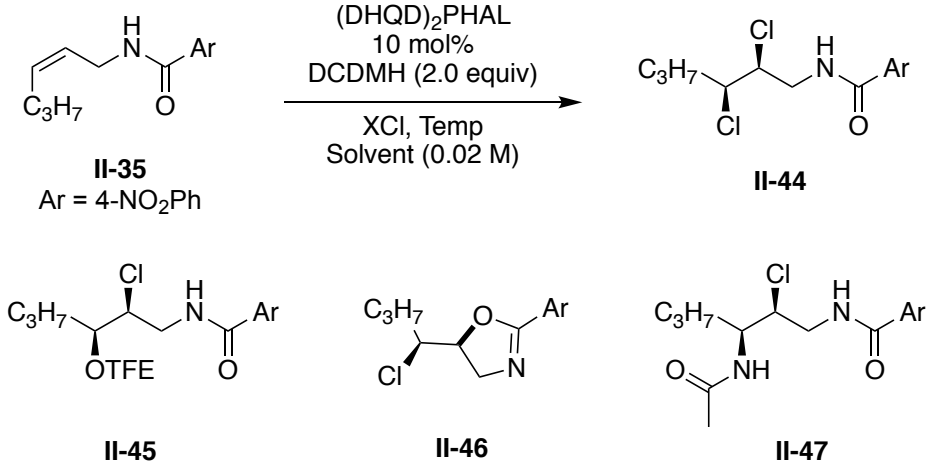

Entry	XCl	Solubility (mol/lit)	XCl (equiv)	**44**:**45**:**46**:**47**[a]	*ee*[b](**5**)
1	**LiCl**	**0.40**	**100**	**95:5:0:0**	**92:8**
2	TEAC	Fully soluble	100	66:34:0:0	93:7
3	NaCl	0.03	100	0:89:11:0	nd
4	CsCl	0.54	100	55:44:3:0	95:5
5[c]	Cl_2 (gas)	nd	Gas	16:43:41:0	50:50

[a]Determined by NMR; [b]Determined by chiral HPLC; [c]Cl_2 gas was generated *in situ* and bubbled into the reaction; TFE = 2,2,2-trifluoroethanol; TEAC = Tetraethylammonium chloride

II-2-5 Substrate scope for asymmetric dichlorination reaction

II-2-5-1 Substrate scope for Z-allyl amide in asymmetric dichlorination reaction

Mapping the generality of the dichlorination reaction, numerous *cis*-substituted allyl amides were examined under the optimized conditions (0.02 M substrate concentration in TFE, 100 equivalents LiCl and 2.0 equivalents of

DCDMH at -30 ^{o}C). Dichlorination of *Z*-aliphatic amides exhibit high diastereoselectivity (Figure II-15, see II-44 and II-48B to II-52B, >99:1 *dr).* The identity of the benzamide motif had little influence on the enantioselectivity of this reaction; products II-44 and II-48B were both formed in 99.5:0.5 *er* (Figure II-15, entries 1 and 2). The other *Z*-alkyl substituted olefins afforded dichlorinated products in complete diastereo- and enantioselectivity (see II-49B, II-50B). The benzyloxysubstituted alkene II-51A gave lower enantioselectivity (88.5:11.5 *er*). Aryl-substituted *Z*-olefins gave corresponding products in high enantioselectivity and regioselectivity (>97:3 *er* and >99:1 *rr,* Figure II-15, see II-53B-II-55B). The diastereoselectivities and yields for these entries are varied (1.7:1 to >20:1 *dr* and 35% to 88% yield); as expected reduced diastereoselectivity was seen with increasing benzylic cation stabilization. The poor yield for substrate II-53A is attributed to the formation of cyclized and TFE incorporated products, while the moderate yield for compound II-54B is due to the formation of TFE incorporated product. Nonetheless, the trifluoromethyl substituted olefin II-55A afforded the dichlorinated product with exquisite yield and stereoselectivity (88% yield, >99:1 *dr*, 99.5:0.5 *er*, Figure II-15, entry 9).

Figure II-15: Substrate scope for *Z*-allyl amides in dichlorination reaction[a,b]

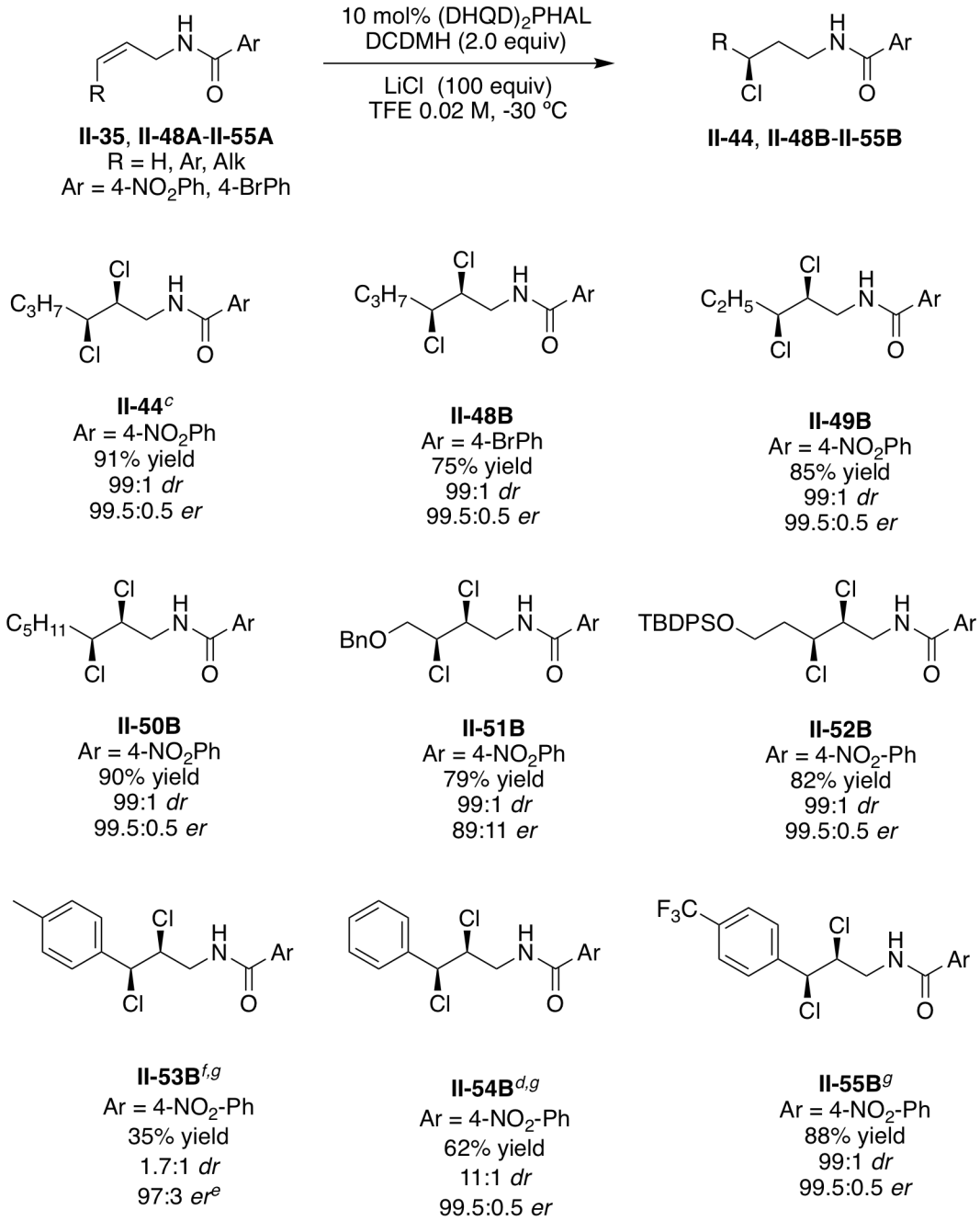

---

[a]Isolated yield on a 0.1 mmol scale; [b]Enantioselectivity determined by chiral HPLC; [c]Performed on 1 g scale with 1% cat.; [d]Mass balance is TFE incorporated products; [e]The minor diastereomer shows 91:9 *er* [f]Mass balance is cyclized and TFE incorporated products; [g]Substrate concentration was 0.2 M

II-2-5-2 Substrate scope for E-allyl amide in asymmetric dichlorination reaction

Trans aliphatic substituted olefins showed high level of diastereoselectivity (>99:1 *dr*, see II-39B, II-56B and II-57B). Changing the 4-bromobenzamide motif to the 4-nitrobenzamide gave identical results (~91:9 *er,* ~80 % yield, see II-39B, II-56B). The benzyloxy protected substrate II-57A formed dichlorinated product in 85% yield and 89:11 *er* (Figure II-16, II-57B). Compound II-58A, with aryl substituent on the alkene gave moderate yield (due to competing production of cyclized and TFE-incorporated products) and moderate enantioselectivity for product II-58B (63% yield, 90:10 *er*, Figure II-16). Trisubstituted alkene II-59A was also compatible with this chemistry and returned the desired product in 73% yield and 92:8 *er*. It warrants emphasis that for trisubstituted and aryl-substituted olefins, a higher substrate concentration (0.20 M) is required for mitigating the formation of TFE incorporated by-product (see Section II-2-6 for concentration studies).

Figure II-16: Substrate scope for *Z*-allyl amides in dichlorination reaction[a, b]

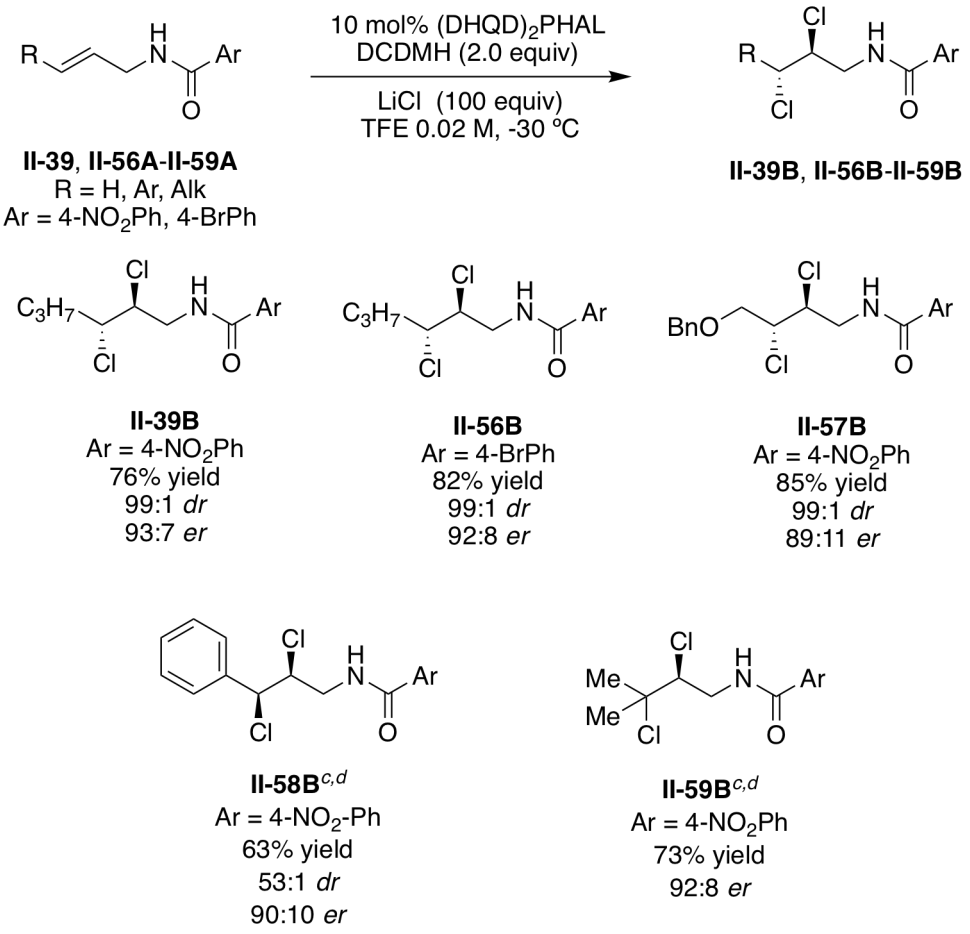

---

[a]Isolated yield on a 0.1 mmol scale; [b]Enantioselectivity determined by chiral HPLC; [c]Mass balance is TFE incorporated products; [d]Substrate concentration was 0.2 M

II-2-5-3 Substrate scope for dichlorination reaction with quasi-enantiomeric $(DHQ)_2$PHAL catalyst

The quasi-enantiomeric catalyst, $(DHQ)_2$PHAL, transformed two substrates (II-35, II-39A) to the corresponding enantiomeric products in comparable yield and selectivity (Figure II-17, *ent*-II-44 and *ent*-II-39B). This

quasi-enantiomeric catalyst forms the mirror image products with similar yields and enantioselectivities when $(DHQD)_2PHAL$ was used (see Figure II-15 and II-16).

Figure II-17: Substrate scope for dichlorination reaction with quasi-enantiomeric $(DHQ)_2PHAL$ catalyst[a, b]

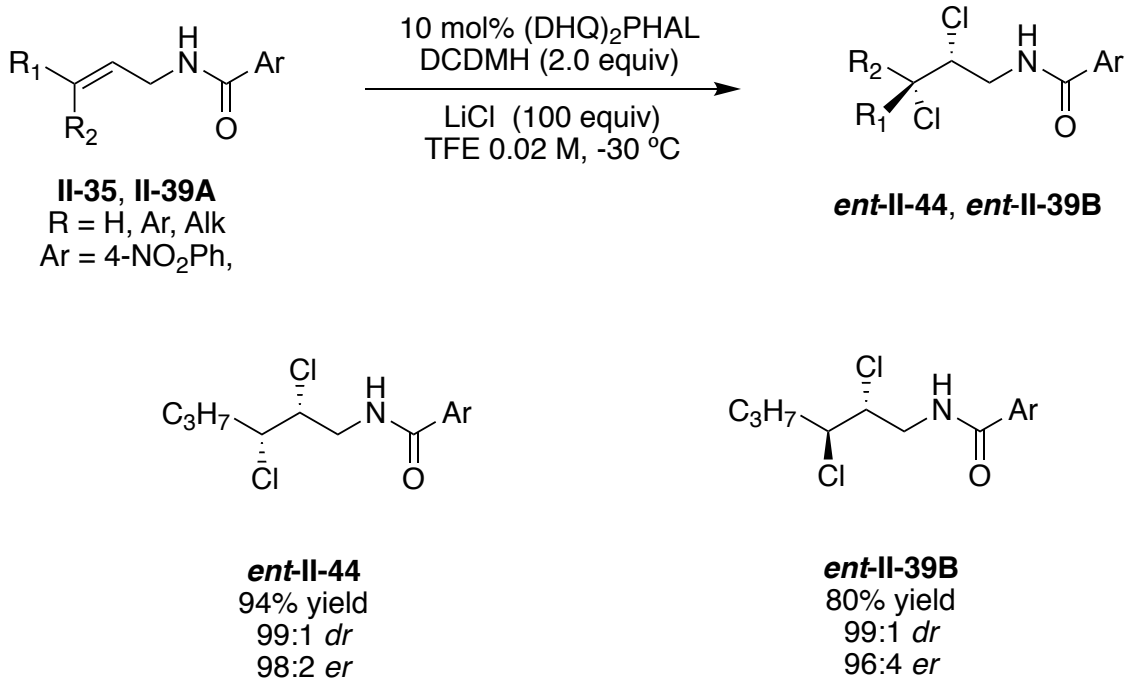

[a]Isolated yield on a 0.1 mmol scale; [b]Enantioselectivity determined by chiral HPLC

II-2-5-4 Substrate scope for regio- and enantioselective hetero-dihalogenation

Gratifyingly, this chemistry also delivers vicinal dibrominated and chloro-brominated products with high stereoselectivity. Treating II-35 in TFE (0.2 M) with 100 equivalents LiCl as the chloride source and 2.0 equivalents of NBS as the

bromenium source gave II-35C in 97% yield and 99.5:0.5 *er* (Figure II-18, entry 1). Using LiBr in conjunction with NBS gave the dibrominated product II-35C' in 90% yield and 84:16 *er* (Figure II-18, entry 2). *Z*-aromatic olefin II-55A returned chlorobrominated product II-55C in 96% yield with high stereoselectivity (99.5:0.5 *er* and >99:1 *dr,* see II-55C, Figure II-18). The chlorobromination of *E*-amides II-39 and II-58A formed desired products II-39C and II-58C in high diastereoselectivity and good enantioselectivity. The yield for aromatic substrate II-58A suffers due to the formation of the cyclized product (58%, see II-58C, Figure II-18). There are solvent and equilibrium optimization studies for hetero-dihalogenation that will be discussed in Section II-2-7.

Figure II-18: Regio- and enantioselective hetero-dihalogenation[a, b]

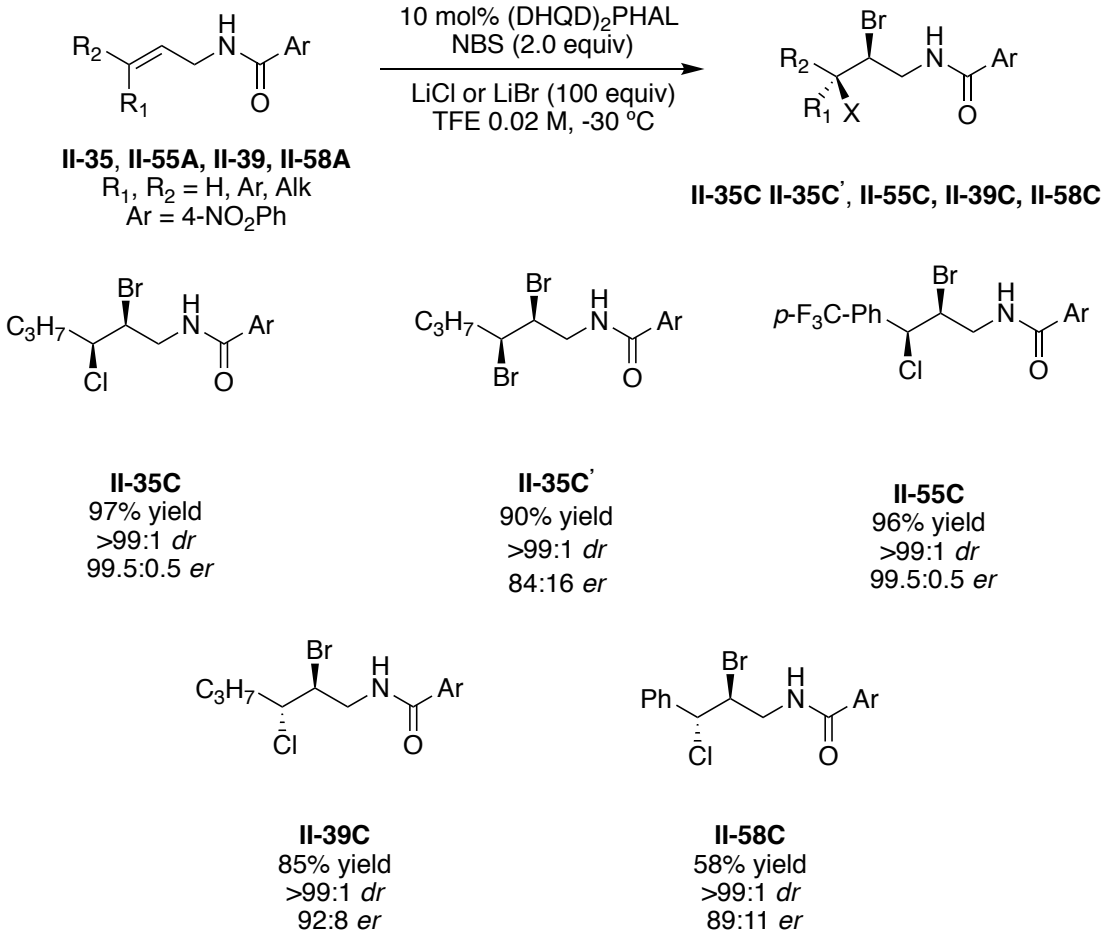

[a]Isolated yield on a 0.1 mmol scale; [b]Enantioselectivity determined by chiral HPLC

II-2-6 Influence of reaction concentration on the yield for the dichlorination of unsaturated aromatic and trisubstituted allyl amides

The dichlorination of aromatic allyl amides (**II-54A**, **II-58A**) in optimized concentration (0.02 M) produced the mixture of dichlorinated product and chloroetherification side product in moderate yield and high diastereoselectivity (entries 1 and 2, Table II-7).

Table II-7: Dichlorination of aromatic and trisubstituted allyl amides

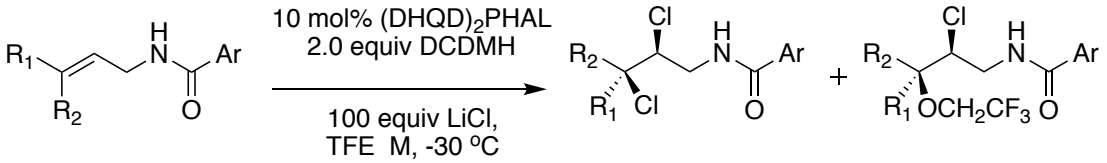

II (54, 58, 59) A
Ar = 4-NO_2Ph

II (54, 58, 59) B

II (54, 58, 59) D

Entry	R_1	R_2	Conc	Prod	%Yield[a]/*dr*[b]	**B**:**D**
1	H	Ph	0.02	**II-54B**	55[c]/10:1	4.2:1
2	Ph	H	0.02	**II-58B**	40[c]/32:1	2.8:1
3	Me	Me	0.02	**II-59B**	44[c]/na	1:1.8
4	H	Ph	0.2	**II-54B**	62[c]/15.6:1	15.6:1
5	Ph	H	0.2	**II-58B**	63[c]/53:1	5.3:1
6	Me	Me	0.2	**II-59B**	73[c]/na	4.4:1

[a]Yield determined by NMR; [b]Diastereoselectivity determined by chiral HPLC;
[c]Rest of mass balance is TFE incorporated product

The trisubstituted olefin **II-59A** formed the desired product **II-59B** in 44% yield (see entry 3, Table II-7). The mass balance for these reactions was TFE-incorporated side product **II-(54, 58, 59)D**. In an attempt to increase the yield and chemoselectivity for these substrates **II-(54, 58, 59)A**, the reaction was performed at a higher concentration (0.2 M). The higher concentration resulted in higher yields and diastereoselectivities of the desired products (see entries 4, 5 and 6, Table II-7).

II-2-7 Influence of solvents and equivalents of lithium chloride on the chlorobromination reactions

Table II-8: Optimization of chlorobromination reactions

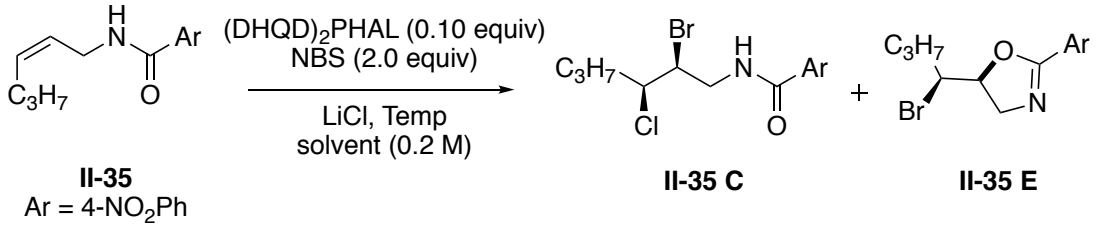

II-35
Ar = 4-NO_2Ph

II-35 C **II-35 E**

Entry	Solvent	Temp	equiv of LiCl	**C**:**E**[a]	*er* (**II-35 C**)[b]
1	ACN	rt	30	1.0:1.0	76:24
2	ACN	-30	100	4.5:1.0	76:24
3	ACN	-30	300	4.9:1.0	76:24
4	TFE	-30	100	>99:1	98:2

[a]The ratio of products, Determined by NMR; [b]Determined by chiral HPLC

Treating allyl amide **II-35** in ACN (0.2 M) with 30 equivalents of LiCl as the chloride source and 2 equivalents of NBS as the bromenium source gave a mixture of products **II-35C**:**II-35E** in ratio of 1:1 with 76:24 *er* for the desired product **II-35C** (entry 1, Table II-8). Using higher equivalents of LiCl slightly increased the chemoselectivity in favor of dihalogenated product **II-35C** (entries 2 and 3, Table II-8). Interestingly, performing the chlorobromination reaction in TFE as solvent forms product **II-35C** with exquisite chemoselectivity and enantioselectivity (98:2 *er*, entry 4, Table II-8).

II-2-8 Various halenium and halide sources for the enantioselective dihalogenation of unsaturated amides were used

Table II-9: Regio- and enantioselective dihalogenation

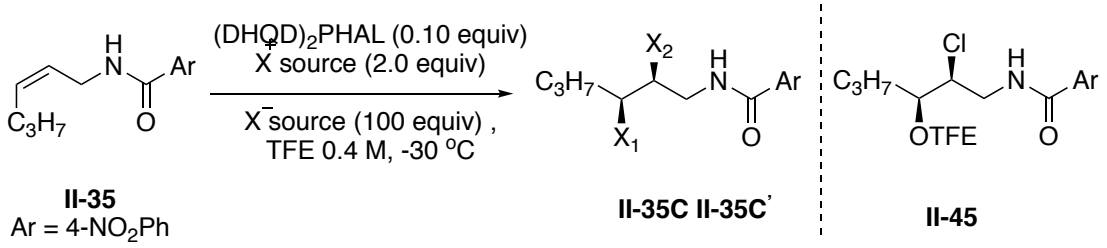

Entry	X^-source	X^+ source	X_1	X_2	Prod	%Conv	%Yield[a]	*er*[b]
1	LiCl	NBS	Cl	Br	**35C**	100	97	98:2
2	LiBr	NBS	Br	Br	**35C'**	100	90	84:16
3	LiBr	DCDMH	Br	Br	**35C'**	100	96	77:23
4	LiF	DCDMH	F	Cl	**45**	100	nd	nd
5	LiI	NIS	I	I	-	0	nd	nd
6	LiI	DCDMH	I	Cl	-	0	nd	nd

[a]Yield determined by NMR; [b]Enantioselectivity determined by chiral HPLC

Treating **II-35** (0.2 M) in TFE with 100 equivalents of LiCl as the chloride source and 2.0 equivalents of NBS as the bromonium source produced **II-35C** in 97% yield and 98:2 *er*. With this result in hand we attempted to form the other regioisomer by changing the X^- and X^+ source. U LiBr and NBS formed the dibrominated product **II-35C'** in 90% yield and 84:16 *er* (Table II-9, entry 2). Surprisingly, employing LiBr and DCDMH led to the dibrominated product **II-35C'** instead of the chlorobrominated product (Table II-9, entry 3). This observation suggests that in the presence of LiBr, DCDMH is converted to DBDMH, or otherwise generates a bromonium. This has led us to devise a simple procedure for the synthesis of a variety of bromenium sources from their corresponding

chlorenium containing parents. These results will discuss in Section II-2-11. Employing LiF as a fluoride source failed to yield chlorofluorinated product and instead returned the TFE incorporated product **II-45** in high yield (Table II-9, entry 4). Lithium iodide does not lead to any product and starting material was recovered (Table II-9, entries 4 and 5).

II-2-9 Product distribution arising due to substrate-control and catalyst-control for the dichlorination reactions

Table II-10: Product distribution in catalyzed and non-catalyzed dichlorination reactions

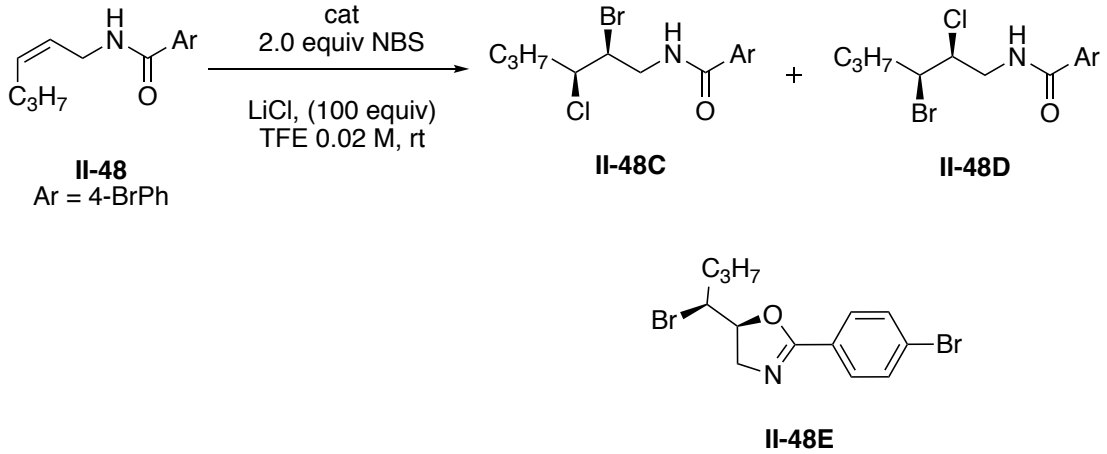

Entry	Catalyst	Ratio (**C**:**D**:**E**)[a]	Regioselectivity[a]	*er* (**II-48C**)[b]
1	None	52:24:24	2:1	50:50
2	$(DHQD)_2PHAL$	90:5:5	18:1	94:6

[a]The ratio of products and regioselectivities, Determined by NMR.; [b] Enantioselectivity determined by chiral HPLC

The dihalogenation reaction without any catalysts gave 3 major products. As shown in the NMR trace (Figure II-19) for the crude reaction, along with the desired product **II-48C**, the regioisomer **II-48D** and the cyclized product **II-48E**

were also formed in a ratio of 52:24:24 (Table II-10, entry 1). On the other hand, employing $(DHQD)_2PHAL$ as the chiral catalyst at ambient temperature gave the desired product in significantly higher selectivity with 94:6 enantioselectivity (Table II-10, entry 2). These results demonstrate that the chiral catalyst is not only responsible for high enantioselectivity but also for the exquisite regioselectivity seen for reactions employing aliphatic substrates.

Figure II-19: NMR trace for product distribution in catalyzed and non-catalyzed chlorobromination reaction

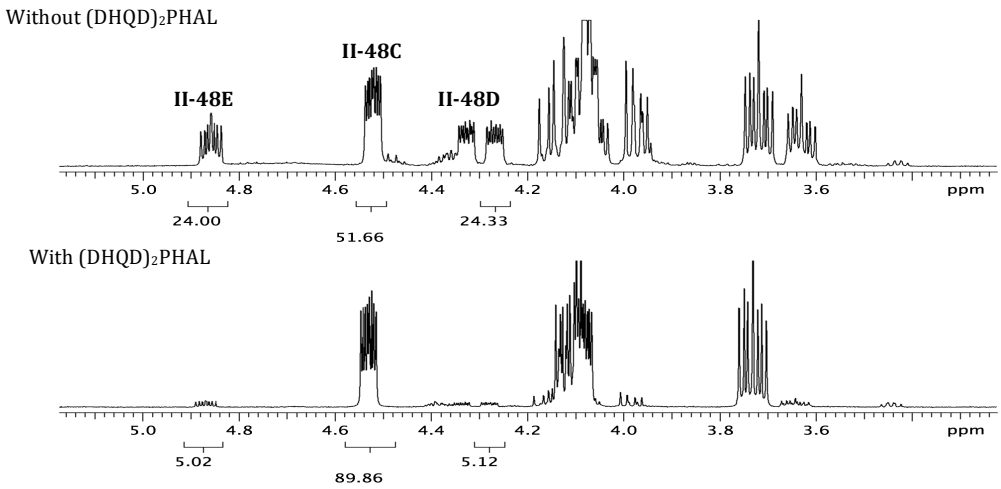

II-2-10 Control experiments indicating that dichlorination reaction occurs on LiCl solid surface

II-2-10-1 Screening selectivity ratio with different concentrations

The fact that these reactions required up to 100 equiv of LiCl for optimal results was counterintuitive given the sparing solubility of LiCl in organic solvents. Additionally, a significant amount of the added LiCl remained undissolved during the reaction and could be recovered at the end. In order to determine whether

suspended LiCl plays a role in this reaction and if indeed the reaction is occurring on a solid-liquid interface, two sets of control experiments were executed. In the first set of experiments, a saturated solution of LiCl in TFE (0.47 M concentration) was prepared and employed in dichlorination reactions with different substrate concentrations (Table II-11, entries 1-4). Two key observations were made. First, all reactions gave similar product ratios regardless of the substrate concentration or the substrate:LiCl ratio (5.8-6.6:1 ratio of II-44:II-45). Second, the ratio of II-44:II-45 was significantly worse than that observed under optimized reaction conditions that employed a large excess of LiCl (>20:1 II-44:II-45); i.e. reactions run in the presence of suspended/undissolved LiCl were significantly more selective (Table II-10, entry 5).

Table II-11: Screening selectivity ratio in different concentrations

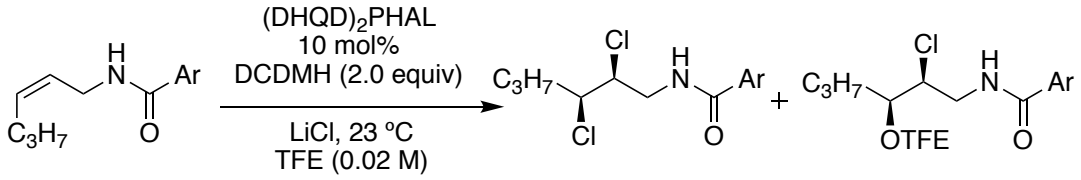

II-35
Ar = 4-NO_2Ph

II-44 **II-45**

Entry	TFE (mL)	Conc. (**35**)	Conc. (LiCl)	LiCl[b] (equiv)	**44**:**45**[a]
1	0.5	0.20	0.47 (soluble)	2	5.8:1
2	0.5	0.08	0.47 (soluble)	5	6.6:1
3	2	0.02	0.47 (soluble)	20	6.4:1
4	7	0.006	0.47 (soluble)	67	6.2:1
5	2	0.02	2.0 (insoluble)	100	>20:1

[a]Ratio determined by NMR; [b]0.47 M solution of LiCl in TFE was prepared by saturating TFE with LiCl, filtering the undissolved LiCl and determining the molarity of the dissolved salt from the difference in mass of recovered LiCl.

II-2-10-2 Effect of rate of stirring (RPM studies) on the selectivity of dichlorination reaction

A second set of control experiments was performed to probe mixing and mass-transfer effects. The stirring speed was altered, first in the soluble regime (15 equiv of LiCl, 0.3 M in LiCl) and then in the insoluble regime. The stirring speed had a remarkable effect on product distribution. In the absence of any stirring (0 rpm) significant amount of by-product II-45 was formed (II-44:II-45= 1:1, Table II-12, entry 1). At 100 and 300 rpm, this ratio improved to 3.5:1 (entries 2 and 3, Table II-12). In the insoluble regime (100 equiv of LiCl, 0.02 M substrate concentration, entries 4 – 7, Table II-12) this effect was even more pronounced.

At 0 rpm, the ratio of II-44:II-45 was 1.5:1. Increasing the rate of stirring to 300 rpm gave the desired product almost exclusively (95% yield, II-44:II-45 = >20:1, Table II-12, entry 5). With a further increase in substrate concentration to 0.20 M, the effects of mass transfer became less pronounced (II-44:II-45 = >20:1 at 0 rpm as well as at 300 rpm, see entries 6 and II-7 in Table II-12). The combination of results from Tables II-6, II-11 and II-12 highlighting the requirement for a Li cation, and also the dependence on the heterogeneous nature of the reaction, strongly suggests that success in greatly limiting the TFE incorporated side product II-45 is due to the reactionpreceding at the liquid-solid interface.

Table II-12: Effect of rate of stirring (RPM studies) in selectivity of the dichlorination reaction

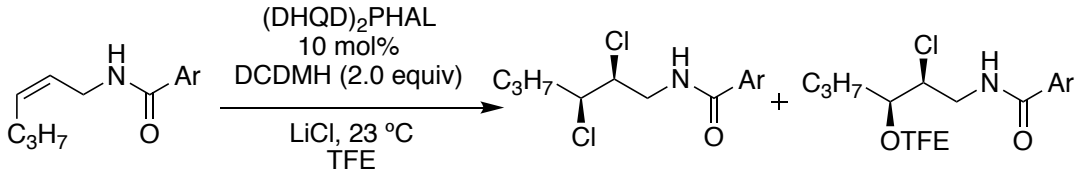

II-35
Ar = 4-NO_2Ph

II-44 **II-45**

entry	Conc	RPM	equiv (LiCl)	Yield	**44**:**45**[a,b]
1	0.02	0	15	95	1.0:1.0
2	0.02	100	15	88	3.5:1.0
3	0.02	300	15	90	3.5:1.0
4	0.02	0	100	90	1.5:1.0
5	0.02	300	100	95	>20:1
6	0.20	0	100	82	>20:1
7	0.20	300	100	87	>20:1

[a]Ratio determined by NMR; [b]1% to 3% of cyclized product was seen by NMR.

II-2-10-3 Effect of LiCl particle size on product distribution of the dichlorination reaction

The suggested role of solid LiCl on the reaction would presume that particle size should have an influence on the reaction outcome. To probe the role of insoluble LiCl on the olefin dichlorination reaction, different particle sizes of lithium chloride were produced by sequential sieving through different mesh screens. This was accomplished by taking the salt particles that passed from a higher mesh size screen (for example 850 mm) and were trapped onto a smaller mesh size screen (such as 300 mm). In the latter example, the particle sizes are

between 850 mm to 300 mm. The mesh ranges in Table II-13 refer to sequential sieving with two different mesh screens as described above. The reactions were ran with 50 equivalents of LiCl in each case, since with larger excess the **II-58B**:**II-58D** ratio would have been less pronounced (at 100 equivalents the majority of the product is the desired **II-58B**). As anticipated for a reaction that is dependent on reaction at the solid interface, LiCl particle size makes a difference in the ratio of products. Entry 1, with the largest particle sizes yields the worst ratio of **II-58B**:**II-58D** (62:38). As the particle sizes become progressively smaller, the ratio favors the desired **II-58B** product, which is presumably aided by the reaction taking place at the solid interface. We would anticipate that the reaction to yield **II-58D** (incorporation of the solvent) is independent of the solid and occurs in the soluble phase. These results corroborate the RPM studies (Table II-12), which also highlights that the dichlorination reaction is aided by the presence of the solid LiCl, suggestive of the fact that the reaction could occur on solid-liquid interface.

Table II-13: Effect of LiCl particle size on product distribution of the dichlorination reaction

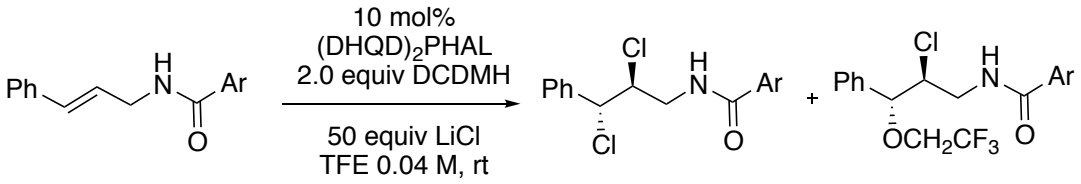

II-58A
Ar = 4-NO_2Ph

II-58B **II-58D**

Entry[a]	LiCl particle size (μm)[b]	Ratio (**B**:**D**)[c]
1	850-300	62:38
2	300-150	66:34
3	150-53	66:34
4	53-45	74:26

[a]For all reactions, 50% of the product was the intramolecularly cyclized compound; [b]LiCl was ground to powder and was sieved to obtain different particle sizes.; [c]Determined by NMR

II-2-10-4 Effect of 12-crown-4 ether on product distribution of dichlorination reactions

12-Crown-4 ether is a specific scavenger for lithium cation, yielding a more soluble chloride in the reaction mixture. In the presence of 15 equivalents of LiCl at ambient temperature the desired product **II-44** was formed predominantly (**II-44:II-45** = 77:23**,** Table II-14, entry 1). Adding 12-crown-4 ether formed **II-44** with diminished selectivity; in presence of 3 equivalents of 12-crown-4 ether the ratio of **II-44:II-45** decreased to 68:32 (Table II-14, entry 2). Employing 20 equivalents of crown ether in presence of 50 equivalants of LiCl gave a mixture of products in worse selectivity (61:39 **II-44:II-45**, Table II-14, entry 6). These results are in line with other control experiments (RPM studies, LiCl particle size) demonstrate that

insoluble LiCl plays an important role for obtaining high selectivity for dichlorination reactions.

Table II-14: Effect of 12-crown-4 ether on product distribution of dichlorination reactions

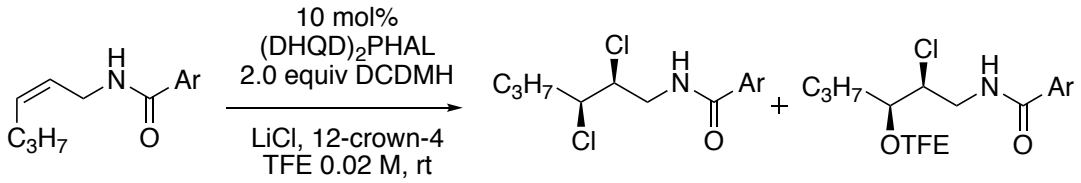

II-35
Ar = 4-NO_2Ph

II-44 **II-45**

Entry	Equiv of LiCl	Equiv of Crown ether	Ratio (**44**:**45**)[a]
1	15	0	77:23
2	15	1	72:28
3	15	3	68:32
4	50	0	89:11
5	50	5	86:14
6	50	20	61:39

[a]Determined by NMR

II-2-11: A new unprecedented transformation for the synthesis of N-haloimides revealed by side product identification in hetero-dihalogenation

During exploring substrate scope for hetero-dihalogenation reaction interesting observations leads us to Expedient access to N-bromo- and N-iodoimides from the corresponding N-chloroimides.

II-2-11-1 The importance of N-haloimides

N-haloimides are among the most widely employed electrophilic halogenating reagents in both academia and industry. These reagents serve as stable and easily handled sources of halogen atoms and often obviate the need to use more corrosive reagents such as molecular chlorine, bromine or iodine. Among this diverse family of reagents, N-bromo and N-iodo imides are particularly useful owing to the higher reactivity of the resulting bromide or iodide products. The typical example, 1,3-dibromo-5,5-dimethyl-hydantoin (DBDMH), has been employed in radical bromination reactions,[53] electrophilic aromatic bromination,[47, 54] oxidation of thiol to disulfides[55] and most recently in enantioselective bromofunctionalization of alkenes.[56] Moreover, DBDMH is used as an active antimicrobial agent; AviBrom® and BoviBrom® are two processing aids that are used for disinfection of beef. Is also more prefered over the corresponding chlorinated counterparts as adisinfectant and bactericide for water sources and food industries because its efficiency is less sensitive to pH.

II-2-11-2 Currently used methods for producing N-haloimides

Two prominent methods are currently used for the synthesis of N-haloimides – 1) Treating the parent imide with molecular bromine or iodine in the presence of a strong base such as sodium hydroxide. Although straightforward, this process is often limited to production facilities that are capable of producing Br_2 or I_2 due to the high cost and hazards associated with the transportation and storage of the highly corrosive reagents.[57] 2) In situ generation of Br_2 or I_2 using readily available bromide or iodide salts by treating with a strong oxidant. While

this process avoids handling molecular Br_2 or I_2, the hazardous nature of the oxidants (such as H_2SO_4, H_2O_2, persulfate salts, Oxone, etc) often preclude the use of such processes on scale (Figure II-20).[58]

Figure II-20: Currently used methods for producing N-haloimides

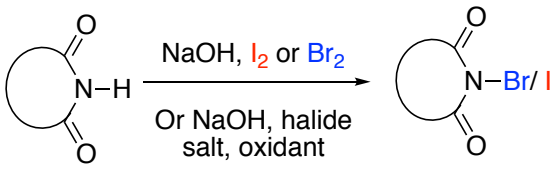

In this Section, we propose an alternative and cost-effective means of generating the N-haloimides *in situ* by reacting readily available and stable N-Chloroimides with inorganic bromide or iodide salts (LiBr, LiI). This process of in-situ transformation of N-chloroimides to the corresponding N-bromo or N-iodo imides is unprecedented. Also, all the reagents are easily handled and shelf-stable.

II-2-11-3 Highly regio- and enantioselective vicinal dihalogenation of allyl amides

As mentioned earlier in this Chapter, we reported the enantioselective vicinal dihalogenation of allyl amides in the presence of (DHQD)2PHAL as a chiral organocatalyst. An electrophilic halenium (X^+) donor along with lithium halide (X^-) is needed for completion of this transformation. The employing of large excess (100 equivalents) of lithium halide is essential to obtain high selectivity and yield, it was indicated that reaction occurs on solid surface of Lithium halide. This methodology is compatible with *E* and *Z* alkenes with both

aryl and aliphatic substituents. Various examples of dihalogenated and heterodihalogenated products was evaluated with up to 97% yield and >99.5:0.5 *er* (Figure II-21).

Figure II-21: Highly regio- and enantioselective vicinal dihalogenation of allyl amides

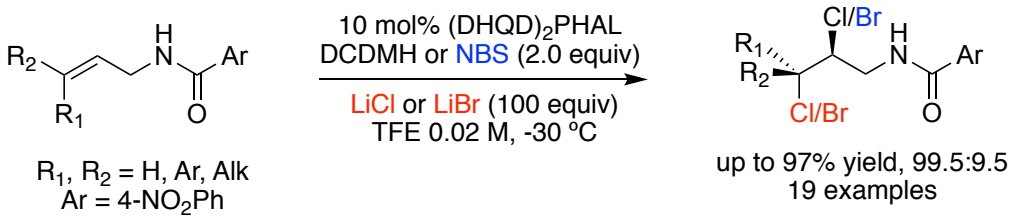

II-2-11-4 Identification of a hetero-dihalogenation reaction's side product

In addition to vicinal dichlorination and dibromination, we were also able to demonstrate heterodihalogenation i.e. bromo-chlorination of the allyl amide. Specifically, when **II-35** was treated with LiCl as the nucleophilic chloride source and DBDMH as the source of electrophilic bromine, chloro- brominated product **II-35C** was formed in 97% yield. In an effort to reverse the regiochemistry, we switched the halide source to LiBr and the electrophilic halogen donor to DCDMH for accessing bromo-chlorinated product **II-35D** (regioisomer of **II-35C**). The reaction did not proceed as planned; instead the dibrominated product **II-35C'** was isolated in 96% yield (Figure II-22a). We surmised that DCDMH must have reacted with LiBr to afford DBDMH in-situ. We were able to confirm this via NMR. When DCDMH was treated with a slight excess of LiBr in CD_3CN, a rapid and quantitative formation of DBDMH was seen based on ^{13}C NMR. It occurred

to us that this might represent a general route to access a variety of N-bromoimides from the corresponding N-chloroimides.

Figure II-22: (a) Regioselective chloro-bromination of allyl amides (b) LiBr-mediated transformation of DCDMH to DBDMH

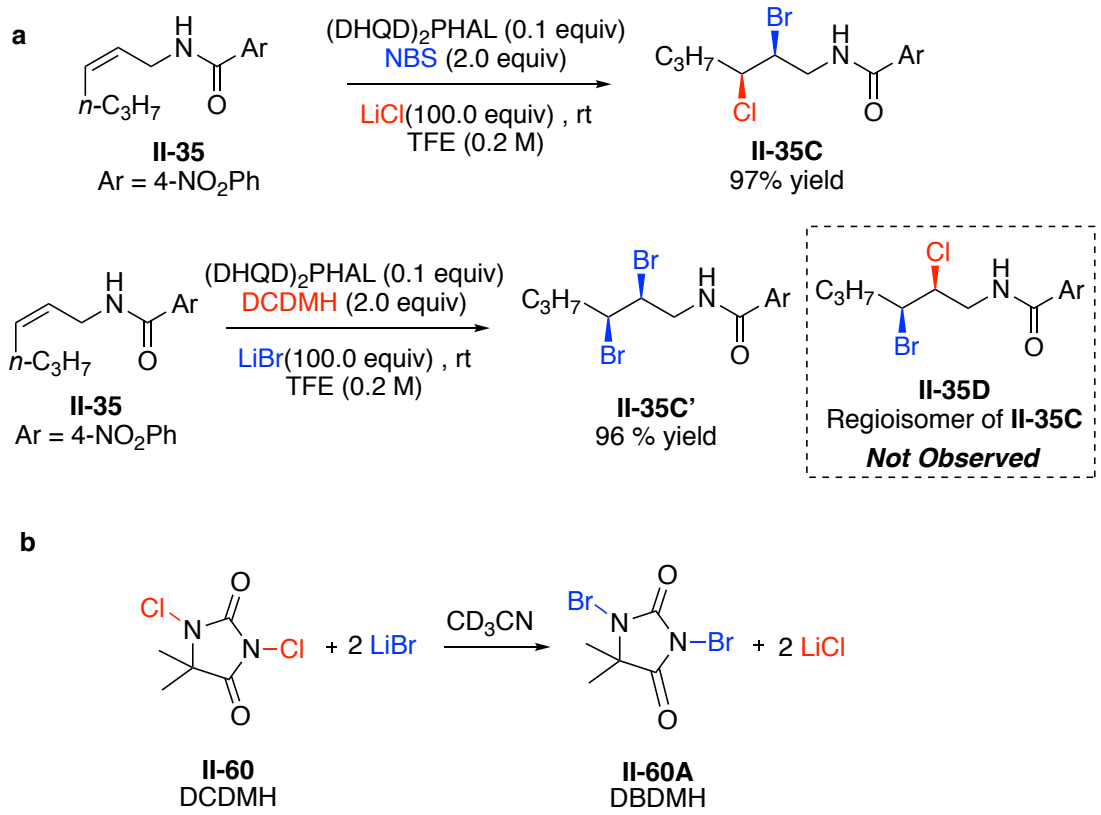

II-2-11-5 Substrate scope for expedient synthesis of N-bromo- and N-iodoimides from the corresponding N-chloroimides

Four of the most commonly employed N-bromoimides were accessed from the corresponding N-chloroimides in high yields. As shown in Figure II-23, DBDMH was isolated in quantitative yield by addition of LiBr to suspended

DCDMH in Acetonitrile. The reaction was complete in 1 hour at ambient temperature. Isolation of the product involved a routine aqueous work-up/extraction protocol followed by recrystallization from EtOAc-Hexanes. This methodology was general. Various N-bromoimides were synthesized by employing LiBr in >90% yield (see products **II-60A**-**II-63A**, Figure II-23).

Figure II-23: Substrate scope for formation of N-bromo and N-iodoimide[a, b]

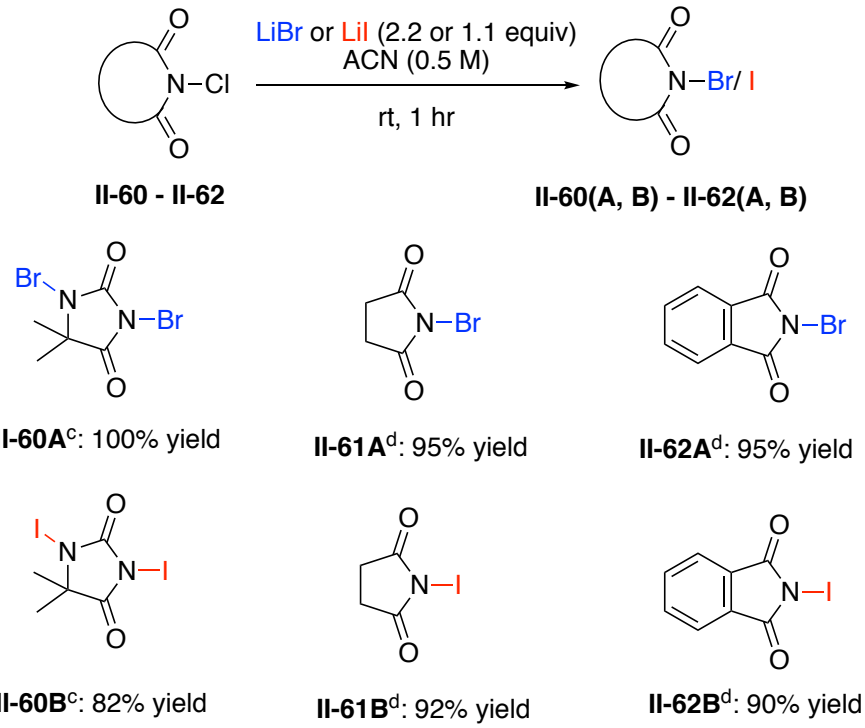

[a]Isolated yield. [b]The reactions were conducted on 10 mmol scales [c]2.2 equivalents of LiBr or LiI were used. [d]1.1 equivalents of LiBr or LiI were used

We then turned our attention to potentially accessing N-iodoimides using an analogous approach. With well-documented stability issues, an expedient access to N-iodoimides from the corresponding shelf-stable N-chloroimides would represent an attractive alternative to freshly recrystallizing these reagents

prior to use. To our delight, employing LiI in lieu of LiBr affords the N-Iodoimides in high yields (**II-60B-II-62B,** Figure II-23). The only by-product formed in this process is LiCl. This is of particular relevance to the synthesis of N-iodoimides – all commercial processes to N-iodoimides produce stoichiometric quantities of inorganic iodide waste (I_2/NaOH system). Most water treatment facilities have strict specifications for iodide content owing to the numerous adverse effects of inorganic iodides on aquatic and terrestrial organisms. The process is rapid and quantitative in most cases that have been examined thus far.

II-2-12 Conclusion

In conclusion, we report an experimentally expedient dihalogenation reaction that is catalyzed with $(DHQD)_2$PHAL, yielding products in high yield and enantioselectivity. Exquisite catalyst controlled regioselectivity has allowed for a broad substrate scope that includes alkyl and aryl substituted allyl amides. The stereochemistry of the double bond is of little consequence, as good results are obtained with both *E* and *Z* olefins. Of particular interest is the role of LiCl, the chloride source for the reaction. Our exhaustive screening demonstrated TFE as the optimal choice for solvent, although its incorporation as the nucleophile in the reaction was initially a problem. Use of excess LiCl drastically reduces the TFE incorporated side product. Our preliminary investigations strongly suggest not only a role for the solid salt in solution, but also for the presence of Li salt in particular, for the success of this transformation. Mechanistic investigations are

underway to further elaborate the nature of interactions, presumably at the solid/liquid interface, that lead to the observed effects.

We report the unprecedented and expedient transformation for generating the N-bromo and N-iodoimides by reacting readily available and stable N-chloroimides with inorganic bromide or iodide salts (LiBr, LiI). All reagents are easily handled, readily available and shelf stable. The transformation is rapid, high-yield and operationally straightforward.

II-2-13 Experimental section

II-2-13-1 General information

Commercially available reagents were purchased from Sigma-Aldrich or Alfa-Aesar and used as received. CH_2Cl_2 and acetonitrile were freshly distilled over CaH_2 prior to use. THF was distilled over sodium-benzophenone ketyl. All other solvents were used as purchased. LiCl and LiBr were purchased from Sigma-Aldrich; the particle size of LiCl and LiBr were <850 mm. ^{1}H and ^{13}C NMR were recorded on 500 MHz Varian NMR machines using $CDCl_3$ as solvent and were referenced to residual solvent peaks. Flash silica gel (32-63 mm, Silicycle 60 Å) was used for column chromatography. The sieves for obtaining different mesh size of LiCl were purchased from H&C sieving systems. Enantiomeric excess for all products was determined by HPLC analysis using DAICEL CHIRALCEL® OJ-H and OD-H or CHIRALPAK® IA and AD-H columns. Optical rotations of all products were measured in chloroform. Allyl amides **II-35, II-39, II-**

(48 to 59)A (except **II-55A**) were synthesized as reported previously.[29] Analytical data for byproducts **II-46** and **II-47** were also reported in the same reference.

II-2-13-2 General procedure for catalytic asymmetric dichlorination of unsaturated amides

The substrate (0.1 mmol, 1.0 equiv) and LiCl (420 mg, 10 mmol, 100 equiv, reagent grade, <850 mm particle size) were suspended in trifluoroethanol (TFE, 5.0 mL) in a screw-capped 20 mL vial equipped with a micro stir bar (7 × 2 mm). The resulting suspension was cooled to -30 °C in an immersion cooler. $(DHQD)_2PHAL$ (7.8 mg, 10 mol%) was then introduced. After stirring for 2 min DCDMH (39.5 mg, 0.2 mmol, 2.0 equiv) was added. The stirring at 300 RPM (as indicated by the stirrer) was continued at -30 °C till the reaction was complete (TLC). The reaction was quenched by the addition of saturated aq. Na_2SO_3 (3 mL) and diluted with DCM (3 mL). The organics were separated and the aqueous layer was extracted with DCM (3 × 4 mL). The combined organics were dried over anhydrous Na_2SO_4 and concentrated in the presence of small quantity of silica gel. Column chromatography (SiO_2/EtOAc – Hexanes gradient elution) gave the desired product.

II-2-13-3 Procedure for gram scale scope analysis for catalytic asymmetric dichlorination of unsaturated amides in presence of 1% of chiral catalyst

II-35 (1.0 g, 4.0 mmol, 1.0 equiv) and LiCl (17 g, 100 equiv) were suspended in trifluoroethanol (TFE, 20.0 mL) in a round-bottom flask equipped with a stir bar. The resulting suspension was cooled to -30 °C in an immersion

cooler. $(DHQD)_2PHAL$ (32.0 mg, 1.0 mol%) was then introduced. After stirring for 2 min DCDMH (1500 mg, 8.0 mmol, 2.0 equiv) was added. The stirring in >300 RPM was continued at -30 °C till the reaction was complete (TLC). The reaction was quenched by the addition of saturated aq. Na_2SO_3 (20 mL) and diluted with DCM (15 mL). The organics were separated and the aqueous layer was extracted with DCM (3 × 15 mL). The combined organics were dried over anhyd. Na_2SO_4 and concentrated in the presence of silica gel. Column chromatography (SiO_2/EtOAc – Hexanes gradient elution) gave the desired product in 91% yield and 98:2 enantioselectivity.

II-2-13-4 Procedure for gram scale scope analysis for synthesis of N-bromo- and N-iodoimides from the corresponding N-chloroimides.

The substrate **II-35** (5 mmol, 1.0 gr) was suspended in acetonitrile (ACN, 10 ml). LiBr (2.2 equiv, 0.95 gr) was then introduced. After stirring for 1 hour, the reaction was quenched by the addition of water (10 mL) and diluted with EtOAC (10 mL). The mixture was extracted with EtOAC (3 × 5 mL), and organic layer concentrated to half of the volume. Following by addition of 5 ml water and extraction with EtOAC (1 × 5 mL). The organic layer was dried over anhydrous Na_2SO_4 and concentrated to the third quarter of the volume. At last, 10 ml of hexane was added to crude and cooled down in fridge to obtain crystalline product **6** in 100% yield.

This methodology is general and the same procedure were used for producing various N-Bromo and Iodoimide

II-2-13-5 Analytical data for products

II-44: *N*-((2*S*,3*S*)-2,3-dichlorohexyl)-4-nitrobenzamide

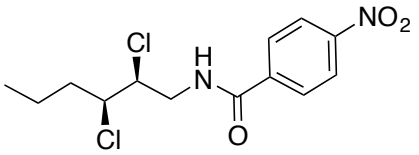

R_f : 0.60 (30% EtOAc in hexanes, UV)

^{1}H NMR (500 MHz, $CDCl_3$) δ 8.30 (d, *J* = 8.5 Hz, 2H), 7.94 (d, *J* = 8.5 Hz, 2H), 6.52 (br s, 1H), 4.41-4.38 (ddd, *J* = 9.5, 4.5, 2.5 Hz, 1H), 4.18-4.15 (ddd, *J* = 9.0, 4.5, 2.0 Hz, 1H), 4.13-4.07 (ddd, *J* = 14.0, 7.5, 4.5 Hz, 1H), 3.66-3.61 (ddd, *J* = 13.5, 8.5, 5.0 Hz, 1H), 1.93-1.80 (m, 2H), 1.62-1.54 (m, 1H), 1.46-1.38 (m, 1H), 0.96 (t, *J* = 7.0 Hz, 3H)

^{13}C NMR (125 MHz, $CDCl_3$) δ 165.77, 149.81, 139.27, 128.22, 123.96, 63.49, 62.76, 44.92, 37.45, 19.67, 13.40

HRMS analysis (ESI): Calculated for $[M+H]^+$: $C_{13}H_{17}Cl_2N_2O_3$: 319.0616; Found: 319.0609

Resolution of enantiomers: DAICEL Chiralcel® AD-H column, 15% IPA-Hexanes, 1.0 mL/min, 254 nm, RT1 (major) = 8.3 min, RT2 (minor) = 10.8 min.

$[\alpha]_D^{20}$ = +47.1 (c 0.65, $CHCl_3$, *er* = >99:1)

Absolute stereochemistry was determined by single crystal X-ray diffraction (XRD). Crystals for XRD were obtained by crystallization from CH_2Cl_2 layered with hexanes in a silicone-coated vial.

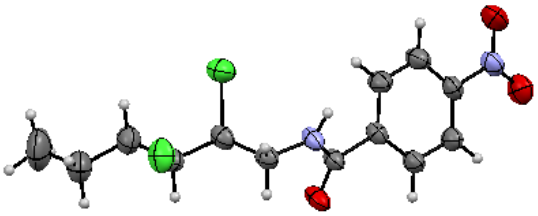

ent-**II-44:** *N*-((2*R*,3*R*)-2,3-dichlorohexyl)-4-nitrobenzamide

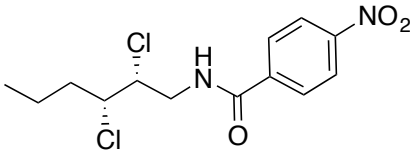

R_f : 0.60 (30% EtOAc in hexanes, UV) 94% yield with $(DHQ)_2PHAL$

^1H NMR (500 MHz, $CDCl_3$) δ 8.30 (d, *J* = 8.5 Hz, 2H), 7.94 (d, *J* = 8.5 Hz, 2H), 6.52 (br s, 1H), 4.41-4.38 (ddd, *J* = 9.5, 4.5, 2.5 Hz, 1H), 4.18-4.15 (ddd, *J* = 9.0, 4.5, 2.0 Hz, 1H), 4.13-4.07 (ddd, *J* = 14.0, 7.5, 4.5 Hz, 1H), 3.66-3.61 (ddd, *J* = 13.5, 8.5, 5.0 Hz, 1H), 3.66-3.61(m, 1H), 1.93-1.80 (m, 2H), 1.62-1.54 (m, 1H), 1.46-1.38 (m, 1H), 0.96 (t, *J* = 7.0 Hz, 3H)

^{13}C NMR (125 MHz, $CDCl_3$) δ 165.77, 149.81, 139.27, 128.22, 123.96, 63.49, 62.76, 44.92, 37.45, 19.67, 13.40

HRMS analysis (ESI): Calculated for $[M+H]^+$: $C_{13}H_{17}Cl_2N_2O_3$: 319.0616; Found: 319.0607

Resolution of enantiomers: DAICEL Chiralcel® AD-H column, 15% IPA-Hexanes, 1.0 mL/min, 254 nm, RT1 (minor) = 8.6 min, RT2 (major) = 11.0 min.

$[\alpha]_D^{20}$ = -45.3 (c 1.0, $CHCl_3$, *er* = 98:2)

II-48B: 4-bromo-*N*-((2*S*,3*S*)-2,3-dichlorohexyl)benzamide

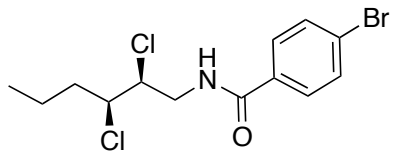

R_f : 0.60 (30% EtOAc in hexanes, UV)

^{1}H NMR (500 MHz, $CDCl_3$) δ 7.64 (d, *J* = 9.0 Hz, 2H), 7.59 (d, *J* = 9.0 Hz, 2H), 6.48 (br s, 1H), 4.40-4.37 (ddd, *J* = 9.0, 4.5, 2.5 Hz, 1H), 4.17-4.14 (ddd, *J* = 9.0, 4.5, 2.5 Hz, 1H), 4.14-4.03 (ddd, *J* = 14.0, 7.0, 4.5 Hz, 1H), 3.64-3.59 (ddd, *J* = 14.0, 8.5, 5 Hz, 1H), 1.93-1.79 (m, 2H), 1.61-1.53 (m, 1H), 1.45-1.38 (m, 1H), 0.94 (t, *J* = 7.5 Hz, 3H)

^{13}C NMR (125 MHz, $CDCl_3$) δ 166.82, 132.56, 131.96, 128.57, 126.68, 63.62, 62.82, 44.82, 37.55, 19.66, 13.40

HRMS analysis (ESI): Calculated for $[M+H]^+$: $C_{13}H_{17}Cl_2NOBr$: 351.9871; Found: 351.9865

Resolution of enantiomers: DAICEL Chiralcel® IA column, 15% IPA-Hexanes, 1.0 mL/min, 254 nm, RT1 (major) = 6.7 min, RT2 (minor) = 10.4 min.

$[\alpha]_D^{20}$ = +40.5 (c 0.8, $CHCl_3$, *er* = >99:1)

II-49B: *N*-((2*S*,3*S*)-2,3-dichloropentyl)-4-nitrobenzamide

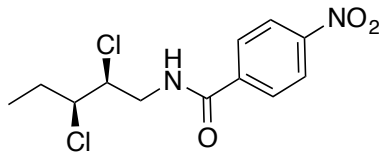

R_f : 0.50 (30% EtOAc in hexanes, UV)

^{1}H NMR (500 MHz, $CDCl_3$) δ 8.30 (d, *J* = 8.5 Hz, 2H), 7.95 (d, *J* = 8.5 Hz, 2H), 6.61 (br s, 1H), 4.43-4.40 (ddd, *J* = 8.5, 4.0, 2.5 Hz, 1H), 4.12-4.05 (m, 2H), 3.67-3.62 (ddd, *J* = 14.0, 9.5, 5.5 Hz, 1H), 1.96-1.90 (m, 2H), 1.06 (t, *J* = 7.5 Hz, 3H)

^{13}C NMR (125 MHz, $CDCl_3$) δ 165.77, 149.82, 139.27, 128.23, 123.97, 64.77, 63.17, 44.95, 28.94, 11.21

HRMS analysis (ESI): Calculated for $[M+H]^+$: $C_{12}H_{15}Cl_2N_2O_3$: 305.0460; Found: 305.0450

Resolution of enantiomers: DAICEL Chiralcel® AD-H column, 15% IPA-Hexanes, 1.0 mL/min, 254 nm, RT1 (major) = 9.9 min, RT2 (minor) = 11.3 min.

$[\alpha]_D^{20}$ = +36.6 (c 0.6, $CHCl_3$, *er* = >99:1)

II-50B: *N*-((2*S*,3*S*)-2,3-dichlorononyl)-4-nitrobenzamide

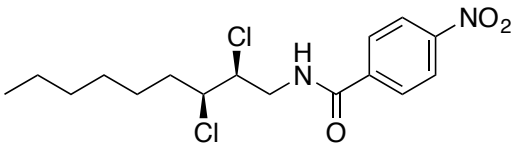

R_f : 0.60 (30% EtOAc in hexanes, UV)

^{1}H NMR (500 MHz, $CDCl_3$) δ 8.30 (d, *J* = 8.5 Hz, 2H), 7.94 (d, *J* = 8.5 Hz, 2H), 6.63 (br s, 1H), 4.41-4.38 (ddd, *J* = 9.0, 4.0, 2.0 Hz, 1H), 4.16-4.07 (m, 2H), 3.66-3.61 (ddd, *J* = 14.0, 9.0, 5.5 Hz, 1H), 1.90-1.85 (m, 2H), 1.57-1.50 (m, 1H), 1.40-1.18 (m, 7H), 0.88 (t, *J* = 7.0 Hz, 3H)

^{13}C NMR (125 MHz, $CDCl_3$) δ 165.77, 149.81, 139.28, 128.22, 123.95, 63.46, 63.10, 44.93, 35.52, 31.52, 28.59, 26.37, 22.50, 14.01

HRMS analysis (ESI): Calculated for $[M+H]^+$: $C_{16}H_{23}Cl_2N_2O_3$ 361.1086; Found: 361.1077

Resolution of enantiomers: DAICEL Chiralcel® AD-H column, 15% IPA-Hexanes, 1.0 mL/min, 254 nm, RT1 (major) = 6.6 min, RT2 (minor) = 8.0 min.

$[\alpha]_D^{20}$ = +27.4 (c 0.7, $CHCl_3$, *er* = >99:1)

II-51B: *N*-((2*S*,3*S*)-4-(benzyloxy)-2,3-dichlorobutyl)-4-nitrobenzamide

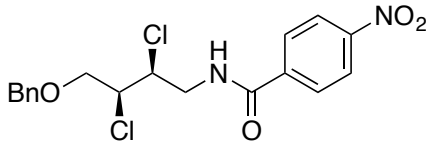

R_f : 0.50 (30% EtOAc in hexanes, UV)

^{1}H NMR (500 MHz, $CDCl_3$) δ 8.28 (d, *J* = 9.0 Hz, 2H), 7.90 (d, *J* = 9.0 Hz, 2H), 7.36-7.29 (m, 5H), 6.65 (br s, 1H), 4.67-4.63 (ddd, *J* = 8.0, 5.0, 2.0 Hz, 1H), 4.57 (s, 2H), 4.29 (dt, *J* = 7.0, 2.5 Hz 1H), 4.07-4.02 (ddd, *J* = 14.0, 7.5, 5.0 Hz, 1H), 3.78 (d, *J* = 6.5 Hz, 2H), 3.76-3.70 (ddd, *J* = 14.0, 8.5, 5.0 Hz, 1H)

^{13}C NMR (125 MHz, $CDCl_3$) δ 165.60, 149.75, 139.33, 137.13, 128.58, 128.21, 128.13, 127.87, 123.91, 73.77, 70.61, 60.12, 59.61, 44.46

HRMS analysis (ESI): Calculated for $[M+H]^+$: $C_{18}H_{19}Cl_2N_2O_4$: 397.0722; Found: 397.0717

Resolution of enantiomers: DAICEL Chiralcel® AD-H column, 15% IPA-Hexanes, 1.0 mL/min, 254 nm, RT1 (major) = 14.7 min, RT2 (minor) = 17.4 min.

$[\alpha]_D^{20}$ = +27.1 (c 0.55, $CHCl_3$, *er* = 89:11)

II-52B: *N*-((2*S*,3*S*)-5-((*tert*-butyldiphenylsilyl)oxy)-2,3-dichloropentyl)-4-nitrobenzamide

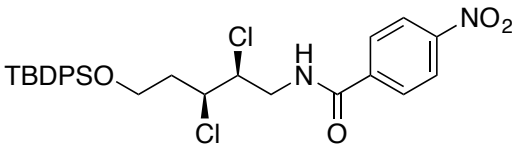

R_f : 0.60 (30% EtOAc in hexanes, UV)

^{1}H NMR (500 MHz, $CDCl_3$) δ 8.29 (d, *J* = 9.0 Hz, 2H), 7.93 (d, *J* = 9.0 Hz, 2H), 7.64-7.60 (m, 4H), 7.42-7.34 (m, 6H), 6.57 (br s, 1H), 4.60 (ddd, *J* = 9.0, 3.5, 2.5 Hz, 1H), 4.48-4.45 (ddd, *J* = 8.5, 5.0, 2.5 Hz, 1H), 4.09-4.04 (ddd, *J* = 14.5, 7.5, 5.5 Hz, 1H), 3.88-3.83 (m, 1H), 3.79-3.71 (m, 2H), 2.15-2.09 (m, 1H), 2.06-1.99 (m, 1H), 0.98 (s, 9H)

^{13}C NMR (125 MHz, $CDCl_3$) δ 165.67, 149.80, 139.27, 135.50, 135.46, 133.21,133.14, 129.81, 129.80, 128.20, 127.77, 127.75, 123.95, 63.38, 59.81, 59.49, 44.73, 38.29, 26.79, 19.17

HRMS analysis (ESI): Calculated for $[M+H]^+$: $C_{28}H_{33}Cl_2N_2O_4Si$: 559.1605; Found: 559.1609

Resolution of enantiomers: DAICEL Chiralcel® AD-H column, 7% IPA-Hexanes, 0.8 mL/min, 254 nm, RT1 (minor) = 12.5 min, RT2 (major) = 13.3 min.

$[\alpha]_D^{20}$ = +21.8 (c 0.45, $CHCl_3$, *er* = >99:1)

Syn-**II-53B**: *N*-((2*S*,3*S*)-2,3-dichloro-3-(*p*-tolyl)propyl)-4-nitrobenzamide

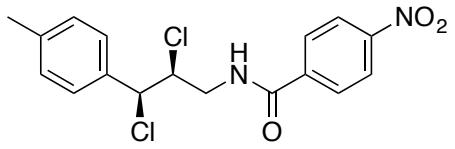

R_f : 0.60 (30% EtOAc in hexanes, UV)

^{1}H NMR (500 MHz, $CDCl_3$) δ 8.28 (d, *J* = 8.5 Hz, 2H), 7.87 (d, *J* = 8.5 Hz, 2H), 7.34 (d, *J* = 8.5 Hz, 2H), 7.19 (d, *J* = 8.5 Hz, 2H), 6.50 (br s, 1H), 5.13 (d, *J* = 5.5 Hz, 1H), 4.56-4.53 (m, 1H), 4.10-4.05 (ddd, *J* = 14.5, 7.5, 4.0 Hz, 1H), 3.50-3.44 (ddd, *J* = 13.5, 9.0, 5.0 Hz, 1H), 2.34 (s, 3H)

^{13}C NMR (125 MHz, $CDCl_3$) δ 165.49, 149.80, 139.30, 139.25, 133.79, 129.42, 128.17, 127.67, 123.92, 65.11, 64.35, 44.30, 21.18

HRMS analysis (ESI): Calculated for $[M+H]^+$: $C_{17}H_{17}Cl_2N_2O_3$: 367.0614; Found: 367.0616

Resolution of enantiomers: DAICEL Chiralcel® AD-H column, 15% IPA-Hexanes, 1.0 mL/min, 254 nm, RT1 (major) = 13.4 min, RT2 (minor) = 20.4 min.

$[\alpha]_D^{20}$ = -19.4 (c 0.4, $CHCl_3$, *er* = 97:3)

Anti-**II-53B**: *N*-((2*S*,3*R*)-2,3-dichloro-3-(*p*-tolyl)propyl)-4-nitrobenzamide

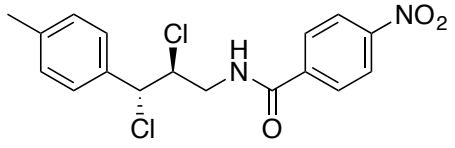

R_f : 0.60 (30% EtOAc in hexanes, UV)

^{1}H NMR (500 MHz, $CDCl_3$) δ 8.30 (d, *J* = 8.5 Hz, 2H), 7.91 (d, *J* = 8.5 Hz, 2H), 7.31 (d, *J* = 8.5 Hz, 2H), 7.19 (d, *J* = 8.5 Hz, 2H), 6.50 (br s, 1H), 4.99 (d, *J* = 8.0

Hz, 1H), 4.58-4.54 (m, 1H), 4.49-4.44 (ddd, *J* = 14.0, 6.5, 3.5 Hz, 1H), 3.67-3.62 (ddd, *J* = 13.5, 8.0, 5.0 Hz, 1H), 2.34 (s, 3H)

^{13}C NMR (125 MHz, $CDCl_3$) δ 165.42, 149.80, 139.39, 139.27, 134.56, 129.50, 128.21, 127.62, 123.92, 64.08, 63.55, 43.90, 21.21

HRMS analysis (ESI): Calculated for $[M+H]^+$: $C_{17}H_{17}Cl_2N_2O_3$: 367.0614; Found: 367.0619

Resolution of enantiomers: DAICEL Chiralcel® AD-H column, 15% IPA-Hexanes, 1.0 mL/min, 254 nm, RT1 (minor) = 14.9 min, RT2 (major) = 18.2 min.

$[\alpha]_D^{20}$ = +4.0 (c 0.3, $CHCl_3$, *er* = 91:9)

II-54B: *N*-((2*S*,3*S*)-2,3-dichloro-3-phenylpropyl)-4-nitrobenzamide

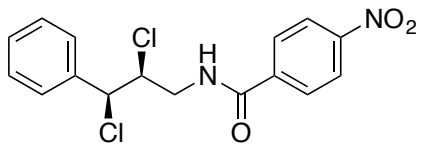

R_f : 0.50 (30% EtOAc in hexanes, UV)

^{1}H NMR (500 MHz, $CDCl_3$) δ 8.29 (d, *J* = 9.0 Hz, 2H), 7.88 (d, *J* = 9.0 Hz, 2H), 7.47-7.35 (m, 5H), 6.50 (br s, 1H), 5.18 (d, *J* = 5.0 Hz, 1H), 4.59-4.55 (m, 1H), 4.14-4.01 (ddd, *J* = 14.0, 7.5, 4.0 Hz, 1H), 3.52-3.46 (ddd, *J* = 14.0, 8.5, 4.5 Hz, 1H)

^{13}C NMR (125 MHz, $CDCl_3$) δ 165.53, 149.81, 139.21, 136.71, 129.23, 128.71, 128.17, 127.80, 123.94, 64.97, 64.25, 44.38

HRMS analysis (ESI): Calculated for $[M+H]^+$: $C_{16}H_{15}Cl_2N_2O_3$: 353.0460; Found: 353.0452

Resolution of enantiomers: DAICEL Chiralcel® AD-H column, 15% IPA-Hexanes, 1.0 mL/min, 254 nm, RT1 (major) = 13.5 min, RT2 (minor) = 27.6 min.

$[\alpha]_D^{20}$ = -11.3 (c 0.6, $CHCl_3$, *er* = >99:1)

II-55B: *N*-((2*S*,3*S*)-2,3-dichloro-3-(4-(trifluoromethyl)phenyl)propyl)-4-nitrobenzamide

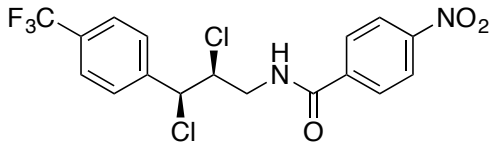

R_f : 0.43 (30% EtOAc in hexanes, UV)

^{1}H NMR (500 MHz, $CDCl_3$) δ 8.30 (d, *J* = 9.0 Hz, 2H), 7.91 (d, *J* = 9.0 Hz, 2H), 7.66 (d, *J* = 9 Hz, 2H), 7.61 (d, *J* = 8.5 Hz, 2H), 6.59 (br s, 1H), 5.27 (d, *J* = 4.5 Hz, 1H) 4.60-4.56 (m, 1H), 4.19-4.14 (ddd, *J* = 14.5, 7.0, 4.0 Hz, 1H), 3.55-3.50 (ddd, *J* = 14.5, 8.5, 4.0 Hz, 1H)

^{13}C NMR (125 MHz, $CDCl_3$) δ 165.75, 149.87, 140.55, 139.02, 131.38 (q, J_{CF} = 32.2 Hz), 128.35, 128.20, 127.2 (q, J_{CF} = 271.6 Hz), 125.63 (q, J_{CF} = 2.8 Hz), 123.99, 64.30, 63.03, 44.62

HRMS analysis (ESI): Calculated for $[M+H]^+$: $C_{17}H_{14}Cl_2N_2O_3F_3$: 421.0322; Found: 421.0334

Resolution of enantiomers: DAICEL Chiralcel® IA column, 15% IPA-Hexanes, 1.0 mL/min, 254 nm, RT1 (major) = 10.5 min, RT2 (minor) = 19.1 min.

$[\alpha]_D^{20}$ = -5.2 (c 1.0, $CHCl_3$, *er* = >99:1)

II-39B: *N*-((2*S*,3*R*)-2,3-dichlorohexyl)-4-nitrobenzamide

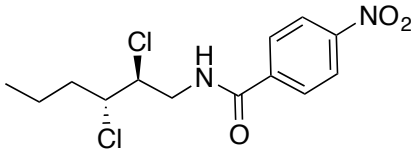

R_f : 0.56 (30% EtOAc in hexanes, UV)

^{1}H NMR (500 MHz, $CDCl_3$) δ 8.31 (d, *J* = 8.5 Hz, 2H), 7.95 (d, *J* = 8.5 Hz, 2H), 6.55 (br s, 1H), 4.40-4.35 (ddd, *J* = 14.0, 7.0, 3.0 Hz, 1H), 4.28-4.24 (ddd, *J* = 10.0, 6.5, 3.0 Hz, 1H), 4.09-4.05 (ddd, *J* = 10.0, 6.5, 3.5 Hz, 1H), 3.59-3.54 (ddd, *J* = 14.0, 8.5, 5.0 Hz, 1H), 2.04-1.97 (m, 1H), 1.85-1.80 (m, 1H), 1.68-1.61 (m, 1H), 1.49-1.44 (m, 1H), 0.97 (t, *J* = 7.0 Hz, 3H)

^{13}C NMR (125 MHz, $CDCl_3$) δ 165.54, 149.79, 139.43, 128.21, 123.96, 64.00, 63.59, 43.66, 37.21, 19.30, 13.41

HRMS analysis (ESI): Calculated for $[M+H]^+$: $C_{13}H_{17}Cl_2N_2O_3$: 319.0616; Found: 316.0610

Resolution of enantiomers: DAICEL Chiralcel® IA column, 10% IPA-Hexanes, 1.0 mL/min, 254 nm, RT1 (major) = 13.0 min, RT2 (minor) = 14.5 min.

$[\alpha]_D^{20}$ = +16.6 (c 0.5, $CHCl_3$, *er* = 92:7)

ent-**II-39B**: *N*-((2*R*,3*S*)-2,3-dichlorohexyl)-4-nitrobenzamide

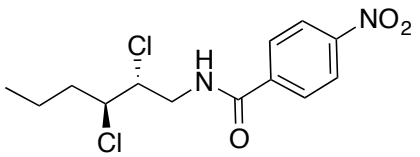

R_f : 0.56 (30% EtOAc in hexanes, UV) 80% yield with $(DHQ)_2$PHAL

^{1}H NMR (500 MHz, $CDCl_3$) δ 8.31 (d, *J* = 8.5 Hz, 2H), 7.95 (d, *J* = 8.5 Hz, 2H), 6.55 (br s, 1H), 4.40-4.35 (ddd, *J* = 14.0, 7.0, 3.0 Hz, 1H), 4.28-4.24 (ddd, *J* = 10.0, 6.5, 3.0 Hz, 1H), 4.09-4.05 (ddd, *J* = 10.0, 6.5, 3.5 Hz, 1H), 3.59-3.54 (ddd, *J* = 14.0, 8.5, 5.0 Hz, 1H), 2.04-1.97 (m, 1H), 1.85-1.80 (m, 1H), 1.68-1.61 (m, 1H), 1.49-1.44 (m, 1H), 0.97 (t, *J* = 7.0 Hz, 3H)

^{13}C NMR (125 MHz, $CDCl_3$) δ 165.54, 149.79, 139.43, 128.21, 123.96, 64.00, 63.59, 43.66, 37.21, 19.30, 13.41

HRMS analysis (ESI): Calculated for $[M+H]^+$: $C_{13}H_{17}Cl_2N_2O_3$: 319.0616; Found: 319.0611

Resolution of enantiomers: DAICEL Chiralcel® OD-H column, 5% IPA-Hexanes, 1.0 mL/min, 254 nm, RT1 (minor) = 13.0 min, RT2 (major) = 14.5 min.

$[\alpha]_D^{20}$ = -15.2 (c 1.0, $CHCl_3$, *er* = 96:4)

II-56B: 4-bromo-*N*-((2*S*,3*R*)-2,3-dichlorohexyl)benzamide

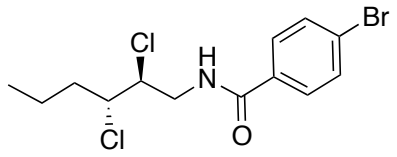

R_f : 0.54 (30% EtOAc in hexanes, UV)

^{1}H NMR (500 MHz, $CDCl_3$) δ 7.65 (d, *J* = 9.0 Hz, 2H), 7.59 (d, *J* = 9.0 Hz, 2H), 6.45 (br s, 1H), 4.36-4.31 (ddd, *J* = 14.0, 7.0, 3.0 Hz, 1H), 4.26-4.23 (m, 1H), 4.10-4.04 (ddd, *J* = 10.0, 6.5, 3.5 Hz, 1H), 3.54-3.38 (ddd, *J* = 13.5, 8.0, 4.0 Hz,

1H), 2.00-1.95 (m, 1H), 1.88-1.80 (m, 1H), 1.68-1.59 (m, 1H), 1.51-1.42 (m, 1H), 0.95 (t, *J* = 7.0 Hz, 3H)

^{13}C NMR (125 MHz, $CDCl_3$) δ 166.58, 132.73, 131.95, 128.53, 126.60, 64.31, 63.70, 43.47, 37.18, 19.35, 13.42

HRMS analysis (ESI): Calculated for $[M+H]^+$: $C_{13}H_{17}Cl_2NOBr$: 351.9871; Found: 351.9863

Resolution of enantiomers: DAICEL Chiralcel® AD-H column, 15% IPA-Hexanes, 1.0 mL/min, 254 nm, RT1 (major) = 8.4 min, RT2 (minor) = 9.5 min.

$[\alpha]_D^{20}$ = +12.4 (c 0.9, $CHCl_3$, *er* = 92:8)

II-57B: *N*-((2*S*,3*R*)-4-(benzyloxy)-2,3-dichlorobutyl)-4-nitrobenzamide

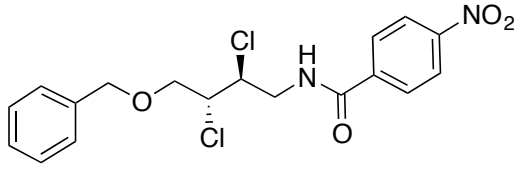

R_f : 0.50 (30% EtOAc in hexanes, UV)

^{1}H NMR (500 MHz, $CDCl_3$) δ 8.26 (d, *J* = 8.5 Hz, 2H), 7.86 (d, *J* = 8.5 Hz, 2H), 7.37-734, 5H), 6.63 (br s, 1H), 4.63-4.56 (dd, *J* = 22.5, 12.0 Hz, 2H), 4.54-4.50 (ddd, *J* = 10.5, 6.5, 4.5 Hz, 1H), 4.25-4.17 (m, 2H), 3.88 (d, *J* = 5 Hz, 2H), 3.78-3.73 (ddd, *J* = 14.0, 8.0, 5.5 Hz, 1H)

^{13}C NMR (125 MHz, $CDCl_3$) δ 165.38, 149.71, 139.41, 137.13 128.60, 128.18, 128.13, 127.85, 123.88, 73.78, 70.75, 61.05, 60.37, 43.53

HRMS analysis (ESI): Calculated for $[M+H]^+$: $C_{18}H_{19}Cl_2N_2O_4$: 397.0722; Found: 397.0725

Resolution of enantiomers: DAICEL Chiralcel® AD-H column, 15% IPA-Hexanes, 1.0 mL/min, 254 nm, RT1 (minor) = 16.1 min, RT2 (major) = 17.6 min.

$[\alpha]_D^{20}$ = +5.1 (c 0.3, $CHCl_3$, *er* = 89:11)

II-58B: *N*-((2*S*,3*R*)-2,3-dichloro-3-phenylpropyl)-4-nitrobenzamide

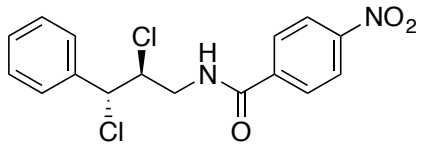

R_f : 0.44 (30% EtOAc in hexanes, UV)

^{1}H NMR (500 MHz, $CDCl_3$) δ 8.29 (d, *J* = 8.5 Hz, 2H), 7.91 (d, *J* = 8.5 Hz, 2H), 7.43-7.35 (m, 5H), 6.56 (br s, 1H), 5.02 (d, *J* = 8 Hz, 1H), 4.59-4.55 (dt, *J* = 11, 3.5 Hz, 1H), 4.49-4.44 (ddd, *J* = 14.5, 7.0, 3.5 Hz, 1H), 3.67-3.62 (ddd, *J* = 13.5, 8.5, 5.0 Hz, 1H)

^{13}C NMR (125 MHz, $CDCl_3$) δ 165.47, 149.77, 139.36, 137.47, 129.22, 128.79, 128.21, 127.75, 123.91, 63.98, 63.55, 43.89

HRMS analysis (ESI): Calculated for $[M+H]^+$: $C_{16}H_{15}Cl_2N_2O_3$: 353.0460; Found: 353.0462

Resolution of enantiomers: DAICEL Chiralcel® AD-H column, 20% IPA-Hexanes, 1.0 mL/min, 254 nm, RT1 (minor) = 10.5 min, RT2 (major) = 11.6 min.

$[\alpha]_D^{20}$ = +5.6 (c 1.0, $CHCl_3$, *er* = 90:10)

II-59B: (*S*)-*N*-(2,3-dichloro-3-methylbutyl)-4-nitrobenzamide

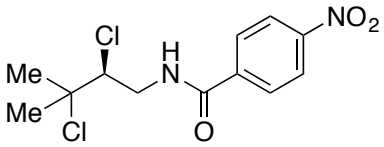

R_f : 0.50 (30% EtOAc in hexanes, UV)

^{1}H NMR (500 MHz, $CDCl_3$) δ 8.30 (d, *J* = 9.0 Hz, 2H), 7.95 (d, *J* = 9.0 Hz, 2H), 6.63 (br s, 1H), 4.58-4.53 (ddd, *J* = 10.5, 7.5, 3.0 Hz, 1H), 4.24 (dd, J = 9.5, 3.0 Hz, 1H), 3.47-3.41 (ddd, *J* = 14.5, 10.0, 4.5 Hz, 1H), 1.78 (s, 3H), 1.70 (s, 3H)

^{13}C NMR (125 MHz, $CDCl_3$) δ 165.57, 149.78, 139.51, 128.22, 123.97, 69.68, 69.44, 43.36, 31.29, 28.47

HRMS analysis (ESI): Calculated for $[M+H]^+$: $C_{12}H_{15}N_2O_3Cl_2$: 305.0460; Found: 305.0446

Resolution of enantiomers: DAICEL Chiralcel® IA column, 2% IPA-Hexanes, 1.0 mL/min, 254 nm, RT1 (major) = 113.4 min, RT2 (minor) = 130.4 min.

$[\alpha]_D^{20}$ = +42.4 (c 0.8, $CHCl_3$, *er* = 92:8)

II-35C: *N*-((2*S*,3*S*)-2-bromo-3-chlorohexyl)-4-nitrobenzamide

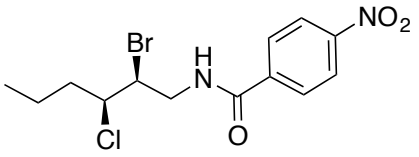

R_f : 0.52 (30% EtOAc in hexanes, UV)

^{1}H NMR (500 MHz, $CDCl_3$) δ 8.31 (d, *J* = 8.5 Hz, 2H), 7.95 (d, *J* = 8.5 Hz, 2H), 6.62 (br s, 1H), 4.52-4.50 (ddd, *J* = 9.0, 4.0, 2.0 Hz, 1H), 4.17-4.12 (ddd, *J* = 15.0, 7.5, 4.5 Hz, 1H), 4.08-4.05 (m, 1H), 3.75-3.70 (ddd, *J* = 14.0, 9.0, 5.0 Hz, 1H), 1.93-1.84 (m, 2H), 1.62-1.54 (m, 1H), 1.46-1.38 (m, 1H), 0.96 (t, *J* = 7.0 Hz, 3H)

^{13}C NMR (125 MHz, $CDCl_3$) δ 165.68, 149.82, 139.29, 128.23, 123.99, 62.70, 57.52, 45.25, 38.51, 19.67, 13.40

HRMS analysis (ESI): Calculated for $[M+H]^+$: $C_{13}H_{17}ClNO_3Br$: 363.0111; Found: 363.0107

Resolution of enantiomers: DAICEL Chiralcel® OD-H column, 10% IPA-Hexanes, 1.0 mL/min, 254 nm, RT1 (minor) = 4.7 min, RT2 (major) = 14.7 min.

$[\alpha]_D^{20}$ = +54.3 (c 0.5, $CHCl_3$, *er* = >99:1)

Absolute stereochemistry was determined by single crystal X-ray diffraction (XRD). Crystals for XRD were obtained by crystallization from CH_2Cl_2 layered with hexanes in a silicone-coated vial.

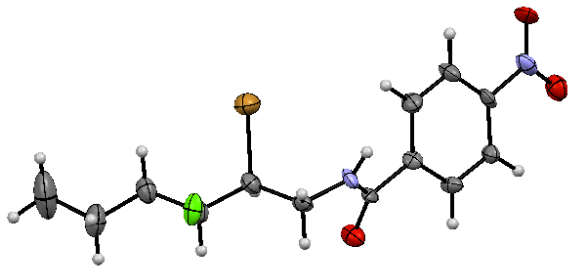

II-35C': *N*-((2*S*,3*S*)-2,3-dibromohexyl)-4-nitrobenzamide

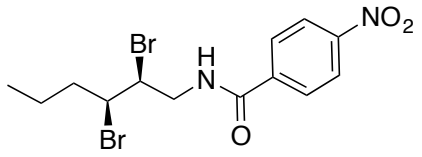

R_f : 0.60 (30% EtOAc in hexanes, UV)

^{1}H NMR (500 MHz, $CDCl_3$) δ 8.31 (d, *J* = 8.5 Hz, 2H), 7.94 (d, *J* = 8.5 Hz, 2H), 6.61 (br s, 1H), 4.50-4.47 (ddd, *J* = 9.0, 4.0, 2.5 Hz, 1H), 4.23-4.15 (m, 2H), 3.75-3.69 (ddd, *J* = 14.5, 9.0, 5.5 Hz, 1H), 1.99-1.93 (m, 2H), 1.62-1.56 (m, 1H), 1.45-1.40 (m, 1H), 0.96 (t, *J* = 7.5 Hz, 3H)

^{13}C NMR (125 MHz, $CDCl_3$) δ 165.64, 149.82, 139.27, 128.23, 123.98, 57.50, 56.06, 45.94, 38.68, 20.75, 13.26

HRMS analysis (ESI): Calculated for $[M+H]^+$: $C_{13}H_{17}N_2O_3Br_2$: 406.9606; Found: 406.9603

Resolution of enantiomers: DAICEL Chiralcel® IA column, 10% IPA-Hexanes, 1.0 mL/min, 254 nm, RT1 (major) = 14.7 min, RT2 (minor) = 17.9 min.

$[\alpha]_D^{20}$ = +32.7 (c 0.4, $CHCl_3$, *er* = 83.0:17.0)

II-55C: *N*-((2*S*,3*S*)-2-bromo-3-chloro-3-(4-(trifluoromethyl)phenyl)propyl)-4-nitrobenzamide

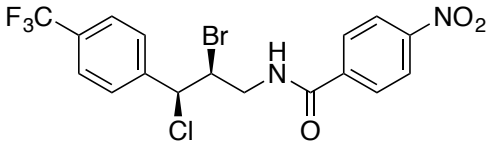

R_f : 0.60 (30% EtOAc in hexanes, UV)

^{1}H NMR (500 MHz, $CDCl_3$) δ 8.29 (d, *J* = 8.0 Hz, 2H), 7.91 (d, *J* = 8.0 Hz, 2H), 7.66 (d, *J* = 9 Hz, 2H), 7.61 (d, *J* = 8.5 Hz, 2H), 6.63 (br s, 1H), 5.29 (d, *J* = 4.0 Hz, 1H) 4.69-4.65 (m, 1H), 4.25-4.20 (ddd, *J* = 14.5, 7.0, 4.0 Hz, 1H), 3.65-3.59 (ddd, *J* = 14.5, 9.0, 5.0 Hz, 1H),

^{13}C NMR (125 MHz, $CDCl_3$) δ 165.68, 149.85, 140.77, 139.04, 131.57 (q, J_{CF} = 32.1 Hz), 128.29, 128.19, 126.77 (q, J_{CF} = 271.8 Hz), 125.57 (q, J_{CF} = 3.7 Hz), 123.99, 63.03, 57.82, 44.98

HRMS analysis (ESI): Calculated for $[M+H]^+$: $C_{17}H_{14}ClBrN_2O_3$: 468.9827; Found: 468.9828

Resolution of enantiomers: DAICEL Chiralcel® AD-H column, 15% IPA-Hexanes, 1.0 mL/min, 254 nm, RT1 (major) = 11.5 min, RT2 (minor) = 21.7 min.

$[\alpha]_D^{20}$ = +2.5 (c 1.0, $CHCl_3$, *er* = >99:1)

II-39C: *N*-((2*S*,3*R*)-2-bromo-3-chlorohexyl)-4-nitrobenzamide

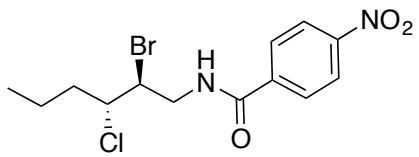

R_f : 0.50 (30% EtOAc in hexanes, UV)

^{1}H NMR (500 MHz, $CDCl_3$) δ 8.30 (d, *J* = 8.5 Hz, 2H), 7.95 (d, *J* = 8.5 Hz, 2H), 6.62 (br s, 1H), 4.41-4.35 (m, 2H), 4.15-4.11 (ddd, *J* = 10.0, 7.0, 3.5 Hz, 1H), 3.69-3.63 (ddd, *J* = 15.0, 10.0, 5.5 Hz, 1H), 2.08-2.02 (m, 1H), 1.91-1.83 (m, 1H), 1.68-1.60 (m, 1H), 1.52-1.44 (m, 1H), 0.967 (t, *J* = 7.5 Hz, 3H)

^{13}C NMR (125 MHz, $CDCl_3$) δ 165.46, 149.77, 139.44, 128.22, 123.95, 63.76, 57.32, 44.11, 38.22, 19.32, 13.38

HRMS analysis (ESI): Calculated for $[M+H]^+$: $C_{13}H_{17}ClN_2O_3Br$: 363.0111; Found: 363.0103

Resolution of enantiomers: DAICEL Chiralcel® IA column, 10% IPA-Hexanes, 1.0 mL/min, 254 nm, RT1 (major) = 13.7 min, RT2 (minor) = 15.0 min.

$[\alpha]_D^{20}$ = +6.6 (c 1.0, $CHCl_3$, *er* = 92:8)

II-58C: *N*-((2*S*,3*R*)-2-bromo-3-chloro-3-phenylpropyl)-4-nitrobenzamide

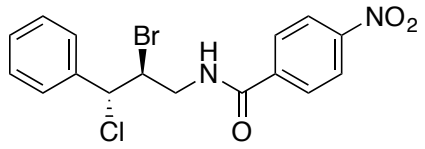

R_f : 0.50 (30% EtOAc in hexanes, UV)

^{1}H NMR (500 MHz, $CDCl_3$) δ 8.30 (d, *J* = 8.5 Hz, 2H), 7.93 (d, *J* = 8.5 Hz, 2H), 7.42-7.35 (m, 5H), 6.57 (br s, 1H), 5.08 (d, *J* = 9.5 Hz, 1H), 4.68-4.64 (dt, *J* = 12.0, 3.5 Hz, 1H), 4.56-4.51 (ddd, *J* = 14, 6.5, 3.0 Hz, 1H), 3.81-3.75 (ddd, *J* = 14.0, 8.0, 5.5 Hz, 1H),

^{13}C NMR (125 MHz, $CDCl_3$) δ 165.35, 149.80, 139.39, 138.30, 129.24, 128.81, 128.23, 127.61, 123.95, 63.62, 56.95, 44.35

HRMS analysis (ESI): Calculated for $[M+H]^+$: $C_{16}H_{15}ClBrN_2O_3$: 369.9955; Found: 369.9939

Resolution of enantiomers: DAICEL Chiralcel® AD-H column, 20% IPA-Hexanes, 1.0 mL/min, 254 nm, RT1 (minor) = 11.4 min, RT2 (major) = 12.5 min.

$[\alpha]_D^{20}$ = +26.3 (c 0.7, $CHCl_3$, *er* = 89:11)

II-2-13-6 Analytical data for byproduct II-45

II-45: *N*-(2-chloro-3-(2,2,2-trifluoroethoxy)hexyl)-4-nitrobenzamide

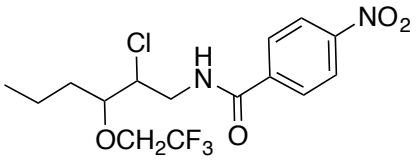

R_f : 0.60 (30% EtOAc in hexanes, UV)

^{1}H NMR (500 MHz, $CDCl_3$) δ 8.30 (d, *J* = 8.5 Hz, 2H), 7.93 (d, *J* = 8.5 Hz, 2H), 6.68 (br s, 1H), 4.28-4.25 (m, 1H), 4.15-4.10 (ddd, *J* = 14.5, 7.0, 4.5 Hz, 1H), 3.99-3.91 (m, 2H), 3.73-3.70 (dt, *J* = 10.5, 3.5 Hz, 1H), 3.59-3.54 (ddd, *J* = 13.5, 9.0, 5.0 Hz, 1H), 1.78-1.73 (m, 1H), 1.67-1.60 (m, 1H), 1.45-1.35 (m, 2H), 0.96 (t, *J* = 7.5 Hz, 3H)

^{13}C NMR (125 MHz, $CDCl_3$) δ 165.63, 149.76, 139.46, 128.16, 127.03 (q, J_{CF} = 277.8 Hz), 123.93, 82.57, 67.33 (q, J_{CF} = 34.1 Hz), 60.76, 43.44, 32.18, 18.53, 13.96

HRMS analysis (ESI): Calculated for $[M+H]^+$: $C_{15}H_{19}ClN_2O_4F_3$: 383.0985; Found: 383.0970

II-2-13-7 Analytical data for products in non-catalyzed reaction (II-48C, II-48D, II-48E)

II-48C: 4-bromo-*N*-((2*S*,3*S*)-2-bromo-3-chlorohexyl)benzamide

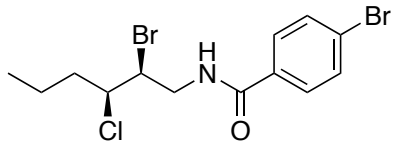

R_f : 0.54 (30% EtOAc in hexanes, UV)

^{1}H NMR (500 MHz, $CDCl_3$) δ 7.64 (d, *J* = 8.0 Hz, 2H), 7.57 (d, *J* = 8.5 Hz, 2H), 6.60 (br s, 1H), 4.51-4.48 (ddd, *J* = 8.5, 5.0, 2.5 Hz, 1H), 4.09-4.03 (m, 2H), 3.73-3.67 (ddd, *J* = 14, 9.0, 5.0 Hz, 1H), 1.92-1.78 (m, 2H), 1.59-1.52 (m, 1H), 1.44-1.37 (m, 1H), 0.94 (t, *J* = 7.0 Hz, 3H)

^{13}C NMR (125 MHz, $CDCl_3$) δ 166.77, 132.56, 131.94, 128.58, 126.66, 62.74, 57.71, 45.15, 38.61, 19.65, 13.39

HRMS analysis (ESI): Calculated for $[M+H]^+$: $C_{13}H_{17}ClBr_2NO$: 395.9365; Found: 395.9374

Resolution of enantiomers: DAICEL Chiralcel® AD-H column, 10% IPA-Hexanes, 1.0 mL/min, 254 nm, RT1 (major) = 10.2 min, RT2 (minor) = 20.8 min.

$[\alpha]_D^{20}$ = +40.1 (c 1.0, $CHCl_3$, *er* = 94:6)

II-48D: 4-bromo-*N*-((2*S*,3*S*)-3-bromo-2-chlorohexyl)benzamide

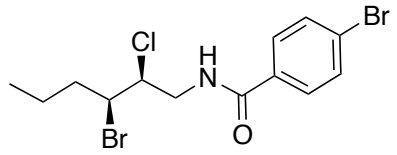

R_f : 0.54 (30% EtOAc in hexanes, UV)

^{1}H NMR (500 MHz, $CDCl_3$) δ 7.64 (d, *J* = 8.5 Hz, 2H), 7.59 (d, *J* = 8.5 Hz, 2H), 6.49 (br s, 1H), 4.32-4.29 (ddd, *J* = 9.0, 4.0, 2.5 Hz, 1H), 4.27-4.24 (ddd, *J* = 9.0, 4.5, 2.0 Hz, 1H), 4.08-4.03 (ddd, *J* = 14.0, 7.0, 4.5 Hz, 1H), 3.65-3.59 (ddd, *J* = 14.5, 9.0, 5,0 Hz, 1H), 1.98-1.87 (m, 2H), 1.62-1.56 (m, 1H), 1.45-1.38 (m, 1H), 0.95 (t, *J* = 7.0 Hz, 3H)

^{13}C NMR (125 MHz, $CDCl_3$) δ 165.80, 132.54, 131.97, 128.57, 126.70, 63.57, 59.32, 45.80, 38.08, 20.72, 13.30

HRMS analysis (ESI): Calculated for $[M+H]^+$: $C_{13}H_{17}ClBr_2NO$: 395.9365; Found: 395.9373

II-48E: (*S*)-5-((*S*)-1-bromobutyl)-2-(4-bromophenyl)-4,5-dihydrooxazole

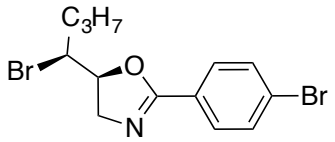

R_f : 0.30 (30% EtOAc in hexanes, UV)

^{1}H NMR (500 MHz, $CDCl_3$) δ 7.80 (d, *J* = 8.5 Hz, 2H), 7.55 (d, *J* = 8.5 Hz, 2H), 4.86-4.82 (m, 1H), 4.16-4.11 (dd, *J* = 15.0, 10.0 Hz, 1H), 4.09-4.05 (dt, *J* = 10.0, 3.5 Hz, 1H), 3.98-3.94 (dd, *J* = 15.0, 7.0 Hz, 1H), 1.89-1.82 (m, 1H), 1.80-1.74 (m, 1H), 1.70-1.63 (m, 1H), 1.50-1.42 (m, 1H), 0.95 (t, *J* = 7.0 Hz, 3H)

^{13}C NMR (125 MHz, $CDCl_3$) δ 163.04, 131.67, 129.72, 126.27, 126.18, 81.21, 58.30, 56.36, 35.42, 20.78, 13.36

HRMS analysis (ESI): Calculated for $[M+H]^+$: $C_{13}H_{16}Br_2NO$: 359.9599; Found: 359.9610

II-2-13-8 Analytical data for substrate II-55A

II-55A: (*Z*)-4-nitro-*N*-(3-(4-(trifluoromethyl)phenyl)allyl)benzamide

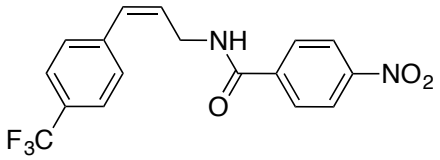

R_f : 0.39 (30% EtOAc in hexanes, UV)

^{1}H NMR (500 MHz, $CDCl_3$) δ 8.20 (d, *J* = 8.5 Hz, 2H), 7.88 (d, *J* = 8.5 Hz, 2H), 7.58 (d, *J* = 7.5 Hz, 2H), 7.34 (d, *J* = 7.5 Hz, 2H), 6.67 (br s, 1H), 6.63 (d, *J* = 12.0 Hz, 1H), 5.86-5.81 (m, 1H), 4.32 (t, *J* = 6.0 Hz, 2H)

^{13}C NMR (125 MHz, $CDCl_3$) δ 165.42, 149.51, 139.68, 139.57, 139.55, 130.84, 129.72 (q, J_{CF} = 32.2 Hz), 129.24, 128.89, 128.10, 127.19 (q, J_{CF} = 270.3 Hz), 125.35 (q, J_{CF} = 3.8 Hz), 38.51

HRMS analysis (ESI): Calculated for $[M+H]^+$: $C_{17}H_{14}N_2O_3F_3$: 351.0957; Found: 351.095

REFERENCES

REFERENCES

1. Gribble, G. W., Naturally occurring organohalogen compounds--a comprehensive survey. *Fortschr. Chem. Org. Naturst.* **1996,** *68*, 1-423.

2. Gribble, G. W., Introduction. *Fortschr. Chem. Org. Naturst.* **2010,** *91*, 1.

3. Gribble, G. W., Occurrence of halogenated alkaloids. *Alkaloids Chem. Biol.* **2012,** *71*, 1-165.

4. Chung, W. J.; Vanderwal, C. D., Stereoselective Halogenation in Natural Product Synthesis. *Angew. Chem. Int. Ed. Engl.* **2016,** *55* (14), 4396-434.

5. Arai, T.; Watanabe, O.; Yabe, S.; Yamanaka, M., Catalytic Asymmetric Iodocyclization of N-Tosyl Alkenamides using Aminoiminophenoxy Copper Carboxylate: A Concise Synthesis of Chiral 8-Oxa-6-Azabicyclo[3.2.1]octanes. *Angew. Chem. Int. Ed. Engl.* **2015,** *54* (43), 12767-71.

6. Ashtekar, K. D.; Marzijarani, N. S.; Jaganathan, A.; Holmes, D.; Jackson, J. E.; Borhan, B., A new tool to guide halofunctionalization reactions: the halenium affinity (HalA) scale. *J. Am. Chem. Soc.* **2014,** *136* (38), 13355-62.

7. Cai, Y.; Zhou, P.; Liu, X.; Zhao, J.; Lin, L.; Feng, X., Diastereoselectively switchable asymmetric haloaminocyclization for the synthesis of cyclic sulfamates. *Chem. Eur. J.* **2015,** *21* (17), 6386-9.

8. Cai, Y. F.; Liu, X. H.; Hui, Y. H.; Jiang, J.; Wang, W. T.; Chen, W. L.; Lin, L. L.; Feng, X. M., Catalytic Asymmetric Bromoamination of Chalcones: Highly Efficient Synthesis of Chiral alpha-Bromo-beta-Amino Ketone Derivatives. *Angew. Chem. Int. Ed.* **2010,** *49* (35), 6160-6164.

9. Castellanos, A.; Fletcher, S. P., Current methods for asymmetric halogenation of olefins. *Chem. Eur. J.* **2011,** *17* (21), 5766-76.

10. Chen, G.; Ma, S., Enantioselective halocyclization reactions for the synthesis of chiral cyclic compounds. *Angew. Chem. Int. Ed. Engl.* **2010,** *49* (45), 8306-8.

11. Chen, J.; Zhou, L., Recent Progress in the Asymmetric Intermolecular Halogenation of Alkenes. *Synthesis-Stuttgart* **2014,** *46* (5), 586-595.

12. Cheng, Y. A.; Yu, W. Z.; Yeung, Y. Y., Recent advances in asymmetric intra- and intermolecular halofunctionalizations of alkenes. *Org. Biomol. Chem.* **2014,** *12* (15), 2333-43.

13. Cheng, Y. A.; Yu, W. Z.; Yeung, Y. Y., Carbamate-catalyzed enantioselective bromolactamization. *Angew. Chem. Int. Ed. Engl.* **2015,** *54* (41), 12102-6.

14. Cresswell, A. J.; Eey, S. T.; Denmark, S. E., Catalytic, stereospecific syn-dichlorination of alkenes. *Nat. Chem.* **2014,** *7* (2), 146-52.

15. Cresswell, A. J.; Eey, S. T.; Denmark, S. E., Catalytic, Stereoselective Dihalogenation of Alkenes: Challenges and Opportunities. *Angew. Chem. Int. Ed. Engl.* **2015,** *54* (52), 15642-82.

16. Denmark, S. E.; Kuester, W. E.; Burk, M. T., Catalytic, asymmetric halofunctionalization of alkenes--a critical perspective. *Angew. Chem. Int. Ed. Engl.* **2012,** *51* (44), 10938-53.

17. Dobish, M. C.; Johnston, J. N., Achiral Counterion Control of Enantioselectivity in a Brønsted Acid-Catalyzed Iodolactonization. *J. Am. Chem. Soc.* **2012,** *134* (14), 6068-6071.

18. Fang, C.; Paull, D. H.; Hethcox, J. C.; Shugrue, C. R.; Martin, S. F., Enantioselective Iodolactonization of Disubstituted Olefinic Acids Using a Bifunctional Catalyst. *Org. Lett.* **2012,** *14* (24), 6290-6293.

19. Hennecke, U., New catalytic approaches towards the enantioselective halogenation of alkenes. *Chem. Asian J.* **2012,** *7* (3), 456-65.

20. Hennecke, U.; Wilking, M., Desymmetrization as a Strategy in Asymmetric Halocyclization Reactions. *Synlett* **2014,** *25* (12), 1633-1637.

21. Jaganathan, A.; Borhan, B., Chlorosulfonamide salts are superior electrophilic chlorine precursors for the organocatalytic asymmetric chlorocyclization of unsaturated amides. *Org. Lett.* **2014,** *16* (14), 3616-9.

22. Jaganathan, A.; Garzan, A.; Whitehead, D. C.; Staples, R. J.; Borhan, B., A catalytic asymmetric chlorocyclization of unsaturated amides. *Angew. Chem. Int. Ed. Engl.* **2011,** *50* (11), 2593-6.

23. Jaganathan, A.; Staples, R. J.; Borhan, B., Kinetic resolution of unsaturated amides in a chlorocyclization reaction: concomitant enantiomer

differentiation and face selective alkene chlorination by a single catalyst. *J. Am. Chem. Soc.* **2013,** *135* (39), 14806-13.

24. Ke, Z.; Tan, C. K.; Chen, F.; Yeung, Y. Y., Catalytic asymmetric bromoetherification and desymmetrization of olefinic 1,3-diols with C2-symmetric sulfides. *J. Am. Chem. Soc.* **2014,** *136* (15), 5627-30.

25. Mizar, P.; Burrelli, A.; Gunther, E.; Softje, M.; Farooq, U.; Wirth, T., Organocatalytic stereoselective iodoamination of alkenes. *Chem. Eur. J.* **2014,** *20* (41), 13113-6.

26. Murai, K.; Fujioka, H., Recent Progress in Organocatalytic Asymmetric Halocyclization. *Heterocycles* **2013,** *87* (4), 763-805.

27. Nakatsuji, H.; Sawamura, Y.; Sakakura, A.; Ishihara, K., Cooperative activation with chiral nucleophilic catalysts and N-haloimides: enantioselective iodolactonization of 4-arylmethyl-4-pentenoic acids. *Angew. Chem. Int. Ed. Engl.* **2014,** *53* (27), 6974-7.

28. Pan, H.; Huang, H.; Liu, W.; Tian, H.; Shi, Y., Phosphine Oxide-Sc(OTf)3 Catalyzed Highly Regio- and Enantioselective Bromoaminocyclization of (E)-Cinnamyl Tosylcarbamates. An Approach to a Class of Synthetically Versatile Functionalized Molecules. *Org. Lett.* **2016,** *18* (5), 896-9.

29. Soltanzadeh, B.; Jaganathan, A.; Staples, R. J.; Borhan, B., Highly Stereoselective Intermolecular Haloetherification and Haloesterification of Allyl Amides. *Angew. Chem. Int. Ed. Engl.* **2015,** *54* (33), 9517-22.

30. Tan, C. K.; Yeung, Y. Y., Recent advances in stereoselective bromofunctionalization of alkenes using N-bromoamide reagents. *Chem. Commun.* **2013,** *49* (73), 7985-96.

31. Tan, C. K.; Zhou, L.; Yeung, Y. Y., Organocatalytic Enantioselective Halolactonizations: Strategies of Halogen Activation. *Synlett* **2011,** (10), 1335-1339.

32. Toda, Y.; Pink, M.; Johnston, J. N., Bronsted acid catalyzed phosphoramidic acid additions to alkenes: diastereo- and enantioselective halogenative cyclizations for the synthesis of C- and P-chiral phosphoramidates. *J. Am. Chem. Soc.* **2014,** *136* (42), 14734-7.

33. Tripathi, C. B.; Mukherjee, S., Catalytic Enantioselective 1,4-Iodofunctionalizations of Conjugated Dienes. *Org. Lett.* **2015,** *17* (18), 4424-7.

34. Veitch, G. E.; Jacobsen, E. N., Tertiary aminourea-catalyzed enantioselective iodolactonization. *Angew. Chem. Int. Ed. Engl.* **2010,** *49* (40), 7332-5.

35. Wang, Y.-M.; Wu, J.; Hoong, C.; Rauniyar, V.; Toste, F. D., Enantioselective Halocyclization Using Reagents Tailored for Chiral Anion Phase-Transfer Catalysis. *J. Am. Chem. Soc.* **2012,** *134* (31), 12928-12931.

36. Whitehead, D. C.; Yousefi, R.; Jaganathan, A.; Borhan, B., An Organocatalytic Asymmetric Chlorolactonization. *J. Am. Chem. Soc.* **2010,** *132* (10), 3298-3300.

37. Wilking, M.; Muck-Lichtenfeld, C.; Daniliuc, C. G.; Hennecke, U., Enantioselective, desymmetrizing bromolactonization of alkynes. *J. Am. Chem. Soc.* **2013,** *135* (22), 8133-6.

38. Xie, W.; Jiang, G.; Liu, H.; Hu, J.; Pan, X.; Zhang, H.; Wan, X.; Lai, Y.; Ma, D., Highly enantioselective bromocyclization of tryptamines and its application in the synthesis of (-)-chimonanthine. *Angew. Chem. Int. Ed. Engl.* **2013,** *52* (49), 12924-7.

39. Yin, Q.; You, S. L., Asymmetric chlorocyclization of indole-3-yl-benzamides for the construction of fused indolines. *Org. Lett.* **2014,** *16* (9), 2426-9.

40. Yousefi, R.; Ashtekar, K. D.; Whitehead, D. C.; Jackson, J. E.; Borhan, B., Dissecting the stereocontrol elements of a catalytic asymmetric chlorolactonization: syn addition obviates bridging chloronium. *J. Am. Chem. Soc.* **2013,** *135* (39), 14524-7.

41. Zeng, X.; Miao, C.; Wang, S.; Xia, C.; Sun, W., Asymmetric 5-endo chloroetherification of homoallylic alcohols toward the synthesis of chiral beta-chlorotetrahydrofurans. *Chem. Commun.* **2013,** *49* (24), 2418-20.

42. Zhang, W.; Liu, N.; Schienebeck, C. M.; Zhou, X.; Izhar, I. I.; Guzei, I. A.; Tang, W. P., Enantioselective intermolecular bromoesterification of allylic sulfonamides. *Chem. Sci.* **2013,** *4* (6), 2652-2656.

43. Zheng, S. Q.; Schienebeck, C. M.; Zhang, W.; Wang, H. Y.; Tang, W. P., Cinchona Alkaloids as Organocatalysts in Enantioselective Halofunctionalization of Alkenes and Alkynes. *Asian J. Org. Chem.* **2014,** *3* (4), 366-376.

44. Denmark, S. E.; Burk, M. T.; Hoover, A. J., On the Absolute Configurational Stability of Bromonium and Chloronium Ions. *J. Am. Chem. Soc.* **2010,** *132* (4), 1232-1233.

45. Nicolaou, K. C.; Simmons, N. L.; Ying, Y. C.; Heretsch, P. M.; Chen, J. S., Enantioselective Dichlorination of Allylic Alcohols. *J. Am. Chem. Soc.* **2011,** *133* (21), 8134-8137.

46. Snyder, S. A.; Tang, Z. Y.; Gupta, R., Enantioselective total synthesis of (-)-napyradiomycin A1 via asymmetric chlorination of an isolated olefin. *J. Am. Chem. Soc.* **2009,** *131* (16), 5744-5.

47. Hu, D. X.; Shibuya, G. M.; Burns, N. Z., Catalytic Enantioselective Dibromination of Allylic Alcohols. *J. Am. Chem. Soc.* **2013,** *135* (35), 12960-12963.

48. Hu, D. X.; Seidl, F. J.; Bucher, C.; Burns, N. Z., Catalytic chemo-, regio-, and enantioselective bromochlorination of allylic alcohols. *J. Am. Chem. Soc.* **2015,** *137* (11), 3795-8.

49. Bucher, C.; Deans, R. M.; Burns, N. Z., Highly Selective Synthesis of Halomon, Plocamenone, and Isoplocamenone. *J. Am. Chem. Soc.* **2015,** *137* (40), 12784-7.

50. Landry, M. L.; Hu, D. X.; McKenna, G. M.; Burns, N. Z., Catalytic Enantioselective Dihalogenation and the Selective Synthesis of (-)-Deschloromytilipin A and (-)-Danicalipin A. *J. Am. Chem. Soc.* **2016,** *138* (15), 5150-8.

51. Nilewski, C.; Geisser, R. W.; Carreira, E. M., Total synthesis of a chlorosulpholipid cytotoxin associated with seafood poisoning. *Nature* **2009,** *457* (7229), 573-6.

52. Chung, W. J.; Carlson, J. S.; Bedke, D. K.; Vanderwal, C. D., A synthesis of the chlorosulfolipid mytilipin A via a longest linear sequence of seven steps. *Angew. Chem. Int. Ed. Engl.* **2013,** *52* (38), 10052-5.

53. Shibatomi, K.; Zhang, Y.; Yamamoto, H., Lewis acid catalyzed benzylic bromination. *Chem. Asian J.* **2008,** *3* (8-9), 1581-4.

54. Ivanov, A.; Ejaz, S. A.; Shah, S. J.; Ehlers, P.; Villinger, A.; Frank, E.; Schneider, G.; Wolfling, J.; Rahman, Q.; Iqbal, J.; Langer, P., Synthesis, functionalization and biological activity of arylated derivatives of (+)-estrone. *Bioorganic & medicinal chemistry* **2017,** *25* (3), 949-962.

55. Khazaei, A.; Zolfigol, M. A.; Rostami, A., 1,3-Dibromo-5,5-Dimethylhydantoin DBDMH as an Efficient and Selective Agent for the Oxidation of Thiols to Disulfides in Solution or under Solvent-Free Conditions. *Synthesis* **2004,** *2004* (18).

56. Tan, C. K.; Yeung, Y.-Y., Recent advances in stereoselective bromofunctionalization of alkenes using N-bromoamide reagents. *Chem. Commun.* **2013,** *49* (73), 7985-7996.

57. Markish, I.; Arrad, O., New Aspects on the Preparation of 1,3-Dibromo-5,5-dimethylhydantoin. *Industrial & Engineering Chemistry Research* **1995,** *34* (6), 2125-2127.

58. de Almeida, L. S.; Esteves, P. M.; de Mattos, M. C. S., Tribromoisocyanuric Acid: A New Reagent for Regioselective Cobromination of Alkenes. *Synlett* **2006,** *2006* (10), 1515-1518.

Chapter III: Highly regio-, diastereo-, and enantioselective chloroamination of alkenes

III-1 Introduction

Molecules that contain amines and halogens in their structure are found in different natural products and bioactive compounds (Figure III-1).[1-4] Additionally, haloamine compounds are versatile motifs in organic synthesis, where the halogens can serve as a leaving group to yield aziridines or can be utilized in cross-coupling reactions.[5-6]

Figure III-1: Biologically active haloamines

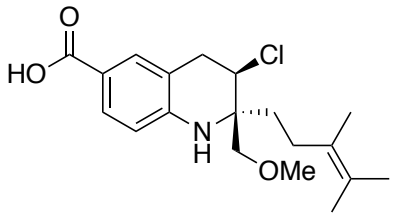

virantmycin
antiviral antibiotic

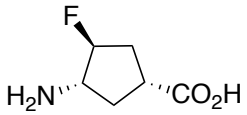

GABA-AT inactivator

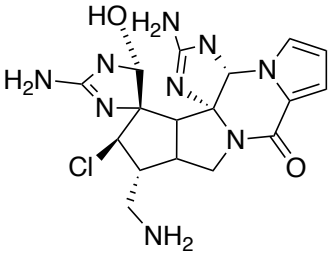

palau'amine
cytoxic and immunosuppressive

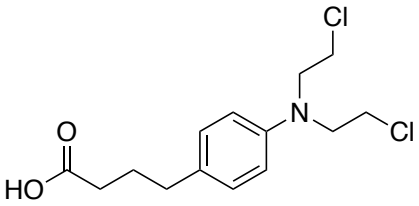

Chloambucil
chemotherapy

One of the common methods for synthesizing haloamines is activating the carbon-carbon double bond with various halogen donors as electrophiles and subsequently nucleophilic attack of the putative halonium ion with different amine sources. Recently our lab suggested that the well-known two-step mechanism in halofunctionalization (1-formation of halonium, 2- nucleophilic attack to halonium ion intermediate) is not the predominant mechanism in many halofunctionalization reactions. Based on kinetic isotopic effect (KIE), NMR and kinetic studies our lab proposed a nucleophile dependent path where the nucleophile pre-polarizes the alkene, leading to a more nucleophilic olefin that can compete effectively with the halenium source for the halogenation. In this manner, the halofunctionalization occurs via a concerted transition state (Figure III-2).[7]

Figure III-2: Nucleophile assisted alkene activation (NAAA)

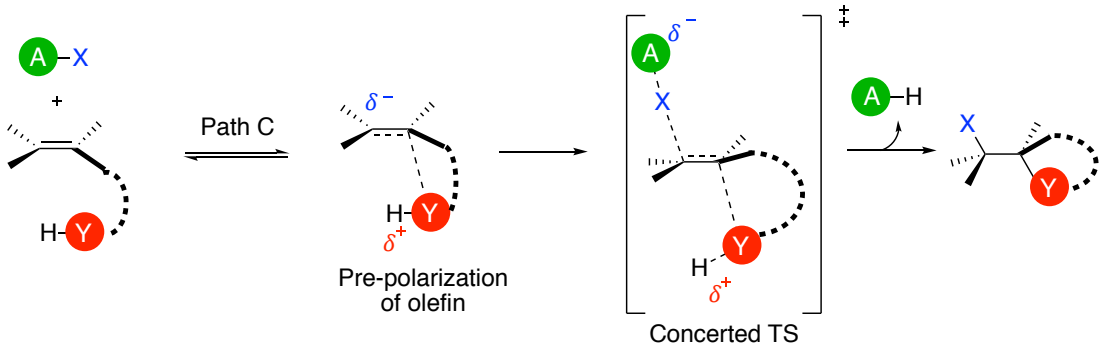

For developing new methodology in haloamination reaction, employing amine sources as the nucleophile in the halofunctionalization reaction is challenging. The basic nature of amines leads to higher halonium affinity. This is apparent if one consults the reported Hal A values for amines.[8] Therefore for developing the

methodologies for haloamination reaction, choosing nucleophilic amine sources with lower halonium affinity is essential.

We have recently begun to explore the intermolecular halofuctionalization of alkenes.[9-10] This possesses additional challenges in comparison to the intramolecular halofunctionalization reactions. Intramolecular reactions always have the nucleophile in close proximity as it is tethered, allowing for a quick capture of the halonium intermediate or a β-halocarbenium ion. A long-lived cation might erode enantioselectivity and diastereoselectivity.[11] Also, intramolecular reactions (cyclization) often rely on ring closure kinetics and molecular geometry leading to the major regioisomer.[12] On the other hand, approaching externally, the intermolecular nucleophile must be able to differentiate between the two possible positions it can attack. Finally, in some cases, the external nucleophile must outcompete the tethered nucleophile for a reaction at the same location. The first intermolecular catalytic asymmetric reaction we developed was a haloetherification reaction. This was done via optimizing conditions such as solvent and concentration to outcompete the cyclization reaction and simultaneously afford high enantioselectivity and yield for the intermolecular reaction. We were able to obtain enantiomeric excesses as high as 99% for this methodology (see Chapter I and Figure III-3a).[9] We then extended this methodology to dihalogenation reactions, such as dichlorination and chlorobromination. This provided the products with high enantioselectivity and yield (see Chapter II and Figure III-3b).[10]

Figure III-3: (a) Highly enantioselective haloetherification of allyl amides (b) Highly enantioselective dihalogenation of allyl amides

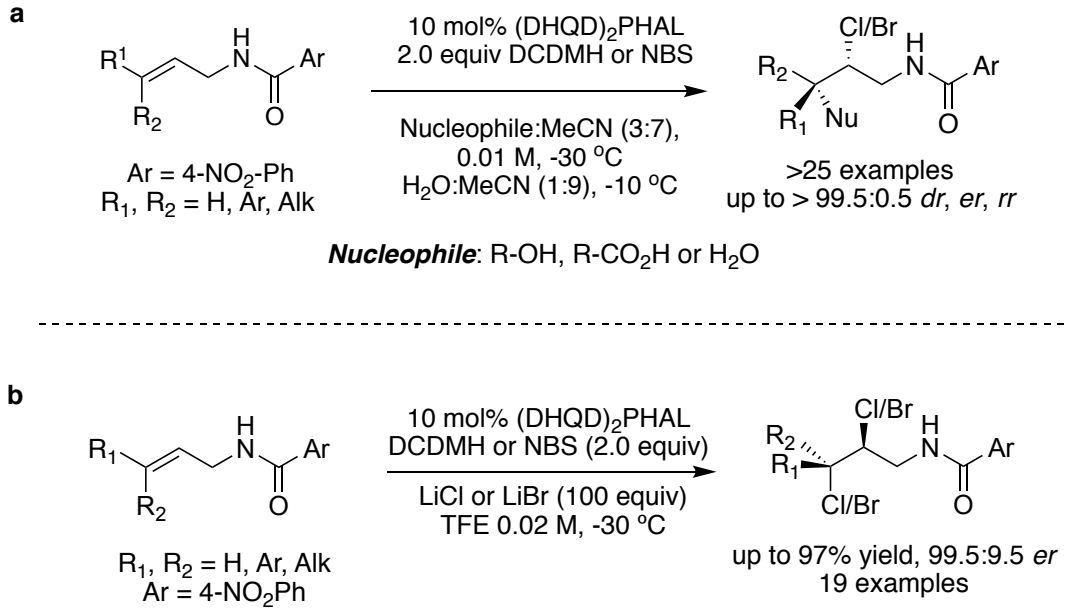

Utilizing our experiences for developing catalytic asymmetric intermolecular haloetherification and dihalogenation reactions of alkenes, we sought to develop a highly enantio-, diastereo- and regioselective haloamination. Our goal was for this methodology to work well for a variety of alkenes, including those with no bias for regioselectivity (alkenes with only alkyl substituents), where other methods have failed.

III-1-1 Literature precedence for catalytic vicinal haloamination of alkenes

III-1-1-1 Literature precedence for catalytic-racemic vicinal haloamination of alkenes

A halogen vicinal to an amine has been a useful intermediate in the synthesis of aminated oligosaccharides. Danishefsky and co-workers reported sulfonamidoglycosylation of glycals, a route to oligosaccharides with 2-aminohexose subunits in 1990.[5] In this report, benzenesulfonamide was employed as an amine nucleophilic source, and IDCP **III-2** was used as iodonium agent to yield haloaminated product **III-3** in 78% yield and >99% diastereoselectivity. Treating haloamine **III-3** with base produced aziridine **III-4**. This aziridine ring was then opened via a nucleophilic attack of sugar to form oligosaccharide **III-5** in 52% yield after two steps (Figure III-4).

Figure III-4: A general procedure for sulfonamidoglycosylation of glycals

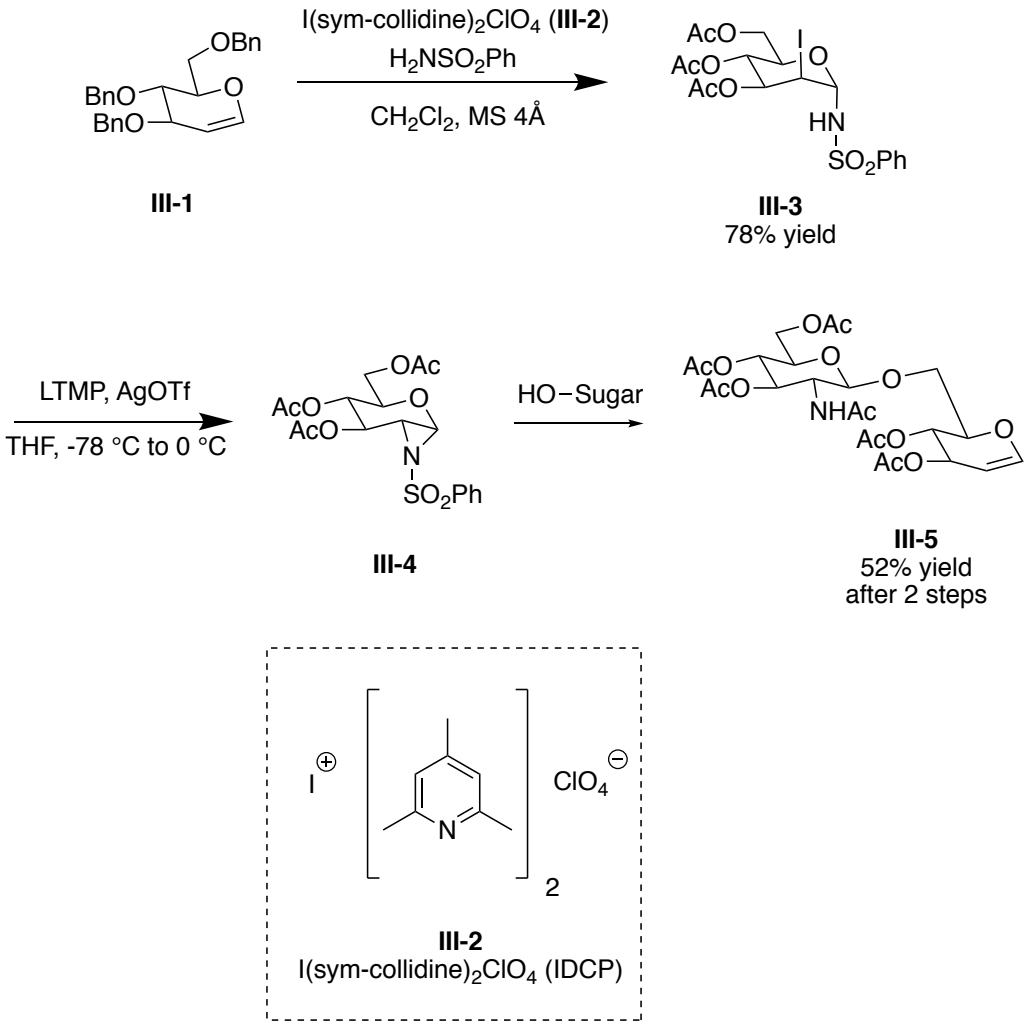

A general process for haloamination of alkenes was developed by E. J. Corey and coworkers in 2006.[13] In this procedure, a Lewis acid catalyzed haloamination of alkenes was reported where *N*-bromoacetamide served as halogen donor, 40 mol% $SnCl_4$ was employed as a Lewis acid catalyst and acetonitrile with a trace amount of water was used as solvent and nucleophile. Substrate scope shows different cyclic alkenes **III-6** were transferred to haloaminated products **III-7** with up to 90% yield (Figure III-5a). The formation of bromonium ion **III-9** followed by nucleophilic attack by acetonitrile generated nitrilium ion **III-10**. The reaction of nitrilium ion with water followed by tautomerization forms final bromoaminated product **III-12** (Figure III-5b).

Figure III-5: A general process for the haloamination of olefins

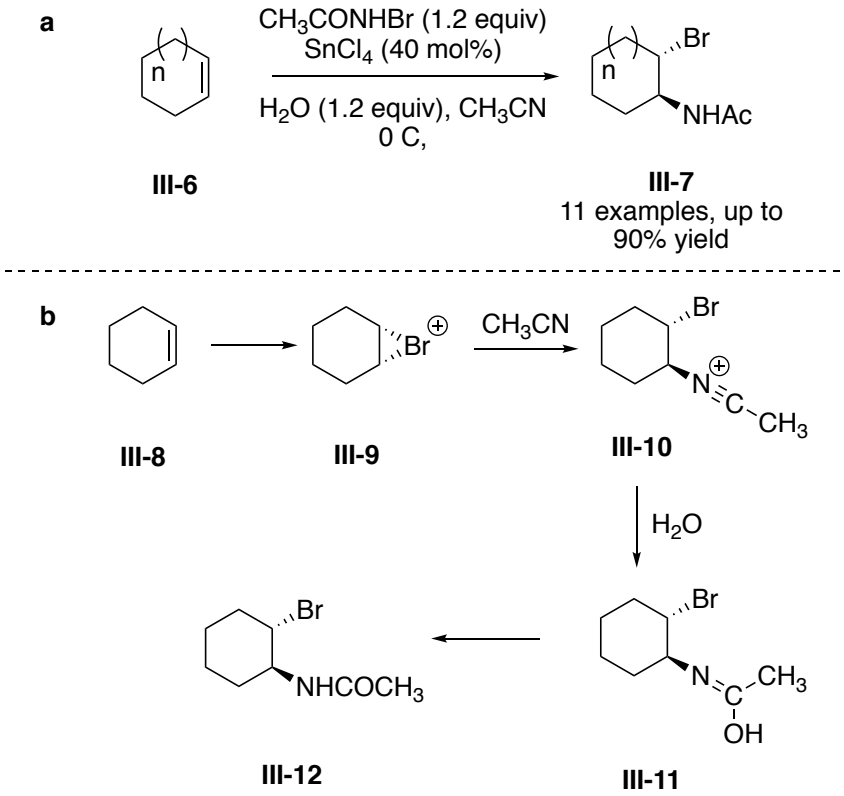

The same group used the above haloamination methodology for the concise synthesis of anti-influenza neuramidase inhibitor (Tamiflu®) **III-15** (Figure III-6).[6]

Figure III-6: Employing bromoamination reaction, a route for the synthesis of neuramidase inhibitor

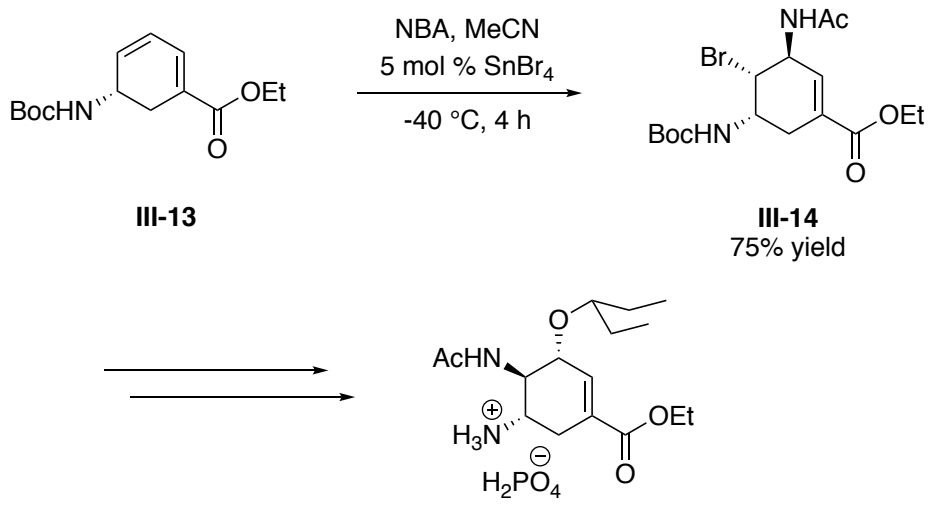

A mechanistically similar Indium (III)-catalyzed aminobromination and aminofluorination of styrenes were reported by Yadav and coworkers in 2009.[14] The NBS and selectfluor were employed as halogen donor to yield aminobrominated product **III-17A** in 87% yield and aminofluorinated product **III-17B** in 90% yield (Figure III-7).

Figure III-7: Indium (III)-catalyzed aminobromination and aminofluorination

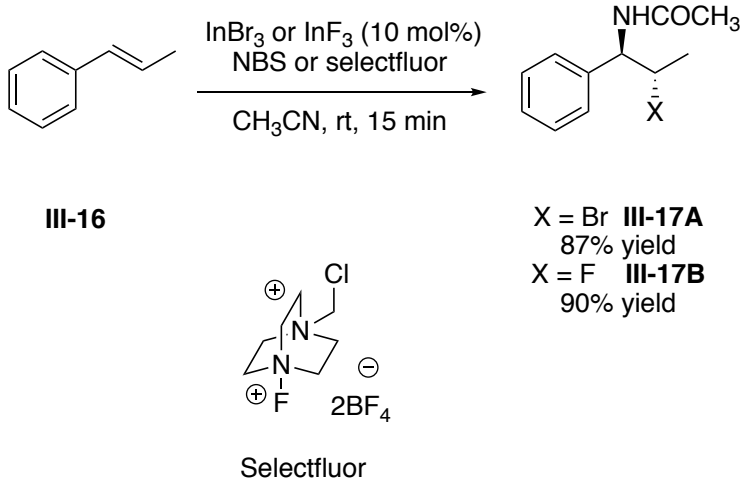

Yeung and coworkers disclosed a racemic chloroamination of olefins in 2013.[15] For facile and efficient chloroamination of alkenes, Lewis basic diphenyl selenide (20 mol%) along with N-chlorosuccinamide (NCS) as chloronium source and acetonitrile as nitrogen source were used, respectively. In these conditions, chloroaminated products **III-19** were formed in up to 89% yield (Figure III-8).

Figure III-8: Lewis basic selenium catalyzed chloroamination of olefins

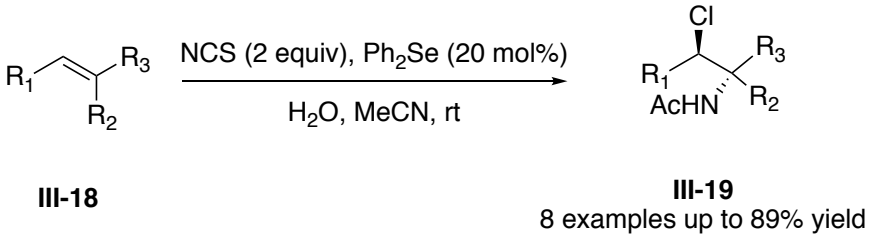

Procopiou and his coworkers developed a racemic Ritter-type reaction for electrophilic diamination of alkenes.[16] It was reported as an one pot reaction involving the addition of *N*-chlorosaccharin **III-21** to the alkene solution in acetonitrile at -42 °C to yield chloroimide **III-23**, followed by addition of potassium

ethoxide in EtOH to hydrolyze the saccharin ring. Warming the reaction mixture to room temperature yielded imidazoline **III-24** in up to 47% yield (Figure III-9).

Figure III-9: A method for electrophilic diamination of alkenes

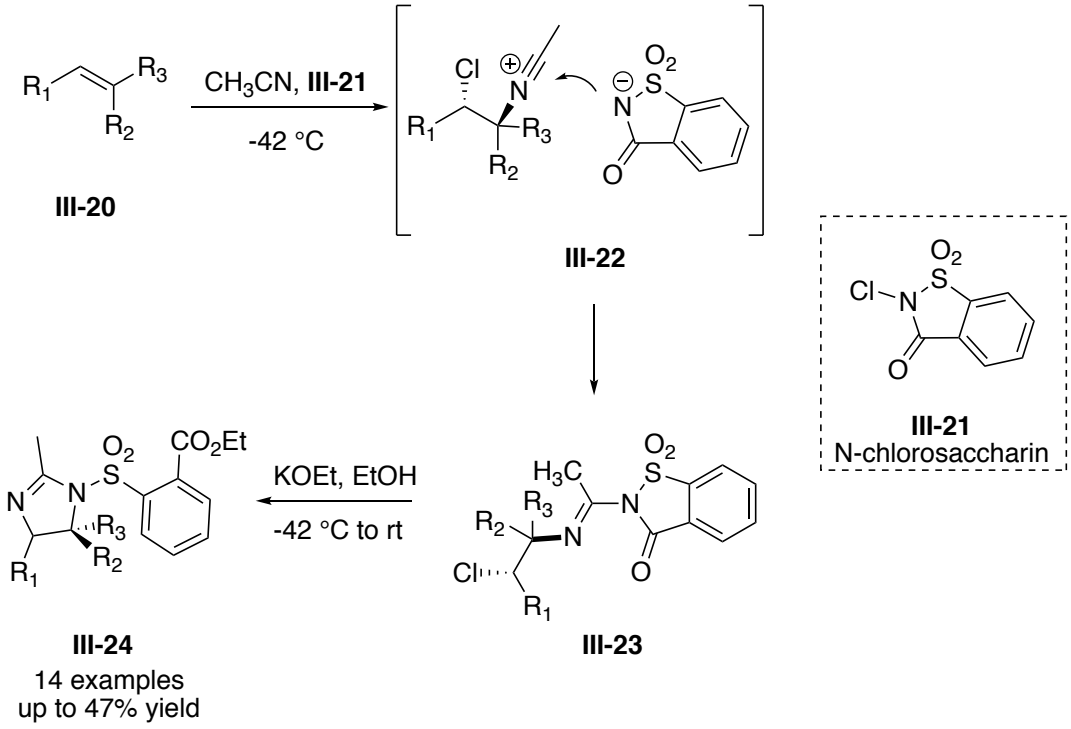

III-1-1-2 Literature precedence for catalytic-asymmetric vicinal haloamination of alkenes

In 2012 Masson and co-workers disclosed the bromoamidation of enecarbamates with high enantioselectivity.[17] They employed a chiral phosphoric acid to catalyze the reaction using NBS as the source of bromonium as well as a source of nucleophilic nitrogen. This transformation proceeds under mild conditions (room temperature) and only 1 mol% of chiral catalyst is needed to produce various α-brominated encarbamates in up to 99% yield and 98% *ee* (Figure III-10a). The proposed transition state **III-27** suggest that the chiral

catalyst acts as a bifunctional entity that activates both NBS and the encarbamate via hydrogen bonding (Figure III-10b).

Figure III-10: Highly enantioselective α-bromination of encarbamates

a

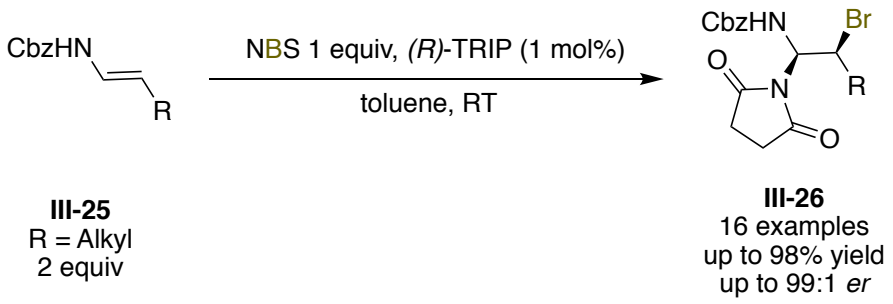

b

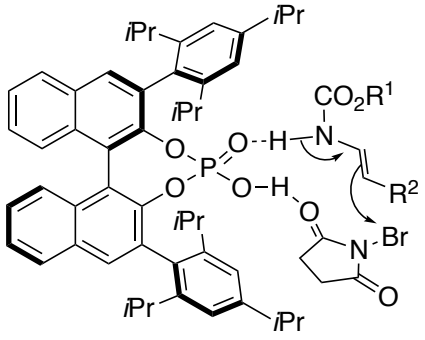

III-27

Feng and coworkers reported their first haloamination using a scandium (III) triflate catalyst with a chiral N,N-dioxane ligand **III-29** along with NBS as the halonium source and sulfonamide as a nitrogen nucleophile to form bromoaminmated products **III-31** in exquisite yields and enantioselectivities.[18] They saw similar results when using NIS as the source of halonium to construct the α-iodo amine products **III-32**.[19] With a slight modification, Feng's system was able to succeed in the chloroamination.[20] The authors changed the halonium

source from a succinimide to the more active N,N-dichloro-4-methylbenzene-sulfonamide and changed the R group of the chiral ligand to the sterically hindered adamantyl group **III-30**. In this case, the reaction was able to proceed with higher yields and similar enantio- and diastereoselectivity to form a chlorinated product (Figure III-11a). A diverse range of aryl and aryl-substituted chalcones **III-28** were examined in these studies. These reactions are believed to proceed through a chiral halonium ion. The scandium as Lewis acid coordinates to the carbonyl of the enone and the oxygen of the sulfonyl group. These coordinations place the counter ion of the dihalo-sulfonamide close to the chiral halonium ion (Figure III-11b).

Figure III-11: $Sc(OTf)_3$-catalyzed enantioselective halogenation of alkenes

a

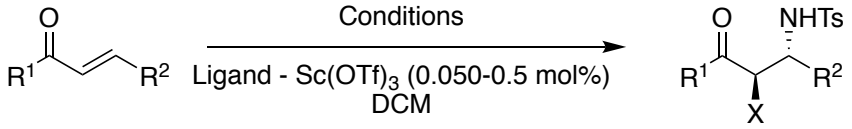

III-28
R_1,R_2 = Ar

III-31 X = Br up to 99% yield
up to >99:1 *er*

III-32 X = I up to 99% yield
up to 99:1 *er*

III-33 X = Cl up to 99% yield
up to >99:1 *er*

Conditions:

X = Br NBS (1.2 equiv.), $TsNH_2$ (1.1 equiv.), 0 °C, Ligand = **III-29**
X = I NIS (1.2 equiv.), $TsNH_2$ (1.1 equiv.), rt, dark, Ligand = **III-29**
X = Cl $TsNCl_2$ (0.6 equiv.), $TsNH_2$ (0.6 equiv.), 35 °C, Ligand = **III-30**

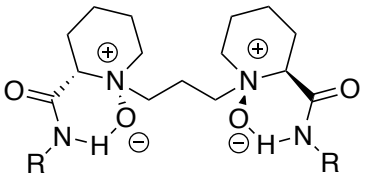

III-29 R = $PhCH_2CH_2$
III-30 R = 1-Adamantyl

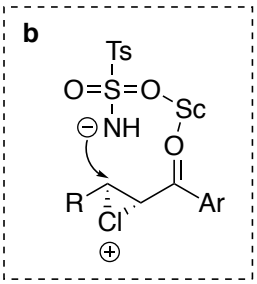

Although enantioselective haloamination and haloamidation reactions have seen success, there are still many limitations. Each method described above can either tolerate alkyl substitution or aryl substitution, never both. Asymmetric chloroamination has only seen success when the scandium catalyst is used; no organocatalytic methods have been reported. The substrate scope was limited to only the chalcone and α,β-unsaturated keto-ester moieties.

III-2 Result and discussion

During my graduate studies, I learned that being detail oriented is essential to be successful. Separation and characterization of side products, even if they are 10% of mass balance, can lead us to new methodologies. Some of these side products can be substantial, valuable and worth attempting to optimize the reaction to get them exclusively.

III-2-1 Discovery of chloroacetamide product III-34D as a side product in enantioselective dichlorination reactions

During dichlorination reactions optimization studies to produce dichlorinated product **III-34A**, competing intermolecular processes such as interception of the intermediate by the solvent leads to side products **III-34B** (from TFE incorporation) or **III-34D** (the Ritter product when CH_3CN is employed).[10] Also, the intramolecular halocyclization path yields the oxazoline **III-34C** as a side product. As listed in Table III-1, numerous chloride sources in different solvents were evaluated for developing an enantioselective dichlorination reaction. It was revealed that employing 100 equivalents of LiCl in TFE (CF_3CH_2OH) in the presence of $(DHQD)_2PHAL$ as a chiral catalyst leads to the desired dichlorinated product **III-34A** in high selectivity and enantio excess (Table III-1, entry 7). Employing 15 equivalents of NaCl in acetonitrile did not provide any desired dichlorinated product. However, chloroacetamide (Ritter type reaction) product **III-34D** was formed in good selectivity (Table III-1, entry 2). We have taken advantage of this previously unintended result for the development of

the first organo-catalytic enantioselective chloroamidation. This is also the first example of an asymmetric Ritter type reaction.

Table III-1: Summary of optimization studies in dichlorination reactions

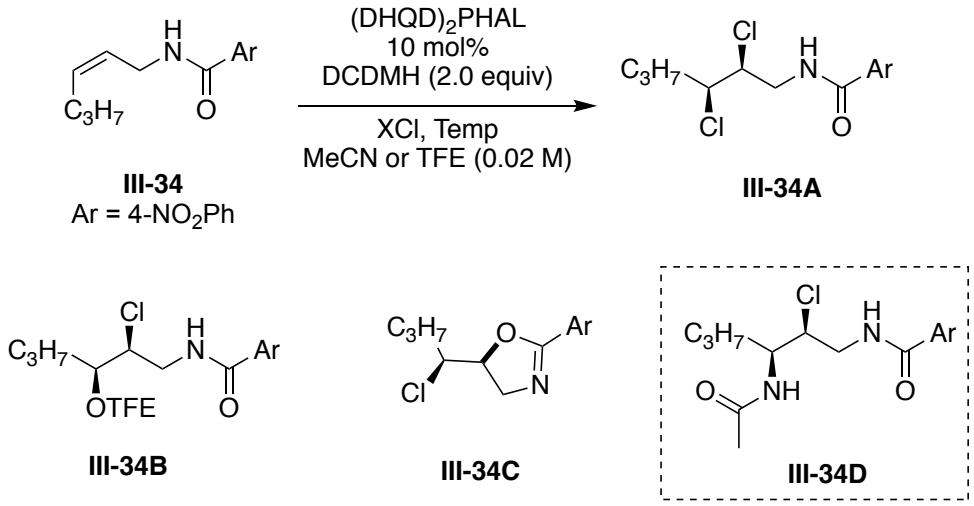

Entry	Solvent	Temp (°C)	XCl	XCl (equiv)	**A**:**B**:**C**:**D**[a]
1	MeCN	23	TEAC	15	55:0:45:0
2	MeCN	23	NaCl	15	0:0:13:87
3	MeCN	23	LiCl	15	79:0:21:0
4	MeCN	-30	LiCl	15	95:0:5:0
5	TFE	-30	LiCl	15	45:56:0:0
6	TFE	-30	LiCl	50	86:14:0:0
7	TFE	-30	LiCl	100	95:5:0:0

[a]Determined by NMR; TFE = 2,2,2-trifluoroethanol; TEAC = Tetraethylammonium chloride

III-2-2 Typical Ritter type mechanism leading to the chloroacetamide product III-34D

The mechanism for the formation of chloroacetamide **III-34D** is shown in Figure III-12. Same as the typical Ritter type reaction, after the chloronium ion intermediate formation, acetonitrile attacks the putative intermediate and forms

the nitrilium ion **III-36**. The trace amount of water in acetonitrile reacts with **III-36** and yields intermediate **III-37**. Subsequently, tautomerization of **III-37** yields the final chloroacetamide product **III-34D** (Figure III-12).[13]

Figure III-12: Proposed mechanism for the formation of the chloroacetamide **III-34D**

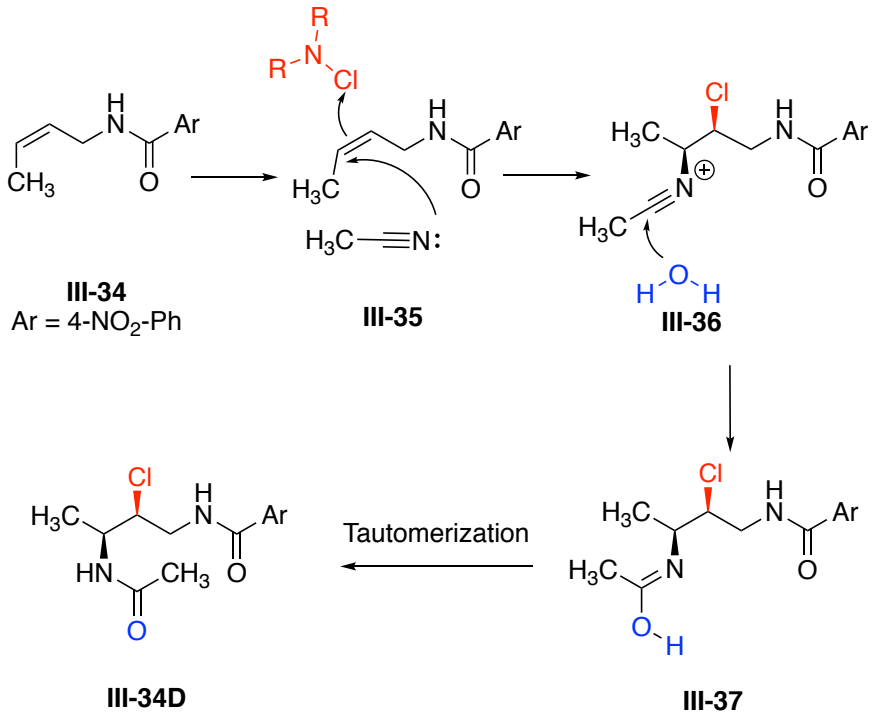

III-2-3 Formation of unknown products as intermediates in chloroamination reaction

For optimizing the reaction to obtain the chloroacetamide product **III-34D** exclusively, the allyl amide **III-34** was treated with two equivalents of DCDMH in acetonitrile along with 10 mol% $(DHQD)_2PHAL$ as a chiral catalyst. Surprisingly, mixtures of unknown products were formed (Figure III-13). Attempting to separate the mixture of products and characterize them was unsuccessful due to

their instability on silica gel. Interestingly, addition of the silica gel to the crude mixture resulted in the conversion of the mixtures of intermediates were transferred to the final chloroacetamiden product **III-34D** as a single diastereomer in 67% yield and 95:5 *er* (Figure III-13a). **)** The NMR spectrums for allyl amide substrate **III-34**, the mixture of unknown products and final chloroacetamide product **III-34D** were shown in Figure III-13b.

Figure III-13: (a) Unknown products as an intermediate were formed in chloroamination reaction (b) The NMR spectra for allyl amide substrate **III-34,** the mixture of unknown products and final chloroacetamide product **III-34D**

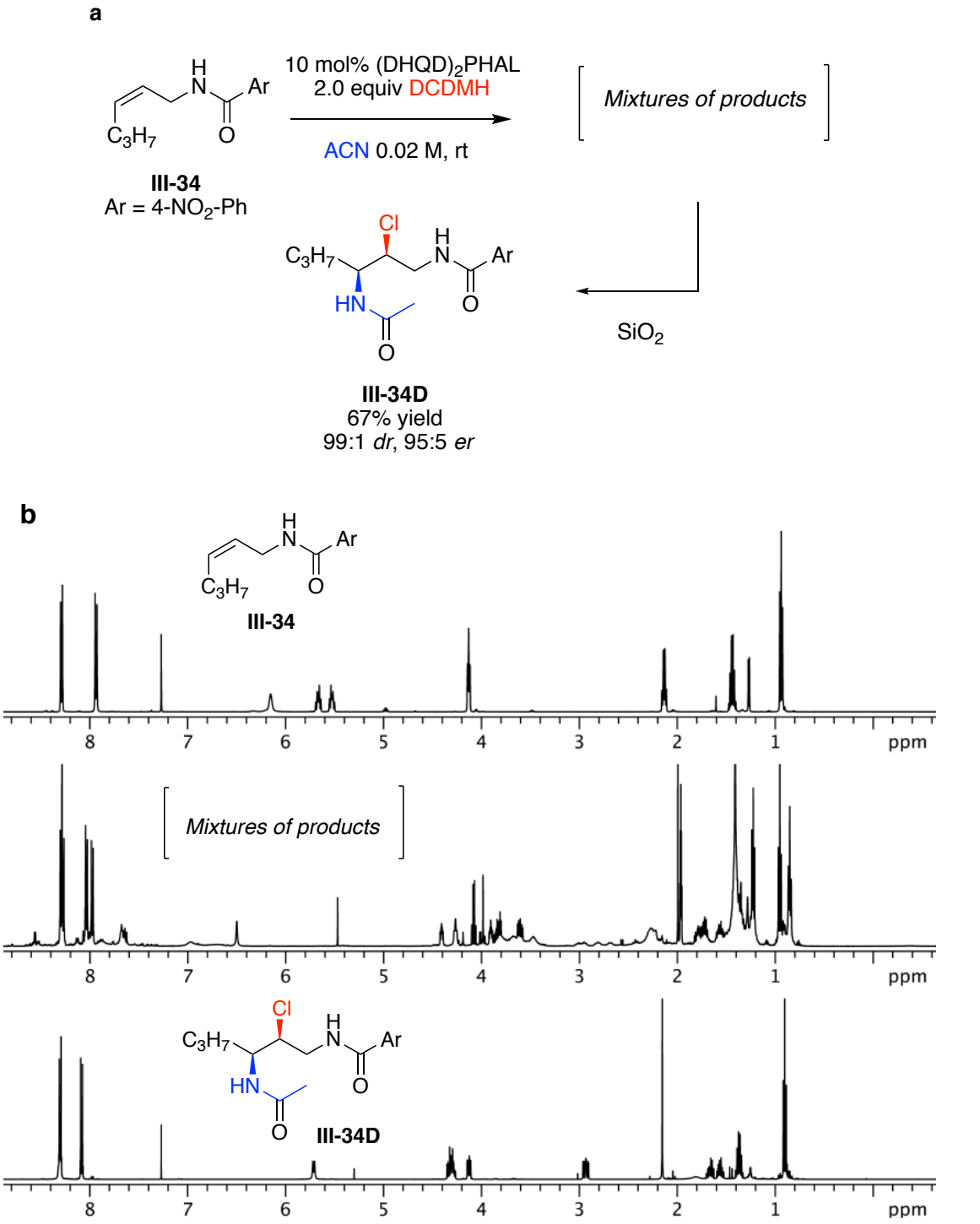

III-2-4 Designing control experiments to determine the structure of mixture of products

Due to the instability of unknown products on silica gel, we designed control experiments to reveal their structure. Under the same conditions, employing $TsNCl_2$ (N,N-dichloro-*p*-toluenesulfonamide) instead of DCDMH yielded single chloroimide product **III-34E** in 78% yield and 95:5 *er* (Figure III-14a). This chloroamidine product **III-34E** was stable to purification on silica gel. This result indicates that the counter ion of the chlorine source must be part of the final chlorinated product **III-34E**. Therefore, in the case of employing DCDMH, we assume the mixture of products is the result of the attack of the two nucleophilic nitrogens atoms in the DCDMH structure. However, the chloroimide product **III-34E** is stable on silica gel, but the combination of products **III-38** in case of using DCDMH is not stable and hydrolyze in the presence of silica gel to form chloroacetamide **III-34D** in 67% yield and 95:5 enantioselectivity (Figure III-14b)

Figure III-14: (a) The counter ion of chlorine source is part of the final product (b) Revealing the structures of the mixture of products

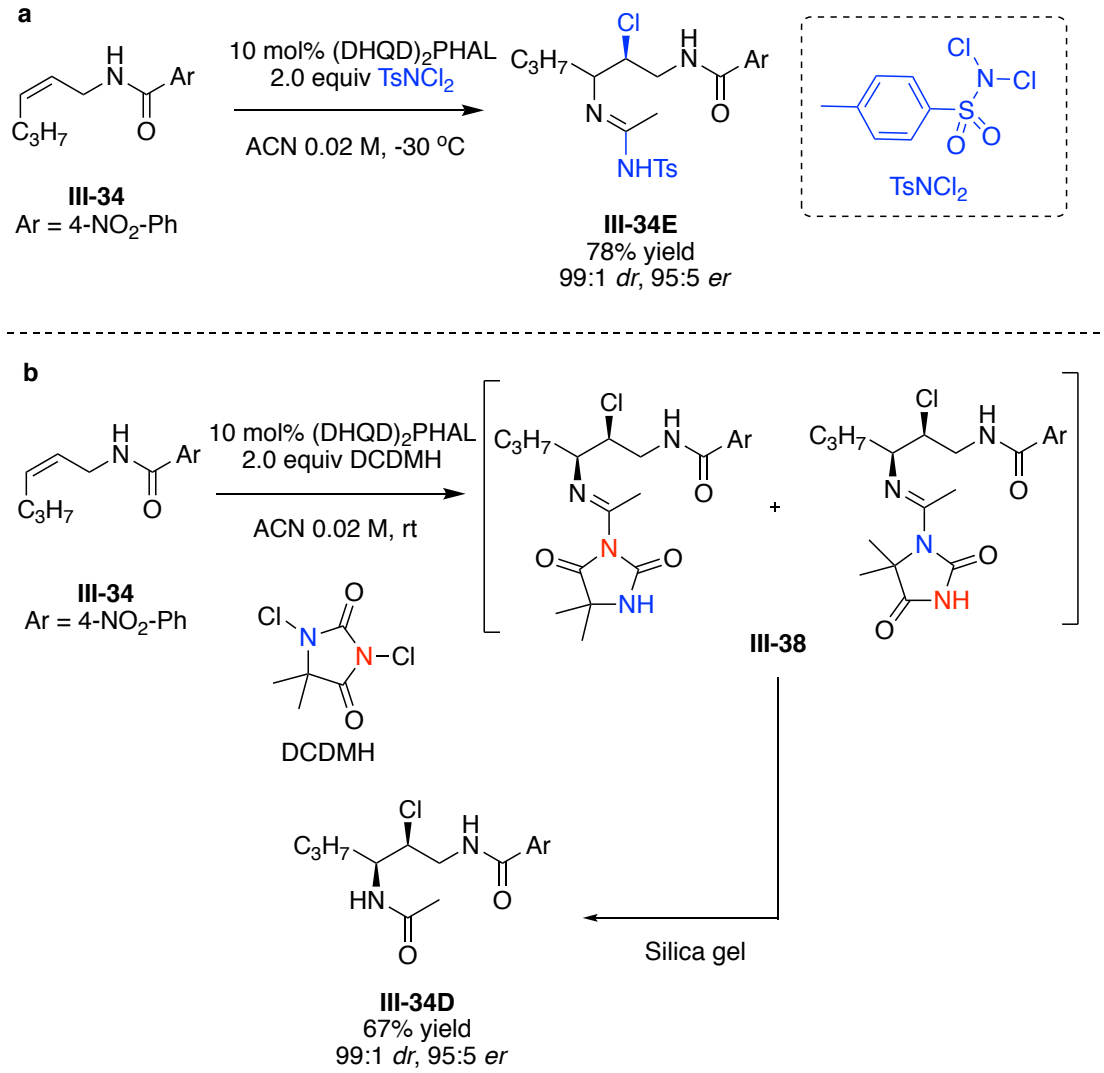

III-2-5 Modified mechanism for the formation of the chloroacetamide III-34D

The updated mechanism for the formation of chloroacetamide was proposed based on the latter results (Figure III-15). In this modified mechanism, the counter ion of the chloronium ion participates in the nucleophilic attack to

yield chloroamidine **III-40**. Subsequently, hydrolysis of the chloroamidine **III-40** forms chloroacetamide **III-34D**.

Figure III-15: The modified proposed mechanism for formation of chloroacetamide **III-34D**

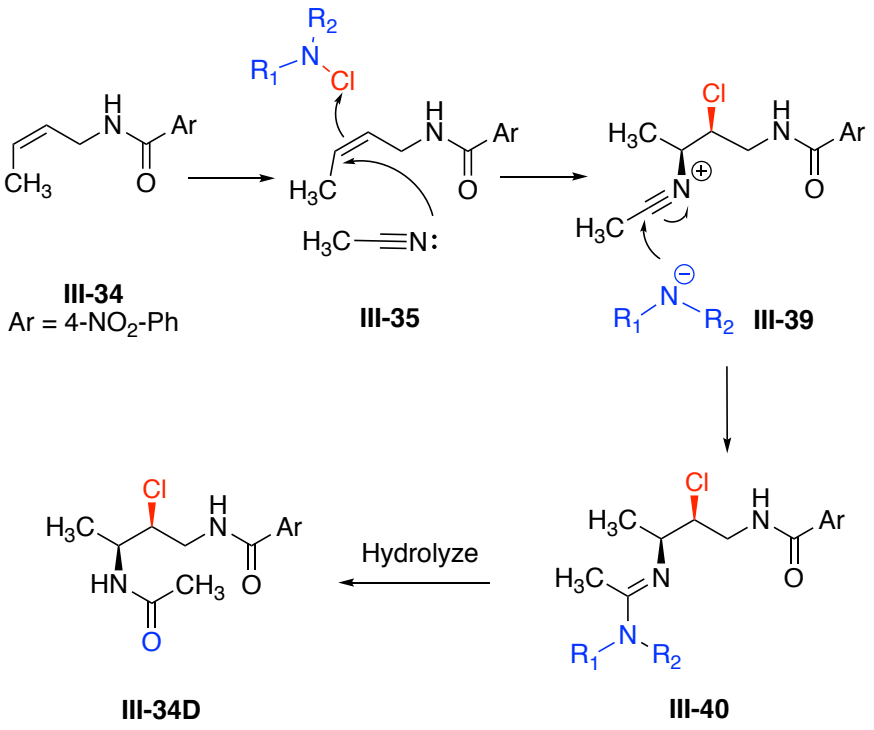

III-2-6 Catalyst-controlled chloroamination reaction

For measuring the background for chloroamidation reaction, the allyl amide **III-34** was treated with DCDMH in acetonitrile at ambient temperature. Surprisingly, a reaction without $(DHQD)_2PHAL$ forms the final chloroacetamide **III-34D** along with the cyclized product **III-34C** in the ratio of 1.0:1.7 (Figure III-16). As mentioned above, in the presence of $(DHQD)_2PHAL$, the two dimethyl hydantoins incorporated imide products **III-38** are formed, which upon addition of silica gel hydrolyze to yield final the chloroacetamide product **III-34D** (Figure III-

14b). Interestingly, without $(DHQD)_2PHAL$, the final product was formed without employing silica gel for hydrolysis. These observations could suggests that, $(DHQD)_2PHAL$ holds DCDMH in the chiral pocket, thus making the counter ion of DCDMH relatively close to the nitrilium ion intermediate, which the traps it to form imide products (see Figure III-15, **III-39**). However, without the chiral catalyst, the trace amount of water in acetonitrile is responsible for the nucleophilic attack of the nitrilium ion to yield the intermediate product **III-37** (see Figure III-12), followed by tautomerization to deliver the chloroacetamide product.

Figure III-16: Chloroamination of allyl amide **III-34** without $(DHQD)_2PHAL$

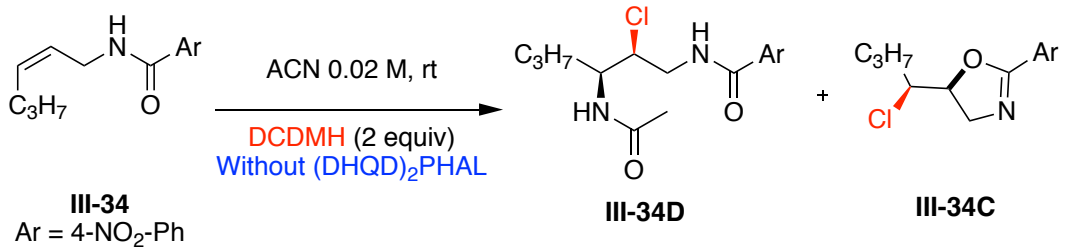

Our lab has previously showen the coordination of *N*,*N*-dichlorohydantoin **III-41** with $(DHQD)_2PHAL$ via NMR studies.[21] The two-gem hydrogen atoms in *N*,*N*-dichlorohydantoin resonate as a singlet at 4.35 ppm in $CDCl_3$. However, adding one equivalent of $(DHQD)_2PHAL$ along with two equivalents of benzoic acid into the NMR tube, leads to the formation of an AB quartet at 4.40 ppm (Figure III-17). We had previously suggested that two scenarios depicted in Figure III-17 as a result of the NMR observations. Both senarios would explain the splitting pattern of the hydrogens atoms of dichlorohydantoin in the presence of $(DHQD)_2PHAL$. The structural suggestion agrees observations above,

highlighting the role of chiral catalyst $(DHQD)_2PHAL$ in the enantioselective chloroamination reactions, yielding the intermediate **III-38** suggested in Figure III-14B.

Figure III-17: Catalyst controlled chloroamination of unsaturated allyl amides

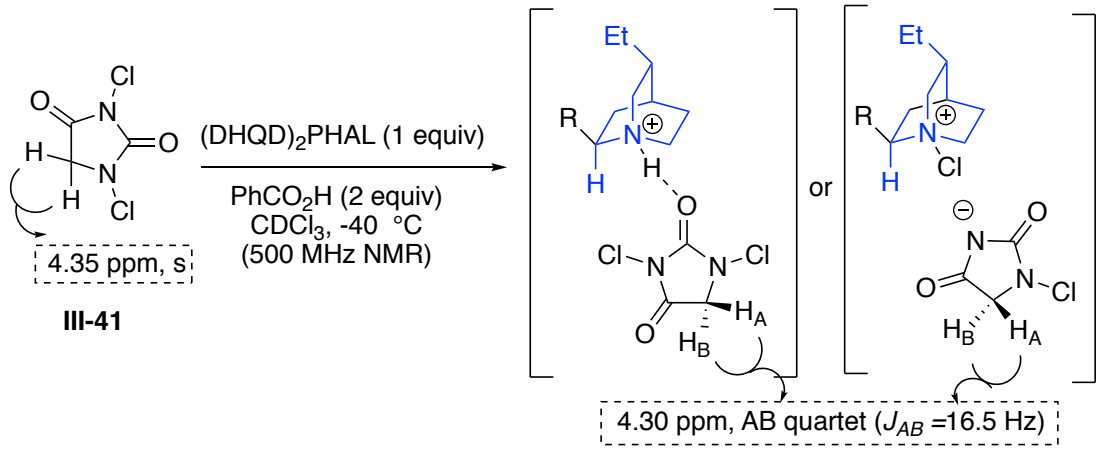

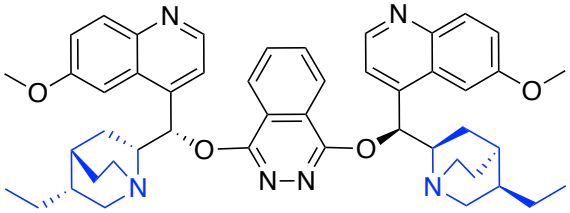

$(DHQD)_2PHAL$

III-2-7 Two distinct types of choloroaminated products were produced from different chlorenium sources

In our system, two different types of chlorenium sources lead to two distinct and precious products. When DCDMH is employed, the Ritter product can undergo facile hydrolysis with silica gel, yielding the amide product **III-34D**

(Figure III-18a). When dichloramine-T ($TsNCl_2$) is employed, we have observed that the Ritter product is more stable and does not hydrolyze as easily, leaving the sulfonamide intact (see **III-34E,** Figure III-18b). These two products have significant synthetic applications and both have the potential to undergo hydrolysis to the chiral 1,3 diamine. The α-chloroamide product has been shown to undergo an aziridination reaction when treated with cesium carbonate (Figure III-18a).[22] As mentioned before, the unmodified α-haloamide itself can be observed in molecules of biological importance. The chloroamidine product **III-34E** can be cyclized using sodium carbonate in 40 °C to form 2-imidazoline product in 72% yield (**III-43**). This chiral imidazoline product could be of interest in medicinal chemistry and can be hydrolyzed to the chiral 1,2,3 triamine product **III-44** (Figure III-18b).

Figure III-18: Two different types of chlorenium sources lead to two distinct products

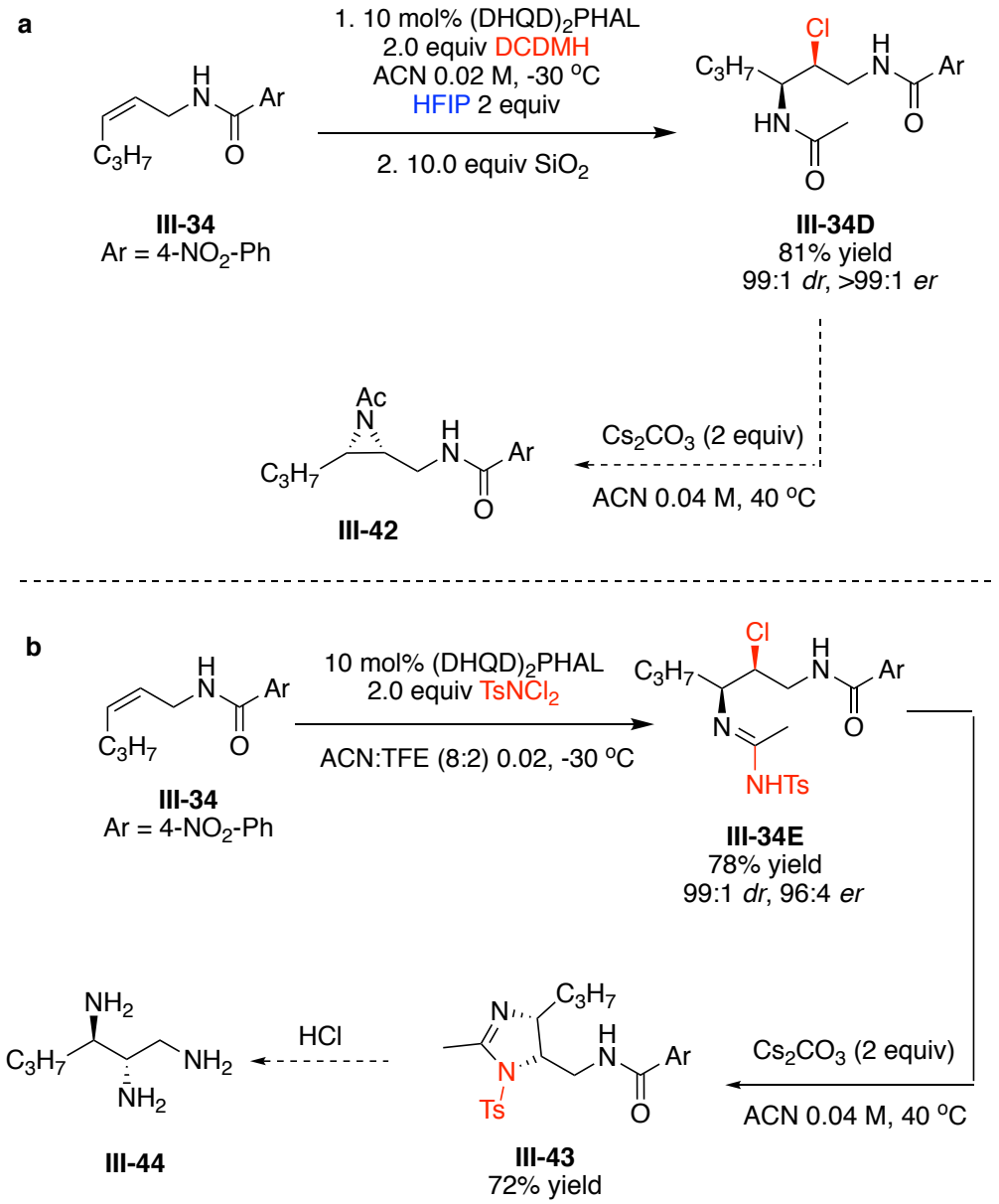

III-2-8 Role of HFIP as an additive in enantioselective chloroamination reactions

Under optimized reaction conditions, either two equivalents of HFIP (hexafluoroisopropanol) as an additive were used in CH_3CN or a mixture of

CH_3CN:TFE (8:2) was employed for the enantioselective chloroamination reactions (Figure III-18a, III-18b). We observed that using fluorinated solvents as additive or co-solvent affected the rate of the reaction. The relatively low pka of the fluorinated solvents presumably protonates the quinuclidine nitrogen atoms, therefore enabling the catalyst to hydrogen bond with DCDMH (see Figure III-17).[21] This coordination can bring the counter ion of the chlorenium source closer to the nitrilium ion intermediate and accelerate the chloroamination reaction. The relative rates with or without HFIP for enantioselective chloroacetamidation of **III-34** were shown in Figure III-19.

Figure III-19: Role of fluorinated additives in chloroamination reactions

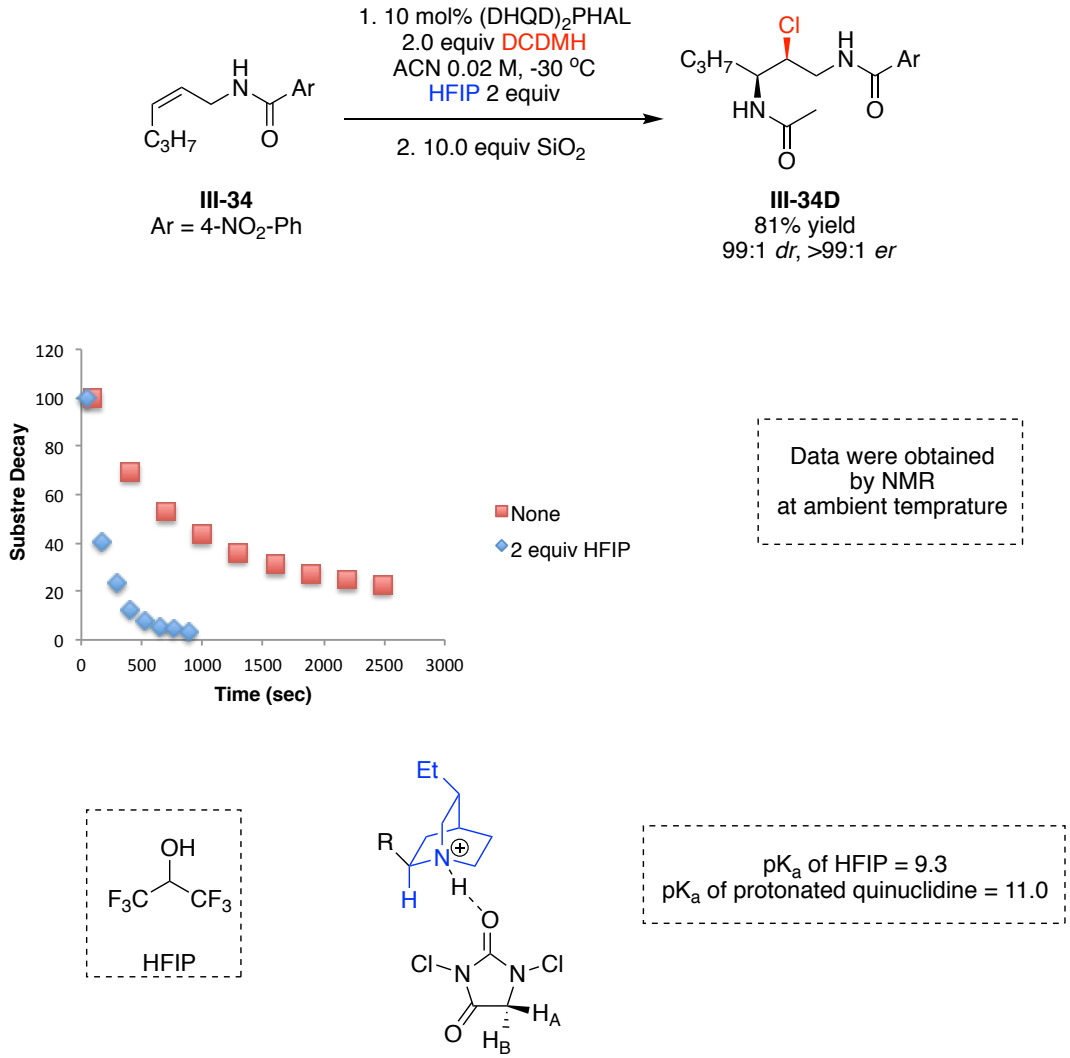

III-2-9 Substrate scope for enantioselective chloroamination reaction by employing DCDMH as the chlorenium source

In an effort to map out the generality of the chloroamination reaction in the presence of DCDMH as the chlorenium source, a number of *cis*-disubstituted allyl amides were initially exposed to the optimized conditions. Compound **III-34** forms the corresponding product **III-34D** in 89% yield with an exquisite level of stereoselectivity (>99:1 *er*, >99:1 *dr*). Switching the substituent on the benzamide

motif to 4-bromobenzamide gave similar results (see **III-45D**). The other *Z*-alkyl substituted olefins (**III-46**, **III-47**) afforded the chloroacetamide products in high yield and stereoselectivity (see Figure III-20, **III-46D** and **III-47D**). Aryl substituted *Z*-alkenes are also compatible with this chemistry and yield final product **III-48D** in 82% yield and >99:1 *er*. The diastereoselectivity for product **III-48D** is poor (4.7:1.0 *dr*), which is presumably due to the carbocation character at the benzylic position. Varying the expandable amide moiety for *E*-alkyl substituted olefins affected the yield and enantioselectivity. The substrate with 4-nitrobenzamide gave slightly higher yield and enantioselectivity compared to the substrate that has 4-bromobenzamide moiety (see **III-49D** and **III-50D**). The aryl substituted *E*-allyl amide **III-51** gave moderate yield (due to competing chlorocyclization) and fair diastereoselectivity (1.5:1 *dr*). Nonetheless, the chloroacetamide product **III-51D** was formed in high enantioselectivity (see Figure III-20, **III-51D**). Benzonitrile can also be employed as nucleophile to furnish the corresponding product with excellent enantioselectivity (see **III-52D**)

Figure III-20: Enantioselective chloroamidation substrate scope

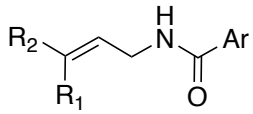

III-34, **III-45** to **III-51**
R_1, R_2 = H, Ar, Alk

DCDMH (2 equiv.)
HFIP (2 equiv.)
CH_3CN (0.05 M), -30 °C
2. SiO_2(10 equiv.)

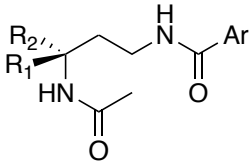

III-34 (D,F), III-45D to III-51D

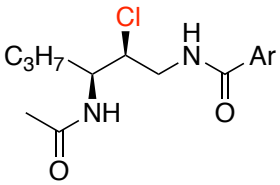

III-34D
Ar = 4-NO_2-Ph
89% yield
>99:1 *er*

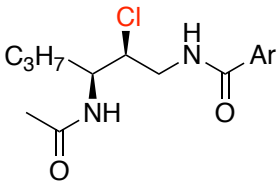

III-45D
Ar = 4-Br-Ph
83% yield
98:2 *er*

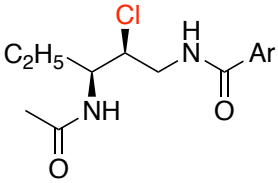

III-46D
Ar = 4-NO_2-Ph
84% yield
99:1 *er*

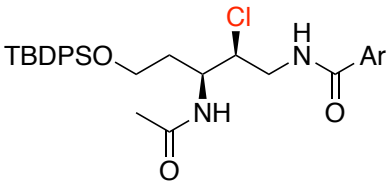

III-47D
Ar = 4-NO_2-Ph
86% yield
>99:1 *er*

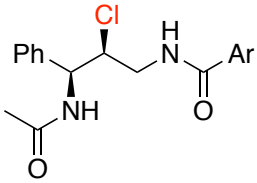

III-48D
Ar = 4-NO_2-Ph
82% yield
>99:1 *er*
4.7:1 *dr*

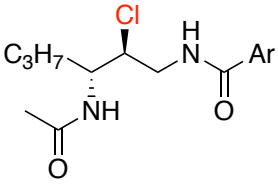

III-49D
Ar = 4-NO_2-Ph
75% yield
98:2 *er*

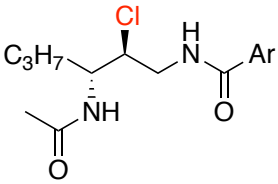

III-50D
Ar = 4-Br-Ph
66% yield
96:4 *er*

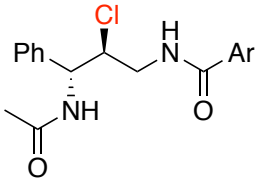

III-51D
Ar = 4-NO_2-Ph
58% yield
96:4 *er*
1.5:1 *dr*

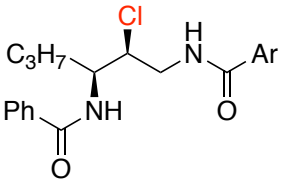

III-34F
Ar = 4-NO_2-Ph
56% yield
99:1 *er*

III-2-10 Optimization studies for the intermolecular enantioselective chloroamidination of *E*-allyl amides

We choose the *E*-aliphatic substituted allyl amide **III-49** to optimize the enantioselective chloroamidination reactions. 10 mol% $(DHQD)_2PHAL$ was employed as the chiral catalyst along with two equivalents of $TsNCl_2$ as the chlorenium and nitrogen source. At ambient temperature in acetonitrile, the desired chlorofunctionalized **III-49E** along with cyclized (**III-49G** and **III-49C**) products were observed in the ratio of 47:35:18, respectively (Table III-2, entry 1). The intermolecular product shows 88:12 *er*, whereas the cyclized products **III-49E** and **III-49G** exhibit lower enantioselectivity (88:12 *er* for **III-49D** and 50:50 *er* for **III-49C**, Table III-2, entry 1). Lower temperature (-30 °C) led to slightly improved selectivity toward desired intermolecular product **III-49E** (Table III-2, entry 2). Decreasing the amount of $TsNCl_2$ (1.1 equiv) shows significantly higher selectivity for the formation of desired acyclic product **III-49C** (Table III-2, entry 3). Employing different additives such as 1.1 equivalents of $TsNH_2$, five equivalents Li_2CO_3 and 5 A° molecular sieves would not increase the selectivity of the chloroamidination reaction (Table III-2, entries 4 to 6). The reaction that was run with 20 mol% $(DHQD)_2PHAL$ in -30 °C shows slightly higher selectivity compared to using 10 mol% chiral catalyst (Table III-2, entries 7 and 8). IN an attempt to reduce the formation of cyclized products (**III-49G** and **III-49C**), the reactions were conducted in -45 °C and -50 °C. Lower temperatures led to the formation of the desired chloroamidinated product **III-49E** exclusively with 96:4 *er* (Table III-2, entries 9 and 10)

Table III-2: Optimization studies for the intermolecular enantioselective chloroamidination of *E*-allyl amides

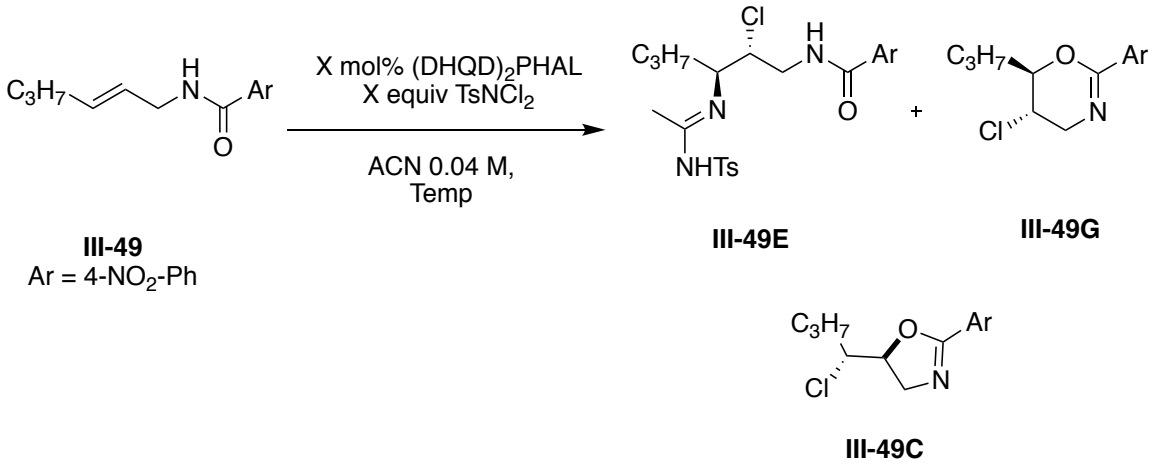

Entry	Temp	Mol% cat	Additive	Equiv of $TsNCl_2$	**E**:**G**:**C**[a]	*er* (**E**)[b]	*er* (**G**)[b]
1[e]	rt	10	None	2	47:35:18	88:12	78:22
2	-30	10	None	2	70:25:5	95.5:4.5	82:18
3	rt	10	None	1.1	63:28:9	89:11	78:22
4[f]	rt	10	$TsNH_2$	1.1	47:34:19	nd	nd
5[g]	rt	10	Li_2CO_3	1.1	59:30:11	89:11	78:22
6	rt	10	5 A° MS	1.1	58:29:13	89:11	78:22
7	-30	10	None	1.1	78:17:5	95.5:4.5	nd
8	-30	20	None	1.1	81:15:5	nd	nd
9[c]	-45	10	None	1.1	90:9:1	96:4	nd
10[d]	-55	10	None	1.1	95:4:1	96:4	nd

[a]Determined by NMR; [b]Enantioselectivity determined by chiral HPLC; [c] Mixture of ACN:TFE (9:1) was used ; [d]Mixture of ACN:TFE (8:2) was used ; [e]The enantioselectivity for compound **III-49C** was 50:50 *er*; [f]1.1 equiv of TsNH2 was used; [g]5 equiv of Li_2CO_3 was used

III-2-11 Substrate scope for enantioselective chloroamination reaction by employing $TsNCl_2$ as the chlorenium source

We sought to explore the scope of this transformation under optimized conditions (1.1 equiv of $TsNCl_2$, 10 mol% $(DHQD)_2PHAL$ and the mixture of CH_3CN:TFE (8:2) as solvent at -50 °C). As mentioned before, products of this reaction are stable on silica gel. Chiral chloroamidine products were formed in high yield and stereoselectivities. *Z*-alkyl-substituted alkenes afforded the desired products in near complete regio-, diastereo-, and enantioselectivity (Figure III-21, see **III-34E**, **III-46E** and **III-47E**). Benzyloxy substituted olefin gave the isolated product in slightly lower yield and enantioselectivity (78% yield and 95:5 *er*) as compared to other *Z*-alkyl substituted allyl amides (see **III-52E**). The *cis* substrate with aryl substituent **III-48** produced chloroimide product in 78% yield and 96:4 *er*. The only *trans* substrate (**III-49)** that was evaluated so far in this chemistry produced the product in 82% yield, >99:1 *dr* and 96:4 *er* (Figure III-21, **III-49E**).

Figure III-21: Enantioselective chloroimidation substrate scope

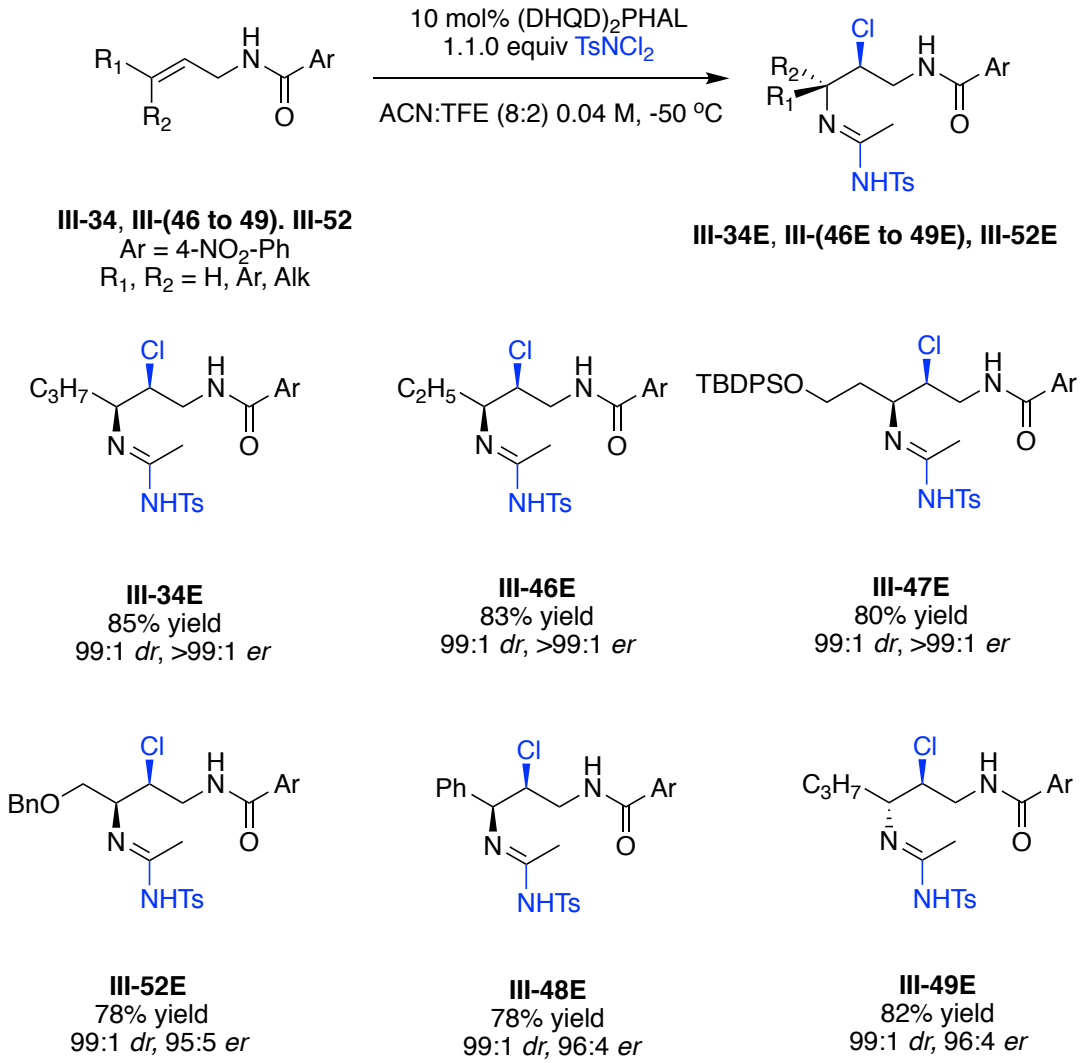

III-2-12 Conclusion

We report the first enantioselective Ritter type reaction. This chemistry is compatible with aryl and aliphatic substituted alkenes. Interestingly, exquisite regioselectivity was observed even with employing aliphatic substituted (unbiased) alkenes. Both *E*- and *Z*-olefins under optimized conditions deliver chloroamide products with high yield and enantioselevtivities. In this system, two

different types of chlorenium sources lead to two distinct and precious products (chloroacetamide and chloroamidines). Expanding the substrate scope for this transformation is underway. The optimized condition for chloroamidination (1.1 equiv of $TsNCl_2$, 10 mol% $(DHQD)_2PHAL$ and the mixture of CH_3CN:TFE (8:2) as solvent at -50 °C) might be improved by employing less amount of $TsNCl_2$ (0.6 equivalents). Exploring substrate scope of chloroamidination reaction in the presence of two equivalents of HFIP as an additive in CH_3CN instead of using the mixture of CH_3CN:TFE (8:2) is necessary (see Figure III-21). Kinetic studies are underway to elaborate on the employing HFIP as an additive and figure out the kinetic order of reactants in enantioselective Ritter type reactions.

III-2-13 Experimental section

III-2-13-1 General procedure for catalytic asymmetric chloroamidation of unsaturated allyl amides

The substrates (0.1 mmol, 1.0 equiv) and $(DHQD)_2PHAL$ (7.8 mg, 0.01 mmol, 10 mol%) were suspended in acetonitrile (2.0 mL) in a 4 mL vial capped with a septum and equipped with a micro stir bar (7 × 2 mm). Hexafluoroisopropanol (21.4 μl, 0.2 mmol, 2.0 equiv) was introduced, and the resulting suspension was cooled to -30 °C in an immersion cooler. After stirring for 2 min DCDMH (39.5 mg, 0.2 mmol, 2.0 equiv) was added. The stirring was continued at -30 °C until the reaction was complete (TLC). The reaction was quenched by the addition of saturated aq. Na_2SO_3 (3 mL), concentrated, and diluted with DCM (3 mL). The organics were separated and the aqueous layer

was extracted with DCM (3 × 4 mL). The combined organics were dried over anhydrous Na_2SO_4 and concentrated in a 20 ml vial. The reaction was then suspended with 2 mL of DCM and SiO_2 (60.4 mg, 1 mmol, 10.0 equiv) was introduced and allowed to stir for 12 h. SiO_2 was then filtered via a cotton stuffed column. The column was rinsed with EtOAc (5 mL). The filtrate was then concentrated in the presence of a small quantity of silica gel. Column chromatography (SiO_2/EtOAc – Hexanes gradient elution) gave the desired product.

III-2-13-2 Analytical data for chloroamide products

III-34D *N*-((2*S*,3*S*)-3-acetamido-2-chlorohexyl)-4-nitrobenzamide

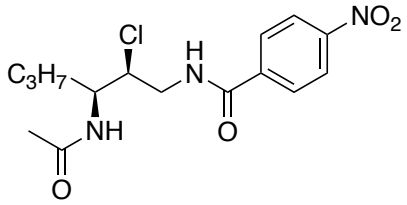

^{1}H NMR (500 MHz, Chloroform-*d*) δ 8.29 (d, *J* = 9.0 Hz, 3H, 2CH, 1NH), 8.08 (d, *J* = 9.0 Hz, 2H), 5.71 (d, *J* = 9.3 Hz, 1H, NH), 4.35 – 4.23 (m, 2H), 4.12 (ddd, *J* = 11.0, 5.2, 1.7 Hz, 1H), 2.93 (ddd, *J* = 13.7, 11.0, 4.4 Hz, 1H), 2.15 (s, 3H), 1.70-1.60 (m, 1H), 1.59-1.49 (m, 1H), 1.41-1.32 (m, 2H), 0.89 (t, *J* = 7.4 Hz, 3H).

^{13}C NMR (125 MHz, Chloroform-*d*) δ 172.2, 164.8, 149.7, 139.2, 128.4, 123.8, 61.2, 49.3, 42.6, 34.7, 23.3, 19.3, 13.7.

Resolution of enantiomers: DAICEL Chiralcel AD-H column, 10% IPA-Hexanes, 1.0 mL/min, 254 nm, RT1 (minor) = 8.8 min, RT2 (major) = 14.3 min

III-45D *N*-((2*S*,3*S*)-3-acetamido-2-chlorohexyl)-4-bromobenzamide

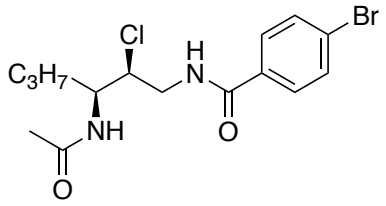

^{1}H NMR (500 MHz, Chloroform-*d*) δ 8.07 (dd, *J* = 8.6, 4.4 Hz, 1H, NH), 7.78 (d, *J* = 8.5 Hz, 2H), 7.59 (d, *J* = 8.5 Hz, 2H), 5.75 (d, *J* = 9.3 Hz, 1H, NH), 4.33-4.24 (m, 2H), 4.12 (ddd, *J* = 10.9, 5.2, 1.7 Hz, 1H), 2.90 (ddd, *J* = 13.5, 10.9, 4.4 Hz, 1H), 2.14 (s, 3H), 1.60-1.68 (m, 1H), 1.50-1.58 (m 1H), 1.3 (h, *J* = 7.4 Hz, 2H), 0.89 (t, *J* = 7.3 Hz, 3H).

^{13}C NMR (125 MHz, $CDCl_3$) δ 171.90, 165.96, 132.49, 131.84, 128.75, 126.45, 61.45, 49.22, 42.46, 34.77, 23.26, 19.24, 13.66.

Resolution of enantiomers: DAICEL Chiralcel AD-H column, 15% IPA-Hexanes, 1.0 mL/min, 254 nm, RT1 (major) = 5.8 min, RT2 (minor) = 7.1 min

III-46D *N*-((2*S*,3*S*)-3-acetamido-2-chloropentyl)-4-nitrobenzamide

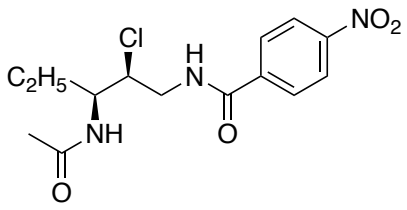

^{1}H NMR (500 MHz, $CDCl_3$) δ 8.32 (d, *J* = 8.8 Hz, 1H, NH), 8.29 (d, *J* = 5.4 Hz, 1H), 8.10 (d, *J* = 8.7 Hz, 1H), 5.59 (d, *J* = 9.3 Hz, 1H, NH), 4.35 (ddd, *J* = 13.7, 8.8, 5.1 Hz, 1H), 4.25-4.08 (m, 2H), 2.94 (ddd, *J* = 13.7, 10.9, 4.3 Hz, 1H), 2.17 (s, 2H), 1.77-1.63 (m, 2H), 0.97 (t, *J* = 7.3 Hz, 3H).

^{13}C NMR (125 MHz, $CDCl_3$) δ 172.24, 164.74, 149.70, 139.17, 128.37, 123.82, 60.80, 51.25, 42.53, 25.88, 23.26, 10.61.

Resolution of enantiomers: DAICEL Chiralcel AD-H column, 15% IPA-Hexanes, 1.0 mL/min, 254 nm, RT1 (major) = 7.7 min, RT2 (minor) = 8.8 min

III-47D *N*-((2*S*,3*S*)-3-acetamido-5-((*tert*-butyldiphenylsilyl)oxy)-2-chloropentyl)-4-nitrobenzamide

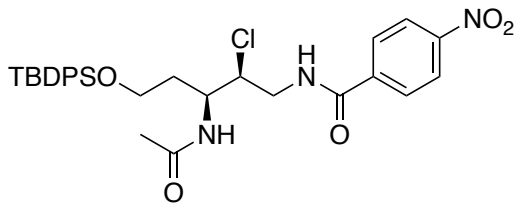

^{1}H NMR (500 MHz, $CDCl_3$) δ 8.48 (dd, *J* = 8.7, 4.2 Hz, 1H, NH), 8.26 (d, *J* = 9.0 Hz, 2H), 8.10 (d, *J* = 9.0 Hz, 2H), 7.58 (ddd, *J* = 9.6, 8.0, 1.4 Hz, 4H), 7.46-7.39 (m, 2H), 7.39-7.32 (m, 4H), 5.56 (d, *J* = 9.3 Hz, 1H, NH), 4.77 (q, *J* = 7.4 Hz, 1H), 4.41 (ddd, *J* = 13.8, 8.9, 5.1 Hz, 1H), 4.17 (ddd, *J* = 11.2, 5.1, 1.6 Hz, 1H), 3.74-

3.61 (m, 2H), 2.93 (ddd, *J* = 13.7, 11.2, 4.3 Hz, 1H), 2.11 (s, 3H), 1.89-1.82 (m, 2H), 0.89 (s, 9H).

^{13}C NMR (125 MHz, $CDCl_3$) δ 172.1, 164.7, 149.6, 139.1, 135.5, 135.4, 133.0, 133.0, 129.8, 129.8, 128.4, 127.8, 127.8, 123.8, 61.5, 59.5, 46.4, 42.4, 35.6, 26.7, 23.3, 19.0.

Resolution of enantiomers: DAICEL Chiralcel OD-H column, 7% IPA-Hexanes, 1.0 mL/min, 254 nm, RT1 (minor) = 22.9 min, RT2 (major) = 26.2 min

III-48D *N*-((2*S*,3*S*)-3-acetamido-2-chloro-3-phenylpropyl)-4-nitrobenzamide

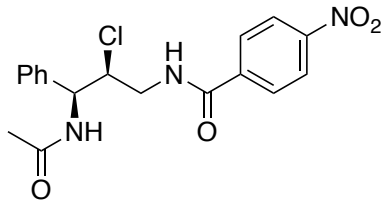

^{1}H NMR (500 MHz, $CDCl_3$) δ 8.32 (d, *J* = 8.8 Hz, 2H), 8.03 (d, *J* = 8.8 Hz, 2H), 7.63 (dd, *J* = 8.7, 3.3 Hz, 1H, NH), 7.44-7.35 (m, 5H), 6.05 (d, *J* = 8.5 Hz, 1H, NH), 5.23 (t, *J* = 8.8 Hz, 1H), 4.52-4.38 (m, 2H), 3.37 (dt, *J* = 14.4, 4.4 Hz, 1H), 2.08 (s, 3H).

^{13}C NMR (125 MHz, $CDCl_3$) δ 170.7, 165.5, 149.7, 139.5, 137.6, 129.2, 128.8, 128.4, 127.5, 123.8, 62.1, 56.3, 42.5, 23.4.

Resolution of enantiomers: DAICEL Chiralcel OD-H column, 20% IPA-Hexanes, 1.0 mL/min, 254 nm, RT1 (major) = 12.8 min, RT2 (minor) = 17.8 min

III-49D *N*-((2*S*,3*R*)-3-acetamido-2-chlorohexyl)-4-nitrobenzamide

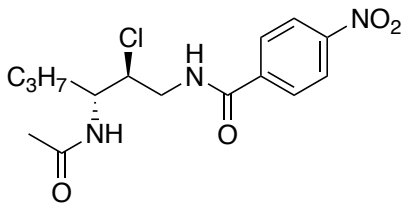

^{1}H NMR (500 MHz, Chloroform-*d*) δ 8.31 (d, *J* = 8.9 Hz, 2H), 8.06 (d, *J* = 8.9 Hz, 2H), 7.60 (d, *J* = 8.4 Hz, 1H, NH), 5.49 (d, *J* = 9.0 Hz, 1H, NH), 4.38 (ddd, *J* = 14.5, 8.8, 3.8 Hz, 1H), 4.20-4.06 (m, 1H), 3.99-3.90 (m, 1H), 3.37 (ddd, *J* = 14.6, 4.8, 3.7 Hz, 1H), 2.09 (s, 3H), 2.01-1.92 (m, 1H), 1.51 – 1.41 (m, 2H), 1.38-1.28 (m, 1H), 0.96 (t, *J* = 7.2 Hz, 3H).

^{13}C NMR (125 MHz, $CDCl_3$) δ 171.30, 165.41, 149.6, 139.65, 128.35, 123.83, 63.14, 51.75, 42.50, 33.22, 23.35, 19.01, 13.72.

Resolution of enantiomers: DAICEL Chiralcel AD-H column, 10% IPA-Hexanes, 1.0 mL/min, 254 nm, RT1 (major) = 10.2 min, RT2 (minor) = 11.4 min

III-50D *N*-((2*S*,3*R*)-3-acetamido-2-chlorohexyl)-4-bromobenzamide

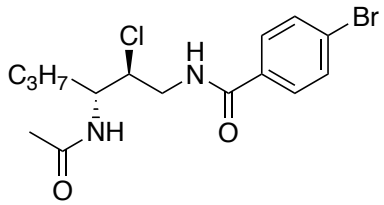

^{1}H NMR (500 MHz, $CDCl_3$) δ 7.73 (d, *J* = 8.5 Hz, 2H), 7.59 (d, *J* = 8.5 Hz, 2H), 7.23 (s, 1H, NH), 5.63 (d, *J* = 9.0 Hz, 1H, NH), 4.27 (ddd, *J* = 14.5, 8.3, 4.0 Hz, 1H), 4.14 (ddd, *J* = 9.9, 7.2, 2.8 Hz, 1H), 4.00 (ddd, *J* = 7.5, 5.7, 4.0 Hz, 1H), 3.37 (ddd, *J* = 14.5, 5.7, 4.0 Hz, 1H), 2.06 (s, 3H), 1.84-1.94 (m, 1H), 1.52-1.39 (m, 2H), 1.39-1.28 (m, 1H), 0.94 (t, *J* = 7.2 Hz, 3H).

^{13}C NMR (125 MHz, $CDCl_3$) δ 171.0, 166.7, 132.8, 131.8, 128.8, 126.4, 63.7, 51.6, 42.7, 32.8, 23.3, 19.0, 13.8.

Resolution of enantiomers: DAICEL Chiralcel AD-H column, 10% IPA-Hexanes, 1.0 mL/min, 254 nm, RT1 (major) = 8.4 min, RT2 (minor) = 10.9 min

III-51D *N*-((2*S*,3*R*)-3-acetamido-2-chloro-3-phenylpropyl)-4-nitrobenzamide

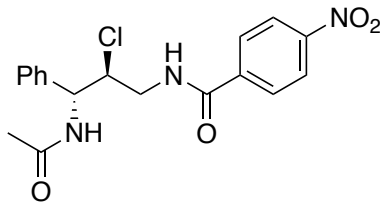

^{1}H NMR (500 MHz, $CDCl_3$) δ 8.32 (d, *J* = 8.8 Hz, 2H), 8.10 (d, *J* = 8.8 Hz, 3H, NH), 7.41-7.29 (m, 5H), 6.26 (d, *J* = 9.7 Hz, 1H, NH), 5.62 (dd, *J* = 9.7, 1.8 Hz, 1H), 4.55 (ddd, *J* = 10.5, 5.4, 1.8 Hz, 1H), 4.39 (ddd, *J* = 13.8, 8.3, 5.4 Hz, 1H), 3.12 (ddd, *J* = 13.8, 10.5, 4.7 Hz, 1H), 2.24 (s, 3H).

^{13}C NMR (125 MHz, $CDCl_3$) δ 171.7, 164.9, 149.8, 139.0, 137.0, 128.8, 128.4, 128.3, 126.6, 123.9, 61.1, 52.2, 43.0, 23.4.

Resolution of enantiomers: DAICEL Chiralcel OJ-H column, 10% IPA-Hexanes, 1.0 mL/min, 254 nm, RT1 (major) = 17.0 min, RT2 (minor) = 23.1 min

III-34F *N*-((2*S*,3*S*)-3-benzamido-2-chlorohexyl)-4-nitrobenzamide

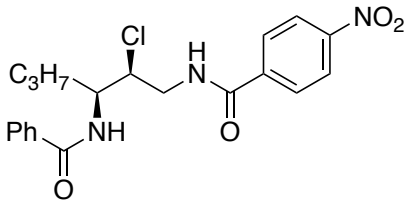

^{1}H NMR (500 MHz, Chloroform-*d*) δ 8.40 (dd, *J* = 8.6, 4.4 Hz, 1H NH), 8.33 (d, *J* = 8.8 Hz, 2H), 8.15 (d, *J* = 8.8 Hz, 2H), 7.83 (d, *J* = 6.9 Hz, 2H), 7.62 – 7.57 (m, 1H), 7.51 (t, *J* = 7.6 Hz, 2H), 6.24 (d, *J* = 9.4 Hz, 1H, NH), 4.53 (tdd, *J* = 9.1, 5.3, 1.6 Hz, 1H), 4.35 (ddd, *J* = 13.8, 8.7, 5.2 Hz, 1H), 4.24 (ddd, *J* = 10.9, 5.2, 1.7 Hz, 1H), 3.00 (ddd, *J* = 13.7, 10.9, 4.4 Hz, 1H), 1.86-1.76 (m, 1H), 1.73-1.63 (m, 1H), 1.48-1.39 (m, 2H), 0.93 (t, *J* = 7.3 Hz, 3H).

^{13}C NMR (125 MHz, Chloroform-*d*) δ 169.30, 164.84, 149.73, 139.22, 133.21, 132.46, 128.96, 128.42, 127.03, 123.88, 61.49, 49.63, 42.68, 34.94, 19.37, 13.71.

Resolution of enantiomers: DAICEL Chiralcel OD-H column, 10% IPA-Hexanes, 1.0 mL/min, 254 nm, RT1 (minor) = 8.8 min, RT2 (major) = 14.3 min

REFERENCES

REFERENCES

1. Gribble, G. W., Naturally occurring organohalogen compounds--a comprehensive survey. *Fortschr. Chem. Org. Naturst.* **1996,** *68*, 1-423.

2. Nakagawa, A.; Iwai, Y.; Hashimoto, H.; Miyazaki, N.; Oiwa, R.; Takahashi, Y.; Hirano, A.; Shibukawa, N.; Kojima, Y.; Omura, S., Virantmycin, a new antiviral antibiotic produced by a strain of Streptomyces. *J. Antibiot.* **1981,** *34* (11), 1408-15.

3. Qiu, J.; Silverman, R. B., A new class of conformationally rigid analogues of 4-amino-5-halopentanoic acids, potent inactivators of gamma-aminobutyric acid aminotransferase. *J Med Chem* **2000,** *43* (4), 706-20.

4. Chemler, S. R.; Bovino, M. T., Catalytic Aminohalogenation of Alkenes and Alkynes. *ACS Catal.* **2013,** *3* (6), 1076-1091.

5. Griffith, D. A.; Danishefsky, S. J., Sulfonamidoglycosylation of glycals. A route to oligosaccharides with 2-aminohexose subunits. *Journal of the American Chemical Society* **1990,** *112* (15), 5811-5819.

6. Yeung, Y. Y.; Hong, S.; Corey, E. J., A short enantioselective pathway for the synthesis of the anti-influenza neuramidase inhibitor oseltamivir from 1,3-butadiene and acrylic acid. *J Am Chem Soc* **2006,** *128* (19), 6310-1.

7. Ashtekar, K. D.; Vetticatt, M.; Yousefi, R.; Jackson, J. E.; Borhan, B., Nucleophile-Assisted Alkene Activation: Olefins Alone Are Often Incompetent. *Journal of the American Chemical Society* **2016,** *138* (26), 8114-8119.

8. Ashtekar, K. D.; Marzijarani, N. S.; Jaganathan, A.; Holmes, D.; Jackson, J. E.; Borhan, B., A new tool to guide halofunctionalization reactions: the halenium affinity (HalA) scale. *J Am Chem Soc* **2014,** *136* (38), 13355-62.

9. Soltanzadeh, B.; Jaganathan, A.; Staples, R. J.; Borhan, B., Highly Stereoselective Intermolecular Haloetherification and Haloesterification of Allyl Amides. *Angew Chem Int Ed Engl* **2015,** *54* (33), 9517-22.

10. Soltanzadeh, B.; Jaganathan, A.; Yi, Y.; Yi, H.; Staples, R. J.; Borhan, B., Highly Regio- and Enantioselective Vicinal Dihalogenation of Allyl Amides. *Journal of the American Chemical Society* **2017,** *139* (6), 2132-2135.

11. Denmark, S. E.; Burk, M. T.; Hoover, A. J., On the Absolute Configurational Stability of Bromonium and Chloronium Ions. *Journal of the American Chemical Society* **2010,** *132* (4), 1232-1233.

12. Jaganathan, A.; Garzan, A.; Whitehead, D. C.; Staples, R. J.; Borhan, B., A catalytic asymmetric chlorocyclization of unsaturated amides. *Angew Chem Int Ed Engl* **2011,** *50* (11), 2593-6.

13. Yeung, Y. Y.; Gao, X.; Corey, E. J., A general process for the haloamidation of olefins. Scope and mechanism. *J Am Chem Soc* **2006,** *128* (30), 9644-5.

14. Yadav, J. S.; Reddy, B. V. S.; Chary, D. N.; Chandrakanth, D., InX3-catalyzed haloamidation of vinyl arenes: a facile synthesis of alpha-bromo- and alpha-fluoroamides. *Tetrahedron Letters* **2009,** *50* (10), 1136-1138.

15. Tay, D. W.; Tsoi, I. T.; Er, J. C.; Leung, G. Y.; Yeung, Y. Y., Lewis basic selenium catalyzed chloroamidation of olefins using nitriles as the nucleophiles. *Org Lett* **2013,** *15* (6), 1310-3.

16. Booker-Milburn, K. I.; Guly, D. J.; Cox, B.; Procopiou, P. A., Ritter-type reactions of N-chlorosaccharin: a method for the electrophilic diamination of alkenes. *Org Lett* **2003,** *5* (18), 3313-5.

17. Alix, A.; Lalli, C.; Retailleau, P.; Masson, G., Highly enantioselective electrophilic alpha-bromination of enecarbamates: chiral phosphoric acid and calcium phosphate salt catalysts. *J Am Chem Soc* **2012,** *134* (25), 10389-92.

18. Cai, Y. F.; Liu, X. H.; Hui, Y. H.; Jiang, J.; Wang, W. T.; Chen, W. L.; Lin, L. L.; Feng, X. M., Catalytic Asymmetric Bromoamination of Chalcones: Highly Efficient Synthesis of Chiral alpha-Bromo-beta-Amino Ketone Derivatives. *Angewandte Chemie-International Edition* **2010,** *49* (35), 6160-6164.

19. Cai, Y. F.; Liu, X. H.; Li, J.; Chen, W. L.; Wang, W. T.; Lin, L. L.; Feng, X. M., Asymmetric Iodoamination of Chalcones and 4-Aryl-4-oxobutenoates Catalyzed by a Complex Based on Scandium(III) and a N,N '-Dioxide Ligand. *Chemistry-a European Journal* **2011,** *17* (52), 14916-14921.

20. Cai, Y. F.; Liu, X. H.; Jiang, J.; Chen, W. L.; Lin, L. L.; Feng, X. M., Catalytic Asymmetric Chloroamination Reaction of alpha,beta-Unsaturated gamma-Keto Esters and Chalcones. *Journal of the American Chemical Society* **2011,** *133* (15), 5636-5639.

21. Whitehead, D. C.; Yousefi, R.; Jaganathan, A.; Borhan, B., An Organocatalytic Asymmetric Chlorolactonization. *Journal of the American Chemical Society* **2010,** *132* (10), 3298-3300.

22. Trost, B. M.; Saget, T.; Hung, C. J., Efficient Access to Chiral Trisubstituted Aziridines via Catalytic Enantioselective Aza-Darzens Reactions. *Angew Chem Int Ed Engl* **2017,** *56* (9), 2440-2444.

Chapter IV: Mechanistic investigation for the observed switch in olefin chlorenium face selectivity

IV-1 Introduction

IV-1-1 Switch of chlorenium face selectivity in two products of dichlorination reaction

In our prior work, we had demonstrated optimized conditions (0.02 M substrate concentration in TFE, 100 equivalents LiCl and 2.0 equivalents of DCDMH at -30 °C) for the enantioselective dihalogenation reactions of alkenes (Figure IV-1a). The fact that these reactions required up to 100 equivalents of LiCl for optimal results was surprising. Based on different control experiments, it was indicated that the reaction is occurring on a solid-liquid interface (see Chapter II). On the other hand, treating allyl amide **IV-1** with 15 equivalents of LiCl in the presence of 10 mol% $(DHQD)_2$PHAL and two equivalents of DCDMH at room temperature produces a mixture of products. In line with the desired dichlorinated product **IV-1A**, the TFE-incorporated product **IV-1B** was formed in 45% yield and 92:8 enantioselectivity (Figure IV-1b). The crystal structure for the dichlorinated product **IV-1A** enabled us to assign the absolute stereochemistry for the two newly formed chiral centers. Unfortunately, different attempts to get single crystal structure for the TFE incorporated product **IV-1B** were not successful. However, varying the expandable amide moiety from 4-nitrobenzamide to 4-bromobenzamide led to get a crystal structure for the TFE-incorporated product **IV-1B**. Examination of the latter results leads to an interesting yet puzzling observation. The chloroetherified side-product **IV-1B** for

the dichlorination reactions is formed with a switch in olefin face selectivity during the addition of the chlorenium, with overall excellent enantioselectivity (Figure IV-1b). To the best of our knowledge, this is the first time that two products are produced in high *ee* under same reaction conditions (same chiral catalyst, solvent, etc.), but with different chlorenium face selectivity.

Figure IV-1: Switch of chlorenium face selectivity for two products of the dichlorination reaction.

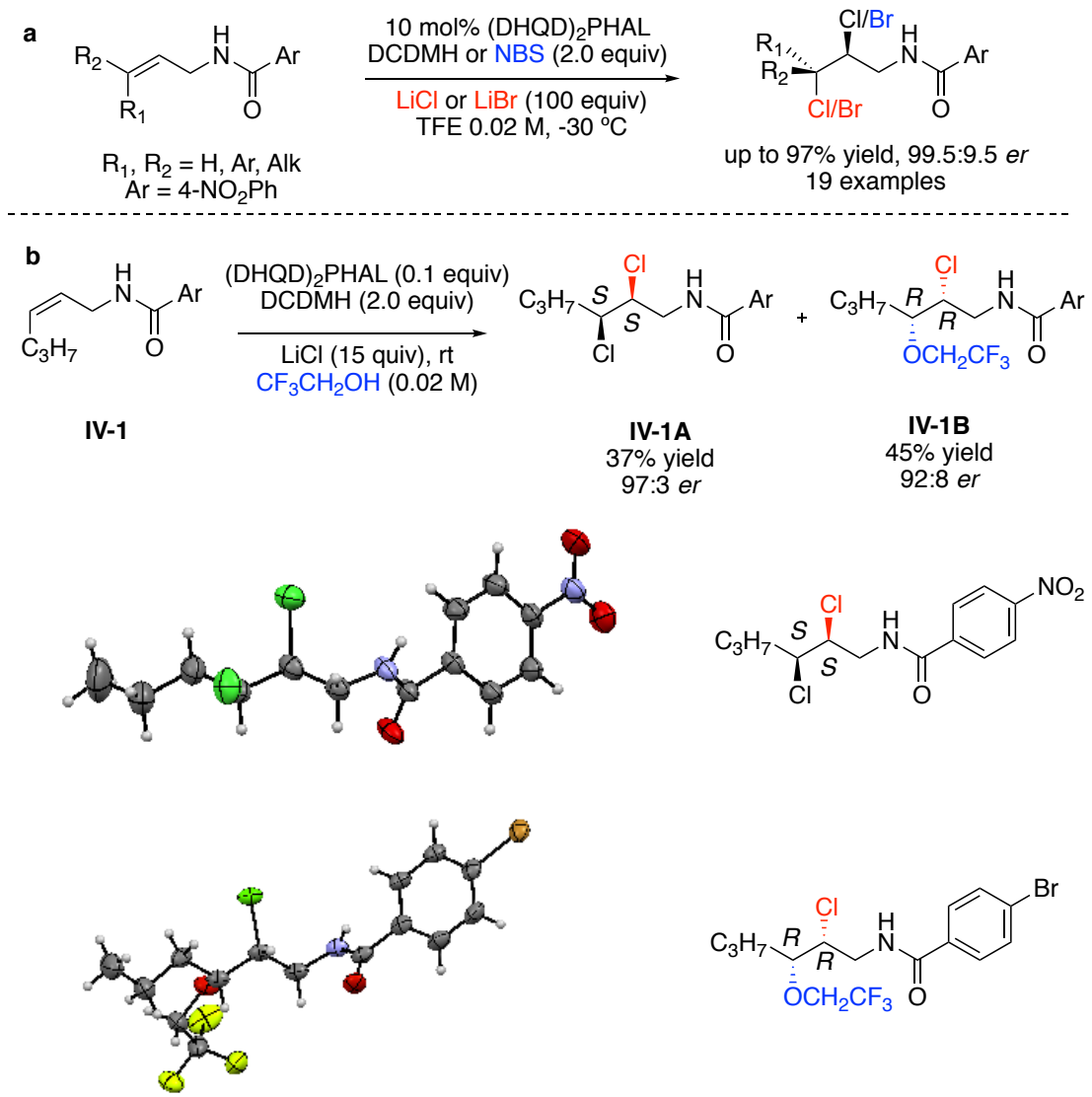

IV-1-2 Switch of chlorenium face selectivity for two products of the chloroetherification reaction.

Based on the results above, we were interested in determining if the switch in chlorenium face selectivity can also occur in the enantioselective haloetherification of alkenes.[1] When *trans*-aryl-substituted alkenes such as compound **IV-2** were subjected to the optimized conditions for the enantioselective haloetherification reactions two products were produced, the desired chloroetherified product **IV-2B** (43% yield and 82:18 *er*) along with the chlorocyclized product **IV-2C** (36% yield and 97:3 *er,* see Figure IV-2). Notably, aliphatic substituted alkenes under the same optimized conditions yielded the desired intermolecular products exclusively in high yield and stereoselectivity.

Figure IV-2: The *trans*-aryl-substituted alkenes form two products during the enantioselective chloroetherification reaction

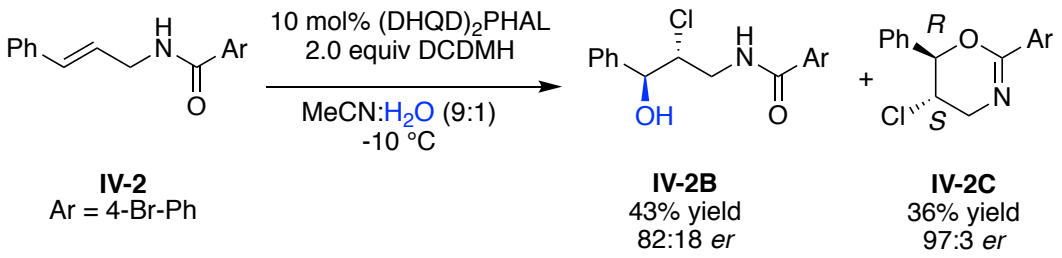

We sought to understand whether the chlorenium face selectivity would switch in these two products (inter- and intramolecular chlorofunctionalized products), similar to the dichlorination case. We were able to a get crystal structure for cyclized product **IV-2C**.[2] However, several attempts to obtain a single crystal for the intermolecular product **IV-2B** failed. In order to unequivocally assign the stereo centers of chloroetherified product **IV-2B**, compound **IV-2C** was transformed to **IV-2B** in two steps as shown in Figure IV-3.

Treating the chlorocyclized product with 1.5 N HCl at reflux followed by protection of the amine with 4-bromobenzoylchloride produces halohydrin *ent*-**IV-2B**. Optical rotation, as well as HPLC co-injection, confirmed that it was indeed the enantiomer of **IV-2B** that had resulted from this transformation (Figure IV-3). These results lead us to conclude that the chlorenium face selectivity switches while the two products are formed during the enantioselective chlorofunctionalization reactions (both the enantioselective dichlorination and haloetherification reactions).

Figure IV-3: Switch of chlorenium face selectivity for the two products of the chloroetherification reaction.

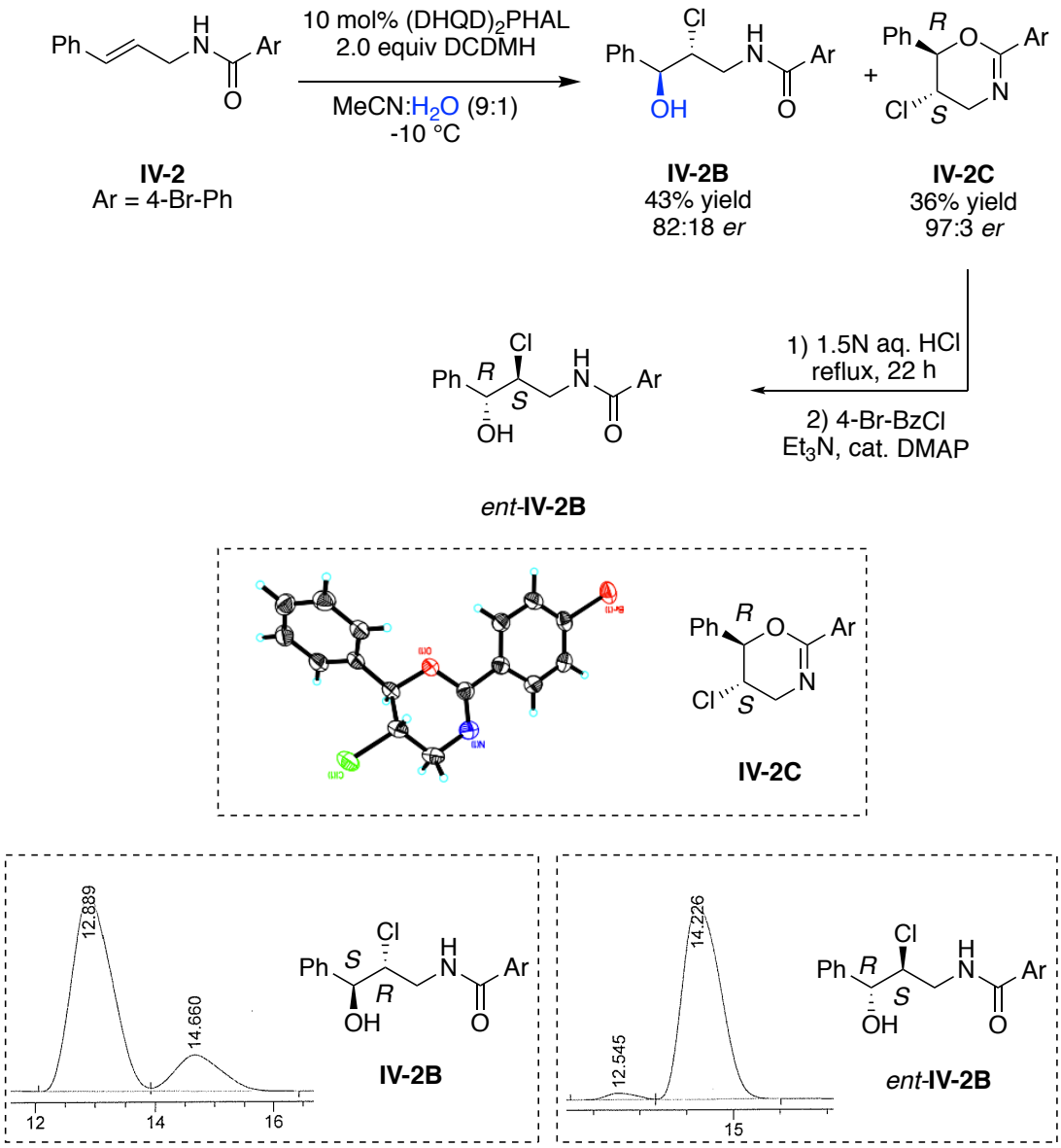

IV-1-3 Classical perception of electrophilic addition to alkenes vs. Nucleophile Assisted Alkene Activation (NAAA)

In a classical way, the chiral catalyst dictates the face selectivity of the alkene (*re* face or *si* face) in the formation of halonium ion intermediates.[3-4] If the chiral catalyst selects one face of the alkene to form the intermediate ion **IV-2'**, the nature of nucleophiles does not effect the halenium face selectivity (Figure IV-4).

However, our results show various nucleophiles can affect the chlorine face selectivity. As depicted in Figure IV-4b, with H_2O as the nucleophile the chlorenium face selectivity for the halohydrin product **IV-2B** has an *R* configuration. On the other hand, when 4-bromobenzamide acts as the nucleophile, the chlorine face selectivity for cyclized product **IV-2C** result in an *S* configuration (Figure IV-4b).

Figure IV-4: (a) The classical way for indicating halenium face selectivity (b) various nucleophiles dictates face selectivity

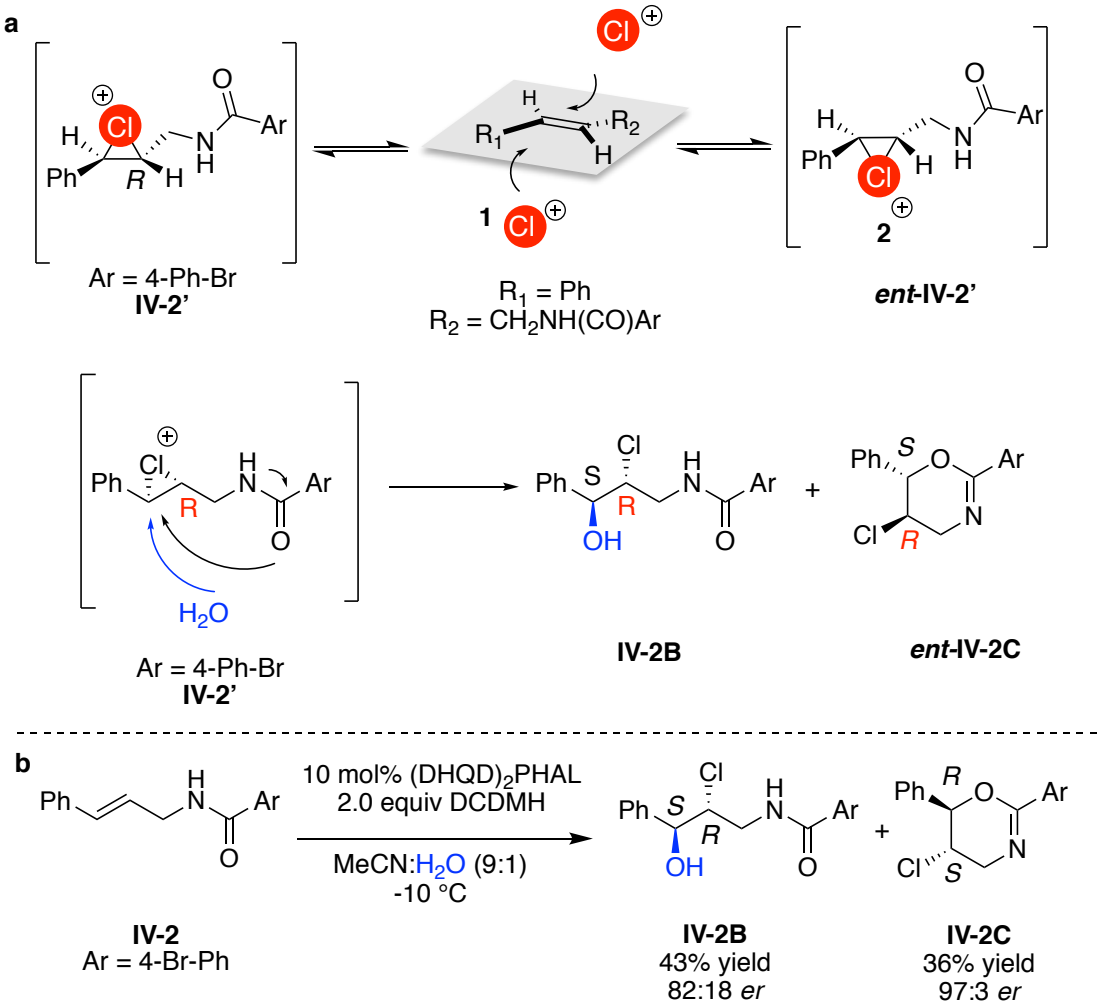

Mechanistic investigations to understand the latter results are underway. Nonetheless, this observation leads credence to our earlier finding on the

halocyclization reaction that showed in lieu of a stepwise activation of alkenes (electrophilic attack on the alkene) and subsequent nucleophilic bond formation, the reaction actually proceeds via a concerted mechanism. Our proposed Nucleophile Assisted Alkene Activation (NAAA) pathway suggests that the proximity of the nucleophile to the olefin leads to the activation of the olefin (pre-polarization) for capturing of the electrophile from its source. Based on the latter supposition, the nucleophile should be part of the rate-determining step and thus can affect the halogen face selectivity (Figure IV-5a, b).[5]

Figure IV-5: (a) Classical perception of the electrophilic addition to alkenes (b) Nucleophile Assisted Alkene Activation (NAAA)

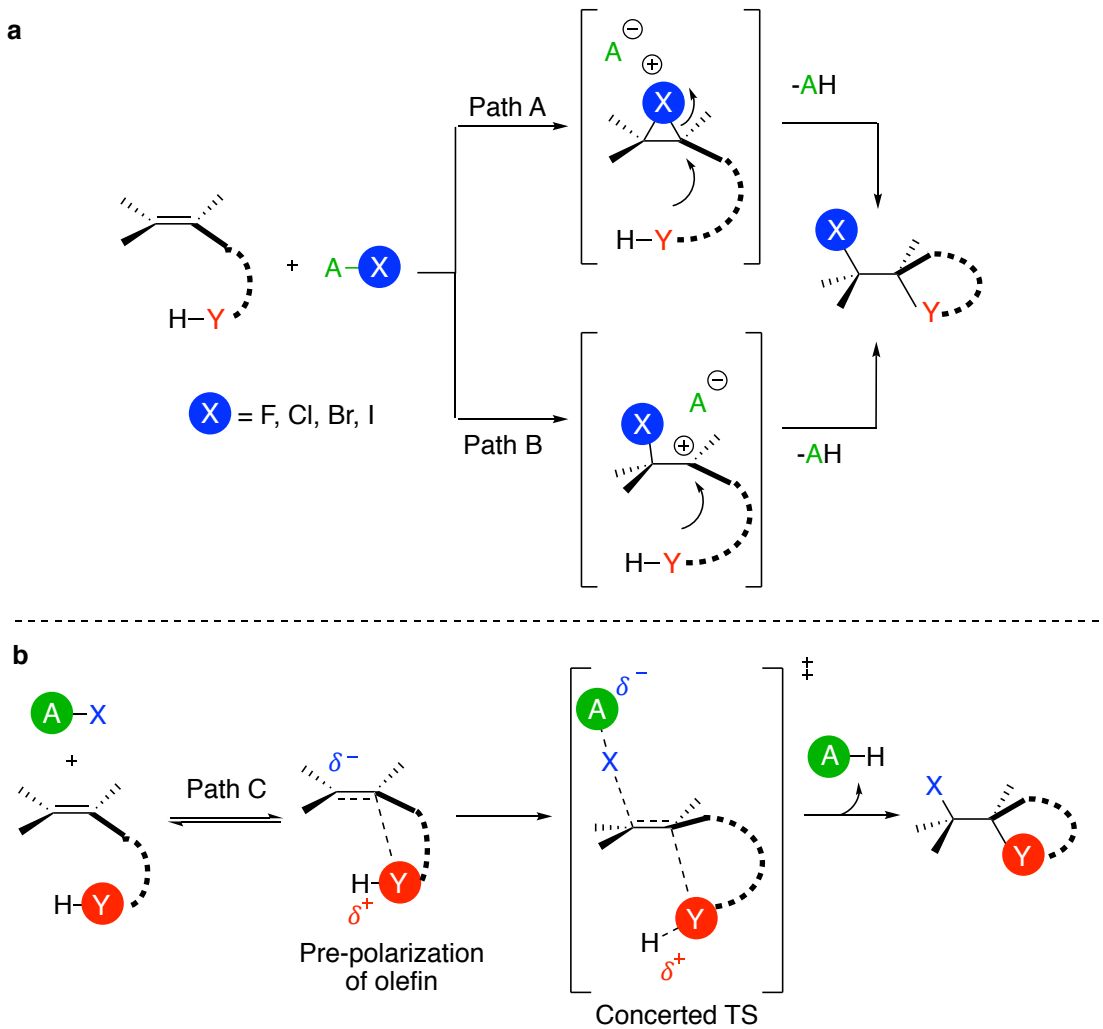

IV-1-3-1 ^{18}O KIE studies prove the role of the nucleophile in the transition states

Different experiments such as transition state calculation, kinetic isotopic effects (KIE) and NMR studies have provided support for the NAAA pathway. The summary of two of the experiments performed by Dr. Kumar Ashtekar would be helpful for readers.[5] The ^{18}O KIE experiment for the racemic chlorolactonization reaction would directly probe the role of nucleophile in the NAAA pathway. The 1:1 mixture of **IV-3**-^{16}O and **IV-3**-^{18}O were treated with 0.1 equivalents of DCDMH in $CHCl_3$ at room temperature to form the mixture of ^{16}O and ^{18}O chlorocyclized products (**IV-3C** and **IV-3C***). The ratio of these products shows a significant ^{18}O KIE ($K^{16}O/K^{18}O$ = 1.026). In contrast, the reaction of 4-methoxy substituted aryl **IV-4** as control experiment shows almost unity value ^{18}O KIE ($K^{16}O/K^{18}O$ = 1.009). These results indicate that the nucleophile should be part of the rate-determining step.

Figure IV-6: ^{18}O KIE experimental results for **IV-3** and **IV-4**

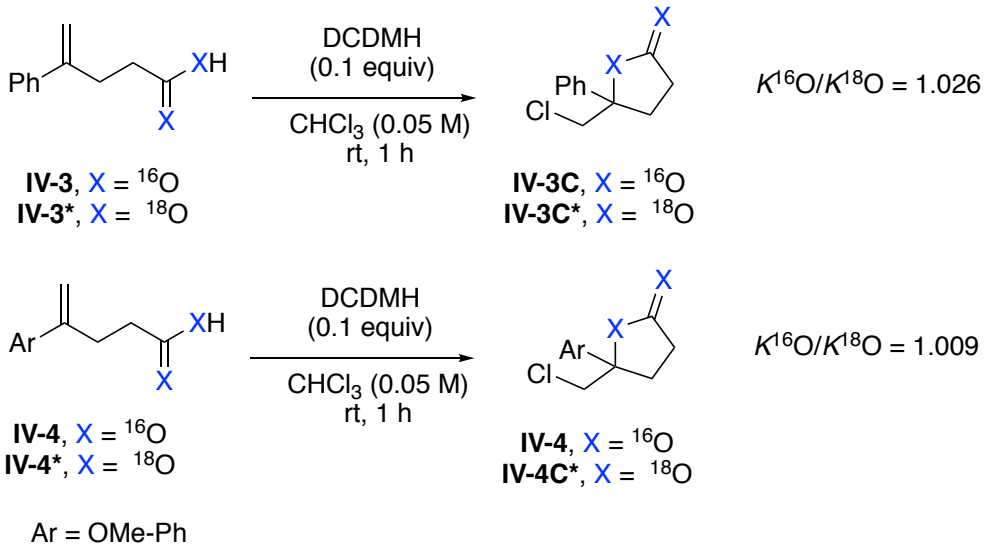

IV-1-3-2 NMR resonance displaying the interaction of nucleophiles with the alkenes

The NMR studies demonstrate the pre-polarization and activation of alkenes by the tethered nucleophile. The free acid displays proton resonance for olefinic hydrogens at 6.50 for H_a and 5.62 for H_b, while ^{13}C resonance appears at 130.4 and 129.8 ppm, respectively. Changing the tethered nucleophile to carboxylate (more nucleophilic than carboxylic acid) leads to shielding of H_a and C-H_a, where as the more proximal H_b and C-H_b deshielded relative to the acid. The above NMR studies indicate that the interaction between the nucleophile and the alkene (pre-polarization) would be an important feature for electrophilic addition reactions such as halofunctionalization.

Figure IV-7: NMR resonance of olefinic C and H displaying the interaction of nucleophiles with the alkenes

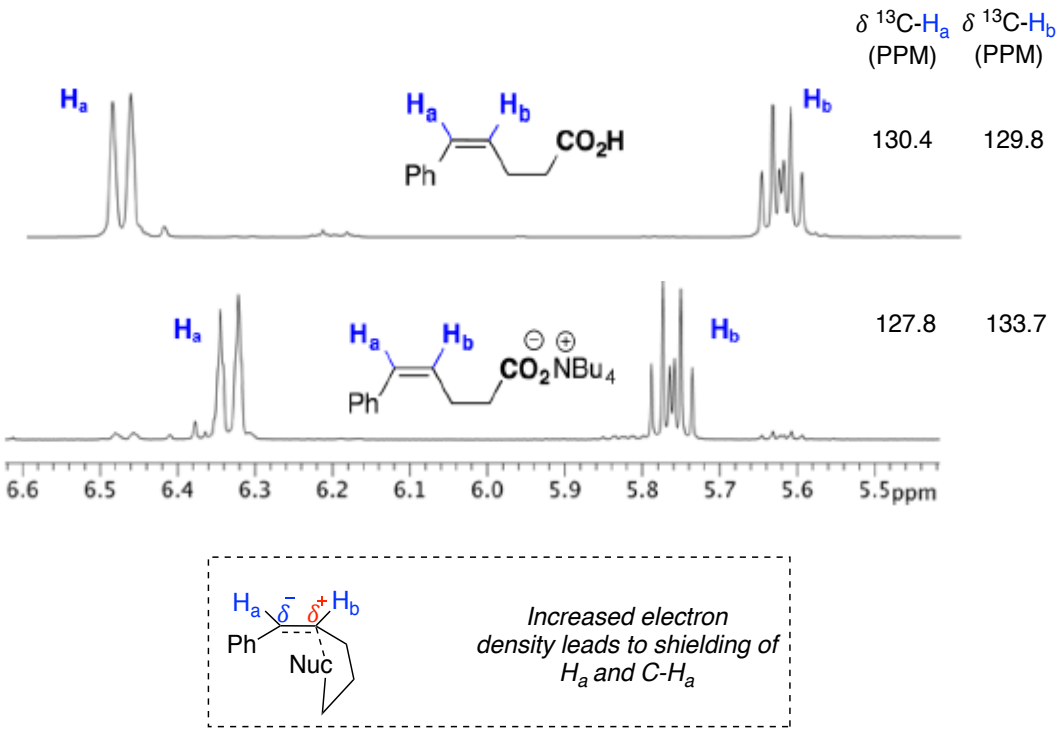

IV-1-4 Kinetic studies

In order to demonstrate that the enantioselective chlorofunctionalization follows the NAAA pathway, illustrating that nucleophile in these reactions is part of the transition state and exhibits first order kinetic is essential. In the classical kinetic studies, pseudo first order approximations are used to figure out kinetic orders of each reactant in reaction. In this approximation excess amount of the reactant ([**B**]) as compared to other reactant is used, thus during the reaction the concentration of compound **B** does not change. By this approximation, the rate of reaction is related to the concentration of one component. In this case, plotting rate vs. concentration of **A** would reveal the order for compound **A** (Figure IV-8).[6]

Figure IV-8: The classical method for kinetic studies (pseudo first order approximation)

$$\mathbf{A} + \mathbf{B} \longrightarrow \mathbf{C}$$

$$r = k\,[A]^n[B]^n \quad \text{If } [B] >> [A] \Longrightarrow r = k'\,[A]^n$$

$$k' = k\,[B]^n$$

n = Order of reactant in reaction
r = Rate of reaction
k = Rate constant

We have demonstrated the use of various nucleophiles for the enantioselective intermolecular chloroetherification.[1] In all cases, the nucleophiles were employed as a co-solvent to out-compete the cyclization reaction and simultaneously furnish the intermolecular products in high yield and selectivity (Figure IV-9). Thus, applying the pseudo first order kinetic approximation to reveal the kinetic order of the nucleophile in the

enantioselective intermolecular chloroetherification would not be applicable due to the large excess of nucleophile under the optimized conditions. Extensive literature research was performed in an attempt to find a solution for the above problem and determine the kinetic order of nucleophiles in this type of reactions.

Figure IV-9: Nucleophiles were used as co-solvents in the enantioselective chloroetherification reactions

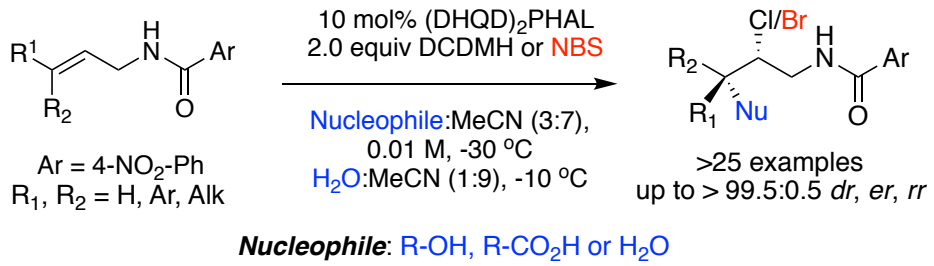

IV-1-5 Kinetic competition studies in HDDA reactions

Hoye and coworkers recently developed a mild and facile path for the synthesis of benzynes as versatile and reactive intermediates.[7] These arynes can be trapped by different nucleophiles. The *in situ* formation of benzyne from triyne **IV-5** at 26 °C followed by intermolecular trapping of the benzyne intermediate **IV-6** produces the complex molecule **IV-7** in 93% yield (Figure IV-10). These one-pot reactions, known as the hexadehydro-Diels-Alder (HDDA) reactions (Figure IV-10), can produce a plethora of interesting products.

Figure IV-10: The hexadehydro-Diels-Alder reaction

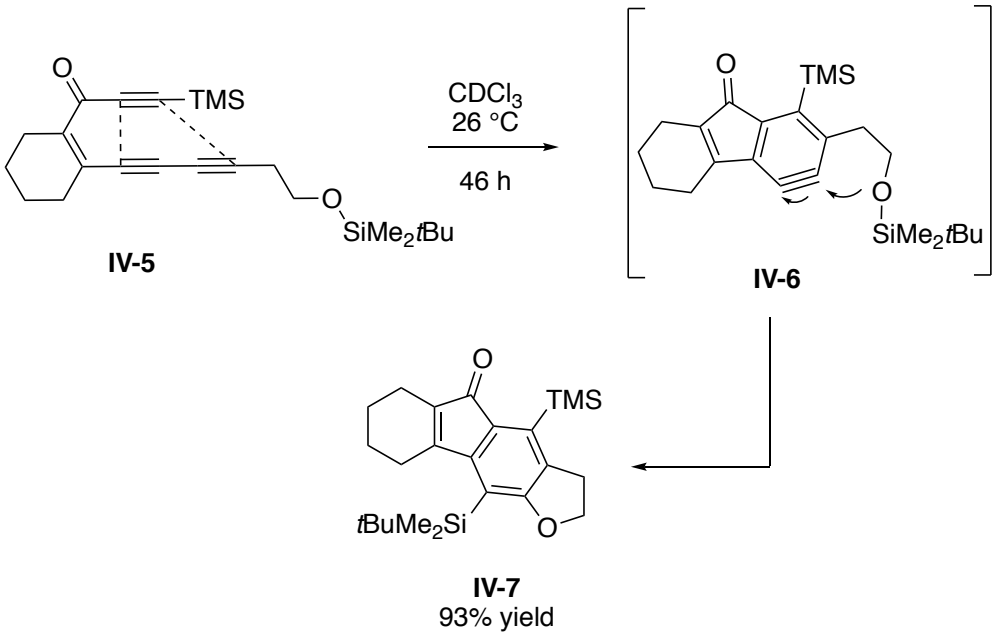

In the course of employing different nucleophiles that would trap the HDDA-derived benzyne **IV-10**, an interesting observation was made. The HDDA-reaction of triyne **IV-8** in neat cyclohexanol **IV-9** produced predominantly the addition products **IV-11** in 80% yield (Table IV-1, entry 1).[8] However, a small amount of reduced benzyne product **IV-12** was observed (**IV-11: IV-12** = 12:1, entry 1). Surprisingly, treating triyne **IV-9** with 1.6 equivalents of cyclohexanol at 85 °C reversed the selectivity of products. (**IV-11: IV-12** = 1:17, entry 2). The reduced benzyne product **IV-12** was formed in 60% yield under these conditions (Table IV-1, entry 2).

Table IV-1: Competitive H_2-transfer vs. addition product in HDDA reaction

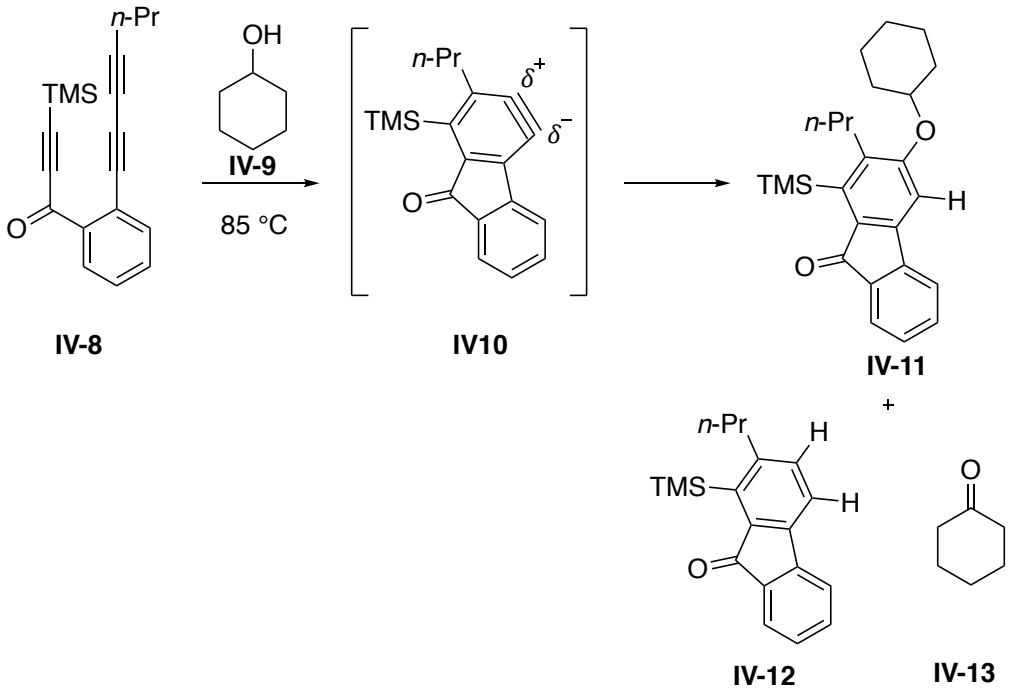

Entry	[**IV-9**]	equiv **IV-9**	**11**:1**2**	Yield
1	9.5 M (neat)	1000	12:1	80%, **IV-11**
2	0.013 M (in $CDCl_3$)	1.6	1:17	60%, **IV-12**

Based on the above results, these two reactions have different kinetic profiles relative to cyclohexanol. The authors investigated the kinetic order of the trapping reagent (such as cyclohexanol) for the addition product **IV-11** and the reduced benzyne products **IV-12**. However, applying pseudo first order approximation to examine the kinetic order of the alcohol (trapping agent) is not possible since an excess amount of cyclohexanol (1000 equivalents) for the formation of alcohol addition products **IV-11** is used (see Table IV-1, entry 1).

Hoye and coworkers cleverly designed the protocol to probe the kinetic order for the benzyne trapping process.[8-9] They designed triyne **IV-14** that contains a competing intramolecular trap serve as an internal clock. By performing the reaction in various concentration of the trapping agent and determining the ratio of products arising from the intramolecular product **IV-15** vs. the product derived from the engagement of trapping agent (bimolecular capture of benzyne such as **IV-16a/b, IV-17**), the kinetic order of the trapping agent can be calculated.

The triyne **IV-14** and *i*-PrOH (70 molar equiv) were dissolved in varying amount of $CDCl_3$ to produce series of solutions with different initial concentration of triyne. Each solution was heated to 68 °C and after 18 h the reactions were quenched and concentrated. Various ratio of intermolecular-Diels-Alder product **IV-15** and intermolecular products that arise from *i*-PrOH engagement (**IV-16a/b, IV-17**) were observed as a function of the concentration of the isopropanol. Notably, the addition products **IV-16a/b** were formed in the same ratio (10:1) regardless of the isopropanol concentration.

Table IV-2: Kinetic competition study employing an internal clock reaction

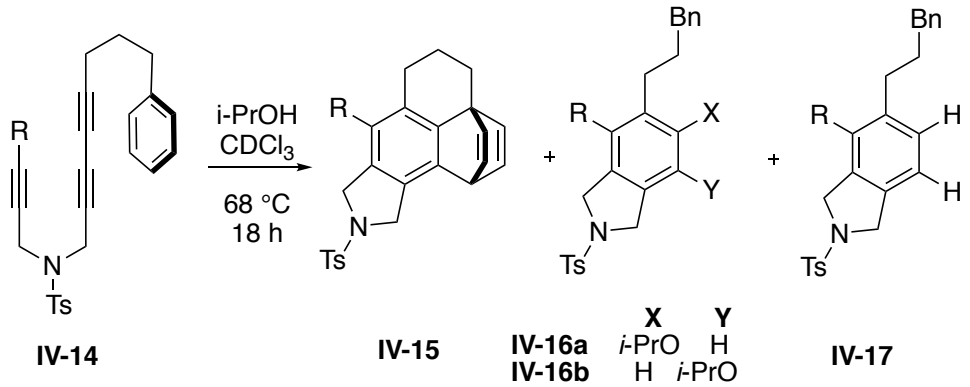

$[\text{i-PrOH}]_{bulk}/[\textbf{IV-14}]_o = 70$

[*i*-PrOH] (Bulk)	[*i*-PrOH] (Monomer)	**16a/15**	**17/15**
1.31	0.83	1.2	0.46
0.66	0.49	0.37	0.26
0.44	0.35	0.19	0.17
0.33	0.28	0.13	0.12

The ratio for the rate expression for the formation of **IV-16a** and **IV-15** is shown in eq (1), and it can be rewritten as eq (2). Since *i*-PrOH is in excess, its concentration approximately remains unchanged during the reaction. Equation (2) can be shown as eq (3), which can also be expressed as eq (4) by mathematical manipulations (Figure IV-11). Plotting ln([**16a**]/[**15**]) vs. ln[*i*-PrOH]$_{mono}$ determines the order of isopropanol for the alcohol addition pathway. The same protocol can be used to determine the kinetic order of *i*-PrOH relative to reduced product **IV-17**. The plot shows that the kinetic order of isopropanol for the alcohol addition pathway is two. However, for the redox reaction pathway, the kinetic order of i-PrOH is one (Figure IV-11).[8]

Figure IV-11: The kinetic Formulas and ln-ln plot, which the kinetic order was obtained

$$\frac{d[\mathbf{16a}]}{d[15]} = \frac{k_1 \cdot [\mathbf{14}] \cdot [iPrOH]^n \cdot dt}{k_2 \cdot [\mathbf{14}] \cdot dt} \quad (1)$$

$$\frac{[\mathbf{16a}]}{[15]} = \frac{\int k_1 \cdot [\mathbf{14}] \cdot [iPrOH]^n \cdot dt}{\int k_2 \cdot [\mathbf{14}] \cdot dt} \quad (2)$$

$$\frac{[\mathbf{16a}]}{[\mathbf{15}]} = \frac{k_1}{k_2} \cdot [iPrOH]^n \quad (3)$$

$$\ln\frac{[\mathbf{16a}]}{[\mathbf{15}]} = n \cdot \ln[iPrOH] + \ln\frac{k_1}{k_2} \quad (4)$$

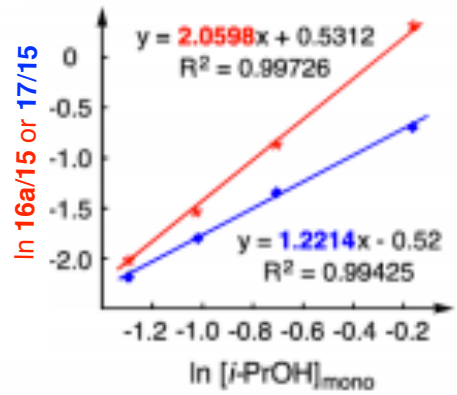

Notably, alcohols aggregate in solutions, the entropy and enthalpy energies for different alcohols were determined experimentally and by calculation. The enthalpy and entropy energy associated with dimerization of isopropanol in CCl_4 has been calculated to be -5.7 kcal/mol and -19.5 kcal/mol, respectively.[10] The free energy was calculated for a particular temperature by applying to the formula $\Delta G = \Delta H - T\Delta S$. Subsequently, the equilibrium constant (K_{eq}) for isopropanol dimerization at 68 °C was obtained by employing the following formula ($\Delta G = -RT\ln K_{eq}$).

IV-2 Results and discussions

IV-2-1 Kinetic competition studies for chloroetherification reactions

The E-aryl-substituted allyl amide **IV-18** in the presence of 10 mol% $(DHQD)_2$PHAL and 100 equivalents of MeOH as a nucleophile in acetonitrile at ambient temperature forms the mixture of products (**IV-18B**, **IV-18B'** and **IV-18C**). Clearly, methanol is engaged in the formation of two diastereomers of the intermolecular chloroetherified products. However, in the chlorocyclized product **IV-18C**, the tethered amide acts as an intramolecular nucleophile. The chlorocyclized product **IV-18C** could be used as an internal clock for the kinetic competition studies similar to what Hoye and coworkers report.[8] Applying kinetic competition formulas as shown in Figure IV-12 yield the kinetic order of the nucleophile (methanol) for the formation of intermolecular products **IV-18B**, **IV-18B'** (Figure IV-12).

Figure IV-12: Kinetic competition studies for enantioselective chloroetherifications

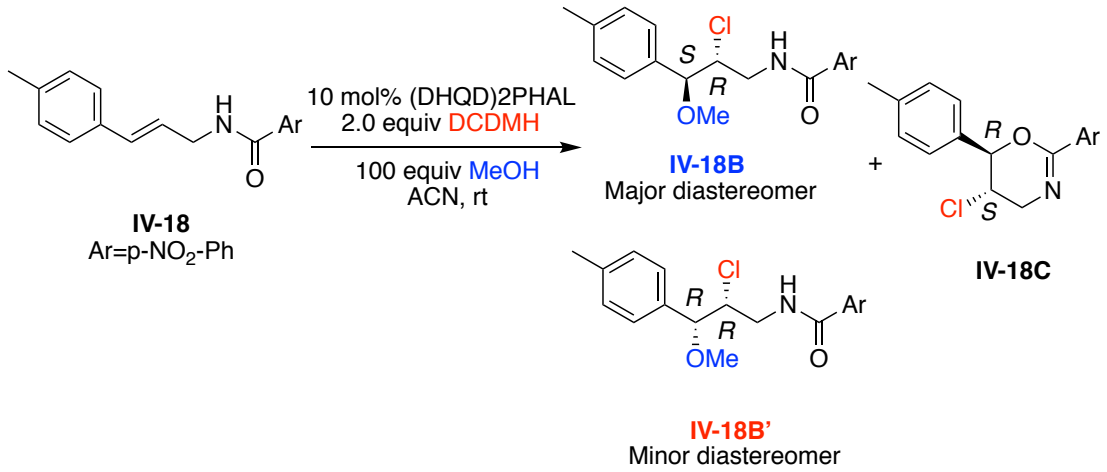

$$\ln\frac{[\mathbf{18B}]}{[\mathbf{18C}]} = n \cdot \ln[\mathrm{MeOH}] + \ln\frac{k_1}{k_2}$$

$$\ln\frac{[\mathbf{18B'}]}{[\mathbf{18C}]} = n \cdot \ln[\mathrm{MeOH}] + \ln\frac{k_1}{k_2}$$

The *E*-allyl amide **IV-18** in the presence of 10 mol% $(DHQD)_2$PHAL and 100 (molar equivalent) of methanol was dissolved in different amounts of acetonitrile. Adding two equivalents of DCDMH to these series of the solution at room temperature forms different ratios of intermolecular products (**IV-18B**, **IV-18B'**) and cyclized products **IV-18C,** as a function of the concentration of methanol (Table IV-3). Conducting the chlorofunctionalization reaction in 1.26 molar methanol gave intermolecular chloroetherified products (major diastereomer **IV-18B** and minor diastereomer **IV-18B'**) and chlorocyclized product **IV-18C** in the ratio of 26.0: 21.8: 52.3, respectively (Table IV-3, entry 1). Applying higher concentration of methanol produced desired chloroetherified diastereomer **IV-18B** with higher selectivity (see entries 1 to 4). Surprisingly, the

amount of minor intermolecular diastereomer did not depend on the concentration of methanol (see entries 1 to 4, the amount of compound **IV-18B'** is constant).

Table IV-3: The ratio of the **IV-18B** and **IV-18C** is related to the concentration of MeOH

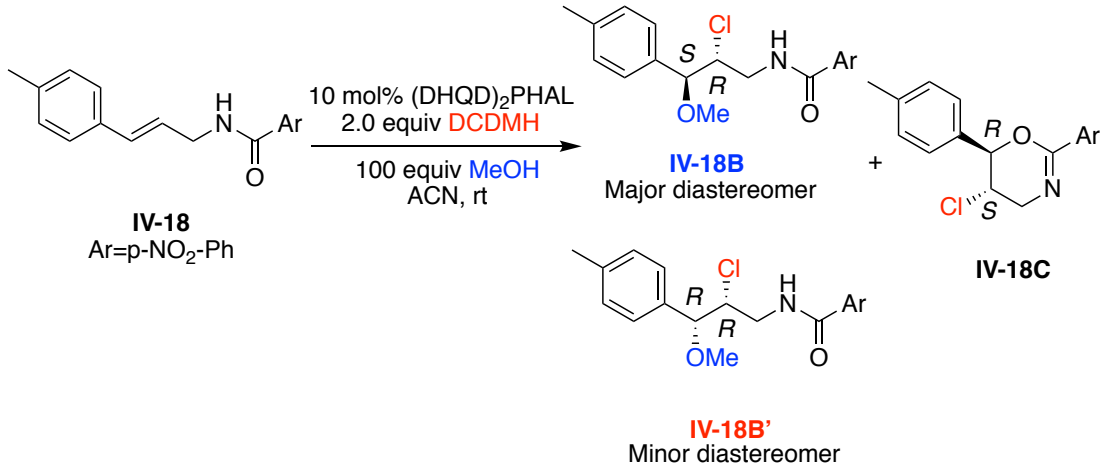

Entry	Conc MeOH (M)	18B: 18B': 18C [a]
1	1.26	26.0: 21.8: 52.3
2	1.85	29.7: 22.2: 48.3
3	3.45	34.3: 21.6: 44.1
4	6.06	38.7: 20.6: 40.7

[a]Determined by NMR

Plotting ln(**18B**/**18C**) vs. $\ln[MeOH]_{mono}$ suggests that the process leading to the major intermolecular diastereomer **IV-18B** is first order for methanol. Interestingly, plotting ln(**18B'**/**18C**) vs. $\ln[MeOH]_{mono}$ indicates that the kinetic order for formation of minor diastereomer **IV-18B'** is zero for methanol (Figure IV-13). These results lead us to conclude that two distinct mechanisms are in play,

leading to either the desired intermolecular products **IV-18B** or the minor intermolecular addition **IV-18B'**.

Figure IV-13: The ln-ln plot from which the kinetic order was obtained

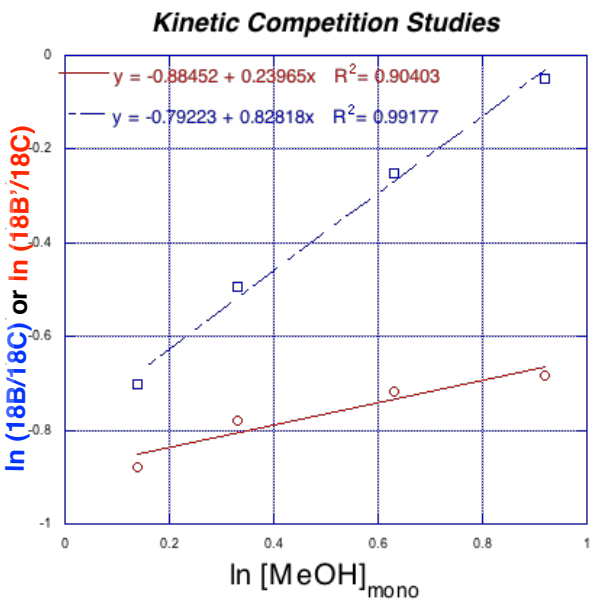

$$\ln\frac{[\mathbf{18B}]}{[\mathbf{18C}]} = n \cdot \ln[\mathrm{MeOH}] + \ln\frac{k_1}{k_2}$$

$$\ln\frac{[\mathbf{18B'}]}{[\mathbf{18C}]} = n \cdot \ln[\mathrm{MeOH}] + \ln\frac{k_1}{k_2}$$

IV-2-2 Proposed mechanism for chlorenium face selectivity switch for products IV-18B and IV-18C

The NAAA pathway suggests, the nucleophile activates alkenes by pre-polarization, and should be part of the transition state. The fact that the kinetic order for the formation of intermolecular product **IV-18B** is one with regards to methanol lead us to suggest the NAAA pathway is a factor in chlorenium face selectivity switch in the enantioselective chloroetherification reactions. The tethered benzamide nucleophile activates (pre-polarization) the alkene from the *re* face. However, the MeOH as an intermolecular nucleophile activates from the other face of the alkene (*si* face). The transition state indicates concerted activation and addition of the electrophilic halogen to alkenes. Our preliminary

mechanistic studies lead us to propose the concerted transition states depicted in Figure IV-14 to explain the divergent chlorenium face selectivity observed in the products of the chloroetherifcation reactions. It merit mentions, mechanistic investigations are under way to elaborate on the nature of interaction for different nucleophiles with the chiral catalyst and alkenes to show how the characteristic

Figure IV-14: Proposed mechanism for switch in chlorenium face selectivity

of the nucleophile can change the face selectivity and enantioselectivity of the products.

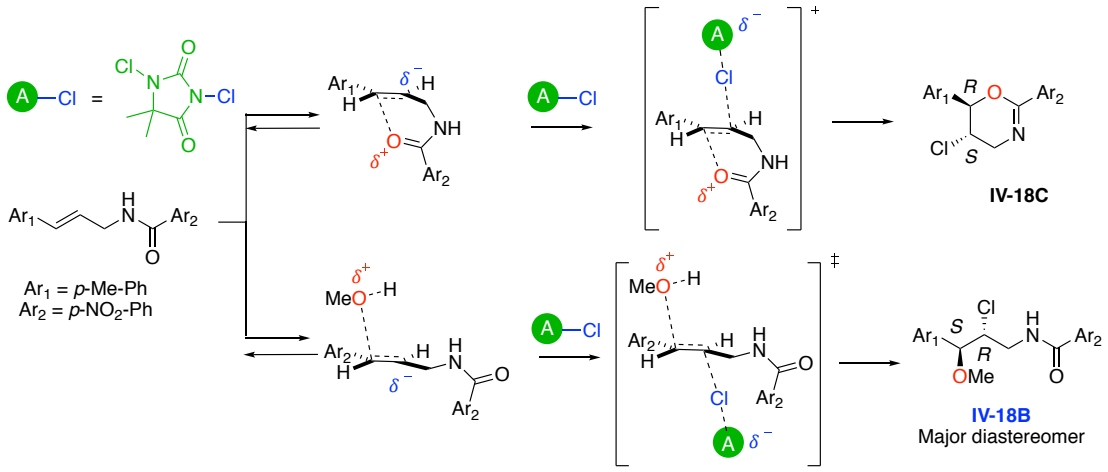

IV-2-3 Exploring mechanism of formation of the minor diasteomer IV-18B'

As described above, the kinetic order of methanol for the formation of the minor diastereomer is zero. Therefore, the NAAA pathway cannot explain the mechanism for the formation of **IV-18B'**. The combined observations described above for the enantioselective intermolecular chloroetherification report leads us to propose a carbocationic mechanism. As depicted in Figure IV-16, varying substituents on the aryl group of Z-aryl-substituted allyl amides resulted in a

significant effect on the diastereoselectivity of the chloroetherified products. Electron donating substituents such as methoxy gave the corresponding products **IV-19B** with 1:1 dr (Figure IV-15). However, reducing the electron donation cause formation of chloroetherified products with higher diastereoselectivity (see products **IV-19B** to **IV-22B**). Employment of trifluoromethyl group as substituent gave chloroetherified product **IV-22B** with >20:1 dr.

Figure IV-15: Different substituents on aryl group of allyl amides effects diastereoselectivities of products

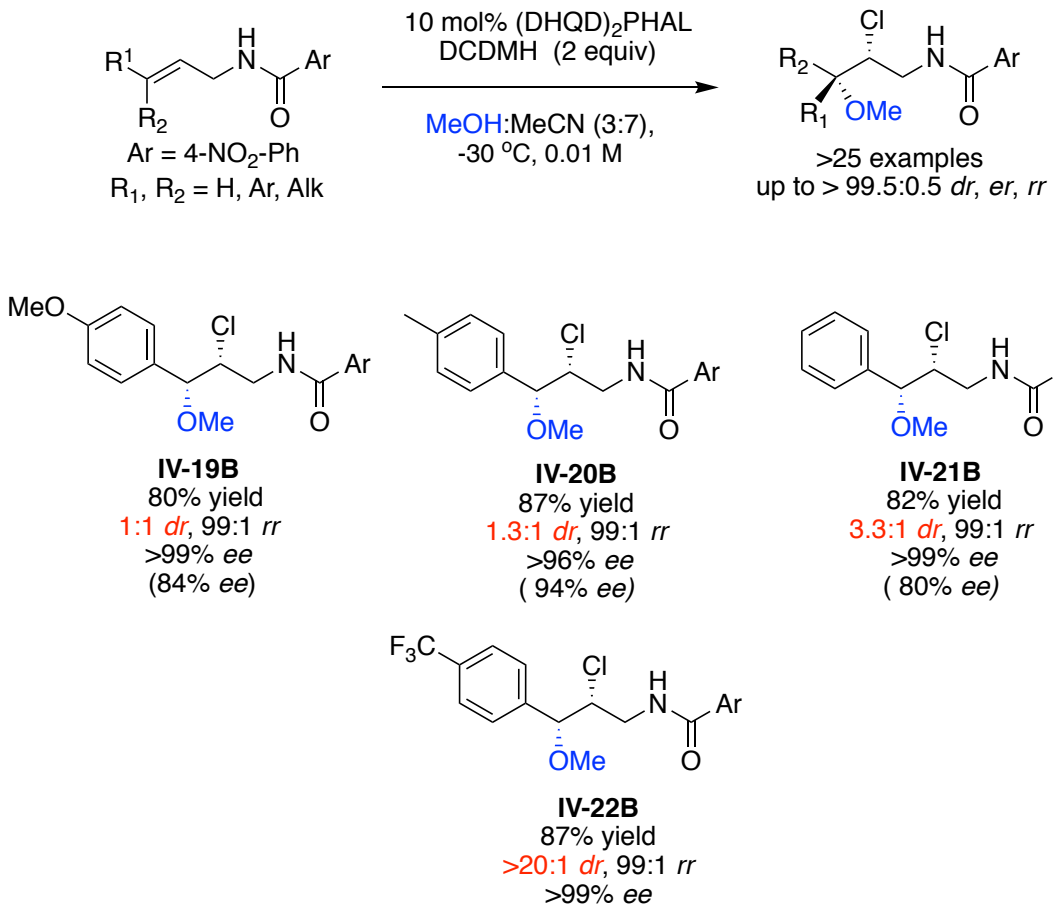

Hammett analysis of the later data by plotting log(**B**/**B'**) vs. σ (Hammett value for different substituents), indicates carbocation formation during the chloroethrification reactions (Figure IV-16).

Figure IV-16: Hammett plot for diastereoselectivities of chloroetherified products

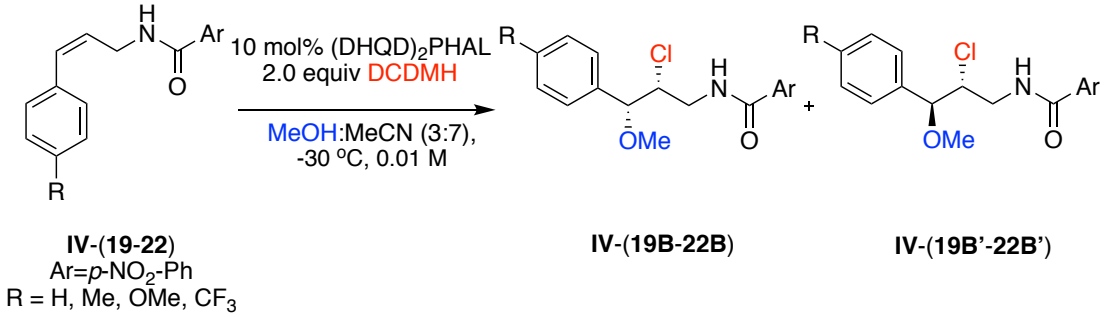

R	Ratio (**B**:**B'**)	σ
OMe	1:1	-0.27
CH_3	1.3:1	-0.14
H	3.3:1	0
CF_3	>20:1	0.53

The mechanism for the formation of two chloroetherified diastereomers and chlorocyclized products is summarized in Figure IV-17. The NAAA pathway suitably explains the chlorenium face selectivity switch for the major interm

Figure IV-17: Proposed mechanism for the formation of intermolecular and intramolecular products in enantioselective chloroetherification reactions

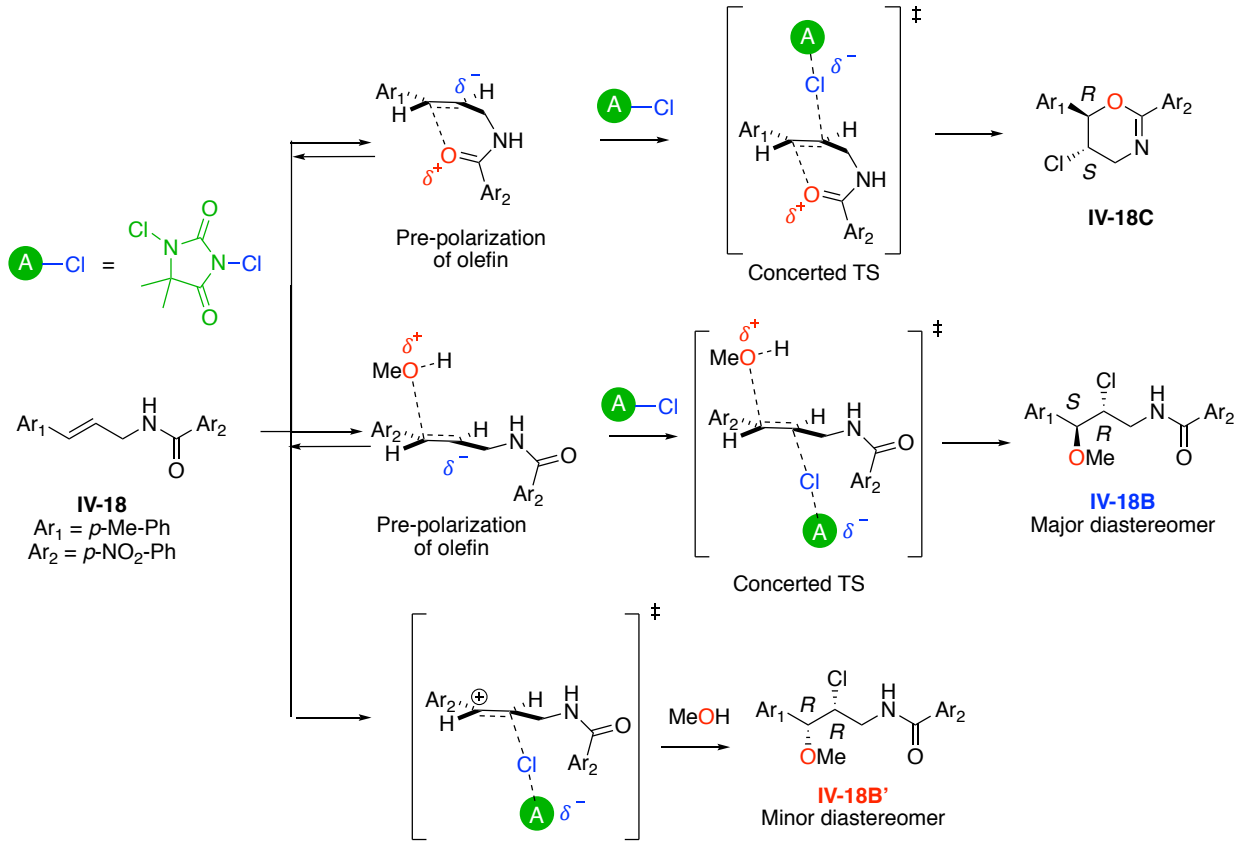

olecular product **IV-18B** and the cyclized product **IV-18c**. Nonetheless, the zero kinetic order of the nucleophile for the formation of the minor diastereomer **IV-18B'** and the Hammett analysis lead us to propose carbocation production for the formation the latter product.

IV-2-4 Experimental section

The *E*-allyl amide **IV-18** (0.04 mmol, 11.8 mg) in the presence of 10 mol% $(DHQD)_2PHAL$ (0.004 mmol, 3.1 mg) and methanol (4 mmol, 160 μl) were dissolved in different amounts of acetonitrile (0.5 mL, 1 mL, 2 mL, 3 mL) in a screw-capped vial equipped with a stir bar. After stirring for 2 min DCDMH (15.8 mg, 0.08 mmol, 2.0 equiv) was added to these series of solution at room temperature. The stirring was continued at room temperature till the reaction was complete (TLC). The reaction was quenched by the addition of saturated aq. Na_2SO_3 (1 mL) and diluted with DCM (3 mL). The organics were separated and the aqueous layer was extracted with DCM (3 × 3 mL). The combined organics were dried over anhyd. Na_2SO_4 and concentrated. The ratio of products **IV-18B**/ **IV-18C** (or **IV-18B'**/ **IV-18C**) resulting from each individual reaction was determined by integrating appropriately resolved resonances in the 1 H NMR spectrum of each crude product mixture.

REFERENCES

REFERENCES

1. Soltanzadeh, B.; Jaganathan, A.; Staples, R. J.; Borhan, B., Highly Stereoselective Intermolecular Haloetherification and Haloesterification of Allyl Amides. *Angew Chem Int Ed Engl* **2015,** *54* (33), 9517-22.

2. Jaganathan, A.; Garzan, A.; Whitehead, D. C.; Staples, R. J.; Borhan, B., A catalytic asymmetric chlorocyclization of unsaturated amides. *Angew Chem Int Ed Engl* **2011,** *50* (11), 2593-6.

3. Cresswell, A. J.; Eey, S. T.; Denmark, S. E., Catalytic, Stereoselective Dihalogenation of Alkenes: Challenges and Opportunities. *Angew Chem Int Ed Engl* **2015,** *54* (52), 15642-82.

4. Denmark, S. E.; Kuester, W. E.; Burk, M. T., Catalytic, asymmetric halofunctionalization of alkenes--a critical perspective. *Angew Chem Int Ed Engl* **2012,** *51* (44), 10938-53.

5. Ashtekar, K. D.; Vetticatt, M.; Yousefi, R.; Jackson, J. E.; Borhan, B., Nucleophile-Assisted Alkene Activation: Olefins Alone Are Often Incompetent. *Journal of the American Chemical Society* **2016,** *138* (26), 8114-8119.

6. Corbett, J. F., Pseudo first-order kinetics. *Journal of Chemical Education* **1972,** *49* (10), 663.

7. Hoye, T. R.; Baire, B.; Niu, D.; Willoughby, P. H.; Woods, B. P., The hexadehydro-Diels-Alder reaction. *Nature* **2012,** *490* (7419), 208-12.

8. Willoughby, P. H.; Niu, D.; Wang, T.; Haj, M. K.; Cramer, C. J.; Hoye, T. R., Mechanism of the reactions of alcohols with o-benzynes. *J Am Chem Soc* **2014,** *136* (39), 13657-65.

9. Niu, D.; Wang, T.; Woods, B. P.; Hoye, T. R., Dichlorination of (hexadehydro-Diels-Alder generated) benzynes and a protocol for interrogating the kinetic order of bimolecular aryne trapping reactions. *Org Lett* **2014,** *16* (1), 254-7.

10. Blanks, R. F.; Prausnitz, J. M., Infrared Studies of Hydrogen Bonding in Isopropanol and in Mixtures of Isopropanol with Poly (n-Butyl Methacrylate) and with Poly(Propylene Oxide). *The Journal of Chemical Physics* **1963,** *38* (7), 1500-1504.